MOLDOVA STATE UNIVERSITY

DOCTORAL SCHOOL OF NATURAL SCIENCES

The title of manuscript:
U.D.C. 582.32:504.3.054:551.4:551.5

CHALIGAVA OMARI

APPLICATION OF MOSSES AS BIOINDICATORS FOR EVALUATION OF ECOLOGICAL STATE OF AIR IN DIFFICULT CLIMATIC AND RELIEF CONDITIONS

Specialty: 166.01. Ecology

APPROVED:

Scientific adviser:  **CEPOI Liliana**, dr.hab., assoc.prof.

Author:  **CHALIGAVA Omari**

CHISINAU 2026

UNIVERSIRTAEA DE STAT DIN MOLDOVA

ȘCOALA DOCTORALĂ ȘTIINȚE ALE NATURII

Cu titlul de manuscript:
C.Z.U. 582.32:504.3.054:551.4:551.5

CHALIGAVA OMARI

APLICAREA MUȘCHILOR CA BIOINDICATORI PENTRU EVALUAREA STĂRII ECOLOGICE A AERULUI ATMOSFERIC ÎN CONDIȚII CLIMATICE ȘI DE RELIEF DIFICILE

Specialitatea: 166.01. Ecologie

APROBAT:

Conducător științific: **CEPOI Liliana**, dr.hab., conf.cerc.

Autor: **CHALIGAVA Omari**

CHIȘINĂU 2026

Contents

ADNOTARE

Chaligava Omari, „Aplicarea mușchilor ca bioindicatori pentru evaluarea stării ecologice a aerului atmosferic în condiții climatice și de relief dificile" teză de doctor în științe ale mediului, Chisinau, 2026

Structura tezei: Adnotare (în engleză şi română), Introducere, Cinci capitole, Concluzii si recomandări, Bibliografie cu 365 surse, 26 figuri, 18 tabele, 140 pagini de text de bază. Rezultatele obținute au fost publicate în 15 lucrări ştiinţifice, inclusiv 6 articole în reviste indexate WoS/Scopus.

Cuvinte-cheie: Biomonitorizarea cu muşchi, depuneri atmosferice, elemente potențial toxice, evaluarea calității aerului, factori climatici, relief și topografie, Republica Moldova, Georgia, metode analitice

Scopul tezei. Elucidarea eficacității metodei de biomonitorizare cu mușchi pentru evaluarea calității aerului atmosferic în zone cu diferite condiții fizico-geografice: studiu de caz pentru Republica Moldova și Georgia.

Obiectivele studiului sunt: Efectuarea biomonitorizării pasive cu mușchi în Republica Moldova și Georgia, regiuni caracterizate prin condiții climatice și de relief contrastante; Determinarea compoziției elementare a probelor de mușchi și analiza comparativă a variabilității lor spațiale și temporale; identificarea și diferențierea surselor naturale (geogene) și antropogene de poluare a aerului atmosferic în regiunile studiate; Evaluarea influenței factorilor climatici și topografici (precipitații, altitudine, pantă) asupra acumulării elementelor în mușchi; Elaborarea principiilor de stabilire a nivelurilor de fond ale poluării în diferite condiții climatice și de relief; elaborarea recomandărilor pentru aplicarea și interpretarea rezultatelor biomonitorizării cu mușchi în regiuni cu caracteristici fizico-geografice contrastante.

Noutatea şi originalitatea ştiinţifică: Noutatea lucrării constă în evaluarea integrată a eficienței biomonitorizării cu mușchi în condiții climatice și de relief contrastante, utilizând o abordare comparativă între Republica Moldova și Georgia. Studiul demonstrează, pentru prima dată, rolul decisiv al factorilor topoclimatici (precipitații, altitudine, teren) în controlul modelelor de depunere atmosferică și acumulare a elementelor în mușchi, dincolo de influența surselor de emisie.

Rezultatul obţinut care contribuie la soluţionarea unei probleme ştiinţifice importante constă în identificarea și fundamentarea factorilor climatici și geomorfologici ca determinanți - cheie ai depunerii atmosferice și ai acumulării elementelor în mușchi, printr-o analiză comparativă a regiunilor cu condiții fizico-geografice contrastante (Republica Moldova și Georgia), ceea ce a condus la o diferențiere mai clară între contribuțiile geogene și antropogene și la o interpretare mai exactă a datelor de biomonitorizare, în contextul aplicării biomonitorizării cu mușchi pentru evaluarea calității aerului în diverse condiții climatice și de relief.

Semnificaţia teoretică a tezei constă în extinderea conceptului de biomonitorizare prin încorporarea factorilor climatici și de relief ca factori cheie ai transportului și acumulării poluanților. Cercetarea contribuie la o înțelegere mai profundă a mecanismelor depunerii atmosferice (depunerea uscată și umedă), și a interacțiunii acestora cu condițiile de mediu în modelarea tiparelor geochimice în biomonitori.

Valoarea aplicativă a tezei: constă în dezvoltarea de recomandări metodologice pentru interpretarea datelor de biomonitorizare cu mușchi în regiuni cu condiții climatice și geomorfologice diferite. Rezultatele susțin stabilirea unor niveluri de fond specifice regiunii, îmbunătățirea strategiilor de monitorizare a mediului și identificarea mai precisă a surselor de poluare, oferind o bază pentru managementul de mediu și politică de dezvoltare.

Implementarea rezultatelor ştiinţifice: Rezultatele obținute în urma acestui studiu au fost incluse în raportul ICP Vegetation, contribuind astfel la dezvoltarea rețelei europene de monitorizare a metalelor grele în Europa și alte state.

ANNOTATION

Chaligava Omari, Application of mosses as bioindicators for evaluation of ecological state of air in difficult climatic and relief conditions. PhD thesis in environmental sciences, Chisinau, 2026

Structure of the thesis: Abstracts (in Romanian and English), introduction, five chapters, conclusions and recommendations, bibliography from 365 sources, 26 figures, 18 tables and 140 pages of main text. The results of the dissertation are reflected in 15 scientific publications, including 6 articles in peer-reviewed journals, indexed in WoS/Scopus.

Keywords: Moss biomonitoring, atmospheric deposition, potentially toxic elements, air quality assessment, climatic factors, relief and topography, Republic of Moldova, Georgia, analytical techniques

The aim of the thesis. To elucidate the effectiveness of the moss biomonitoring method for assessing the quality of atmospheric air in areas with different physico-geographical conditions: case study of Republic of Moldova and Georgia.

The objectives of the study are: carrying out passive moss biomonitoring in the Republic of Moldova and Georgia, regions characterized by contrasting climatic and relief conditions; determination of the elemental composition of moss samples and comparative analysis of their spatial and temporal variability; identification and differentiation of natural (geogenic) and anthropogenic sources of atmospheric air pollution in the studied regions; assessment of the influence of climatic and topographical factors (precipitation, altitude, slope) on the accumulation of elements in mosses; elaboration of principles for establishing background levels of pollution under different climatic and relief conditions; development of recommendations for the application and interpretation of moss biomonitoring results in regions with contrasting physico-geographical characteristics.

The novelty and scientific originality: The novelty of the work consists in the integrated evaluation of moss biomonitoring efficiency under contrasting climatic and relief conditions, using a comparative approach between the Republic of Moldova and Georgia. The study demonstrates, for the first time, the decisive role of topoclimatic factors (precipitation, altitude, terrain) in controlling atmospheric deposition patterns and element accumulation in mosses, beyond the influence of emission sources.

A result that contributes to the solution of a scientific problem consists in the identification and substantiation of climatic and geomorphological factors as key drivers of atmospheric deposition and element accumulation in mosses, through a comparative analysis of regions with contrasting physico-geographical conditions (Republic of Moldova and Georgia), which led to improved differentiation between geogenic and anthropogenic contributions and to more accurate interpretation of biomonitoring data, in the context of applying moss biomonitoring for air quality assessment under diverse climatic and relief conditions.

The theoretical importance of the work lies in extending the conceptual framework of biomonitoring by incorporating climatic and relief factors as key drivers of pollutant transport and accumulation. The research contributes to a deeper understanding of the mechanisms of atmospheric deposition, including dry and wet processes, and their interaction with environmental conditions in shaping geochemical patterns in biomonitors.

The applied value of the work consists in the development of methodological recommenddations for the interpretation of moss biomonitoring data in regions with different climatic and geomorphological conditions. The results support the establishment of region-specific background levels, improvement of environmental monitoring strategies, and more accurate identification of pollution sources, providing a basis for environmental management and policy development. **The implementation of the results:** The obtained results of this study were included in ICP Vegetation survey report, thereby contributing to the European monitoring network for heavy metals across Europe and beyond.

LIST OF TABLES

LIST OF FIGURES

LIST OF ABBREVIATIONS

This list will contain all the abbreviations included in the sentence that are not in common use.

Abbreviations	Discription
a.s.l.	Above sea level
AAS	Atomic Absorption Spectroscopy
ATP	Adenosine triphosphate
CF	Contamination Factor
CRMs	Certified reference materials
CV%	Coefficient of variation
DMA-80	Direct Mercury Analyzer
DNA	Deoxyribonucleic acid
EPA	United States Environmental Protection Agency
GDP	Gross Domestic Product
GIS	Geographic Information Systems
HPGe	High-Purity Germanium
ICP-MS	Inductively Coupled Plasma Mass Spectrometry
ICP-OES	Inductively Coupled Plasma Optical Emission Spectrometry
IN	Ice nuclei
LLI 1	First long-lived isotopes
LLI 2	Second long-lived isotopes
LRTAP	Convention on Long-range Transboundary Air Pollution
MAD	Median Absolute Deviation
NAA	Neutron Activation Analysis
ND	Not detected
NEE	Non-exhaust emissions
PAHs	Polycyclic aromatic hydrocarbons
PCA	Principal Component Analysis
PCs	Principal components
PER	Potential Ecological Risk Index
PLI	Pollution Load Index
PM	Particulate matter
PM_{10}	Particulate matter with a diameter of 10 micrometers or less
$PM_{2.5}$	Particulate matter with a diameter of 2.5 micrometers or less
PMF 5.0	Positive Matrix Factorization
POPs	Persistent organic pollutants
PTEs	Potentially Toxic Elements
Q1	First quartile (the 25th percentile of a dataset)
Q3	Third quartile (the 75th percentile of a dataset)
RI	Ecological Risk Index
ROS	Reactive oxygen species
RP	Reference Plant – A standardized plant material with a certified inorganic composition published by Markert

SD	Standard deviation
SLI	Short-lived isotopes
TF	Toxic-response factor
UCC	Upper Continental Crust
UFPM	Ultra-fine particulate matter less than 0.1 micrometers in diameter
UV	Ultraviolet
VOCs	Volatile organic compounds
XRF	X-ray Fluorescence

INTRODUCTION

The importance and relevance of the topic:

Atmospheric air quality is a critical determinant of human health, shaped by a combination of anthropogenic emissions and natural environmental factors. According to the World Health Organization, exposure to particulate matter ($PM_{2.5}$ – particulate matter with a diameter of 2.5 μm or less, and PM_{10} – particulate matter with a diameter of 10.0 μm or less), a key component of ambient air pollution, causes approximately 4.2 million deaths annually. The observed mortality has been associated with pollution-induced cases of stroke, cardiovascular disease, lung cancer, lower respiratory tract infections and chronic obstructive pulmonary disease [1–3]. Fine particulate matter is considered the most harmful air pollutant due to its ability to penetrate deeply into the respiratory system and to serve as an efficient carrier of toxic substances, including trace metals and metalloids [2, 4–6].

In addition to emission sources, the distribution, transport, and deposition of atmospheric pollutants are strongly influenced by climatic conditions and topographical features. Factors such as precipitation patterns, temperature regimes, wind dynamics, and atmospheric stability directly affect both wet and dry deposition processes [7, 8]. At the same time, relief characteristics, including altitude, slope, and valley–mountain systems, play a critical role in modifying air mass circulation, pollutant dispersion, and accumulation zones [9, 10]. As a result, regions with contrasting physico-geographical conditions may exhibit substantially different patterns of pollutant deposition even under comparable emission scenarios.

To assess air quality, it is necessary to carry out a complex analysis of aerosol particles to determine the concentrations of those pollutants that pose a threat to living organisms. The most important hazard criteria are: the degree of toxicity, potential carcinogenicity, the stability of compounds, their solubility, the degree of bioaccumulation by living organisms, the quantitative release into the atmospheric air and the concentration in the environment [11, 12]. According to all these criteria, heavy metals and metalloids especially: Al, As, Cd, Cr, Cu, Fe, Hg, Ni, Pb, Sb, V, and Zn are considered harmful and pose ecological and health risks even at very low concentrations [13–15]. While some of these elements (e.g., Cu, Fe, Zn) are essential micronutrients at trace levels, others (e.g., Cd, Hg, Pb, As) have no known biological function and are toxic even at minimal exposure [13, 15, 16]. Their environmental behavior depends strongly on chemical speciation, solubility, and redox state, which influence mobility and bioavailability. Although heavy metals are natural components of the earth’s crust, their multiple industrial, domestic, agricultural, medical, and technological applications, as well as soil erosion,

deforestation, urbanization, and land degradation have significantly increased the contribution to elevated metal concentrations in airborne particulate matter. Once emitted, metals can easily attach to atmospheric particles and be transported over long distances before being deposited via dry and wet processes, a phenomenon addressed under the Convention on Long-range Transboundary Air Pollution [13, 17, 18].

In mountainous regions, orographic effects can enhance precipitation and consequently increase wet deposition rates, while valleys may act as accumulation zones due to reduced air circulation and temperature inversions. In contrast, lowland and open terrains are typically characterized by more uniform dispersion patterns, but may be more exposed to long-range transport of pollutants and resuspended dust [19, 20]. These differences complicate the interpretation of atmospheric deposition data and raise important questions regarding the comparability of monitoring results across regions with distinct climatic and geomorphological characteristics.

The monitoring of the composition of atmospheric deposition is an important task of environmental protection. Detailed chemical characterization of atmospheric deposition provides insight into emission sources, atmospheric transport mechanisms, transformation processes, and long-term environmental impacts on terrestrial and aquatic ecosystems.

To evaluate these processes, diverse air pollution monitoring techniques have been developed, combining direct atmospheric measurements with analytical assessment of deposited materials.

As mentioned above, atmospheric deposition is governed by two fundamentally different mechanisms: wet and dry deposition. As these mechanisms differ in terms of removal efficiency and physicochemical behavior, separate methodological approaches are necessary for accurate quantification. Consequently, monitoring systems are designed to selectively capture either precipitation-associated inputs or deposition occurring under non-precipitating conditions.

In humid regions, the contribution of dry deposition is typically minor relative to wet deposition and does not significantly modify the chemical characteristics of precipitation. However, in arid and semiarid environments, where intense dust loadings are common, dry deposition can represent the dominant flux, highlighting the need to differentiate between these two processes [8]. Furthermore, under high precipitation regimes, wet deposition is primarily associated with long-range transport, while dry deposition is more closely linked to local pollution sources and is the dominant process for the deposition of pollutants in highly industrialized areas [8].

Wet deposition is commonly monitored using bulk collectors or wet-only samplers. Bulk collectors remain open continuously and collect both wet and dry deposition, whereas automated wet-only collectors equipped with precipitation sensors, open only during precipitation events, minimizing contamination from particles settling during dry periods. The collected samples are analyzed for pH, conductivity, major anions and cations, and trace metals. Long-term datasets from such systems are fundamental in assessing acid deposition and evaluating the effectiveness of emission control policies [21].

In contrast, deposition under dry atmospheric conditions involves gravitational settling of coarse particles, turbulent transfer of fine particles, and direct adsorption of gaseous pollutants onto surfaces. Monitoring this pathway requires open-surface collectors, surrogate deposition plates, or passive accumulation devices that continuously capture particles and reactive gases over defined exposure periods. These systems must consider aerodynamic resistance, surface characteristics, and potential resuspension effects, all of which influence deposition velocity [8, 22].

High-volume samplers are commonly used to capture PM_{10} or $PM_{2.5}$ fractions, which are later analyzed for mass concentration and chemical composition, including heavy metals, sulfates, nitrates, ammonium, and organic compounds. Following collection, PM mass concentration is determined gravimetrically under controlled temperature and relative humidity conditions to reduce hygroscopic bias. Water-soluble anions (e.g., SO_4^{2-}, NO_3^-) and cations (e.g., NH_4^+) are routinely quantified by ion chromatography, which provides low detection limits and high selectivity for atmospheric aerosol applications [23–25]. Trace and heavy metals are commonly determined after acid digestion using inductively coupled plasma mass spectrometry (ICP-MS), which offers multi-element capability and low detection limits suitable for urban and background environments [26, 27]. Atomic absorption spectroscopy (AAS), while increasingly supplemented by ICP-based techniques, remains applicable for targeted elemental analysis in regulatory contexts [28].

Organic compound characterization, including polycyclic aromatic hydrocarbons (PAHs) and other semi-volatile organic compounds, is generally conducted using gas chromatography coupled with mass spectrometry. Methodological refinements such as thermal desorption and solvent extraction protocols have enhanced compound recovery and reduced matrix interferences [29–31].

For gaseous pollutants, continuous automated analyzers are often employed and provide high temporal resolution. SO_2 is predominantly measured using ultraviolet (UV) fluorescence analyzers, which exploit SO_2 excitation-emission properties and demonstrate high stability under

field conditions [32–34]. Nitrogen oxides are typically quantified using chemiluminescence detection based on the reaction of NO with ozone, with molybdenum or photolytic converters employed for NO_2 determination; recent evaluations have addressed converter interferences and measurement biases [35]. Carbon oxides monitoring commonly relies on nondispersive infrared spectroscopy, with gas filter correlation improving selectivity and drift correction [36, 37]. Ozone is measured using UV photometry at 254 nm, a method standardized in regulatory frameworks due to its linearity and robustness across ambient concentration ranges [38, 39].

These instrumental techniques constitute the technical backbone of national and international air quality monitoring networks. Such networks operate under quality assurance and quality control protocols consistent with international regulatory standards and guidelines issued by bodies such as the World Health Organization and implemented within regional frameworks [40].

Despite their technical sophistication, these conventional monitoring techniques present several limitations. They often require expensive instrumentation, stable power supply, regular calibration, and skilled personnel for maintenance and data interpretation. Monitoring stations are usually sparsely distributed due to financial constraints, reducing representativeness in remote or complex terrains. Many instruments provide high temporal resolution but only at specific points. Furthermore, chemical analyses typically reflect short-term concentrations rather than cumulative exposure or ecological impact over extended periods. These constraints highlight the need for complementary approaches that can integrate pollutant accumulation over time and provide broader spatial coverage with lower operational demands.

In addition to ground-based methods, remote sensing has become a widely adopted tool for atmospheric assessment. Satellite-based instruments enable large-scale assessment of atmospheric column concentrations of pollutants including nitrogen dioxide, sulfur dioxide, and particulate aerosols. However, remote sensing methods have several notable disadvantages. Satellite measurements provide vertically integrated column concentrations rather than ground-level values, which are typically most relevant for human exposure. Retrieval algorithms rely on modeling assumptions and are sensitive to cloud cover, surface reflectance, and atmospheric conditions, which introduce uncertainties and data gaps [41, 42].

In Republic of Moldova, according to Government decision air pollution is regulated by the operation of two systems: National Inventory System of Air Pollutant Emissions and National Integrated Air Quality Monitoring System. In addition, air quality monitoring is performed by the State Hydrometeorological Service, which has a network of 17 stations, located in five urban centers: Chisinau (6), Bender (4), Tiraspol (3), with Balți and Ribnița each hosting 2 stations [43].

Air samples are collected manually, only three times per day, and analyzed for multiple pollutants, including PM, SO_2, CO, NO_2, soluble sulfates, NO, phenol, and formaldehyde [43]. A significant methodological limitation of this network is its spatial resolution, being limited primarily to urban areas, it cannot evaluate spatial patterns of atmospheric deposition across the entire territory, particularly in rural and background regions.

In Georgia, the national air quality monitoring system employs both indicative and automatic methods [44]. Since 2015, indicative measurements have been carried out quarterly across 25 cities [44]. The automatic network has seen significant expansion, growing from 7 stations in 2019 to 15 by 2023, delivering continuous data from major urban centers, namely: Tbilisi, Rustavi, Telavi, Akhaltsikhe, Kutaisi, Batumi, Zugdidi, and Mestia [44]. Furthermore, since 2021, the monitoring program has been progressively enhanced to include the measurement of heavy metals, such as Ni, Cd, Pb, and As [44]. Despite these improvements, monitoring infrastructure remains concentrated in populated areas, and high operational costs limit the establishment of dense spatial networks.

In both countries, the concentrations of pollutants often exceed national limits and monitoring stations are operated mainly in cities and towns. Lack of stations, their low prevalence and high operating costs make traditional monitoring expensive and less informative particularly when assessment of the pollution spread on the large territory needs to be performed [45, 46].

Biomonitoring using mosses is considered an adequate alternative method for obtaining data about air pollution. The advantage of the moss biomonitoring technique is its low cost and applicability for investigations on large territories, what increases the confidence and precision in estimation. The use of epiphytic plants as passive biomonitors is an established and approved method of determining atmospheric deposition of heavy metals, radionuclides, ozone and nitrogen. Mosses absorb nutrients and contaminants directly from atmospheric deposition. This physiological characteristic makes them particularly suitable as passive samplers of airborne trace elements. In Scandinavia, mosses have been used as biomonitors for determining pollution with heavy metals since the late 1960s. Numerous projects have since been carried out with mosses; the method has been developed systematically and also used in large-scale European studies. Since 2001, the European biomonitoring program has been coordinated by the International Cooperative Program on Effects of Air Pollution on Natural Vegetation and Crops (UNECE ICP Vegetation) under the Convention on Long-range Transboundary Air Pollution (LRTAP Convention). The program conducts continent-wide surveys at five-year intervals, generating spatially comparable datasets on atmospheric metal deposition.

The ICP Vegetation report of moss survey of 2015-2016 [47] highlighted the necessity to unravel factors primarily contributing to the very high metal concentrations in mosses, especially assess the role of wind-blown dust and/or soil contamination in the areas dominated by mineral soils. The question rises of how suitable the moss biomonitoring technique is for determining the contribution of current primary sources of anthropogenic emissions of atmospheric metal deposition and long-range transboundary air pollution.

Republic of Moldova, as well as Georgia joined the moss biomonitoring program of UNECE ICP Vegetation for the first time in 2015. According to the Moss Survey 2015-2016 report, both countries showed higher levels of the elements compared to other countries participating in the program [47]. Republic of Moldova and Georgia share several characteristics relevant to atmospheric deposition processes: both countries are located in the same temperate zone, both are influenced by the Black Sea, in both soil erosion is one of the main source of elements emission in the atmosphere, and the same species of mosses are available. At the same time, these countries have many differences, for example, Republic of Moldova is relatively lowland and hilly, while approximately two-thirds of Georgia is mountainous, and 20% of the country is located at an altitude of 2000 meters or more above sea level. Moldova is a predominantly rural country, 74% of its total area is agricultural land, in Georgia the same parameter is only 43%. The main economic activities also differ in many ways [45, 46]. These geographic and economic contrasts provide a valuable framework for comparative analysis of metal deposition patterns.

The general objective of the project:

To elucidate the effectiveness of the moss biomonitoring method for assessing the quality of atmospheric air in areas with different physico-geographical conditions: case study of Republic of Moldova and Georgia.

Specific objectives:

- Carrying out passive moss biomonitoring in the Republic of Moldova and Georgia, regions characterized by contrasting climatic and relief conditions.
- Determination of the elemental composition of moss samples and comparative analysis of their spatial and temporal variability.
- Identification and differentiation of natural (geogenic) and anthropogenic sources of atmospheric air pollution in the studied regions.
- Assessment of the influence of climatic and topographical factors (precipitation, altitude, slope) on the accumulation of elements in mosses.

- Elaboration of principles for establishing background levels of pollution under different climatic and relief conditions.
- Development of recommendations for the application and interpretation of moss biomonitoring results in regions with contrasting physico-geographical characteristics.

Hypothesis

Moss biomonitoring captures spatiotemporal variability in atmospheric deposition through the integrated effects of climate and relief on trace element accumulation, and, when coupled with advanced multivariate statistics and supplementary environmental data, enables robust discrimination between geogenic and anthropogenic sources across diverse climatic and geomorphological gradients.

The synthesis of the research methodology and justification of the research methods:

A nationwide assessment of atmospheric heavy metal and metalloid pollution was conducted using moss biomonitoring. This method enabled a spatially comprehensive evaluation of pollution. Initial sampling in Georgia utilized multiple moss species to achieve maximum territorial coverage, while in the Republic of Moldova only one species was used. The elemental analysis of moss tissues was performed using complementary analytical methods: Neutron Activation Analysis (NAA), Atomic Absorption Spectrometry (AAS), and Inductively Coupled Plasma Optical Emission Spectrometry (ICP-OES). To isolate the effects of environmental variables on metal accumulation in mosses, a comparison was designed between two countries with distinct climates and geologies. For this controlled comparison, a single moss species was selected to eliminate interspecies variability. Furthermore, to isolate the influence of natural environmental factors and minimize distortion from samples associated with direct anthropogenic activity or local pollution hotspots, the Grubbs' test was applied to identify and exclude statistical outliers. A comprehensive multivariate statistical analysis was performed to extract meaningful patterns from the compositional data. Principal Component Analysis (PCA) served to reduce dimensionality and identify latent factors representing common pollution sources. Associations between elemental concentrations and key environmental variables were evaluated using Spearman's rank correlation coefficient. Finally, the non-parametric Kruskal-Wallis test was applied to detect statistically significant differences in metal accumulation across different geographical or ecological groupings.

The scientific novelty of the work is as follows:

The novelty of the work consists in the integrated evaluation of moss biomonitoring efficiency under contrasting climatic and relief conditions, using a comparative approach between the Republic of Moldova and Georgia. The study demonstrates, for the first time, the decisive role

of topoclimatic factors (precipitation, altitude, terrain) in controlling atmospheric deposition patterns and element accumulation in mosses, beyond the influence of emission sources.

The impact of the results:

The theoretical importance of the work lies in extending the conceptual framework of biomonitoring by incorporating climatic and relief factors as key drivers of pollutant transport and accumulation. The research contributes to a deeper understanding of the mechanisms of atmospheric deposition, including dry and wet processes, and their interaction with environmental conditions in shaping geochemical patterns in biomonitors.

The applied value of the work consists in the development of methodological recommendations for the interpretation of moss biomonitoring data in regions with different climatic and geomorphological conditions. The results support the establishment of region-specific background levels, improvement of environmental monitoring strategies, and more accurate identification of pollution sources, providing a basis for environmental management and policy development.

Summary of the dissertation sections:

The dissertation consists of an introductory part and 5 chapters. The first chapter presents an analytical review of scientific literature, applicable to the problem considered in the dissertation. In the second chapter, material and research methods are presented. In the third and fourth chapters, the experimental part is described and analyzed. The fifth chapter describes the comparative analysis of moss biomonitoring data from the Republic of Moldova and Georgia, demonstrating that elemental accumulation in *Hypnum cupressiforme* is controlled by a complex interaction between geogenic background, anthropogenic inputs, and environmental factors, particularly climatic conditions and relief characteristics.

The first chapter establishes the scientific foundations for using mosses as biomonitors of atmospheric pollution. It characterizes air pollutants, particularly potentially toxic elements associated with particulate matter, and examines factors governing their spatial distribution, including climate, topography, and atmospheric transport processes. The chapter then introduces biomonitoring as a cost-effective complement to traditional monitoring, detailing moss morphological and physiological traits that enable pollutant accumulation from atmospheric deposition. Key methodological approaches and analytical techniques are reviewed, alongside persistent knowledge gaps regarding climatic and topographic influences on data interpretation.

The second chapter details the methodological framework for assessing atmospheric deposition using moss biomonitoring across Georgia and the Republic of Moldova. It describes study area characteristics, sampling strategies, analytical techniques (INAA, AAS, ICP-OES,

DMA-80), and quality control protocols. Statistical approaches include correlation analysis, PCA, PMF, contamination indices, and GIS-based spatial analysis incorporating climatic, topographic, and population variables.

The third chapter presents two national moss surveys in Georgia (2014–2017, n=120; 2019–2023, n=95). Results identify significant pollution hotspots from mining and industry, while multivariate statistics reveal dominant geogenic crustal influences alongside anthropogenic contributions. The pollution load indices confirming localized ecological risks.

The fourth chapter presents Moldova's second national moss biomonitoring survey, analyzing 35 elements from 41 sites. Results show significant declines in toxic metals like Pb (75%) and Cd (66%) since 2015, though urban hotspots persist. Factor analysis identifies terrigenous, agricultural, combustion, and industrial sources. Despite localized urban contamination, national ecological risk remains low.

The fifth chapter investigates factors controlling elemental content in mosses through a comparative study of surveys from Moldova and Georgia. Using *Hypnum cupressiforme* to avoid interspecies variability, outlier test removed local contamination hotspots. Results reveal strong lithogenic associations (Al, Co, Cr, Fe, Ni, V) and distinct topoclimatic controls, with elevation, precipitation, and slope driving Pb and Cd accumulation via wet deposition processes.

The work ends with general conclusions and recommendations, a list of cited bibliographic sources.

1. MOSS BIOMONITORING AS EFFICIENT TOOL OF THE AIR POLLUTION ASSESSMENT

Air pollution is a complex environmental problem, governed not only by emission sources but also by atmospheric processes and environmental conditions that control the transport and deposition of pollutants. In recent decades, increased attention has been paid to the spatial variability of atmospheric contaminants, especially potentially toxic elements associated with suspended particles. Traditional monitoring techniques, although highly accurate, are often limited by high operational costs and insufficient spatial coverage, especially in regions with heterogeneous relief and climatic conditions. In this context, biomonitoring has emerged as a complementary approach capable of providing integrated information on pollutant deposition over extended periods. Among biological indicators, mosses have proven to be particularly effective due to their unique morphological and physiological characteristics, including the absence of a root system and their direct interaction with atmospheric deposition. Their ability to accumulate pollutants from both wet and dry deposition makes them reliable indicators of air quality at local, regional and continental scales. Furthermore, the applicability of moss biomonitoring in large-scale international programs has demonstrated its value in identifying spatial patterns of pollution and long-term environmental trends.

However, the interpretation of biomonitoring data is not straightforward and can be influenced by a number of environmental factors, including climate, relief and local ecological conditions. These factors can significantly affect pollutant accumulation processes and limit the comparability of results across regions. Therefore, a comprehensive understanding of the theoretical background, mechanisms and limitations of moss biomonitoring is essential for its proper application in environmental assessment.

This chapter presents the scientific foundations of air pollution assessment using moss biomonitors, including the characteristics of air pollutants, the factors influencing their spatial distribution, the principles of biomonitoring, and the biological and ecological characteristics of mosses that determine their suitability for this purpose.

1.1. Air Pollution: Composition and Pollutant Types

Air pollution is a serious worldwide problem caused by anthropogenic activities, and is closely related to the environmental situation, economics, and human health. Air is a mixture of gases, most of which occur naturally, and also contains water in all three phases (liquid, solid and gas), but it is incomplete without its non-gaseous components. It contains dispersed materials in both solid and liquid phases, collectively known as aerosols. These components, ranging from fine

droplets and mists to complex particles, vary widely in their origin, size, and composition. The terminology reflects this complexity: a droplet is clearly a liquid, but a particle may be solid, liquid, or a hybrid, such as a solid core coated with liquid. Due to the difficulty in distinguishing the actual phase, the term particulate matter (PM) is often used as a general term that does not specify phase. An aerosol describes the entire suspension, meaning the air plus dispersed particles [21]. These atmospheric particles and droplets range dramatically in size, from a few nanometers to approximately 100 micrometers in diameter. Because they often have irregular shapes, their "diameter" is typically not a geometric measurement but is instead defined by how they behave during separation, such as through filtration or aerodynamic methods.

Ambient air pollution consists of gaseous components and PM. Air pollutants that are released directly from sources are called primary air pollutants and include: carbon monoxide (CO), nitrogen oxides (NO_x), sulfur dioxides (SO_2), volatile organic compounds (VOCs), hydrocarbons, lead, and PM. Secondary air pollutants are formed as a result of chemical reactions of the primary pollutants and include: ozone (O_3), sulfuric acid (H_2SO_4), nitric acid (HNO_3), secondary PM and more. Forest fires, volcanic eruptions, industrial activity and combustion engines play a major role in the occurrence of fine particulate matter. A significant amount of man-made air pollutants is harmful to breathing, and some cause global warming. Pollutants in gaseous or vapor-phase including O_3, NO_2, VOCs, CO, and SO_2, make up 90% of the total mass of pollutants in urban areas [48].

According to World Health Organization, ambient air pollution has caused approximately 4.2 million deaths in 2016 [1]. Particulate matter air pollution has been identified as the most prominent leading risk factor causing disease, especially fine particulate matter, which can penetrate deep into the lungs and bloodstream and cause respiratory (lung cancer, lower respiratory infections, chronic obstructive pulmonary disease) cardiovascular (heart disease) and cerebrovascular (stroke) complications. Particulate matter itself can be divided into fractions based on particle size. They include PM_{10}, $PM_{2.5}$ and ultra-fine particulate matter (UFPM). Material with an aerodynamic diameter of approximately 2.5 μm or greater is typically designated as coarse particulate material, while particles with an aerodynamic diameter of 2.5 μm or less are classified as fine. A subset of fine particles, known as ultrafine particles, are those with diameters less than 0.1 μm. These ultrafine particles are primarily formed from gases and vapors. Subsequently, they can increase in size through coagulation with one another to form fine particles. Fine particles, in turn, can grow further via aggregation with other fine particles and through the heterogeneous sorption of gases and low-volatility vapors onto their surfaces [21].

The size of an aerosol particle fundamentally determines its behavior in both the atmosphere and the human respiratory system. First, coarse particles are subject to rapid removal via gravitational settling, resulting in atmospheric residence times on the order of minutes to hours. This rapid removal from the atmosphere restricts their spatial influence, limiting transport to a scale of tens of kilometers from the source [3, 21]. Fine particles, however, evade such rapid deposition and can be transported over intercontinental distances, spanning hundreds to thousands of kilometers.

The light scattering properties of particles, which are heavily influenced by size, have a dual impact on the atmosphere: they reduce visibility and affect Earth's heat balance, contributing to climate forcing [21]. The underlying principles of this dual impact will be explored in the following section.

Second, particle size dictates the region and probability of deposition within the pulmonary system, a critical factor in assessing inhalation health impacts. Particles larger than 10 μm are mainly filtered by the nose and upper respiratory tract, while PM_{10}, $PM_{2.5}$ and UFPM reach the lower respiratory tract. The smaller the particle, the deeper it can deposit in the lower respiratory tract [2, 5, 49].

Particulate matter can be composed of a variety of organic and inorganic elements, the composition of which varies depending on local geographic, temporal, and meteorological conditions [50]. PM composition may include metals, elemental and organic carbon, ammonium, sulphates and nitrates, peroxides, aldehydes, quartz, silicates, sea salt, pollens, as well as other constituents [51]. Primary particulate matter is generated by fuel combustion, wear on road-surfaces, tires and brakes, re-suspended crustal matter and organic matter such as pollen. Secondary PM is formed by photo-chemical reactions of PM in the atmosphere, with the nucleation of pollutant gases such as ammonium nitrate and sulfur dioxide [52].

Particulate matter can generate free radical oxidants in both cellular and acellular experimental systems. Organic compounds induce oxidative stress through the redox cycle of quinone-based radicals, while metals directly support electron transport to form oxidants and also reduce antioxidant levels. Cells respond to oxidative stress that occurs after PM exposure and activate kinase cascades and transcription factors and release inflammatory mediators, eventually leading to cell damage or apoptosis, which in turn leads to morbidity and mortality [53].

It is currently estimated that non-exhaust emissions (NEE) account for up to 90% by mass of total PM emissions from road traffic. NEE are mainly composed of heavy metals, such as Cu, Fe, Pb, and Zn. Particulate matter emissions are most affected by road type and vehicle weight, with vehicle speed having a lesser influence. In the case of electric vehicles, the additional weight

of the batteries results in a significant increase in the amount of resuspended dust, tire and road wear emissions, which together compensate for the lack of emissions due to exhaust pipe and brake wear [54].

Heavy metals are steady in the environment and are subject to bioaccumulation in food-chains. They are released to the environment from a range of anthropogenic and natural sources, such as mining, urbanization, industrial activities, deforestation, soil erosion, combustion of wood or agricultural waste, and land degradation [55]. The large surface area per unit of mass of fine particles allows them to act as a reaction layer for heavy metals, facilitating their binding [56]. This interaction may lead to instability of the heavy metals and increase their biological activity [57, 58], leading to negative consequences to environment compartments and living systems.

1.2. Potentially Toxic Elements Associated with Particulate Matter

Atmospheric particulate matter represents a major pathway for the dispersion of potentially toxic elements (PTEs) [59–61]. The term "potentially toxic elements" refers to a group of metallic and non-metallic elements that may pose risks to ecological systems and human health when exposure exceeds natural background levels. For instance, the presence of PTEs in soil can reduce microbial activity and diversity, which in turn can significantly inhibit the biodegradation of organic contaminants [62]. PTEs are predominantly composed of heavy metals, which are conventionally defined as metallic elements with a density exceeding 5 g/cm^3, alongside specific non-metals such as As and Se (Table 1.1) [59]. A defining characteristic of many PTEs is their environmental persistence and their capacity to induce toxic effects in biota, even at relatively low concentrations [59, 63]. It is crucial to distinguish between non-essential PTEs and those that are biologically essential. Several elements classified as heavy metals serve as essential micronutrients or trace elements, playing vital roles in metabolic processes (Table 1.1). The potential for toxicity in these essential elements is concentration-dependent; they become hazardous only when present in elevated, bioavailable concentrations that exceed homeostatic control mechanisms. Similarly, non-metals like Se are an example of this duality, acting as a functional micronutrient at low doses in plants and humans while exhibiting toxic properties at higher concentrations [64, 65].

Table 1.1. Classification of Potentially Toxic Heavy Metals and Non-Metals According to Biological Role [59].

Biological Function	Heavy Metals	Non-Metals
No physiological function, highly toxic	Cr, Cd, Hg, Pb	As
Essential for biological processes, toxic at high concentrations	Mn, Fe, Co, Ni, Cu, Zn, Mo	Se

Although PTEs enter the atmosphere from natural processes like volcanic activity, dust storms, wildfires, wind erosion, and sea spray, anthropogenic activities represent the dominant source of these contaminants in airborne particles, particularly within industrialized regions where natural contributions are considerably smaller. High-temperature industrial processes are responsible for the majority of anthropogenic trace element emissions. Specifically, the production of primary non-ferrous metals is the dominant source of atmospheric As, Cd, Cu, and Zn, and is a notable contributor of Pb and Se. Within the energy generation sector, the combustion of coal is the primary source of Hg, Mo, and Se release, and also represents a major source for As, Cr, Mn. In contrast, the combustion of oil is identified as the most significant source of anthropogenic V and Ni emissions [14].

These elements can persist in the environment, bioaccumulate within food chains, and exert toxic effects even at relatively low concentrations [11, 15]. Fine particles carry a disproportionately high metal load per unit mass compared to coarser fractions, and their small aerodynamic size allows them to penetrate deep into the alveolar region of the lung [66, 67].

Inhalation represents the most relevant route of heavy metal exposure via PM. Once inhaled, particle-bound metals may be solubilized in the respiratory lining fluid, absorbed across pulmonary epithelial cells, and distributed systemically via the bloodstream and lymphatic system. The bioavailability of metal species from PM depends on multiple physicochemical factors, including the oxidation state of the metal, particle solubility, pH of respiratory fluids, and the presence of complexing ligands. For instance, hexavalent Cr associated with PM exhibits substantially greater solubility and cellular uptake than its trivalent form, making its inhalation particularly hazardous [68, 69]. The table 1.2 reviews the sources, exposure pathways and molecular mechanisms of toxicity of some of the PTEs.

Table 1.2. Sources, exposure pathways, and molecular mechanisms of toxicity of some of the PTEs.

PET	Source	Exposure pathway	Key feature	Mechanisms of toxicity	References
As	• Anthropogenic: metallurgy, glassmaking, semiconductor manufacturing, pesticide production; • Natural: geological processes	• Inhalation; • Ingestion	• As(III) > As(V); • Phosphate mimicry • Zn displacement	• Sulfhydryl groups binding → enzyme inhibition; • ROS↑; • DNA repair↓; • ATP synthesis↓	[13, 70–77]
Cd	• Anthropogenic: fossil fuel combustion, waste incineration, iron and steel production, non-ferrous metal smelting, battery and pigment manufacturing, phosphate fertilizers, cigarette smoking (major personal source).	• Inhalation	• renal accumulation; • metal displacement (Zn^{2+}, Ca^{2+}, Fe, Cu)	• ROS↑ (indirect; Fe/Cu displacement); • Zn/Ca competition; • DNA repair↓; • oncogene↑	[13, 78–82]
Cr	• Anthropogenic: metallurgy, chromate and chrome pigment manufacturing, leather tanning, chrome-plating facilities.	• Inhalation	• Cr(VI) cell entry; • Cr(III) poorly absorbed	• Intracellular reduction of Cr(VI) → ROS↑; • DNA damage (strand breaks, adducts); • mutagenesis	[13, 83–87]
Co	• Natural: geological; • Anthropogenic: fossil fuel burning, sewage sludge, cobalt processing plants, hard-metal industry, diamond polishing; cobalt-chromium orthopedic joint replacements	• Inhalation; • Systemic (implants)	• HIF stabilization (hypoxia mimicry); • Ion mimicry (Ca^{2+})	• mimicking hypoxia and stimulating erythropoietin production; • Ca competition; • DNA damage; • lysosomal dissolution ("Trojan-horse") → Co^{2+} release	[88–90]
Cu	• Natural: environmental; • Anthropogenic: copper pipes, cookware, fungicides	• Ingestion; • Inhalation; • Dermal; • Parenteral	• Redox-active metal	• Cu(I)/Cu(II) cycling → ROS↑; • lipid/DNA damage; • metal displacement; • apoptosis signaling	[91–93]
Fe	• Anthropogenic: iron and steel production, welding, foundries, iron ore mining; underground railways (brake-wheel friction dust); engineered nano-iron oxides (toner manufacturing); medical (blood transfusions, therapeutic iron)	• Inhalation; • Parenteral	• Non-transferrin-bound iron formation	• Fenton chemistry → ROS↑; • mitochondrial dysfunction (ATP↓); • organ damage (liver, heart, endocrine)	[94–97]

Pb	• Natural: geological; • Anthropogenic: mining, battery manufacturing, smelting, electronic waste recycling, deteriorating lead-based paints, aging plumbing systems; historical leaded gasoline	• Inhalation; • Ingestion; • Dermal	• Ion mimicry (Ca^{2+}, Zn^{2+},Fe^{2+})	• mitochondrial dysfunction (ATP↓); • ROS↑; • enzyme inhibition; • endoplasmic reticulum stress; • epigenetic changes	[13, 98–104]
Mn	• Natural: geological; • Anthropogenic: mining, steel production, fireworks, dry-cell batteries, fertilizers, paints, ceramics, cosmetics, gasoline additive, fungicides	• Ingestion; • Inhalation; • Parenteral	• Basal ganglia accumulation (manganism); • Transport across brain barriers via DMT-1, ZIP8, ZIP14, transferrin, and calcium channels.	• ROS↑; • mitochondrial dysfunction; • endoplasmic reticulum stress; • apoptosis;	[105–108]
Hg	• Natural: geological; • Anthropogenic: approximately 2320 megagrams/year from mining (37.5%), stationary industrial and power plants (19%), cement production (10.5%), non-ferrous metal production (10.3%), gold production (3.8%); coal combustion, waste incineration	• Inhalation; • Ingestion; • Dermal	• Methylmercury biomagnification; • Affinity for S, Se, P ligands	• ROS↑; • mitochondrial dysfunction; • Ca/glutamate disruption; • protein denaturation; • lipid peroxidation; • DNA damage; • neurotoxicity	[13, 14, 109]
Ni	• Natural: volcanic activity, windblown dust, weathering of rocks (24th most abundant element); • Anthropogenic: mining, smelting, fossil fuel combustion, electroplating, stainless steel production, nickel-cadmium battery manufacturing	• Inhalation; • Ingestion; • Dermal	• Epigenetic carcinogen • replacement of Fe in non-heme iron dioxygenases	• ROS↑; • histone/DNA modification; • DNA repair↓; • apoptosis (mitochondrial/death receptor)	[110–112]

Zn	• Natural: essential trace element in soil; • Anthropogenic: dietary sources (seafood, meat, legumes, nuts, whole grains); excessive supplementation; denture adhesive creams (up to 34 mg/g Zn); occupational (welding, smelting).	• Inhalation; • Ingestion; • Dermal	• Induces Cu deficiency	• Metallothionein↑ → Cu depletion; • ROS↑; • mitochondrial dysfunction; • immune suppression; • apoptosis • neurotoxicity	[113, 114]
ROS↑ = increased reactive oxygen species **DNA repair↓** = impaired DNA repair **ATP↓** = reduced ATP production					

Arsenic occurs in both particulate and gaseous atmospheric forms, with concentrations ranging from 1 to 3 ng/m^3 in remote areas, to 20–100 ng/m^3 in urban environments, and substantially higher levels in occupational settings [13]. It is predominantly associated with $PM_{2.5}$ as inorganic As(III) and As(V), with speciation governed by environmental redox conditions [70]. The more toxic As(III) dominates under reducing conditions. Methylated arsenic species, including monomethylarsonic and dimethylarsinic, are also present and undergo rapid photochemical degradation, with half-lives of hours under UV light versus days to weeks in darkness [73, 74]. Trimethylarsine is the most abundant methylated species (66–69%) and is stable in PM_{10} [70]. Inhalation is a minor exposure pathway versus ingestion for the general population, but arsenic in PM is a Group 1 carcinogen linked to lung, bladder, kidney, skin, liver, and prostate cancers, posing significant risks near emission sources [13, 75].

The solubility of inhaled arsenic-bearing PM is a principal determinant of its pulmonary toxicokinetics and subsequent health effects. Upon deposition in the respiratory tract, soluble arsenic compounds rapidly dissolve in epithelial lining fluid, generating a short-term but high local concentration that is available for direct cellular uptake. This bioavailable fraction is then quickly absorbed into the systemic circulation, contributing to the total body burden of arsenic. In contrast, poorly soluble arsenic compounds initiate a cascade of cellular defense mechanisms. They are targeted for clearance by alveolar macrophages, a process that, while protective, can lead to their prolonged retention, either within the alveolar lumen or following translocation to interstitial lymph nodes. This retention creates a depot of persistent, low-level arsenic exposure of pulmonary tissue. This sustained, localized exposure is a key mechanistic driver in the pathogenesis of arsenic-induced lung disease, most notably in the development of lung carcinoma [75].

The molecular mechanisms underlying arsenic toxicity are complex and multifactorial. A primary mechanism involves the high affinity of trivalent arsenite for sulfhydryl groups found in

the cysteine residues of proteins [76, 77]. This binding can alter a protein's structure and inhibit its function, leading to the disruption of critical biological processes. Arsenic may inactivate up to 200 enzymes [77]. These include enzymes essential for energy production (such as pyruvate dehydrogenase), the cellular antioxidant defense system (like thioredoxin) and DNA repair mechanisms (zinc finger proteins). For instance, the xeroderma pigmentosum group A protein contains a zinc finger domain where zinc is complexed by four cysteine residues; trivalent arsenicals, particularly the methylated one, can bind to these cysteines and displace the essential zinc, thereby compromising nucleotide excision repair [77]. The pentavalent arsenic toxicity arises primarily through molecular mimicry of phosphate. Arsenate competitively replaces phosphate in biochemical reactions by forming unstable arsenate esters, potentially interfering with ATP generation and phosphate-dependent signaling pathways [77].

Cadmium is a persistent environmental contaminant with a biological half-life of 10–30 years, leading to progressive accumulation, particularly in renal tissue [80]. Airborne Cd exhibits considerable atmospheric persistence and can undergo long-range transport before deposition. Inhalation exposure, constitutes a significant environmental pathway for populations near industrial sources [80, 81]. On a personal level, another major source is cigarette smoking, where tobacco plants take up Cd from contaminated soils [79, 80]. Chronic inhalation of Cd particulates causes characteristic lung damage, manifested as emphysematous changes, decreased lung function, and radiographic abnormalities [13]. Occupationally exposed workers demonstrate olfactory impairment, reflecting upper respiratory tract damage [81]. Chronic exposure is strongly associated with proximal tubular dysfunction, nephropathy, decreased bone mineral density, and osteoporosis, the latter attributable to Cd interference with calcium and phosphate metabolism [80, 82]. Cardiovascular and reproductive effects have been documented, including associations with reduced birth weight [80]. The lung represents the primary site of Cd carcinogenesis; consistent epidemiological evidence demonstrates elevated lung cancer risk among exposed workers, corroborated by rodent studies showing pulmonary adenocarcinomas following chronic inhalation [13, 80]. Accordingly, the International Agency for Research on Cancer classifies Cd as a Group 1 human carcinogen [78]. Associations with prostate, kidney, liver, and hematopoietic cancers have also been reported [13].

The molecular toxicology of Cd involves convergent mechanisms. Although Cd does not participate directly in Fenton-type redox reactions, it potently induces oxidative stress. It displaces redox-active metals like Fe and Cu from proteins such as ferritin; these free ions then generate reactive oxygen species (ROS) via Fenton chemistry. This oxidative challenge is made worse by the depletion of cellular antioxidants, particularly glutathione and selenium, the latter being

essential for the antioxidant enzyme glutathione peroxidase [80]. Cadmium interferes with essential metal homeostasis, competing with Zn and Ca for protein-binding sites and displacing these elements from metalloenzymes. At low concentrations, it activates signal transduction pathways through inositol polyphosphate formation, elevates cytosolic calcium, and blocks Ca channels, collectively perturbing cell signaling [82]. Cadmium upregulates proto-oncogenes (c-fos, c-jun, c-myc), stimulates stress-response proteins (metallothioneins, heme oxygenases, heat-shock proteins, glutathione S-transferases), and decreases DNA repair capacity by reducing nucleotide excision repair activity. These combined effects, oxidative damage, impaired DNA repair, and altered gene expression, underlie cadmium's carcinogenic potential [80].

Chromium's hexavalent form [Cr(VI)], which predominates in industrial aerosols and PM released from high-temperature processes, is the toxicologically critical species, as it is classified as a human carcinogen. The health effects of Cr depend critically on its oxidation state. Inhalation of Cr(VI)-containing PM is the primary cause of occupationally related respiratory cancers [84]. Hexavalent Cr exposure is also responsible for occupational asthma and allergic contact dermatitis, the latter being particularly prevalent among construction workers exposed to chromate in cement [85]. Systemic absorption following inhalation leads to multi-organ toxicity including cardiovascular, gastrointestinal, hematological, hepatic, and neurological consequences [13, 83].The toxicological distinction between Cr(VI) and Cr(III) reflects their contrasting cellular pharmacokinetics. Cr(VI), being an oxyanion, is transported into cells through anion channels (mimicking sulfate and phosphate), whereas Cr(III) is poorly absorbed across cell membranes [83]. Once inside the cell, Cr(VI) undergoes stepwise intracellular reduction, generating reactive free radicals that attack DNA, proteins, and membrane lipids, disrupting cellular integrity and function [83, 86]. This intracellular reduction of Cr(VI) is considered the key activating step in Cr genotoxicity, as the resulting Cr(III)-DNA adducts and oxidative DNA lesions, including chromosomal aberrations, DNA strand breaks, and DNA fragmentation, are responsible for the mutagenic and carcinogenic effects [83, 87]. The solubility of inhaled Cr(VI) particles is an important modifier of carcinogenic risk, less soluble Cr(VI) compounds are retained longer in the lung and are considered more potent carcinogens [13, 84].

Cobalt is a transition metal naturally present in the earth's crust that exists in multiple oxidation states, with Co(II) ion being the most biologically relevant form. It serves as an essential micronutrient as a component of vitamin B_{12}, though inorganic cobalt deficiency has never been described in humans [88]. In human cells, cobalt uptake occurs through shared transport pathways with Ca, with the uptake being essentially irreversible as cobalt binds effectively in the cytosol. It also competes with Ca for binding proteins, inhibits calcium signaling, and displaces divalent

cations from metalloenzymes [88]. In lung epithelial cells, cobalt oxide particles are internalized via clathrin-dependent endocytosis and accumulate within lysosomes. The acidic lysosomal environment (pH 4.5) promotes partial solubilization, leading to the intracellular release of Co(II) ions through a "Trojan-horse" mechanism [90].

Cobalt toxicity operates through multiple molecular pathways. The primary mechanism involves stabilization of hypoxia-inducible factor by inhibiting oxygen-dependent hydroxylases, mimicking hypoxia and stimulating erythropoietin production [88]. This activates numerous genes including angiogenic factors and glycolytic enzymes, some with carcinogenic potential. The genotoxic effects include DNA damage and inhibition of DNA repair mechanisms, leading to chromosomal aberrations [89]. Remarkably, studies demonstrate that the minute intracellular solubilized Co fraction (as low as 0.07% of total cellular cobalt) is responsible for the overall toxicity, not the particulate form itself [90].

Copper is an essential trace element found naturally in soil, water, and air, with concentrations of approximately 50 ppm in soil and 4-10 μg/L in natural water [91]. Human exposure occurs through multiple pathways, including dietary intake (1-5 mg daily from foods like liver, crustaceans, nuts, and beans), drinking water (contributing 6-13% of daily intake), and environmental sources such as copper pipes, cookware, and fungicides [92]. Copper-based pesticides, including copper sulfate, copper oxychloride, and Bordeaux mixture, are extensively used in agriculture [93].

At the molecular level, copper toxicity primarily involves redox cycling between cuprous Cu(I) and cupric Cu(II) ions, generating reactive oxygen species through Fenton and Haber-Weiss reactions [91]. This process produces highly destructive hydroxyl radicals that initiate lipid peroxidation, protein modification, and DNA strand breaks. Copper binds readily to DNA, forming adducts that promote local hydroxyl radical production and oxidative damage [93]. Excess copper also displaces other metals from metalloproteins, disrupting enzymatic functions and protein conformations [92]. Cellular copper homeostasis is tightly regulated by transporters (CTR1, ATP7A, ATP7B) and chaperones (CCS, Atox1, Cox17). Disruption of this homeostasis leads to toxicity through several mechanisms: altered lipid metabolism with downregulation of cholesterol synthesis; activation of acidic sphingomyelinase and ceramide release triggering hepatocyte apoptosis; alpha-synuclein aggregation in neurons; and impaired copper distribution in hepatocytes [91].

Iron toxicity is primarily mediated by the formation of reactive oxygen species (ROS) through Fenton chemistry. Inhaled iron-containing particles deposit in the lungs, where they may be cleared by alveolar macrophages or retained in tissue, contributing to localized exposure [94].

When Fe exceeds the binding capacity of transferrin, non-transferrin-bound iron appears in plasma. A redox-active component, labile plasma iron, can enter cells and catalyze hydroxyl radical formation. Intracellularly, Fe catalyzes reactions producing ROS that damage lipids, proteins, and DNA [95, 96]. This oxidative stress particularly affects mitochondria, impairing respiratory chain function [95]. Target organs particularly susceptible to iron toxicity include liver (fibrosis, cirrhosis, hepatocellular carcinoma), heart (cardiomyopathy, arrhythmias), pancreas (diabetes), and endocrine glands (hypogonadism) [95].

Lead is a non-essential, toxic heavy metal with no known biological function. Humans are primarily exposed through inhalation of polluted air and dust particles, ingestion of contaminated water or food, and to a lesser extent through dermal absorption [98]. The respiratory tract absorbs lead particles at approximately 69% efficiency, while gastrointestinal absorption ranges from 10-15% in adults and up to 50% in children, who are particularly vulnerable due to higher absorption rates and ongoing neurodevelopment [98, 103].

Lead toxicity operates primarily through ion mimicry, wherein Pb(II) imitates essential divalent cations such as Ca(II), Zn(II), and Fe(II), competing with or displacing them at critical binding sites in proteins and enzymes [13, 98]. This disrupts normal cellular function, as Pb(II) cannot fulfill their physiological roles. Mitochondria represent primary targets, with Pb accumulating in the mitochondrial matrix, reducing respiratory chain enzyme activities (especially complexes II and III), and decreasing ATP synthesis [98]. Lead exposure also induces oxidative stress through reactive oxygen species (ROS) generation and antioxidant depletion, including glutathione and enzymes like superoxide dismutase and catalase [103, 104]. Additional mechanisms include endoplasmic reticulum stress through unfolded protein response activation, interference with neurotransmitter systems, DNA damage through oxidative stress and repair inhibition, and epigenetic modifications including altered DNA methylation and histone modifications [98]. These multifaceted molecular disruptions explain Pb systemic toxicity affecting nervous, cardiovascular, renal, and reproductive systems.

Manganese is the twelfth most abundant element in the earth's crust, with global reserves approximating 570 million tons [105]. Diet is the main source of human Mn intake. The highest levels are found in cereals, rice, tea leaves, nuts, and legumes [106]. Average daily intake ranges from 2.3-8.8 mg, though only 1-5% is absorbed gastrointestinaly [105]. Inhalation poses greatest occupational risk for miners, welders, and smelters, as Mn enters the body through the olfactory tract and travels directly to the brain, avoiding biliary excretion [107]. Vulnerable populations include infants (poorly developed biliary systems), individuals with liver dysfunction, those

receiving total parenteral nutrition, and people with SLC30A10 gene mutations causing hypermanganesemia [107].

Mn preferentially accumulates in basal ganglia, particularly globus pallidus and substantia nigra, inducing manganism, a Parkinsonian-like syndrome [108]. Transport across brain barriers involves transferrin, calcium channels, solute carriers, including DMT-1, ZIP8 and ZIP14, while efflux occurs via ferroportin, SLC30A10, and ATP13A2 [107]. Mechanistically, Mn generates oxidative stress through redox cycling between Mn(II) and Mn(III), disrupts mitochondrial complex II, triggers endoplasmic reticulum stress, and activates apoptotic pathways [108].

Mercury is a globally distributed pollutant. Mining operations are responsible for approximately 37.5% of air Hg emissions [109]. Stationary industrial and power plants burning fossil fuels contribute 19%, followed by cement production (10.5%), non-ferrous metal production (10.3%), and large-scale gold production (3.8%) [109]. Unlike many other heavy metals, mercury can exist in elemental gaseous form, allowing long-range atmospheric transport before deposition. The biogeochemical cycle of Hg involves complex transformations between elemental Hg, inorganic mercury Hg(II), and organic methylmercury (MeHg), one of the most toxic environmental contaminants [14, 109]. In aquatic systems, anaerobic bacteria convert inorganic mercury to methylmercury, which bioaccumulates in organisms and biomagnifies through food chains, reaching highest concentrations in predatory fish [109]. Humans are primarily exposed through consumption of contaminated seafood. Mercury primarily affects the central nervous system and can also damage the kidneys, immune system, and cardiovascular system [13].

At the molecular level, Hg toxicity is largely related to its high affinity for sulfhydryl groups in proteins and enzymes. Mercury strongly attracts ligands containing sulfur, selenium, and phosphorus [109]. This interaction disrupts protein structure and enzyme function by binding to thiol-containing amino acids. Mercury compounds induce oxidative stress through generation of reactive oxygen species, cause mitochondrial dysfunction, and disrupt Ca and glutamate homeostasis [109]. These mechanisms lead to protein denaturation, lipid peroxidation, DNA damage, and impaired cellular antioxidant defenses, ultimately resulting in neurodegeneration and organ damage [13].

Nickel toxicity involve multiple pathways. Ni(II) enter cells through phagocytosis of insoluble particles or via Ca channels for soluble forms [110]. Once intracellular, nickel induces oxidative stress by generating reactive oxygen species (ROS) through Fenton-like reactions, depleting antioxidants like glutathione, and causing lipid peroxidation, protein damage, and DNA oxidation [111]. Nickel exhibits carcinogenic properties primarily through epigenetic mechanisms rather than direct DNA mutagenesis. Ni(II) can replace Fe in non-heme iron dioxygenases,

inhibiting histone demethylases (JMJD1A) and DNA repair enzymes (ABH2), leading to histone hypermethylation, chromatin condensation, and tumor suppressor gene silencing [112]. Nickel also triggers apoptosis through both intrinsic (mitochondrial) and extrinsic (death receptor) pathways, involving cytochrome c release, caspase activation, and PARP cleavage [112].

Zinc is an essential trace element obtained primarily through dietary sources. Seafood and meat products are rich in zinc with high bioavailability, while plant-based foods like legumes, nuts, and whole grains contain zinc but also phytate, which inhibits absorption by forming non-absorbable complexes [113]. Exposure pathways include oral intake, inhalation, and dermal contact. Oral exposure through diet rarely causes toxicity, but excessive supplementation or denture adhesive creams (containing up to 34 mg/g of Zn) can exceed the tolerable upper intake level (25 mg/day by EFSA or 40 mg/day by FDA) [113]. Inhalation exposure primarily affects workers in welding or smelting industries, causing metal fume fever, and can lead to acute respiratory distress syndrome at high concentrations [113]. Dermal exposure from zinc oxide in sunscreens or wound treatments presents minimal toxicological risk [114].

Molecular mechanisms of toxicity involve several pathways. Zinc-induced Cu deficiency occurs when elevated Zn upregulates metallothionein in enterocytes, which binds Cu with higher affinity than Zn, leading to Cu excretion and subsequent anemia, neutropenia, and neurological symptoms [113]. In neurons, excessive Zn influx causes oxidative stress, mitochondrial dysfunction, and activation of apoptotic pathways including p75NTR and caspase activation [114]. Zinc also suppresses immune function by inhibiting T and B cell responses at concentrations above 100 μM and can induce pro-inflammatory cytokine production from monocytes [113]. At the cellular level, Zn accumulation causes dissipation of mitochondrial membrane potential, cytochrome c release, and both apoptotic and necrotic cell death [114].

Overall, the diversity of sources, exposure pathways, and toxicity mechanisms of PTEs associated with particulate matter underscores the complexity of their environmental behavior and biological effects. This complexity highlights the need for integrative monitoring approaches capable of capturing cumulative deposition patterns, supporting the application of biomonitoring methods such as moss-based assessment in air quality studies.

1.3. Factors Influencing the Spatial Distribution of Pollutant Emissions into the Atmosphere

The spatial distribution of pollutant emissions depends on many factors, such as the emission source, the concentration, composition, physical and chemical properties, and state of aggregation of the released substances, as well as the location of the emission source, topographic

characteristics, the state of the atmosphere, air pressure, humidity, weather conditions, temperature, time of year, amount of precipitation, air flows, etc [21, 22, 115].

Atmospheric transport processes are fundamentally governed by vertical motion mechanisms, primarily convection and temperature inversion layers. Convection occurs when the Earth's surface is heated by solar radiation, causing the overlying air to warm, become less dense, and rise [116]. This vertical uplift carries pollutants from near-surface sources to higher altitudes, where stronger wind fields can facilitate long-range transport [115, 117–122]. The intensity of convective mixing is directly proportional to the temperature gradient between the surface and the upper air. During daytime hours under clear skies, convection can disperse pollutants vertically, reducing ground-level concentrations but potentially exporting them to regional scales [117]. c

Conversely, temperature inversion layers represent a critical constraint on pollutant dispersion. An inversion occurs when a warm air layer overlies cooler air near the surface, suppressing vertical motion. The formation of a strong, persistent temperature inversion acts as a formidable cap on vertical motion. Radiation inversions, which form on calm, clear nights due to rapid surface cooling, are particularly common in valleys and basins. Under such conditions, emissions from vehicles, industrial stacks, and residential heating accumulate near ground level, leading to severe pollution episodes [117, 123]. In complex basin terrain like the Sichuan Basin, these stable layers ensure that pollution is dominated by local emissions rather than long-range transport. Feng et al. [123] found that inversions occur frequently at two distinct heights: within the boundary layer below 600 m and as a unique Lower-Troposphere Inversion layer between 2200 and 3500 m. The combination of these persistent caps, occurring on >90% of winter days, effectively seals the basin, trapping locally generated pollutants from the underlying urban agglomerations and resulting in a high probability of severe air quality degradation. Lorint et al. [9] also describe how mountain ranges typically block air mass movement, and the shelter they provide inhibits the ventilation of depressions, with thermal inversion during winter promoting formation of an inverse temperature layer that complicates pollutant dispersion.

The influence of meteorological parameters, such as temperature, precipitation, and humidity, on pollutant distribution is multifaceted. Higher temperatures accelerate photochemical reaction rates, promoting the formation of secondary pollutants such as tropospheric ozone and secondary organic aerosols. On a hot day, elevated temperatures shift the equilibrium toward the gas phase, reducing particulate nitrate but potentially increasing the formation of secondary organic aerosol through enhanced biogenic hydrocarbon emissions. Conversely, a cold night can drive these gases back into the particle phase, leading to morning peaks in fine particulate matter.

This temperature-dependent partitioning creates a diurnal cycle for many aerosol components that is independent of emissions, and is a fundamental characteristic of photochemical smog [21].

Aerosol removal from the atmosphere is dominated by wet scavenging, specifically rainout and washout. Rainout occurs when a particle acts as a cloud condensation nucleus, forming a cloud droplet that eventually coagulates into falling precipitation like rain or graupel. This process is exclusive to the troposphere, making it particularly effective for removing volcanic emissions but irrelevant for stratospheric particles. Washout differs slightly; it involves falling precipitation physically capturing interstitial particles or those suspended in clear air below cloud base. When precipitation is absent, sedimentation and dry deposition take over. Sedimentation is the gradual gravitational settling of particles; while effective for coarse dust over short distances, particles smaller than 0.5 μm may require several years to descend just one kilometer. Finally, dry deposition transfers particles directly to surfaces via turbulence and molecular diffusion. While more efficient than sedimentation for near-surface small particles over short periods, it is far less significant globally than precipitation scavenging. Gases, being far lighter and often chemically inert, are removed much more slowly by these physical processes than PM [117].

When the air is humid but not quite saturated, pollution particles soak up moisture and expand. Once their diameters approach the wavelength of visible light, they scatter all colors equally, creating a characteristic whitish haze. This water-induced haze is frequently observed in sunlit urban areas where pollution particles are abundant [117].

Low ground temperatures reduce vertical mixing and wind speed. Conversely, warmer surfaces enhance convection and increase near-surface wind speeds. While faster near-surface winds promote the dispersion of near-surface pollutants, they may simultaneously elevate the resuspension of loose soil dust and other PM from the ground. Higher temperatures lead to increased water vapor, which may raise relative humidity in some regions but lower it in others. An increase in relative humidity boosts the uptake of liquid water by aerosol particles, thereby expanding the surface area for gas condensation and the volume for gas dissolution. Consequently, global warming can increase PM where relative humidity rises, and decrease it where relative humidity falls. Additionally, higher temperatures may directly lower particulate matter by volatilizing certain organic and inorganic aerosol constituents [117].

Mountain barriers, valleys, and altitude gradients fundamentally shape atmospheric pollution transport by redirecting airflow and altering the thermodynamic state of airmasses. Tall mountain ranges act as formidable obstacles to the movement of airmasses within the lower troposphere, effectively blocking or channeling airflow. When a polluted airmass encounters such relief, it is forced to ascend along the windward slopes. This orographic lifting induces adiabatic

cooling, leading to condensation, cloud formation, and precipitation. This process not only generates heavy rainfall and potential flooding on the windward slopes but also effectively scavenges pollutants from the atmosphere. While this wet deposition cleanses the airmass aloft, it simultaneously delivers a concentrated load of pollutants to sensitive mountain ecosystems. As the air descends on the leeward side, it undergoes drying and warming due to latent heating, often creating rain shadows where pollution accumulation can differ markedly from the windward side [115, 124].

However, the interaction of atmospheric flow with complex topography extends beyond simple uplift. When a stable air mass lacks the kinetic energy to overcome an obstacle, it undergoes flow splitting. This dynamic causes air to accelerate as it passes through mountain passes and canyons. These gaps act as funnels, and flow channeling can transport urban pollutants deep into rural or pristine mountain valleys. Furthermore, the terrain itself generates thermally driven circulations, such as slope and valley winds, which are a key mechanism for mass exchange between the valley floor and the free atmosphere aloft, often enhancing vertical export of pollutants beyond what is observed over flat terrain. Lehner and Rotach [124] identify slope winds as providing a particularly effective mechanism of transport from valley floor to mountain peaks, with vertical mass flux over a valley up to eight times larger than over a plain, as shown by idealized simulations.

Low pressure systems create wet and windy conditions. A passing storm can wash pollutants out of the atmosphere or transport them to a new location. However, it is important to note that the contaminants do not actually disappear, but are transferred to a new location. In high-pressure systems, air stops moving, causing pollutants such as vehicles and factory exhaust to concentrate in a specific area. Air pollution is often diurnal; the highest values in urban areas typically occur during daytime (e.g., photochemical reactions are required to form ozone) and during rush hour due to traffic[125].

The characteristics of the pollutants themselves influence the range of emissions. For example, larger and heavier particles settle close to the source, while lighter ones are transported over longer distances. Some metals, such as Hg and Se, can be transported over long distances in air masses in the gas phase. Relatively volatile heavy metals can easily attach to air-borne particles that ensure their widely dispersion throughout the atmosphere, often being deposited far away from the site of primary release [55]. The information in Table 1.3 includes data on the scale of disturbances in biogeochemical cycles and health concern.

Table 1.3. Trace Metal Perturbations: Spatial Scale and Health Implications [14].

Metal	Scale of perturbation			Health concern
	Local (< 100 km)	Regional (100–1000 km)	Global (1000 km >)	
Antimony (Sb)	+	+	-	+
Arsenic (As)	+	+	-	+[b]
Cadmium (Cd)	+	+	-	+
Chromium (Cr)	+	+*	-	+[c]
Copper (Cu)	+	+	-	E
Lead (Pb)	+	+	+	+
Manganese (Mn)	+	+*	-	E
Mercury (Hg)	+	+	+	+[a]
Molybdenum (Mo)	+	+	-	E
Nickel (Ni)	+	+	-	E
Selenium (Se)	+	+	+	E
Tin (Sn)	+	+	+	+[a]
Vanadium (V)	+	+*	-	+
Zinc (Zn)	+	+	-	E

Geochemical Cycle Perturbations:
+: Significant disturbances
–: No significant disturbances
*: Effect enhanced by mobilization of Earth's crust materials

Human Health Concern:
+: Toxic in excess
E: Essential element for health
Note a: Only organometallic forms are toxic.
Note b: Trivalent (III) forms are toxic; pentavalent (V) forms are essential.
Note c: Hexavalent (VI) forms are toxic; trivalent (III) forms are essential.

Air pollution is largely influenced by climate conditions. During extreme heat, ozone and particulate pollution increase. It also directly contributes to global warming, which in turn leads not only to climate change, but also to an increase in the frequency of extreme weather events and natural disasters such as floods, earthquakes, volcanic eruptions, snowstorms, hurricanes or tornadoes [125].

Mineral dust, containing large variety of heavy metals is an important component of aerosol due to its impact on climate. It affects local and global climate by absorbing and scattering solar radiation. Dust particles can mix with highly hygroscopic water-soluble aerosols through heterogeneous reactions with acid gases and turn into coated dust particles. As a result, the size and morphology of dust particles will be changed, and therefore the optical properties and direct climatic effects will be different. Heterogeneous reactions in dust and their consequences are not yet fully studied. Due to higher hygroscopicity, coated dust can become more efficient cloud condensation nuclei, or ice nuclei (IN), compared to pure dust particles, changing the indirect climate impact of dust aerosols [126–128].

Dust aerosols, which originate from various deserts and semi-desert areas around the world, have been shown to serve as effective IN and potentially enhance precipitation in mixed-phase

clouds. A mixed-phase cloud in comparison with liquid-only cloud initiates precipitation more quickly, due to the higher growth rate of ice particles compared to droplets. IN are atmospheric particles that catalyze the freezing of supercooled cloud droplets, producing ice crystals that would not form otherwise at warmer, mixed-phase cloud temperatures. The presence, absence, and abundance of IN can thus affect the intensity and spatial distribution of precipitation events. Some types of biological aerosols, such as bacteria, have also been shown to be effective IN at relatively high temperatures; however, recent modeling studies have concluded that they are of minor importance for global IN concentrations and precipitation processes [129, 130].

Intercontinental transport of dust from Asia and Africa is well known. Due to rapid economic development, East Asia countries experience severe transboundary air pollution. Almost 50% of the yellow dust in South Korea comes directly from the Gobi Desert [131, 132]. These dust storms mainly occur during the winter and spring seasons. They path through economic regions of China, where incidents of extreme air pollution occur quite often, so they also pick up pollutants. Anthropogenic emissions of NO_x at low temperatures and high relative humidity (which explains the seasonal nature of this factor) lead to the deposition of large quantities of N in the form of HNO_3 and nitrates and have strong impacts on ecosystems [131, 133].

Dust particles can be transported over thousands of kilometers, significantly impacting remote environments. Recent investigations indicate that Sahara dust can influence cloud formation and precipitation in the Western United States [129] and also contributes to the fertilization of the Amazon rainforest [134]. In Asia, dust activity follows seasonal patterns: the Taklamakan Desert can loft material as early as February, reaching maximum concentrations between April and May [135, 136]. Although largely frozen in winter, the Gobi Desert becomes a significant source of Asian dust during severe storms from Siberia. In contrast, the Sahara's year-round emissions make it a persistent source with the potential to affect ice formation in clouds throughout the year [129]. During dust storms, it has been observed that the topographic relief greatly changes the horizontal flow of dust relative to different heights. This is caused by wind blowing sand and dust from nearby natural dunes [137].

A significant source of dust emission stems from the disturbance of semi-arid loess soils, which are particularly vulnerable to wind erosion. This vulnerability is acutely realized in agricultural fields subject to intensive practices such as post-harvest grazing or mechanical cultivation. These activities strip the land of protective vegetation and break up the soil structure, which exposes the fine particles, making them vulnerable to wind and leading directly to increased airborne particulate matter [138].

1.4. Monitoring Necessity and the Concept of Biomonitoring

To assess air quality, it is necessary to carry out a complex analysis of aerosol particles to determine the concentrations of those pollutants that pose a threat to living organisms. Information about air pollution can be obtained in two ways: by directly measuring the concentrations of pollutants emitted by sources, or by analyzing the variability in pollutant deposition across different locations. However, neither of these two methods should be considered sufficient. Direct measurements of pollutants require expensive equipment. On the one hand, the second method makes it possible to confirm dispersion models, as well as the ability to detect the presence of unknown sources. This is where traditional atmospheric deposition monitoring plays a crucial role. This methodology, primarily conducted via wet, dry or bulk samplers, provides the fundamental long-term data on the elemental and ionic composition of precipitation and particulates necessary for such analyses [8, 139]. The standard approach involves collecting depositing material into a collector, typically on a weekly or monthly basis, followed by laboratory analysis. While this yields essential baseline information for environmental assessment and model validation, the technique itself is constrained by significant limitations. These include high operational costs, the requirement for consistent technical maintenance, low temporal resolution, low-frequency sampling that obscures episodic events, potential sample contamination or evaporation, introducing analytical uncertainty. These factors collectively restrict spatial deployment density. To address the limitations of traditional deposition monitoring, biomonitoring has been established as a robust and complementary methodology. Its core strength lies in enabling cost-effective, large-scale spatial surveys, providing high-resolution data on contamination patterns across extensive geographical areas [8, 140].

The term biomonitoring refers to obtaining information about certain characteristics of the biosphere by means of biological organisms [141]. Organisms that are used in this process are called biomonitors or bioindicators, there is a difference between these two terms. The term bioindicator refers to a living organism that serves to qualitatively describe the state of the environment by showing visible symptoms; biomonitors, on the other hand, provide quantitative information about quality of the environment. They are in general less sensitive to pollution, and accumulate pollutants onto and into their tissues [141].

The main advantage of biomonitoring is that sampling process is simple and do not require expensive tools. An effective organism for air pollution biomonitoring must meet several key criteria [142]:

- Widespread: commonly found throughout the study area.
- Air-Focused Uptake: primarily absorb elements from the atmosphere, not the soil.

- Pollution Tolerant: able to survive in highly polluted environments.
- Low Background Levels: naturally low content of the target elements.
- Responsive: show measurable changes in response to varying pollution levels.
- Easily Analyzed: enable accurate, quick, and simple measurement with chosen analytical technique.

A biomonitor that meets the relevant requirements provides an opportunity to conduct retrospective monitoring of air pollution with small financial costs. The use of such non-mobile monitors is particularly effective when the purpose of the study is to determine the temporal trends of concentrations of heavy and trace elements in a specific area [143–146].

The earliest applications of lichens and mosses as biomonitors of atmospheric pollution are documented in Scandinavia [147–149]. This region pioneered large-scale investigations into atmospheric deposition to assess the ecological impacts of heavy metal contamination.

The feasibility of mosses in determining the concentrations of heavy and trace elements in different geographical areas has been studied and demonstrated in many studies [145, 150–159]. Moss biomonitoring as a method to study heavy metals atmospheric precipitation was used initially on a national and multinational scale since 1960 [147, 148, 160]. Numerous projects have since been carried out with mosses; the method has been developed systematically and also used in large-scale European studies [161–163].

The International Cooperative Program on Effects of Air Pollution on Natural Vegetation and Crops (ICP Vegetation) was established in 1990 and operates under the Working Group on Effects (WGE) of the UNECE Convention on LRTAP, covers most European countries. Twenty-one European countries contributed to the first campaign of the project [164]. Since 2001, the European biomonitoring program has been coordinated by ICP Vegetation. One of the key activities of this program is conducting moss surveys every 5 years since 1990 to assess spatio-temporal changes in air quality [47]. The majority of the studies using mosses as biomonitors are carried out within the framework of this program. The results of these surveys contribute to a broader understanding of air pollution distribution and its effects on ecosystems across Europe and beyond. In 2005, determination of the nitrogen concentration in mosses was included in the program. The results of these studies [165, 166] provide cumulative insights into the use of moss as a nitrogen monitoring method. Since 2010, some countries also determined the concentration of selected persistent organic pollutants (POPs) and particularly polycyclic aromatic hydrocarbons (PAHs). A general trend of decreasing contamination from 2010 to 2015 for the POPs was observed in Norwegian Moss survey [167]. The complementarity of air pollution modeling and

moss biomonitoring was confirmed in several studies [168, 169]. Preliminary results indicate that mosses are effective for biomonitoring of airborne microplastics [170, 171].

The moss biomonitoring technique is widely used in European countries, mostly to identify the most polluted areas and characterize different pollution sources [172–174]. After adjusting for moss biomonitor species and geographic locations, results from several moss surveys are compared to see the dynamics of the distribution of potentially toxic elements [175, 176].

The first moss survey in Georgia and the Republic of Moldova, conducted between 2014 and 2017, laid the groundwork for ongoing efforts to monitor and understand the impacts of air pollution on countries environment and population [177–180]. According to moss Survey 2015-2016 report in both countries' elements concentration was higher comparable with other countries participating in the program [47].

1.5. Mosses, their Distribution and Ecology

Bryophytes are very specific to certain microhabitats; during their evolution, they have greatly diversified ecologically. The largest class of mosses – Bryopsida, consists of at least 10,000 species which is approximately 95% of all moss species. To simplify, Bryopsida can be divided into two main types:

- In Acrocarpous mosses, the main stem is almost always erect, and reproductive organs develop at its tips. They are mainly found on terrestrial substrates, rocks and soil.
- In Pleurocarpous mosses, the main stem is usually creeping, it is highly branched and reproductive organs develop laterally. In the tropics Pleurocarpous mosses are often epiphytic.

Three main organs of a moss gametophore are stem, leaves and rhizoids. The stem can be branched (usually lateral and never dichotomous) or unbranched, and erect or prostrate, depending on a species. The great majority of Bryophytes are ectohydric (without internal conducting tissues). They absorb water and nutrients over the whole surface of the gametophyte. Water moves through externally, in capillary spaces around the bases of the leaves. The main photosynthetic organs of the gametophore are leaves. The leaves are spirally arranged on the stem. Their basal part is usually broad. In most of the species each leaf has a midrib, the exception is e.g., *Sphagnum*. Leaf shape varies greatly between species. They are normally one cell thick with a thin, poorly developed cuticle.

Rhizoids are multicellular, well-branched and septate, brown or dark brown in color. Rhizoids are not major sites of water and nutrient uptake, but can enhance capillary movement of water along the outer surface of the stem [181]. The septa in moss rhizoids are oblique. They keep the plants attached to the substratum. They function primarily as anchoring structures [182].

Mosses are particularly dependent on such an environmental factor as water. For sexual reproduction bryophytes need water, to transfer swimming sperm to the egg. The majority of mosses are dioicous, having archegonia and antheridia on separate plants. In some taxa, the male and female plants are geographically very separated. Thus, it is not surprising that bryophytes have evolved many types of asexual reproduction and dispersal. Asexual reproduction encompasses a spectrum of mechanisms, ranging from the formation of specialized propagules (gemmae, tubers) to the regeneration of thalli from unspecialized gametophyte fragments. A third distinct process is clonal reproduction, which typically involves the vegetative growth and subsequent independence of new shoots [183].

The gametophyte in Bryopsida is the dominant generation and has two main morphological stages. The first stage is filamentous protonema, which grows from germinating spore. The protonema produces buds, from which the leafy moss plant arises. Mosses have exceptional ability to reproduce vegetatively, due to which they form dense mats over large areas. Almost all parts of moss gametophore are capable of vegetative reproduction [184].

All these morpho-physiological characteristics of the gametophyte lead to the fact that in the process of evolution, mosses first settled in a moist environment. Water and nutrients are taken up by the entire surface of the body, from dry and wet deposition. This is facilitated by the fact that mosses, especially the carpet-forming species, have a well-developed surface. Most bryophytes live in conditions of intermittent water availability. They spend their lives either fully turgid or dry and metabolically inactive. Desiccation tolerance has evolved in many bryophytes. Some species can lose almost all of their water without disruption of cell structures [184, 185].

Mosses have a wide geographical distribution - from the tropics to the polar zone, almost to the limits of the distribution of vegetation. Mosses are mainly distributed in moist places in the temperate and cold zone; In the tropics, they grow mainly in mountain forests [184, 186].

Bryophytes exhibit a wide range of substrate specificity, colonizing surfaces from soil and rock to tree bark and even anthropogenic materials (p. 554). The most fundamental autecological classification distinguishes between species based on their relationship to substrate pH and calcium content, dividing them into calcicoles and calcifuges [183]. Calcicole (or alkaliphilic) bryophytes are species that grow predominantly on calcium carbonate-rich substrates, such as limestone rocks and basic soils. In contrast, calcifuge (or acidophilic) species, are restricted to acidic, calcium-poor substrates like granite or sandstone. A third group, neutrocline taxa, requires near-neutral conditions, while many other species are pH-indifferent (e.g., *Hypnum cupressiforme*) [183].

The underlying causes of this specificity are not fully understood but are linked to substrate chemistry. The critical pH thresholds for many species appear to be around 4.7 and 7.2, possibly

relating to aluminum toxicity at the lower end and phosphate/iron availability at the upper end [183]. Furthermore, studies have observed that calcicole species often have a higher cation exchange capacity than calcifuges. This is hypothesized to be either an adaptation for efficient Ca uptake in calcicoles or a mechanism in calcifuges to exclude toxic Al ions [183]. However, the relationship with Ca itself is not straightforward; for instance, *Sphagnum* (a calcifuge) is not negatively affected by high Ca concentrations as long as the substrate remains acidic [183]. This suggests that the complex interaction of pH, metal ion availability, and nutrient uptake ultimately determines a bryophytes success on a given substrate.

Bryophytes execute important ecosystem functions, include nitrogen fixation, nutrient cycling, food chains and animal interactions, colonization, vascular plant facilitation, mycorrhizae relationships (liverworts), and others. In the Arctic, the Antarctic, in alpine habitats in mountains above treeline and in bogs, fens, and larger peatlands, bryophytes are often the dominant plants in terms of both biomass and productivity. Much of the earth's boreal and arctic zones are covered by peatlands in which species of *Sphagnum* are dominant. These peatlands are very important as carbon sinks and are currently being impacted by climate change [187, 188]. Mosses are capable of absorbing and retaining large amounts of water, thus playing an important role in regulating the water balance of landscapes. There are a number of sources of nutrients that bryophytes accumulate with both wet and dry deposition. Experiments have shown that they also obtain nutrients from the substrate on which they are growing [189]. Bryophytes capture mineral nutrients by "facilitated diffusion," which involves ion channels and carrier proteins and depends on the existing gradients of concentration and electric charge across membranes. The efficient uptake of mineral nutrients in bryophytes is facilitated by their high surface-area-to-volume ratio. Dissolved nutrients are primarily absorbed from the water film that envelops the thalli and leaves, which originates from precipitation or soil moisture [183]. An early study by Tamm [190] showed that *Hylocomium splendens* growing under a Norwegian forest canopy received most of its mineral nutrients from leachates from the tree canopy. In addition, [191] found that bryophytes can obtaining nutrients from dust and litter before they can be taken up by rooted vascular plants. Experiments by Van Tooren et al. [192] demonstrated that bryophytes in Dutch chalk grasslands absorb nutrients and grow during fall and winter while higher plants are inactive, and release nutrients by decomposition in spring and fall; these nutrients are then used by higher plants [193].

1.6. Mosses as Biomonitors of Air Pollution

Moss fully meets all requirements for biomonitoring of air pollution. The developed surface of its above-ground part is in good contact with the ambient air and effectively concentrates

heavy metals and other contaminants from both wet and dry deposition, literally representing an analogue of an air filter [154, 194–196].

One of the important advantages of using mosses in heavy metal research is that mosses accumulate metals in higher concentrations than in air, rain or snow. The probability of sample contamination during their collection and analysis is very small, and the collection process of samples is simple.

Surface properties of the moss cuticle facilitate the penetration of metal ions into the cells [148, 197] Some species of mosses, such as *Hylocomium splendens*, *Pleurozium schreberi* and *Hypnum cupressiforme*, are widespread in the temperate climate zone. As a rule, they have tolerance to high levels of pollution. The growing part of *Hylocomium splendens* is such that the annual growth segments can be easily identified. Collecting and analyzing moss samples is easier than analyzing atmospheric precipitation. It is also easy to determine the exposure period. As a rule, a 3-year growth segment of moss is taken for analysis. Through segments of annual growth, it is possible to study temporal trends [198–201].

The properties that make mosses useful for biomonitoring:

• They obtain nutrients from wet and dry deposition.

• They have no real roots. Although rhizoids visually resemble roots, their main function is anchoring to the substrate, while water and nutrient uptake is negligible.

• Getting nutrients from the atmosphere is facilitated by their weakly developed cuticle.

• Undeveloped vessels facilitate better absorption compared to vascular plants.

• Low growth rates allow long-term accumulation of pollutants.

• The accumulation of heavy metals in high concentrations is facilitated by the high permeability of the cation exchange in moss tissues.

Atmospheric pollutants are deposited on mosses in three different forms: aqueous solution, gaseous form and solid particles. Their accumulation takes place through several different mechanisms:

• Mechanical retention and formation of layers on the surface of cells.

• Embedding into the outer cell wall during ion exchange.

• Metabolically controlled entry into the cell [202].

The binding of particles depends on their size and the surface structure of the moss. Ion exchange is a rapid physiological-chemical process, which is influenced by the number and type of cation exchange sites, as well as the age of cells and their response to desiccation, growth conditions, temperature, amount of precipitation, pH, composition of pollutants [197]. In the

process of ion exchange, cations and anions bind to the functional organic groups of the cell wall, mainly through chelating-bond [203].

The knowledge of mosses as biomonitors is systematically expanding. Concentrations of air pollutants in mosses depend on many natural factors associated with: 1) morphological and physiological characteristics of mosses; 2) with the place of moss growth and the surrounding environment. Natural differences in chemical composition can be observed in different species of mosses. The age of the moss is also important. Older parts of the moss were found to have higher concentrations of heavy metals; thus, the moss provides a historical and interactive record of heavy metals in the environment. It was revealed that, the composition of trace elements and rare earth elements in mosses is highly influenced by throughfall composition, and reflects the interaction of atmospheric deposition with the forest canopy [204–206]. Uptake of some elements by the moss, such as Mn, may be reduced under certain conditions (related with the environment, moss ecophysiology and source and type of emission), even though atmospheric inputs and inputs from vegetation remain the same [207].

The chemical composition of precipitation affects the accumulation of pollutants in mosses, owing to the fact that the absorption efficiency of mosses for different elements is different. The absorption efficiency of heavy metals in mosses is in the following order: Pb > Co, Cr > Cu, Cd, Mo, Ni, V > Zn > As [208]. The accumulation of the largest part of pollutants in mosses is associated with wet precipitation. The amount, duration and intensity of precipitation affect the accumulation [209]. The role of dry precipitation increases in arid climates. The adsorption of metals in mosses is significantly affected by sea salt and acid rain. Usually, the best correlations between mosses and wet precipitation were observed for those elements with high sorption capacity in wet sediments (e.g., Pb, Cd, Co, Cu) [200]. In areas with poor vegetation cover, arid climate or exposed mineral soils, the concentrations of Fe, Cr, Al, Ti and other major elements in the composition of rocks increase [210]. With the increase in altitude, the amount of precipitation, the formation of dust and biomass changes, which is also reflected in mosses [211–213].

1.7. Techniques Commonly Applied for Moss Elemental Analysis

The primary analysis in moss biomonitoring involves determining the content of major and trace elements in moss samples. This is typically done using techniques like Instrumental Neutron Activation Analysis (INAA), or spectroscopic methods such as Atomic Absorption Spectroscopy (AAS), Inductively Coupled Plasma Optical Emission Spectrometry (ICP-OES), Inductively Coupled Plasma Mass Spectrometry (ICP-MS), X-ray Fluorescence (XRF), Direct Mercury

Analyzer (DMA-80). The last one is used to determine mercury concentrations in liquid and solid samples. Each of these techniques has its own advantages and limitations [214, 215].

INAA is a highly sensitive, multi-elemental analytical technique based on the principle of neutron-induced radioactivity. Upon bombarding a sample with neutrons, stable nuclides within a sample are transformed into radioactive ones. These radionuclides subsequently de-excite by emitting gamma rays with element-characteristic energies. By measuring these gamma rays using high-resolution gamma-ray spectrometry, the elemental composition of a sample can be both identified and quantified. This technic offers high sensitivity for numerous elements across the periodic table and often requires minimal sample preparation, as samples can be analyzed in their original form or after simple drying and weighing [216]. However, access to a nuclear reactor or other intense neutron source is required, which typically limits its availability compared to other analytical techniques.

Spectroscopic methods are primarily based on atomic emission spectroscopy, which involves exciting atoms to emit light at characteristic wavelengths. They are more widely available due to lower operational costs and broader accessibility of instrumentation, but they generally require more extensive sample preparation, including dissolution or digestion of solid samples into solutions or suspensions, except for XRF which can be non-destructive depending on the configuration, and DMA-80, where no sample dissolution process is required. ICP-MS offers the highest sensitivity, followed by ICP-OES, then AAS. ICP-based techniques offer simultaneous multi-element analysis and better tolerance of complex sample matrices, while AAS is more cost-effective and simpler to maintain, typically analyzing one element at a time [217–220].

The choice between different spectroscopic methods depends on factors such as the specific analytical requirements, detection limits needed, sample matrix complexity, and budget considerations. Each technique has its unique advantages and is suited for particular applications in various fields including environmental monitoring, metallurgy, geology, and food safety. Regardless of the method chosen, strict quality control is of paramount importance. This is typically achieved by the analysis of certified reference materials (CRMs), which have known, certified concentrations of elements. By comparing the measured values in the CRM to the certified values, the accuracy and precision of the entire analytical procedure, from digestion to final measurement, can be validated [221].

The moss samples are usually measured and analyzed within the same year of sampling. In this study, four distinct analytical methods were employed for the determination of the elemental composition of the samples. Samples from the first Georgian moss survey and the Moldovan survey were analyzed by INAA and AAS, whereas those from the second Georgian moss survey

were analyzed by ICP-OES and DMA-80. This variation in methodology was due to the temporary unavailability of the IBR-2 reactor, during the period when the second Georgian moss survey samples were analyzed.

1.8. Knowledge Gaps and Research Needs

Despite the extensive application of moss biomonitoring for the assessment of atmospheric deposition of PTEs, several important scientific and methodological gaps remain insufficiently addressed.

First, although numerous studies have demonstrated the effectiveness of mosses as biomonitors at regional and continental scales, the influence of climatic conditions on element accumulation in moss tissues remains only partially understood. Variations in precipitation regimes, humidity, temperature, and seasonal dynamics can significantly affect both wet and dry deposition processes, as well as the physiological state of mosses and their capacity to retain pollutants. However, comparative studies conducted under markedly different climatic conditions are still limited, and the extent to which these factors influence data comparability remains unclear.

Second, the role of relief and topography in shaping spatial patterns of atmospheric pollution and its subsequent accumulation in mosses is insufficiently quantified. Mountainous areas, valleys, and plains differ substantially in terms of air mass circulation, pollutant dispersion, and deposition intensity. Orographic effects, such as enhanced precipitation and pollutant trapping in valleys, may lead to spatial heterogeneity in element distribution. Nevertheless, the integration of geomorphological factors into moss biomonitoring studies is often superficial, and systematic evaluations across contrasting relief conditions are lacking.

Third, although international programs such as ICP Vegetation have established standardized protocols for moss biomonitoring, the issue of comparability between regions with different environmental conditions remains unresolved. Differences in species composition, local ecological conditions, and sampling strategies may introduce variability that complicates the interpretation of results across countries. In particular, there is a need to better understand how environmental gradients influence baseline concentrations and accumulation patterns.

Another important limitation concerns the establishment of background levels of pollutants. In regions with complex climatic and geographical characteristics, distinguishing between natural geochemical background and anthropogenic contributions remains challenging. This is especially relevant in areas influenced by long-range transport of dust and aerosols, where natural and anthropogenic sources may overlap.

Furthermore, while the advantages of moss biomonitoring are well documented, its methodological limitations require further consideration. Factors such as species-specific accumulation capacity, age of sampled tissue, canopy effects, and local microenvironmental conditions can influence the measured concentrations of elements. These sources of variability are not always consistently accounted for, which may affect the reliability of inter-regional comparisons.

Finally, despite the growing body of literature, there is a lack of integrated studies that simultaneously consider climatic, geographical, and ecological factors in the interpretation of moss biomonitoring data. Most existing research focuses on either large-scale surveys or local case studies, without bridging these perspectives.

In this context, the present research addresses these gaps by evaluating the effectiveness of moss biomonitoring under contrasting physico-geographical conditions, using the Republic of Moldova and Georgia as case studies. The study aims to contribute to a better interpretation of biomonitoring data, and to support the development of more robust approaches for assessing air quality in regions with diverse environmental conditions.

1.9. Conclusions for Chapter 1

Air pollution represents a complex and dynamic mixture of gaseous components and particulate matter, the latter of which is defined not merely by chemical composition but critically by aerodynamic size and phase state. The distinction between PM_{10}, $PM_{2.5}$, and UFPM particles is paramount, as size dictates both atmospheric residence time and, more importantly, the depth of pulmonary penetration. Furthermore, the role of fine particles as vectors for heavy metals amplifies their toxicological potential. Given that NEE are projected to dominate road transport emissions, especially with the increasing weight of electric vehicles, future mitigation strategies cannot rely solely on reducing combustion exhaust; they must urgently address the growing fraction of non-exhaust emissions from road traffic and industrial wear. Without targeted interventions to reduce resuspended dust and metal contamination, the health benefits of transitioning to cleaner energy sources may be partially offset by the persistent, effects of respirable PM on cardiovascular and respiratory morbidity.

Atmospheric particulate matter serves as a major vector for PTEs. PTEs distinguish between non-essential elements (e.g., Pb, Cd, As) and essential micronutrients (e.g., Zn, Cu, Se) that become hazardous only at elevated bioavailable doses. While natural sources exist, anthropogenic activities, specifically non-ferrous metal production and fossil fuel combustion, dominate emissions. A key focus is the inhalation pathway. $PM_{2.5}$ enriched with metals deposits

deep in the alveolar region, where particle solubility and metal speciation (such as the higher toxicity of Cr(VI) vs. Cr(III) or As(III) vs. As(V)) govern the rate of systemic absorption and the onset of toxicological effects.

The spatial distribution of atmospheric pollutants is governed by interactions between emission sources, meteorology, topography, and pollutant properties. Convection lifts pollutants to higher altitudes for long-range transport, while temperature inversions trap emissions near the surface, especially in valleys and basins. Precipitation acts as the main natural removal mechanism, though humidity can enhance haze by swelling particles. Mountains block or channel airflow, causing orographic scavenging on windward slopes. Dust from deserts (Sahara, Gobi, Taklamakan) travels intercontinentally, acting as ice nuclei and carrying heavy metals, while human activities like agriculture disturb loess soils, adding local emissions.

Traditional air pollution monitoring is accurate but expensive and spatially limited. Biomonitoring, particularly using mosses, offers a cost-effective, large-scale alternative. The ICP Vegetation program coordinates European moss surveys every five years, providing critical data on spatial and temporal trends of pollutants. Mosses are ideal biomonitors due to their widespread nature and air-focused uptake. Moss species are classified by substrate ecology as calcicoles on alkaline substrates, calcifuges on acidic ones, or pH-indifferent, while playing key ecosystem roles that include dominating peatlands as major carbon sinks, and regulating landscape water balance. Moss is an ideal biomonitor for air pollution due to its high surface contact with air, lack of true roots and weakly developed cuticle, forcing it to absorb nutrients and contaminants directly from wet and dry atmospheric deposition. Accumulation occurs via mechanical retention, ion exchange, and cellular uptake. Metal uptake efficiency follows Pb > Co, Cr > Cu, etc., and is affected by precipitation, sea salt, acid rain, and altitude.

Despite widespread use of moss biomonitoring, critical gaps remain regarding how climate, topography, and local ecological factors affect element accumulation, as well as how to ensure comparability across regions with different environmental conditions. This study addresses these limitations by evaluating moss biomonitoring effectiveness in Moldova and Georgia, aiming to improve data interpretation and air quality assessment in diverse physico-geographical settings.

2. MATERIALS AND METHODS

The research presented in this chapter was carried out over multiple sampling campaigns conducted during the periods 2014-2023 covering both the Republic of Moldova and Georgia. These investigations combined field sampling, laboratory analyses, and spatial–statistical approaches to assess atmospheric deposition and its variability under different climatic and relief conditions. Particular emphasis is placed on the selection of study areas, sampling strategy, and analytical techniques, as well as on the application of statistical and spatial analysis tools. The methodological framework combines standardized biomonitoring protocols with advanced analytical and data-processing techniques to ensure the reliability, comparability, and interpretability of the results.

Special attention is given to the incorporation of environmental variables, including climate, relief, and anthropogenic factors, which are expected to influence atmospheric deposition processes and pollutant accumulation patterns.

2.1. Study Area: Georgia and Republic of Moldova

This study leverages a comparative analysis of two countries in the Black Sea basin: the Republic of Moldova and Georgia. Both countries are defined by stark geomorphological and socioeconomic differences. Moldova is a predominantly lowland, agrarian country, with over 80% of its land below 200 m in elevation and 74% of its land dedicated to agriculture. Its economy remains heavily focused on cereals, sunflowers, and viticulture. In contrast, Georgia is characterized by its rugged topography, with approximately two-thirds of its territory at high elevations and approximately 20% exceeding 2,000 m. This mountainous terrain supports a more diversified economy, including tourism, mining, and hydropower, with a significantly smaller proportion of agricultural land (43%) [45, 46]. Despite these pronounced differences in relief and land use, both countries share overlapping climate zones according to the Köppen-Geiger classification (Figure 2.1) and host the same species of mosses.

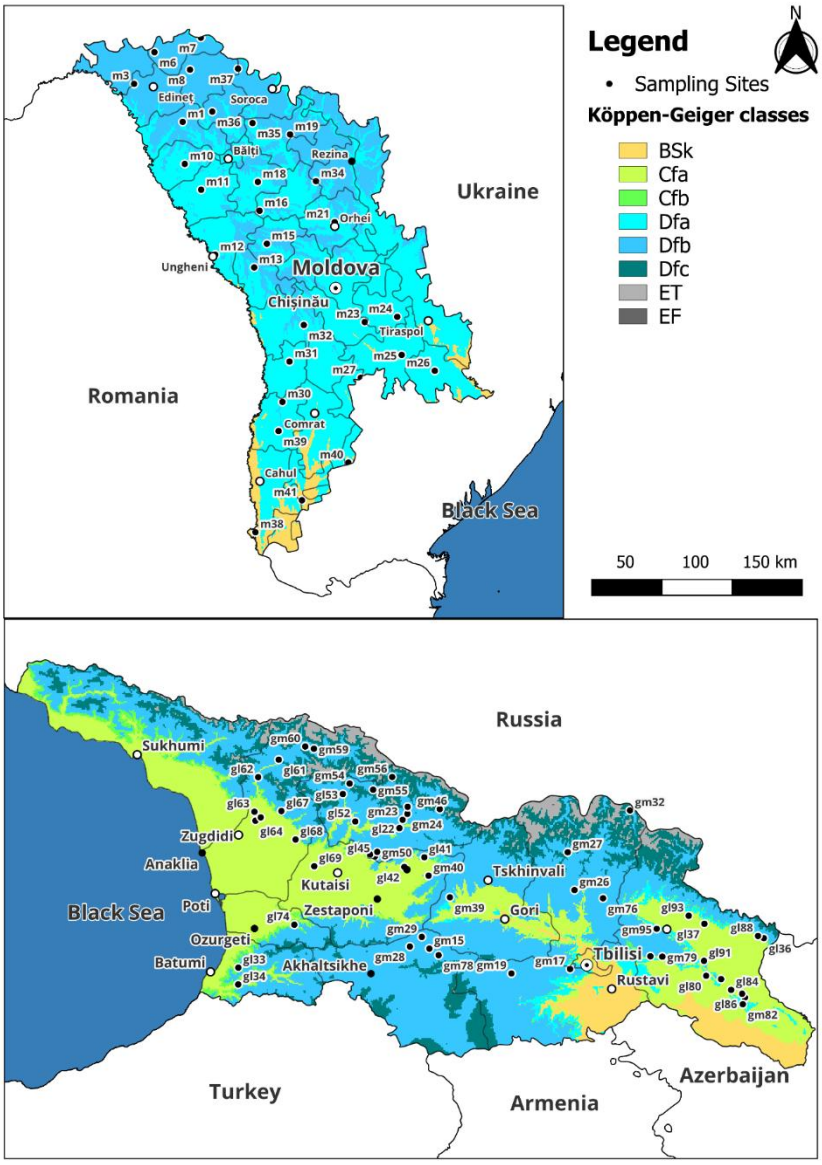

Figure 2.1. Köppen-Geiger classification for the sampling sites. (BSk – Arid, steppe, cold; Cfa – Temperate, no dry season, hot summer; Cfb – Temperate, no dry season, warm summer; Dfa – Cold, no dry season, hot summer; Dfb – Cold, no dry season, warm summer; Dfc – Cold, no dry season, cold summer; ET – Polar, tundra; EF – Polar, frost [222]).

This unique combination of shared climatic factors and the presence of the same moss species against a backdrop of significant geophysical contrasts provides a valuable opportunity for analyzing the environmental drivers of elemental accumulation in mosses.

2.1.1. Georgia: geographical position, natural conditions, economic development and environmental challenges

Georgia is a transcontinental country, situated in the Caucasus region at the intersection of Eastern Europe and Western Asia, with a coastline on the Black Sea [223]. It shares borders with four countries: Russia to the north and northeast, Azerbaijan to the southeast, Armenia to the south, and Turkey to the southwest [223]. Encompassing 69,700 km² and a population of approximately

3.7 million, the country's landscape is predominantly characterized by its mountains [223]. The Greater Caucasus range forms its principal northern orographic barrier, which in turn supports a wide array of ecosystems and contributes to high levels of biodiversity. This mountainous terrain is the dominant factor controlling Georgia's climate, inducing variations in meteorological elements such as temperature and precipitation through hypsometrical zonality, effectively overriding the influence of latitude [223, 224].

The atmospheric circulation patterns are significantly altered by a combination of factors: the complex topography of the Greater and Lesser Caucasus ranges, the uplands of southern Georgia, and the influence of nearby seas. This distinct combination of geographical factors results in a wide spectrum of climatic conditions within a relatively small region. As a result, arid steppes receiving under 400 mm of annual precipitation exist in close proximity to extremely humid regions receiving over 4000 mm. Precipitation levels vary considerably, from 1600–1900 mm in the Kolkheti coastal area to 400–1800 mm in eastern Georgia [223]. The highest levels of rainfall occur on the seaward slopes of the Meskheti Range, with an annual average of 4500 mm at Mount Mtirala, while the lowest levels are found in the southeastern part of eastern Georgia, which receives under 400 mm. These disparities are further influenced by the wind regime, which is determined by the seasonal distribution of atmospheric pressure over Eurasia and the adjacent Black and Caspian Seas, and interacts with local topography. This process is definitively illustrated by the case of Western Georgia, where in winter, easterly terrestrial winds flow from the continental interior, while in summer, westerly marine winds carry moisture from the Black Sea. The interaction of this flow with the mountains forces orographic lift, concentrating precipitation. Furthermore, local wind systems, including coastal breezes and descending foehns, introduce significant microclimatic influences, creating a complex and highly localized climatic landscape. Acting as a key climatic barrier, the Likhi Range modifies wind patterns and contributes to the country's pronounced climatic contrasts [223, 224].

The post-Soviet period in Georgia marks a distinct phase of economic liberalization, defined by the state's transition from a centrally planned economy to a strategy of deregulation and privatization aimed at integrating into global markets. The principal outcome of this strategy has been the structural transformation of the economy, towards a services-oriented economy, where sectors such as transport and logistics, trade, and tourism have become primary contributors to Gross Domestic Product (GDP) growth [225–230]. The industrial sector continues to demonstrate robust activity, predominantly driven by the metallurgy and mining sub-sectors [231, 232]. Furthermore, energy security and export capacity are increasingly linked to the exploitation of hydropower resources, leveraging the country's orographic and hydrological conditions [233].

Despite the relative decline of agriculture in its contribution to national GDP, the sector retains critical socio-economic importance due to its high rate of employment absorption in rural areas [226, 234].

Georgia faces severe environmental challenges that threaten public health, natural resource integrity, and sustainable development. Studies indicate that both ambient and indoor air quality pose significant risks, with urban centers frequently exceeding international guidelines for particulate matter [235, 236]. The discharge of untreated municipal and industrial wastewater compromises surface and groundwater quality, impacting aquatic ecosystems and limiting access to clean water [237]. The natural resource sector suffers from weak regulatory oversight, leading to phenomena such as rampant illegal logging, which undermines forest ecosystems and biodiversity [235]. The mining industry, still operating under an antiquated Soviet-era legal framework, presents a legacy of abandoned sites with no clear accountability for remediation. For example, manganese mines abandoned without proper conservation in the Chiatula municipality continue to threaten both human and environmental health through the leaching of heavy metals and sediment runoff into surrounding water bodies [235, 238]. On land, a combination of unsustainable agricultural practices, the worsening impacts of climate change, and more frequent natural disasters, have led to the degradation or erosion of approximately 35% of the country's agricultural soil [239]. Furthermore, poorly managed municipal landfills and accumulated hazardous waste continue to be major sources of environmental contamination. For example, unspecified quantities of obsolete pesticides scattered throughout agricultural areas, combined with approximately 2,800 tons of such chemicals temporarily stored under improper conditions at the Ialguja site, represent significant and ongoing sources of soil and groundwater pollution [235].

2.1.2. Republic of Moldova: geographical position, natural conditions, economic development and environmental challenges

The Republic of Moldova is a landlocked Eastern European country of 33,800 km², with a population of 3.5 million, and is bordered by Ukraine to the north, east, and south and Romania to the west. The Prut and Dniester (Nistru) rivers are the major waterways, which also serve as significant natural borders, defining the western and eastern borders respectively. Beyond these major waterways, Moldova's internal river systems consist largely of smaller tributaries. These watercourses are frequently seasonal in nature, experiencing reduced flow or drought conditions during periods of low precipitation, which poses challenges for water management and agriculture [240–242].

In terms of topography, Moldova is characterized by a gently undulating landscape of hills and low-lying plains. The northern and central regions are predominantly hilly, while the southern part of the country transitions into the Bugeac Steppe, a semi-arid plain. This generally moderate relief is conducive to agricultural activity, which dominates land use across the nation.

The country is predominantly rural, with 76% of its land dedicated to agricultural purposes, a figure that underscores the sector's importance. This is supported by the presence of deep, fertile chernozem (black earth) soils, particularly in the northern and central regions. In contrast, forest cover is limited, accounting for only about 9.6% of the territory. It should be noted that soil erosion, especially on cultivated slopes, is an acute problem that threatens the long-term viability of black earth [45].

Moldova lies under a continental climate characterized by mild winters averaging −5°C to −3°C and warm summers with limited rainfall, where annual precipitation ranges from about 600 mm in the north to 500 mm in the south, with the heaviest precipitation usually falling in early summer and October.

The economy remains closely tied to its agricultural sector, with a significant portion of the GDP and labor force dedicated to cultivating high-value crops like wine grapes, sunflowers for oil, and walnuts [243, 244]. The most significant industrial activity is food and beverage processing. The wine industry, in particular, is a point of national pride and a key export commodity, supported by a network of wineries and bottling plants. This economic structure exists within the context of limited domestic mineral resources, reinforcing the economy's dependency on the land and its produce [45, 245]. To support its crucial exports of wine, sunflower oil, and fruit, the sector relies heavily on fertilizers and pesticides, resulting in significant non-point source pollution. This agricultural runoff is the principal cause of nutrient loading in the Black Sea basin, leading to eutrophication and "dead zones," and it compromises the quality of groundwater and surface waters, including the strategic Nistru River [246, 247]. Industrial activity, while smaller in scale, contributes to localized "hotspots" of pollution. The older industries, such as the massive cement plant in Rezina and unmanaged chemical waste from the Soviet-era pesticide stockpiles, pose risks of heavy metal and toxic chemical contamination to soil and water [245, 248]. Furthermore, the widespread practice of burning agricultural stubble contributes to seasonal air pollution [249, 250]. In urban and industrial zones, contamination can occur from poorly managed industrial sites and aging infrastructure, while air quality is predominantly affected by emissions from an aging fleet of vehicles and the widespread use of biomass for residential heating [248, 251].

2.2. Moss Sampling

The first comprehensive moss survey in Georgia, hereafter referred to as the "Moss Survey 2015", was executed between 2014 and 2017. This biomonitoring study focused on the most ubiquitous moss species across nine administrative regions. A total of 120 specimens were collected: *Hylocomium splendens* (Hedw.) Schimp. (n = 34), *Hypnum cupressiforme* Hedw. (n = 64), and *Pleurozium schreberi* (Brid.) Mitt. (n = 22). Sampling sites were restricted to natural environments with organic-rich surface soils, spanning forests, foothills, and the subalpine to alpine belts. The altitudinal distribution of sampling points ranged from 161 m to 2763 m a.s.l. [179].

A second series of moss surveys, hereafter termed "Moss survey 2020", was conducted in both Georgia and the Republic of Moldova. In Georgia, sampling took place between 2019 and 2023 during late spring and summer to ensure comprehensive national coverage. In Moldova, a survey was conducted in April 2020. In Georgia, 95 samples were collected, primarily of the species *Hypnum cupressiforme* Hedw. (n = 70). In locations where *Hypnum cupressiforme* was absent, supplementary samples of other species were taken: *Abietinella abietina* (Hedw.) M. Fleisch. (n = 14), *Pleurozium schreberi* (Brid.) Mitt. (n = 5), and *Hylocomium splendens* (Hedw.) Schimp. (n = 6). This multi-species methodology, used by numerous countries to ensure full territorial coverage [47, 252, 253]. Sampling elevations ranged from 2 to 2123 m a.s.l., with *Hypnum cupressiforme* occurring only up to 1,800 m a.s.l.

In Moldova, sampling focused only on *Hypnum cupressiforme.* The survey covered 41 locations, which included a re-survey of 33 sites from a 2015 study [180] and the addition of 8 new sites in the country's south [254, 255] to ensure comprehensive coverage. In Georgia, a total of 33 of the original sampling sites from the 2015 survey were successfully resampled, defined as those that remained identical or fell within a 10 km radius and allowed for the collection of the same moss species. The sampling locations of moss survey 2020 are shown in Figure 2.2.

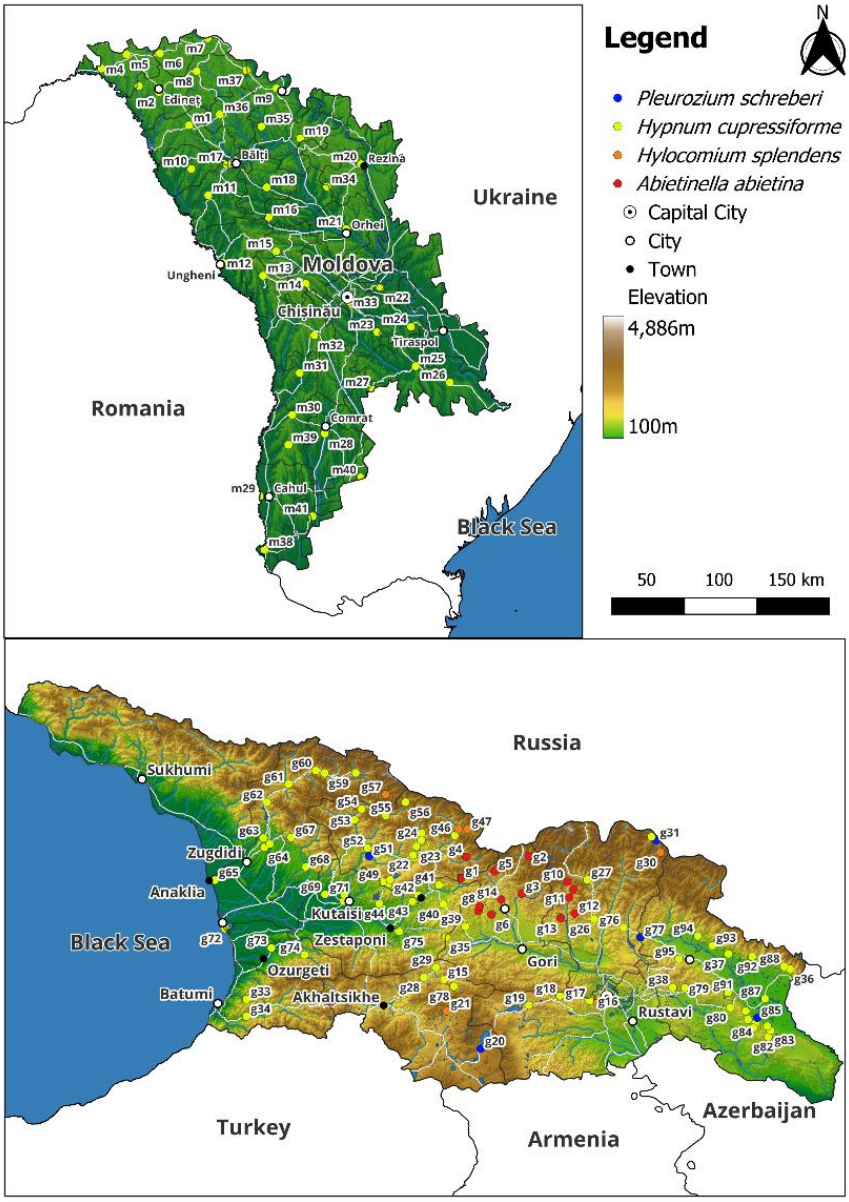

Figure 2.2. Geographic distribution of moss sampling sites across Georgia and Moldova during the 2020 moss survey.

Samples were collected following the ICP Vegetation monitoring manual, targeting a density of at least 1.5 samples/1000 km^2 [256]. The implemented grid had an approximate spacing of 30 km × 30 km. For both surveys, standard precautions were applied: sites were at least 300 m from villages and industrial areas, and 100 m from minor roads. At each site, approximately one litre of fresh moss was collected, consisting of five to ten subsamples of the same species. Samples were collected using separate polyethylene gloves per site and stored in air-permeable bags.

2.3. Sample Preparation and Analysis

The initial stage in preparing the moss samples for analytical purposes involves selecting shoots that represent the most recent 2–3 years of growth. Typically, this entails choosing green

shoots that reflect the current vegetative state of the moss sample. To reduce the risk of sample contamination, disposable polyethylene gloves and plastic tweezers were employed during the cleaning process to remove extraneous materials. Post-cleaning, the samples were dried until they reached a constant weight, specifically at 105 °C for a duration of 48 hours. The next stage involves homogenization. A Fritsch Pulverisette 6 planetary mill (Idar-Oberstein, Germany), equipped with an agate grinding bowl and balls, was used to pulverize the samples to a uniform consistency. The subsequent stages exhibit variations across different methodologies.

2.3.1. Sample Analysis using Instrumental Neutron Activation Analysis

Moss samples were subjected to the instrumental neutron activation analysis (INAA) at the experimental installation REGATA of the IBR-2 reactor of Frank Laboratory of Neutron Physics, Joint Institute for Nuclear Research FLNP, JINR (Dubna, Russia). For INAA, approximately 0.3 g of mosses were pelletized in pressforms. Then the samples were precisely weighed. Moss samples for short-term irradiation were heat-sealed in polyethylene foil bags, whereas the samples for long-term irradiation were packed in aluminum cups.

The samples were irradiated in the channels equipped with a pneumatic system installed at the IBR-2 pulsed nuclear reactor of FLNP with the average power of 1.5 MW. To determine the elements with short-lived isotopes (SLI) (Mg, Al, Cl, Ca, Ti, V, Mn) in the moss samples, each sample was irradiated for 3 min at a thermal neutron flux of 1.2×10^{12} n/cm^2/s, followed by a direct measurement for 15 minutes using a High-Purity Germanium (HPGe) detector with a resolution of 2.5–3 keV for the 1332 keV line of the ^{60}Co [254, 255]. Similarly, the long-lived isotopes (Na, K, Sc, Cr, Fe, Co, Ni, Zn, As, Se, Br, Rb, Sr, Sb, Cs, Ba, La, Ce, Sm, Eu, Tb, Hf, Ta, Th, and U) were irradiated for 4 days in the Cd-screened channel under the epithermal neutron flux of 1.1×10^{11} n/cm^2/s [254, 255]. Following repacking, the samples underwent two measurements. The initial 30-minute measurement was performed after 4 days of decay to determine a specific set of elements, referred to as the first long-lived isotopes (LLI 1), which included Na, K, As, Br, La, Sm, and U. A second, longer measurement of 1.5 hours was conducted after a 20-day decay period to determine a subsequent set of elements, defined as the second long-lived isotopes (LLI 2): Sc, Cr, Fe, Co, Ni, Zn, Se, Rb, Sr, Sb, Cs, Ba, Ce, Eu, Tb, Hf, Ta, and Th. The analysis of gamma spectra was performed with the Genie 2000 software. For the subsequent quantification of elemental concentrations, custom software developed at the FLNP was employed [257]. The analytical errors of the concentrations of the elements of interest range from 3 to 15%.

2.3.2. Sample Analysis using Direct Mercury Analyzer

The content of Hg was determined using a direct mercury analyzer (DMA-80 evo, Milestone Srl, Sorisole, BG, Italy) [223, 258, 259]. Mercury levels were determined directly, without sample dissolution. A weighed and milled sample was placed in a nickel-coated sample boat and inserted into the analytical instrument. The temperature within the device was gradually raised to 700°C, creating conditions suitable for combustion of the samples using oxygen flow. The resulting combustion products were directed through a catalyst tube, where any remaining oxidation processes were completed. All mercury species present in the sample were converted to elemental mercury vapor during this stage. The mercury vapor was selectively trapped on a gold-wire amalgamator while other products were flushed out of the system. The amalgamator was then rapidly heated to 900°C to release the mercury vapor, which was carried towards an atomic absorption spectrophotometer. By measuring the absorbance at a wavelength of 253.7 nm and taking into account the mass of the sample analyzed, the DMA-80 software calculated the mercury concentration in the sample.

2.3.3. Sample Analysis using Atomic Absorption Spectroscopy

For the analysis of Cu, Cd, and Pb by atomic absorption spectrometer approximately 0.2 g of moss sample was digested using a microwave digestion system (Mars, CEM, Matthews, NC, USA). The digestion was performed in a Teflon vessel with 2 mL of concentrated HNO_3 (69%) and 1 mL of H_2O_2 (30%). All chemicals were of analytical grade from Merck (Darmstadt, DE, Germany). The microwave digestion protocol involved a two-stage process: a 15-minute temperature ramp to 160 °C, followed by a 10-minute hold at the target temperature, with power and pressure maintained at 400 W and 20 bar, respectively. After digestion, the samples were quantitatively transferred to 100 mL volumetric flasks and diluted to volume with bi-distilled water [255].

The digests were analyzed using an iCE 3300 atomic absorption spectrometer (Thermo Fisher Scientific, Waltham, MA) equipped with a graphite furnace. The instrument was calibrated using standards of known concentration. In AAS, the sample is injected directly into a graphite tube, which is then heated to atomize the elements. Light from a hollow cathode lamp, tuned to a specific wavelength for the target element (e.g., Cu, Cd, or Pb), is passed through the atom cloud. The atoms in the vapor absorb a fraction of this light, and the decrease in intensity is measured by a detector. This absorbance is proportional to the concentration of the element in the sample, allowing for quantitative determination.

2.3.4. Sample Analysis using Inductively Coupled Plasma Optical Emission Spectrometry

The samples intended to be analyzed using ICP-OES were subjected to dissolution processes, namely approximately 0.5 g of moss sample was digested in a microwave digestion system (Mars, CEM, Matthews, NC, USA) using chemicals of analytical grade, namely a mixture of 5 mL concentrated HNO_3 (69%, Merck, Darmstadt, DE, Germany) and 2 mL H_2O_2 (30%, Merck, Darmstadt, DE, Germany), at 180 °C. The microwave digestion procedure follows that outlined in the AAS section. After digestion, the resulting solution was transferred to a 50 mL volumetric flask and diluted to the mark with bi-distilled water.

The concentrations of 15 elements (Al, Ba, Cd, Co, Cr, Cu, Fe, Mn, Pb, Ni, S, Sr, V, Zn) were determined using an ICP-OES system (PlasmaQuant PQ 9000 Elite, Analytik Jena, Jena, Germany). The sample solutions were aspirated into a high-temperature argon plasma (~10,000 K), exciting the atoms and causing them to emit element-specific light. This emission was measured in either radial or axial view, and the intensities were quantified by a multi-element spectrometer and detector.

The minimum detection levels obtained were 0.4965, 0.0041, 0,0001, 0,0004, 0,0001, 0,0005, 1.024, 0.1136, 0.0001, 0.001, 0.2215, 0.0034, 0.0014, 0.0009 and 1 mg/kg respectively for Al, Ba, Cd, Co, Cr, Cu, Fe, Mn, Pb, Ni, S, Sr, V, and Zn.

2.3.5. Quality Control of Performed Measurements

To ensure reliable results, both studies implemented strict protocols to minimize contamination and performed quality control for the ICP-OES, NAA, AAS, and DMA-80 analyses using certified reference materials (CRMs), as detailed in Table 2.1.

Table 2.1. Quality Control of Measurements and LOD Values for the Determined Elements.

	Elements	M2			OBTL-5			LOD, mg/kg
		Experimental value, mg/kg	Certified value, mg/kg	Recovery, %	Experimental value, mg/kg	Certified value, mg/kg	Recovery, %	
ICP-OES	Al	163.51	175	93	1840.8	1981	93	0.4965
	Ba	17.23	17.6	98	64.8	67.4	96	0.0041
	Cd	0.45	0.454	99	2.30	2.64	87	0.0001
	Co	0.89	0.9	99	0.90	0.98	92	0.0004
	Cr	0.93	0.92	101	ND	ND	ND	0.0001
	Cu	66.75	68.1	98	9.60	10.1	95	0.0005
	Fe	255.95	245	104	1496	1491	100	1.024
	Mn	322.03	357	90	162	180	90	0.1136
	Ni	14.11	14.8	95	6.7	8.5	79	0.0001
	Pb	6.56	5.86	112	1.81	2.01	90	0.001
	Sr	ND	ND	ND	97.6	105	93	0.0034
	V	1.37	1.21	113	3.50	4.12	85	0.0014
	Zn	35.8	35.2	102	49.8	52.4	95	0.0009
NAA*	**Elements**	**CRMs**			**Experimental value, mg/kg**	**Certified value, mg/kg**	**Recovery, %**	**LOD, mg/kg**
	Al	1575a			557	580	96	3.2
	Ba	2711			726	726	100	1.7
	Co	1633c			42.5	42.9	99	0.03

	Cr	2709a	113	130	87	1.3
	Fe	2709a	32232	33600	96	0.9
	Mn	1547	94	98	96	0.08
	Ni	1632c	9.30	9.32	100	1.4
	Sr	2711	257	245	105	1.5
	V	2710	75.8	76.6	99	0.18
	Zn	1632c	10.7	12.1	88	0.4

AAS	**Elements**	**OBTL-5**			**LOD, mg/kg**
		Experimental value, mg/kg	**Certified value, mg/kg**	**Recovery, %**	
	Cd	2.59	2.64	98	0.0001
	Cu	9.8	10.1	97	0.0005
	Pb	1.94	2.01	97	0.001
DMA-80	**Element**	**OBTL-5**			
		Experimental value, mg/kg	**Certified value, mg/kg**	**Recovery, %**	
	Hg	0.0216	0.0209	103%	

* Since NAA relies on relative comparison, results from just one reference material (experimental vs. certified value) are included.

The quality control of ICP-OES results using CRMs such as M2 (*Pleurozium schreberi*), and INCT-OBTL-5 (Oriental Basma Tobacco Leaves), demonstrated recovery rates for the majority of measured elements within acceptable ranges. Specifically, the recovery rates were 90–113% for M2, and 79–100% for INCT-OBTL-5 [223].

To ensure the quality of NAA results, all samples were analyzed alongside certified reference materials, yielding recovery rates of 87–105%. The CRMs included: NIST SRM 1547 (Peach Leaves), NIST SRM 1575a (Pine Needles), NIST SRM 2709a (San Joaquin Soil), NIST SRM 2711 (Montana Soil), and INCT-OBTL-5 (Oriental Basma Tobacco Leaves) [254, 255]. The limited number of certified elements in plant reference materials required the use of standards from alternative matrices to certify a wider range of elements in moss samples. This approach is applicable in NAA because, unlike many other analytical techniques, it is virtually free from chemical matrix effects, particularly when analyzing small samples in terms of size and mass.

The accuracy of the AAS analysis was verified using CRMs: NIST SRM 1570a (Spinach Leaves), NIST SRM 1575a (Pine Needles); and INCT-OBTL-5 (Oriental Basma tobacco leaves). The results showed excellent agreement, with recoveries ranging from 97% to 98% relative to the certified values.

The quality control of DMA-80 results utilizing certified reference material INCT-OBTL-5 demonstrated that the variability in Hg content between certified and measured values ranged from 3% to 6%.

The use of a common reference material INCT-OBTL-5 for ICP-OES, NAA, AAS, and DMA-80 enabled consistent validation of accuracy across all analytical methods [223, 254, 255, 260].

2.4. Statistical Tools Applied to Describe Obtained Results

Statistical analysis is essential for interpreting the complex data generated by moss biomonitoring studies. By applying various statistical techniques, it is possible to identify relationships between elements, potential pollution sources, and environmental factors influencing element accumulation in mosses, providing valuable insights into air quality and ecosystem health [261].

2.4.1. Correlations Analysis

To investigate the associations between element concentrations, a correlation analysis was conducted. Given the non-normal distribution of the data, the non-parametric Spearman's rank correlation coefficient was used. All analyses were performed with the ggstatsplot package in R. To ensure robustness and control for the increased risk of false positives (Type I errors) arising

from multiple comparisons, the p-values were adjusted using the Holm method (also referred to as the Holm-Bonferroni correction) [262].

2.4.2. Nonparametric Statistical Comparisons

Comparative moss surveys are a powerful tool for tracking pollution shifts and assessing trends in air quality, providing a critical evidence base for environmental policy. To ensure the robustness of such comparisons, appropriate statistical methods are required.

Given that biomonitoring data frequently contain asymmetry and outliers, nonparametric methods were chosen. Specifically, the Mann–Whitney U test was used to compare results between two independent groups, such as previous versus recent survey periods. When comparing elemental content across more than two independent groups (e.g., different species, site types, or multiple survey periods), the Kruskal–Wallis test was applied. This test is conceptually similar to the Mann–Whitney U test but extends the comparison to three or more groups, making it the appropriate choice for multi-group analyses. For instances where the Kruskal–Wallis test indicated significant differences, post-hoc pairwise comparisons were performed using Dunn's test, with p-values adjusted via the Holm method to control for multiple comparisons. The results of these analyses were visualized using boxplots created with the ggstatsplot package in R, which effectively displays distributional differences and integrates statistical annotations directly into the figures [223, 260, 262].

2.4.3. Principal Component Analysis

Principal Component Analysis (PCA) is a cornerstone technique for dimensionality reduction, widely used in fields like biomonitoring to manage complex, high-dimensional datasets. Its core function is to simplify data without losing essential information by projecting it onto a new set of orthogonal axes called principal components (PCs).

This transformation works by identifying the directions of greatest variance in the data. The first PC is aligned to capture the maximum possible variance, representing the single most significant pattern or trend. Each subsequent component is then calculated to capture the next greatest amount of remaining variance while being constrained to be uncorrelated (orthogonal) to all preceding components. This orthogonality ensures that each PC provides unique, non-redundant information. A key mathematical consequence is that the total number of possible PCs is constrained by the lesser of the number of samples (observations) or original features (variables).

In practical terms, PCA serves two primary purposes: it reduces noise by concentrating information into fewer dimensions, and it enables visualization of major patterns that might be hidden in high-dimensional space. For this analysis, PCA was implemented using the FactoMineR

package [263] in R, which performed the numerical computation and eigenvalue decomposition. The results were then visualized using the factoextra package [264] to create informative graphs, such as biplots and scree plots, illustrating the contribution of variables and the distribution of samples across the new principal components.

2.4.4. Positive Matrix Factorization Analysis

Positive Matrix Factorization (PMF), particularly version 5.0, is an advanced mathematical receptor model developed by the United States Environmental Protection Agency (EPA). As a powerful multivariate statistical tool, it is designed to interpret complex environmental datasets from diverse sources, including soil, sediments, surface water, wet deposition, and ambient air, by reducing dimensionality. Specifically, PMF decomposes a matrix of measured element concentrations (X) into the product of two strictly non-negative matrices: a matrix of source contributions (G) and a matrix of source profiles (F), plus a residual matrix (E), as shown in Equation 2.1:

$$X = G\,F + E, \qquad (2.1)$$

The non-negativity constraint ensures that the mathematically derived sources reflect physical reality, since a source cannot emit negative amounts of element, nor can it contribute negatively to a sample. The factorization is achieved through a weighted least-squares minimization algorithm, where each data point is weighted by its measurement uncertainty. This approach allows PMF to robustly handle missing data and values below the detection limit. Crucially, PMF does not require a priori knowledge of source profiles; instead, it identifies latent sources directly from the elemental data. Consequently, it is particularly effective for discovering hidden patterns and uncovering the influences of pollution sources that are not immediately apparent from the raw concentration data [265, 266].

2.4.5. Background Calculation

Widespread environmental contamination poses a significant challenge to finding truly pristine sites that can serve as elemental baselines. The method proposed by Krahovska [267] involves ranking sampling points for each element by concentration from lowest to highest, summing the ranks for each point, and defining the baseline concentration as the mean of the lowest 5% of values.

Due to the limited size of the dataset, 10% of the data were utilized in this study. To prevent distortion from unrepresentative extremes, outliers were assessed using Grubbs' test at a significance level of 0.05. Furthermore, bootstrapping was applied to determine the upper limit of the 95% confidence interval for the mean, thereby improving the robustness of the baseline

estimate by accounting for natural variability in elemental concentrations across sampling sites [223].

However, a limitation of this approach lies in its dependence on the representativeness of the sampled population. The derived background is inherently biased by the initial sampling strategy. If the dataset is skewed, for example, if all samples originate from polluted sites or, conversely, exclusively from pristine areas, the calculated background will reflect that bias, respectively overestimating or underestimating true geogenic background concentrations. Therefore, the resulting baseline is strictly valid only within the context of the collected samples and may not be generalizable to the wider environment.

2.5. Evaluating Environmental Contamination: Indices and Risk Characterization

Interpretation of results requires understanding of element sources, environmental factors, and biological interaction. Several indices are commonly used to quantify pollution levels and assess environmental impact. The Contamination Factor (CF) measures the degree of contamination relative to background levels and classifies it into categories ranging from no contamination to extreme contamination. The Pollution Load Index (PLI) provides an integrated measure of overall pollution across multiple elements through geometric mean calculation and is categorized on a descriptive scale from unpolluted to extremely high pollution. The Potential Ecological Risk Index (PER) and its cumulative form, the Ecological Risk Index (RI), incorporate both contamination levels and element-specific toxic-response factors to assess ecological risks according to established risk level classifications.

2.5.1. Contamination Factor

The Contamination Factor (CF) is a quantitative metric employed to assess the degree of environmental contamination attributable to specific elements within a study area. It is derived by comparing the concentration of an element in collected moss samples to its established background concentration, as defined by the equation 2.2:

$$CF = \frac{C_m}{C_b}, \qquad (2.2)$$

In this expression, C_m denotes the measured concentration of the target element, while C_b signifies its corresponding background or reference concentration in an uncontaminated environment. The magnitude of the calculated CF is interpreted according to a classification scheme, which defines varying levels of contamination [268], as detailed in Table 2.2.

Table 2.2. Classification of Contamination Factor (CF).

Contamination Factor (CF) Value	Degree of Contamination
CF < 1	No Contamination
1 < CF < 2	Suspected
2 < CF < 3.5	Slight
3.5 < CF < 8	Moderate
8 < CF < 27	Severe
CF > 27	Extreme

2.5.2. Pollution Load Index

The Pollution Load Index (PLI) is a diagnostic tool used to evaluate the integrated contamination level of an environmental sample. By computing the geometric mean of the CF for a defined set of monitored elements, the PLI synthesizes multiple individual pollution metrics into a single, dimensionless value. This integrative approach allows for a comprehensive assessment of site pollution status, facilitates spatial and temporal comparisons, and aids in identifying areas experiencing significant multi-element stress. For easier interpretation, PLI values are often categorized on a descriptive scale from 0 to 6 (table 2.3) [269].

Table 2.3. Classification of Pollution Load Index (PLI).

PLI Value Range	Pollution Level Classification
0 < PLI ≤ 1	Unpolluted
1 < PLI ≤ 2	Minimal to moderate pollution
2 < PLI ≤ 3	Moderate pollution
3 < PLI ≤ 4	Moderate to severe pollution
4 < PLI ≤ 5	Severe pollution
5 < PLI ≤ 6	Severe to extremely high pollution
PLI > 6	Extremely high pollution

2.5.3. Potential Ecological Risk Index

The Potential Ecological Risk Index (PER) provides an integrated assessment of the ecological risks associated with chemical elements found in moss samples. It combines the contamination factor (CF) and the toxic-response factor (TF) for each element using the formula 2.3:

$$PER_i = CF_i \times TF_i, \qquad (2.3)$$

where CF_i represents the contamination factor for element *i*, and TF_i is its toxic-response factor. TF values are assigned to each element according to their relative toxicities, as established in the literature. The following toxic-response factors are commonly applied: Mn and Zn (TF = 1); Cr and V (TF = 2); Cu, Pb, and Ni (TF = 5); Cd (TF = 30); and Hg (TF = 40) [270].

To assess the cumulative risk from multiple elements, the overall Ecological Risk Index (RI) is calculated as the sum of individual PER values:

$$RI = \sum_{i=1}^{n}(PER_i)_n, \quad (2.4)$$

The ecological risk is interpreted using standardized classification schemes for both the single-element (PER) and composite (RI) indices, as detailed in Table 2.4. These classifications facilitate the identification of areas with significant environmental degradation due to metal contamination.

Table 2.4. Risk Level Classifications for the Potential Ecological Risk (PER) and Ecological Risk Index (RI)

Potential Ecological Risk (PER)	Ecological Risk Index (RI)	Risk Level
PER < 40	RI < 150	Low
40 ≤ PER < 80	150 ≤ RI < 300	Moderate
80 ≤ PER < 160	300 ≤ RI < 600	Considerable
160 ≤ PER < 320	RI ≥ 600	High
PER ≥ 320	—	Extreme

2.6. Spatial Distribution Analysis

The spatial analysis was designed to (i) identify spatial patterns of element accumulation, (ii) detect potential pollution sources, and (iii) evaluate the influence of environmental variables such as climate, relief, and population density on pollutant distribution.

Geographic Information Systems (GIS) technology significantly enhances moss biomonitoring for assessing atmospheric deposition. It facilitates the creation of detailed pollution distribution maps, which are critical for pinpointing pollution sources (e.g., industrial clusters, major roads). Furthermore, GIS allows for the standardization and comparison of data across different regions and participating countries, contributing to a macro-scale understanding of air quality. Time-series analysis, enabled by compiling multi-year GIS data, reveals temporal trends in pollution. In this study, QGIS software [271] was utilized to generate spatial representations of contamination, employing the PLI to quantify and illustrate pollution levels across the studied area.

To clarify the characteristics of the sampling site, the Köppen-Geiger climate classification map at high spatial resolution (~1 km^2) for the 1991–2020 period was applied [222]. This selection was driven by the map's high accuracy, which is derived from advanced statistical techniques and contemporary climatological data sources. The fine spatial resolution permits precise identification of microclimatic boundaries, minimizing spatial uncertainty in the representation of local

conditions at the sampling location. The selected temporal frame corresponds to the World Meteorological Organization's standard 30-year climate normal [272], ensuring alignment with recent climatic baselines. The methodological rigor of the map, including validation through peer-reviewed procedures and consistency with in situ observational records, confirms its suitability for ecological and environmental research. Application of this resource enabled systematic contextualization of regional climate variability and supports replicable comparison with other studies employing the Köppen-Geiger classification system globally.

To characterize the population density at each sampling point, a 2-km radius buffer was applied. All 1-km resolution grid cells from the Global Human Settlement Layer Settlement Model (GHS-SMOD) falling within this buffer were aggregated. The GHS-SMOD classifies grid cells into distinct settlement typologies based on the Degree of Urbanization methodology. For this study, these typologies were consolidated into a five-category density scale, as detailed in Table 2.5.

Table 2.5. Population Density Classification.

Class Code	Settlement Typology (GHS-SMOD)	Description	Assigned Category
11	Very Low Density Rural	< 50 inhabitants/km²	Very Low Density
12	Low Density Rural	50–300 inhabitants/km²	Low Density
13	Rural Cluster	≥ 300 inhabitants/km² in clustered rural settlements	Rural
21	Suburban or Peri-Urban	Moderate density transitional zones	Suburban
22, 23, 30	Semi-dense Urban, Dense Urban Clusters, Urban Centres	≥ 1500 inhabitants/km²	Urban

The dominant density class for each sampling point was assigned based on the highest-order class present within its buffer, with a hierarchical rule prioritizing urban typologies [273].

The terrain at each sampling location was classified based on topographic analysis of slope angle. Areas exhibiting a slope ≤3° were designated as plains, while those with steeper gradients were classified as slopes [274]. High-resolution digital elevation data were employed to ensure accurate derivation of slope parameters [275, 276]. Relief-related variables, including slope and altitude, were considered to influence pollutant dispersion and accumulation, with plains favoring deposition and slopes facilitating redistribution processes.

In parallel, the elevation of each site was recorded via GPS. Sampling locations were subsequently grouped into three altitudinal zones: Lowland (0–500 m a.s.l.), Foothill (500–

1000 m a.s.l.), and Mountain (1000–2500 m a.s.l.). This zonation system captures elevation-dependent gradients in ecological and climatic conditions. Lowland zones are typically characterized by warmer temperatures and relatively flat terrain; foothill zones represent transitional ecosystems with moderate slopes; and mountain zones are characterized by cooler climates and pronounced high-elevation topography. Altitudinal zonation was used to evaluate elevation-dependent variations in pollutant accumulation and to distinguish between lowland and highland deposition patterns.

Site-specific mean annual precipitation was derived from a 3 arc-second geospatial data [275, 277]. The harmonized global dataset provides long-term mean annual precipitation for each grid cell. For temporal consistency with the sampling campaign, data from the specific year of sampling were used.

All environmental variables (climate group, precipitation, altitude, slope, and population density) were integrated with the elemental dataset and used as explanatory variables in subsequent statistical analyses to assess their influence on pollutant accumulation.

Spatial distribution maps were interpreted in conjunction with statistical results to identify relationships between pollution patterns and environmental factors, as well as to distinguish between local and long-range sources of contamination.

This integrated spatial approach allows for a more accurate assessment of how climate and relief modulate atmospheric deposition patterns, which is a central objective of the present study.

2.7. Conclusions for Chapter 2

The methodological framework developed in this study provides a comprehensive and robust basis for assessing atmospheric pollution using moss biomonitoring. The combination of standardized sampling protocols, complementary methods for elemental analysis, and rigorous quality control ensures the reliability and accuracy of the obtained data.

The comparative design, involving two countries with different climatic and geomorphological conditions, enables the investigation of environmental factors influencing pollutant accumulation. The integration of statistical tools such as correlation analysis, nonparametric tests, PCA, and PMF allows for the identification of patterns, relationships, and potential pollution sources within complex datasets.

The inclusion of spatial analysis through GIS, together with environmental parameters such as climate classification, altitude, slope, precipitation, and population density, enhances the interpretability of the results and supports the evaluation of environmental drivers of pollution distribution.

At the same time, certain methodological limitations were identified, particularly related to sampling design, representativeness of background levels, and potential variability introduced by environmental heterogeneity. These aspects must be considered in the interpretation of results and highlight the importance of integrated, multi-factor approaches in biomonitoring studies.

The applied methodology is suitable for large-scale environmental assessment and provides a solid foundation for the analysis and discussion of results presented in the subsequent chapters.

3. THE ASSESSMENT OF HEAVY METAL DEPOSITION IN GEORGIA USING MOSS BIOMONITORING APPROACH

3.1. First Comprehensive Baseline Moss Survey (2014–2017) in Georgia

For the first time in Georgia, a comprehensive baseline dataset for 41 elements was established through the analysis of 120 moss samples (*Hylocomium splendens* (Hedw.) Schimp., *Hypnum cupressiforme* Hedw., and *Pleurozium schreberi* (Brid.) Mitt.), which were collected across nearly the entire country between 2014 and 2017 [179]. Two complementary analytical techniques, INAA and AAS, were employed for the analysis of the collected moss species. Table 3.1 provides a complete summary of the descriptive statistics calculated for the first moss survey in Georgia.

The mean Al content was determined to be 5137 ± 3707 mg/kg, ranging from 759 mg/kg at site No. 23 (Abastumani District, Zekari Pass) to 24500 mg/kg at site No. 114 (Imereti, Chiatura). Exceptionally high concentrations were measured for zirconium, with a mean of 13.1 ± 10.7 mg/kg and a range from 1.19 mg/kg (No. 24) to 67.9 mg/kg (No. 83). The elevated Zr content observed across all moss species can be described by the Zr/Sc ratio, which was calculated to be equal to 10 on average. This value is interpreted as a reliable indicator of sediment recycling processes. Therefore, the high Zr content are associated with a crustal origin and can be explained by weathering processes affecting felsic volcanic rocks and andesites [278]. The locations of peak concentrations for Zr, along with As, Th, and U, were found to be proximal to the Tkibuli coal mine (No. 83), providing a clear explanation for the elevated levels of these elements through mining-related mobilization.

The significant contribution of Mn in the study is associated with the mining areas in Chiatura. The Chiatura mining region in western Georgia sits within one of the world's largest sedimentary manganese ore basins [279]. Manganese extraction in this area began in 1879, and over a century of intensive activity has made it a site of significant anthropogenic transformation. By 1990, total extraction had reached approximately 203 million tons [280]. The landscape is dominated by a complex of mining infrastructure, including numerous tunnels totaling roughly 200 km in length, open-cast mines, and waste heaps [280]. The region suffers from intense geodynamic processes, including landslides, rockslides, and erosion.

Table 3.1. Descriptive Statistics of Element Content (mg/kg) in 120 Moss Samples from the First Georgian Moss Survey.

Element	Range	Mean ± SD	Median ± MAD	CV%	Skewness	Kurtosis	RP
Na	101–3000	713±503	581±235	71	1.65	3.28	150
Mg	1220–11600	3545±1682	3060±770	47	1.80	4.72	2000
Al	759–24500	5137±3707	4295±1500	72	2.55	8.50	80
Cl	57.3–1080	220±150	185±63.5	68	3.26	15.1	2000
K	2030–15000	5967±1862	5935±1245	31	1.00	3.42	19000
Ca	4620–17100	8831±2882	8255±2050	33	0.68	−0.23	10000
Sc	0.17–6.58	1.39±1.09	1.11±0.4	78	2.36	6.79	0.02
Ti	68.6–2100	458±378	350±171	82	2.12	5.53	5
V	1.71–54	11.91±8.92	9.4±4.12	75	2.01	5.00	0.5
Cr	2.04–39	10.16±6.57	7.75±2.65	65	1.98	4.66	1.5
Mn	21.7–2530	238±366	141±54.7	154	5.02	27.5	200
Fe	404–14100	3631±2599	2725±1050	72	1.85	3.67	150
Co	0.23–8.12	1.93±1.45	1.43±0.61	75	1.97	4.24	0.2
Ni	1.92–24.2	6.81±4.07	5.56±1.8	60	1.81	3.96	1.5
Cu	0.13–143.07	7.04±13.15	5.54±2.26	187	9.50	98.3	10
Zn	7.15–75.2	31.6±13.0	28.9±8.9	41	0.75	0.45	50
As	0.18–83.3	2.02±7.56	1.05±0.56	375	10.6	115	0.1
Se	0.07–0.65	0.25±0.13	0.23±0.09	50	0.87	0.35	0.02
Br	2.33–25.2	6.63±2.95	6.31±1.46	44	2.42	12.5	4
Rb	2.92–34.2	11.6±6.4	10.6±3.56	55	1.57	2.84	50
Sr	17.2–157	50.2±25.2	43.9±12.9	50	1.78	4.20	50
Zr	1.19–67.9	13.1±10.7	10.6±5.32	82	2.24	6.97	0.1
Mo	0.15–2.1	0.42±0.27	0.35±0.1	66	3.20	14.4	0.5
Pb	0.18–19.1	5.46±3.23	5.57±2.33	59	0.85	2.08	1
Cd	0.01–0.58	0.18±0.12	0.15±0.07	68	1.26	1.67	0.05
Sb	0.05–1.36	0.2±0.16	0.16±0.06	80	4.52	27.6	0.1
I	0.58–11.8	2.9±1.99	2.48±1.09	69	1.89	4.70	3
Cs	0.04–2.67	0.49±0.35	0.42±0.19	73	2.64	11.9	0.2
Ba	4.98–365	70±58	51.3±23.8	82	2.17	6.23	40
La	0.34–12	2.82±2.11	2.15±0.91	75	2.22	6.20	0.2
Ce	0.32–21.7	5.0±3.8	3.75±1.75	75	2.05	5.38	0.5
Nd	0.45–10.7	2.75±2.11	2.04±0.87	77	1.92	3.77	ND
Sm	0.03–2.74	0.43±0.37	0.34±0.16	86	2.97	13.7	0.04
Eu	0.02–0.52	0.12±0.08	0.1±0.04	67	2.01	5.78	0.008
Tb	0.01–0.31	0.06±0.05	0.05±0.02	76	2.19	6.50	0.008
Yb	0.02–0.8	0.2±0.15	0.15±0.07	74	1.62	2.81	0.02
Hf	0.04–1.81	0.36±0.29	0.27±0.13	81	2.10	5.94	0.05
Ta	0.01–0.28	0.07±0.05	0.06±0.02	71	1.93	4.38	0.001
W	0.03–0.67	0.14±0.11	0.11±0.04	80	2.24	5.92	0.2
Th	0.06–2.9	0.7±0.55	0.51±0.23	78	2.13	5.42	0.005
U	0.02–1.25	0.21±0.17	0.16±0.07	81	2.68	10.9	0.01

According to the findings of Salukvadze et al. [280], mining waste containing Mn compounds serves as a persistent source of contamination for the Kvirila River. The study identifies Mn ion concentrations as high as 3.9 mg/L, nearly 40 times the permissible limit of 0.1 mg/L. Furthermore, soil contamination in some locations reaches an extraordinary 127,338 mg/kg, exceeding both EU (1500 mg/kg) and Georgian (700 mg/kg) standards. In our study, maximum concentrations of Mn (2530, 2470, and 2010 mg/kg) were observed in 2017 at the sites No. 113, 114, and 112. Despite the general limitations of terrestrial moss biomonitoring for atmospheric Mn deposition assessment [207], the extreme values recorded here are accepted as indicative of local pollution, given the region's profound local geogenic enrichment of Mn and the presence of multiple open-pit mines.

The arsenic content dataset was characterized by a single extreme value of 83.30 mg/kg, measured at location No. 87 in 2016. This outlier is attributed to proximity to the historical arsenic mining and chemical factory complex in Uravi village (Ambrolauri district, Kvemo Racha). This site represents one of Georgia's most severe Soviet-era industrial pollution legacies, where arsenic ore (realgar-auripigment) was processed for approximately 50 years until the 1990s [281]. The Uravi facility processed ore with 10-15% arsenic content, generating substantial waste including sulphide ash, metallic arsenic, and arsenic oxides, now scattered across the abandoned plant territory. The scale of contamination at Uravi is extreme, with soil samples from the former plant's sedimentation pond and workshops showing As concentrations as high as 131,000 mg/kg and 164,000 mg/kg, respectively [281]. During the 2013 flood, approximately 15 tons of white arsenic were washed from the Uravi site into the Lukhuni River [281]. This incident highlighted the vulnerability of the concrete "sarcophagus," which stores an estimated 60,000 tons of arsenic waste, and the ongoing mobilization of hazardous materials from the site [281, 282]. The contamination then flowed into the Rioni River, a major tributary of the Black Sea [283]. Later assessments confirm the persistence of this hazard. A 2020 expedition found that soil samples from Uravi continued to exceed safe limits by significant margins, with concentrations up to 6,300 mg/kg, reinforcing the ongoing risk to local residents [282]. While Georgia contains other arsenic-contaminated sites like the Tsana deposit in Lower Svaneti (where the 2020 study found levels as high as 13,000 mg/kg [282]), Uravi remains particularly concerning due to its proximity to residential areas, where courtyard samples have ranged from 27.2 to 772 mg/kg. The risk is compounded by the fact that locally grown food comprises approximately 70% of residents' diets, creating a direct pathway for chronic exposure [281]. Our study did not show As level anomalies at rest of the sites. The overall mean As concentration was calculated to be 2.02 ± 7.56 mg/kg (range: 0.18–83.30 mg/kg) [179, 284, 285].

In contrast, Sc content displayed a lower mean and variability, with a mean of 1.39 ± 1.09 mg/kg (range: 0.17–6.58 mg/kg). The spatial maximum for Sc was identified at sites No. 23 and No. 100 near Chakvistavi village (Kobuleti district, Adjara).

Titanium concentrations averaged 458 ± 377 mg/kg, ranging from 68.6 mg/kg (sample No. 93) to 2100 mg/kg (sample No. 82). The geospatial maximum was identified in the vicinity of Tkibuli (Imereti region, western Georgia), which is interpreted as a consequence of anthropogenic impacts from coal mining. Iron displayed a mean concentration of 3631 ± 2599 mg/kg, with extremes of 404 mg/kg and 14,100 mg/kg noted for samples No. 23 and No. 8, respectively. The peak Fe concentration, located in the Borjomi District of the Lesser Caucasus, is largely attributed to a natural abundance of Fe derived from upper continental crustal material.

Cobalt was also identified as a significant contributor. A mean concentration of 1.92 ± 1.45 mg/kg was determined, while the extreme values of 0.23 and 8.12 mg/kg were recorded at sampling sites No. 23 and No. 100, respectively. The maximum Co content was revealed near the village of Chakvistavi (Kobuleti district, Adjara autonomous republic). Given the absence of local anthropogenic inputs, this Co anomaly is attributed to crustal weathering.

Slightly elevated concentrations of elements were observed in *Hypnum cupressiforme* compared to *Pleurozium schreberi* and *Hylocomium splendens*. However, no statistically significant differences in mean elemental values were found among the species.

Moderate variability was observed in the content of trace elements in moss samples, with coefficients of variation (CV%) ranging from 30% to 85%. Notably higher variability was calculated for Cu, Mn, Ti, V, and As (186%, 162%, 105%, 104%, and 238%, respectively), while the smallest CV% was identified for K (31.2%). Skewness and kurtosis were found to range from 0.68 and -0.23 (for K) to 9.5 and 98 (for Cu), respectively. Elevated CV (>75%), positive skewness (>0), and kurtosis (>3) are interpreted as evidence for deviation from a normal distribution, suggesting that elemental concentrations are affected by external factors. Such a distribution may be caused by outliers associated with anomalously high concentrations or be influenced by a limited sample size [286–288].

Following the confirmation of non-normal distribution for the majority of elements, the dataset was subjected to normalization against the standard values for the Reference Plant (RP) published by Markert [289]. The boxplot in Figure 3.1 compares these normalized data for 40 elements across the three moss species.

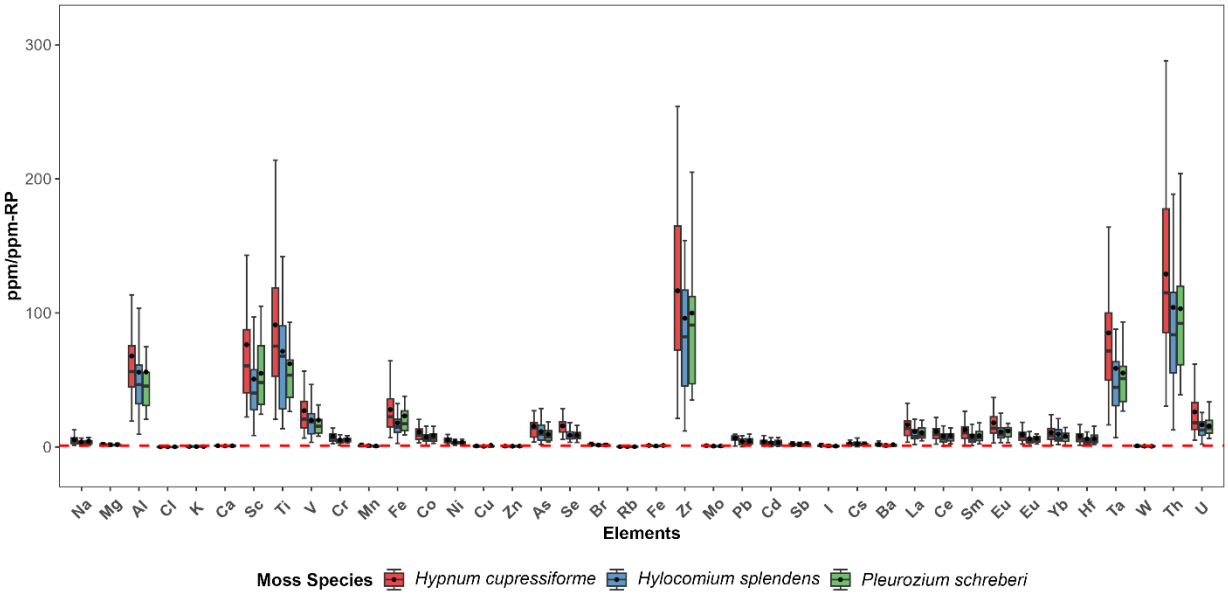

Figure 3.1. Normalized concentrations of 40 major and trace elements in the studied moss species. The dashed red line represents the normalization baseline.

Elevated normalized concentrations were observed for Al, Sc, Ti, V, Fe, As, Zr, Ta, Th, and several rare earth elements (La, Ce, Sm, Eu, Tb, Yb).

Inter-species differences in mean elemental deposition were assessed via a Tukey test. The results indicated that with the exception of the pair *Hylocomium splendens* vs. *Hypnum cupressiforme* ($p = 0.04$), no significant interspecific differences were detected (*Pleurozium schreberi* vs. *Hypnum cupressiforme*, $p = 0.35$; *Pleurozium schreberi* vs. *Hylocomium splendens*, $p = 0.79$). The significant contrast is likely explained by interspecific variation in deposition and accumulation efficiency, compounded by the non-uniform distribution of contamination across sampling localities. It is also noted that *Hylocomium splendens* was primarily located in relatively uncontaminated areas, further contributing to the observed disparity.

A comparative analysis of median elemental concentrations was conducted between the obtained results and existing literature data. The complete dataset for this comparison is given in Table 3.2. ND in the table indicates that elements were either not analyzed or fell below detection limits. For each element, the data is presented as median ± median absolute deviation for Georgia, and simply median values for the other countries, along with the range of concentrations observed.

The median values determined in this work were found to be in good agreement with those published for Macedonia [290], Bulgaria [174], and Norway [291]. Notably, higher median values were recorded for distinct element sets from each country relative to our study, specifically, Mn, Cd, and Zn in Macedonia; Mn, Cu, and Pb in Bulgaria; and Mn, Zn, Se, and Rb in Norway.

Table 3.2. A Comparative Analysis of Median Element Content in Moss: Insights from the First Georgian Moss Survey and Published Studies from Macedonia [290], Bulgaria [174], and Norway [291].

Element	Georgia, 2014–2017, (n=120)		North Macedonia, 2015 (n=72)		Bulgaria, 2015/2016 (n=115)		Norway, 2015 (n=229)	
	Median ± MAD	Range	Median	Range	Median	Range	Median	Range
Na	581±235	101–3000	190	140–380	225	79–1560	210	60–800
Mg	3060±770	1220–11600	1900	1200–3800	2080	514–8550	1350	470–3280
Al	4295±1500	759–24500	2100	750–7400	2310	569–10900	460	100–3050
Cl	185±63.5	57.3–1080	ND	ND	78.8	16.6–861	ND	ND
K	5935±1245	2030–15000	6000	3100–14000	5670	3250–14200	3560	1770–6400
Ca	8255±2050	4620–17100	6900	3500–13000	6630	606–14200	3030	1820–7230
Sc	1.11±0.4	0.17–6.58	ND	ND	0.41	0.10–3.13	0.09	0.02–1.4
Ti	350±171	68.6–2100	ND	ND	143	46.4–764	24	6–152
V	9.4±4.12	1.71–54	3.3	0.47–11	3.89	1.3–22.7	1.2	0.3–14
Cr	7.75±2.65	2.04–39	5.7	1.8–31	2.73	0.219–25	0.7	0.2–17
Mn	141±54.7	21.7–2530	160	33–510	180	39–551	400	40–1660
Fe	2725±1050	404–14100	1700	510–4600	1190	376–7240	310	78–8125
Co	1.43±0.61	0.23–8.12	0.6	0.16–2	0.59	0.197–3.29	0.2	0.06–23
Ni	5.56±1.8	1.92–24.2	3.5	0.68–63	2.1	0.45–13.5	1.1	0.4–550
Cu	5.54±2.31	0.13–143	4.6	3.0–8.3	7.36	3.2–46.88	4.2	1.8–370
Zn	28.85±8.9	7.15–75.2	30	12–66	28	9–101	31	8–409
As	1.05±0.56	0.18–83.3	0.54	0.13–1.4	0.45	0.20–3.57	0.13	0.04–4.72
Se	0.23±0.09	0.068–0.65	ND	ND	0.2	0.008–0.67	0.3	0.009–2
Br	6.31±1.46	2.33–25.2	ND	ND	2.8	1.2–9.4	ND	ND
Rb	10.55±3.56	2.92–34.2	5.3	2.2–28	7.38	2.24–50.7	12.4	1.4–81
Sr	43.85±12.85	17.2–157	25	6.5–220	25	11.3–122	13.6	3.8–60

Zr	10.55±5.32	1.19–67.9	ND	ND	ND	ND	ND	ND
Mo	0.35±0.1	0.14–2.1	0.17	0.08–0.51	ND	ND	ND	ND
Cd	0.15±0.07	0.01–0.58	0.23	0.018–0.88	0.1	0.02–1.56	0.08	0.02–1.33
Sb	0.16±0.06	0.049–1.36	ND	ND	0.11	0.04–0.51	0.07	0.007–0.38
I	2.48±1.09	0.58–11.8	ND	ND	1.28	0.48–2.99	ND	ND
Cs	0.42±0.19	0.036–2.67	ND	ND	0.207	0.072–1.8	0.16	0.02–1.63
Ba	51.3±23.75	4.98–365	42	9.7–180	46	14.2–309	25	5.3–130
La	2.15±0.91	0.34–12	ND	ND	1.35	0.39–22.6	0.32	0.07–3.5
Ce	3.75±1.75	0.31–21.7	ND	ND	2.4	0.5–29.2	0.61	0.10–4.78
Nd	2.04±0.87	0.45–10.7	ND	ND	1.3	0.2–24.1	0.23	0.01–2.24
Sm	0.34±0.16	0.031–2.7	ND	ND	ND	ND	0.05	0.004–0.38
Eu	0.1±0.04	0.023–0.52	ND	ND	0.07	0.009–0.92	0.04	0.01–0.19
Tb	0.05±0.02	0.011–0.31	ND	ND	0.03	0.005–0.42	0.01	< 0.001–0.09
Yb	0.15±0.07	0.022–0.8	ND	ND	0.1	0.03–1.08	0.003	< 0.001–0.016
Hf	0.27±0.13	0.041–1.81	ND	ND	0.16	0.04–1.44	ND	ND
Ta	0.06±0.02	0.0069–0.28	ND	ND	0.04	0.009–0.28	ND	ND
W	0.11±0.04	0.026–0.67	ND	ND	0.1	0.02–1.44	ND	ND
Pb	5.57±2.33	0.18–19.1	4.9	2.2–14	10.7	3.72–102.8	0.05	0.001–0.4
Th	0.51±0.23	0.063–2.9	ND	ND	0.39	0.09–2.8	0.03	0.007–1.5
U	0.16±0.07	0.021–1.25	ND	ND	0.12	0.03–3.2	0.006	0.002–0.08

Georgia exhibits the highest median concentrations for Na at 581±235 mg/kg, with a range extending to 3000 mg/kg, significantly surpassing the medians of approximately 190–225 mg/kg in the other three nations. A similar pattern is observed for Mg, where Georgia's median of 3060±770 mg/kg is notably higher than Bulgaria's 2080 mg/kg, North Macedonia's 1900 mg/kg, and Norway's 1350 mg/kg. For Al, a typically crustal element, Georgia again shows the highest median concentration 4295±1500 mg/kg, followed by North Macedonia (2100 mg/kg) and Bulgaria (2310 mg/kg), while Norway's median is substantially lower at 460 mg/kg. Another lithophilic element, Ti, shows a dramatic variation, with Georgia's median (350±171mg/kg) being more than double that of Bulgaria (143 mg/kg) and an order of magnitude higher than Norway's (24 mg/kg), and was ND in North Macedonia. Chlorine was reported only in Georgia and Bulgaria, with Georgia's median (185±63.5 mg/kg) more than double Bulgaria's (78.8 mg/kg). Potassium and calcium are relatively consistent across Georgia, North Macedonia, and Bulgaria, with median K values around 5600–6000 mg/kg and Ca medians between 6630–8255 mg/kg. Norway presents lower medians for both elements, at 3560 mg/kg for K and 3030 mg/kg for Ca.

For the first-row transition metals, Georgia frequently exhibits the highest median concentrations. This is particularly evident for V (9.4±4.12 mg/kg), Cr (7.75±2.65 mg/kg), Fe (2725±1050 mg/kg), Co (1.43±0.61 mg/kg), and Ni (5.56±1.8 mg/kg). In each of these cases, the Georgian median is approximately 2–10 times higher than the corresponding medians in Bulgaria and North Macedonia, and substantially higher than in Norway.

Manganese presents a different pattern, with Norway showing the highest median concentration (400 mg/kg), followed by Bulgaria (180 mg/kg), North Macedonia (160 mg/kg), and Georgia (141±54.7 mg/kg). The ranges for Mn are also wide, reaching up to 2530 mg/kg in Georgia and 1660 mg/kg in Norway.

Copper and zinc medians are relatively similar across the four countries, though Bulgaria has a slightly elevated Cu median (7.36 mg/kg) and its range extends to 46.88 mg/kg. Georgia shows a very wide range for Cu, up to 143 mg/kg. Arsenic median concentrations are low in all countries, but Georgia's median of 1.05±0.56 mg/kg is notably higher than Norway's 0.13 mg/kg, with Bulgaria and North Macedonia falling in between. Selenium was reported in all countries except North Macedonia, with medians ranging from 0.2 to 0.3 mg/kg. The median for Ce in Georgia is 3.75±1.75 mg/kg, compared to 2.4 mg/kg in Bulgaria and 0.61 mg/kg in Norway. Heavy elements like Hf, Ta, and W were only reported in Georgia and Bulgaria.

A striking difference is observed for Pb. Bulgaria shows the highest median concentration for Pb at 10.7 mg/kg, with a range extending to 102.8 mg/kg, followed by Georgia (5.57±2.33

mg/kg) and North Macedonia (4.9 mg/kg). In contrast, Norway's median Pb concentration is exceptionally low at just 0.05 mg/kg.

The extracted correlation coefficients facilitated an assessment of chemical symmetries for the elements within the moss samples [173]. A map of the inter-element correlations is presented in Figure 3.2, where low correlations (approaching -1) are displayed in cold (deep blue) colors and high correlations (approaching 1) are indicated in hot (deep red) colors. The analysis revealed high positive correlations among the majority of measured elements, with the exceptions of Cl and Cu. Correlation coefficients exceeding 0.95 were observed for the following pairs: Ti-V; Ce-Hf, Sm, Ta, Tb, U; Cr-Co, Fe, Ni; La-Co, Hf, Sm, Ta, Tb, U; Sc-Cr, Fe, Hf. Such high correlations may indicate common geochemical origins. A correlation coefficient greater than 0.6 was observed between U and Th.

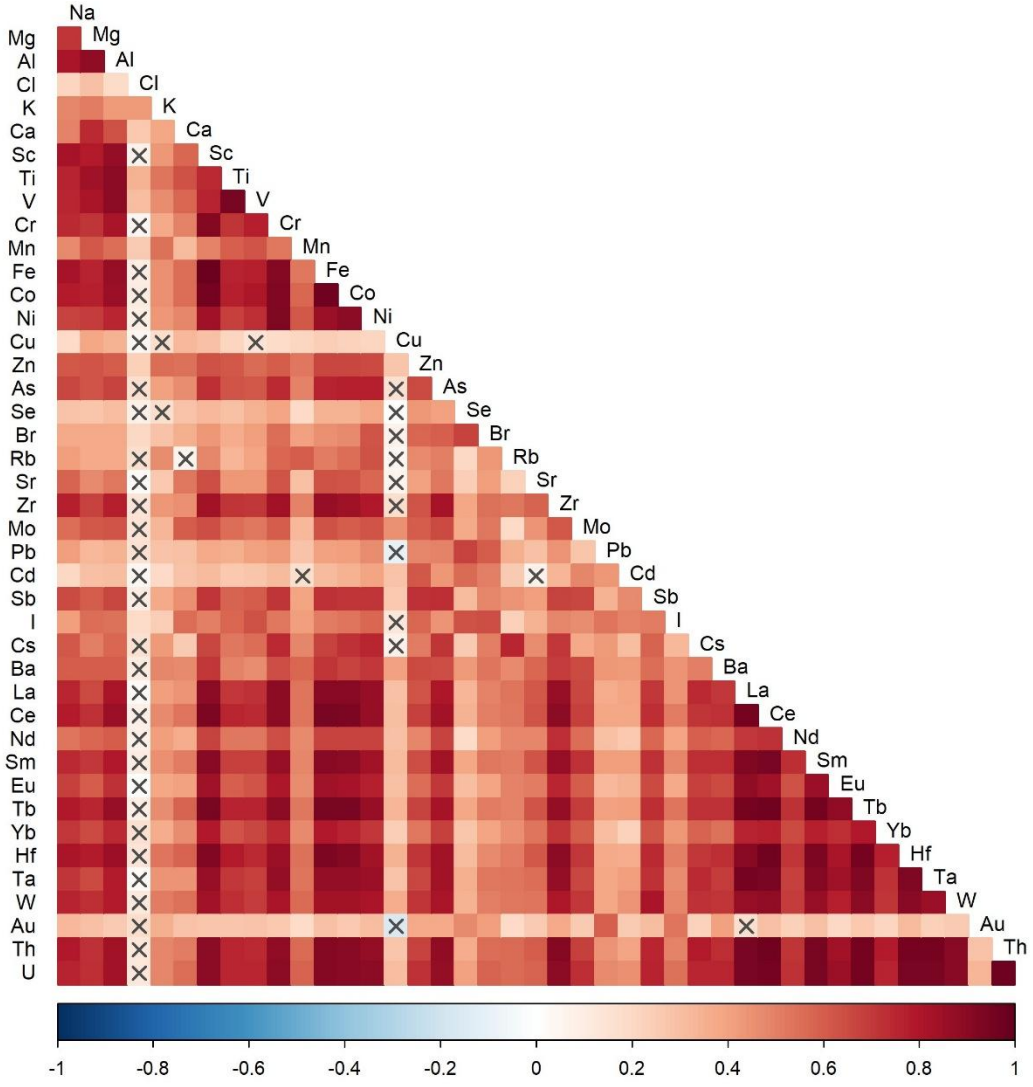

Figure 3.2. Spearman correlation matrix of measured variables from the first moss survey in Georgia.

The spatial distribution of the Pollution Load Index (PLI) was mapped utilizing a GIS technology, as presented in Figure 3.3. Peak PLI values were recorded at four sampling locations. Site No. 38 is proximate to the Tskhenistsqali River, downstream from the villages of Tsana and Koruldashi. These upstream villages are documented repositories of arsenic-contaminated waste originating from the Soviet period [281, 292, 293]. Sampling site No. 53 is located near Telavi. The surrounding area is characterized by facilities producing inert and construction materials, which are the likely source of local particulate matter. Sampling site No. 64, is located in proximity to facilities producing construction materials and asphalt. The elevated PLI at sampling site No. 12 is likely due to the local geology, which is characterized by Pleistocene andesitic-to-dacitic lava formations within a volcanic mountain environment [294, 295]. Furthermore, elevated risk to human and environmental health was identified at secondary clusters. These include sites: No. 44 and No. 97, situated near the Kutaisi Auto Mechanical Plant and Zestafoni Ferroalloy Plant respectively; sites No. 82–84, influenced by coal mining activities in Tkibuli; and sites No. 112–114, associated with the Chiatura mining complex.

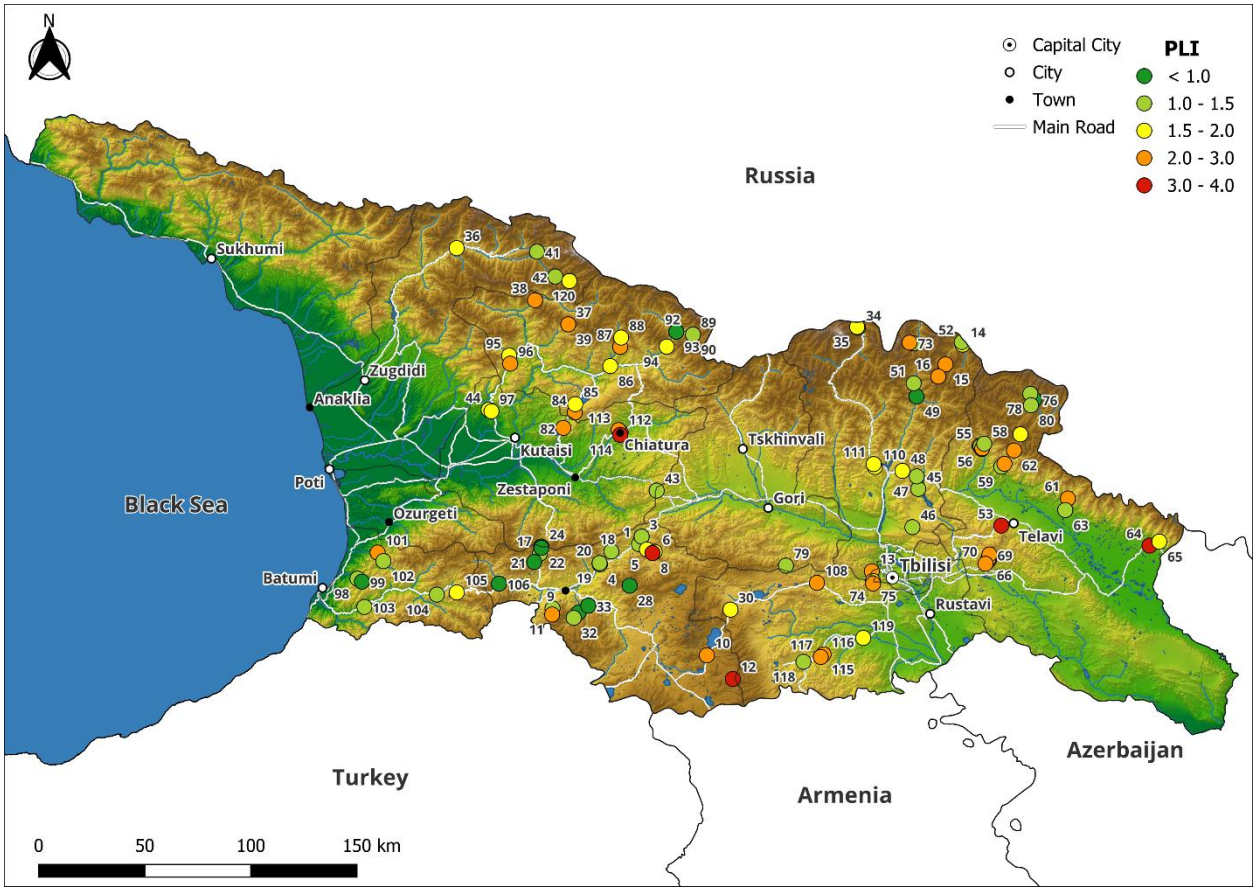

Figure 3.3. Spatial distribution of the Pollution Load Index (PLI) across the first moss survey in Georgia.

A Potential Ecological Risk Index (PER) assessment was conducted for the elements Zn, As, Cr, Pb, Ni, Cu, and Cd. According to the PER classification Zn, Cr, Pb, Ni, and Cu were found

to pose negligible ecological risk, whereas considerable risk was identified for As and Cd. The latter point can be explained by the impact of mining activities, such as As mining in Uravi, gold-copper mining in Kazreti, and Mn mining in Chiatura.

The ternary diagram for Sc-La-Th is illustrated in Figure 3.4, with comparative data like the compositional data for the upper continental crust (UCC), compiled by Rudnick and Gao [296], the values reported for Norway in the moss survey by Steinnes et al.[291], and reference plants (RP) element concentrations established by Markert [289].

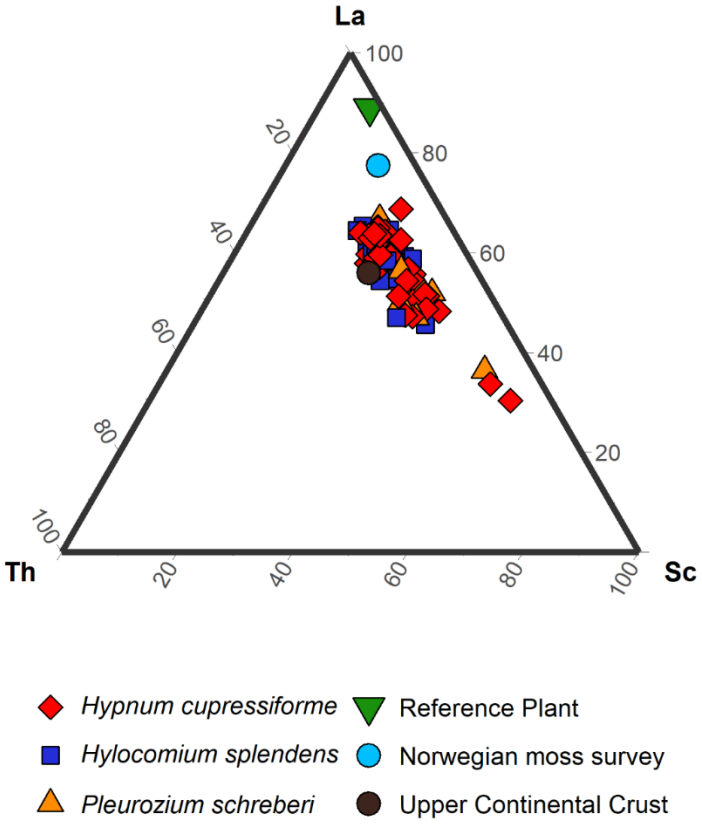

Figure 3.4. Sc-La-Th discriminatory diagram. Comparative data includes UCC [296], Norwegian moss survey [291], and reference plants [289].

The elemental data for the moss species are distributed symmetrically and are located in close proximity to both the UCC field and the Norwegian values. A distinct separation, however, is observed from the reference plant values. This spatial relationship is interpreted as evidence of a strong crustal influence on the moss composition, as indicated by the clustering of the three moss species near the UCC field in the ternary diagram.

Cumulative variance of 51.86% was explained by the first three principal components (PCs), which had eigenvalues of 8.29, 4.34, and 2.4, explaining 28.59%, 14.95%, and 8.3% of the total variance, respectively. As the first two PCs provided sufficient explanatory power, they were

utilized for subsequent clustering. Variables were plotted based on these first two PCs and grouped using the K-means method in a Q-mode biplot (Figure 3.5A). Three clusters were revealed by the analysis. Cluster 1 (Na, Al, Sc, Ti, V, Fe, Co) was defined as geogenic elements with anthropogenic association. Cluster 2, a mixture of geogenic and anthropogenic sources, grouped elements with shared geochemical behavior (Th:U, Hf:Zr, REEs) and included As, whose presence is influenced by nearby arsenic mining. Cluster 3 (Mg, Cl, K, Ca, Mn, Ni, Zn, Br, Rb, Sr, I, Ba) was composed primarily of crustal elements. Within this cluster, Br and I were attributed to marine aerosol transport, and elevated Mn concentrations were associated with regional manganese mining.

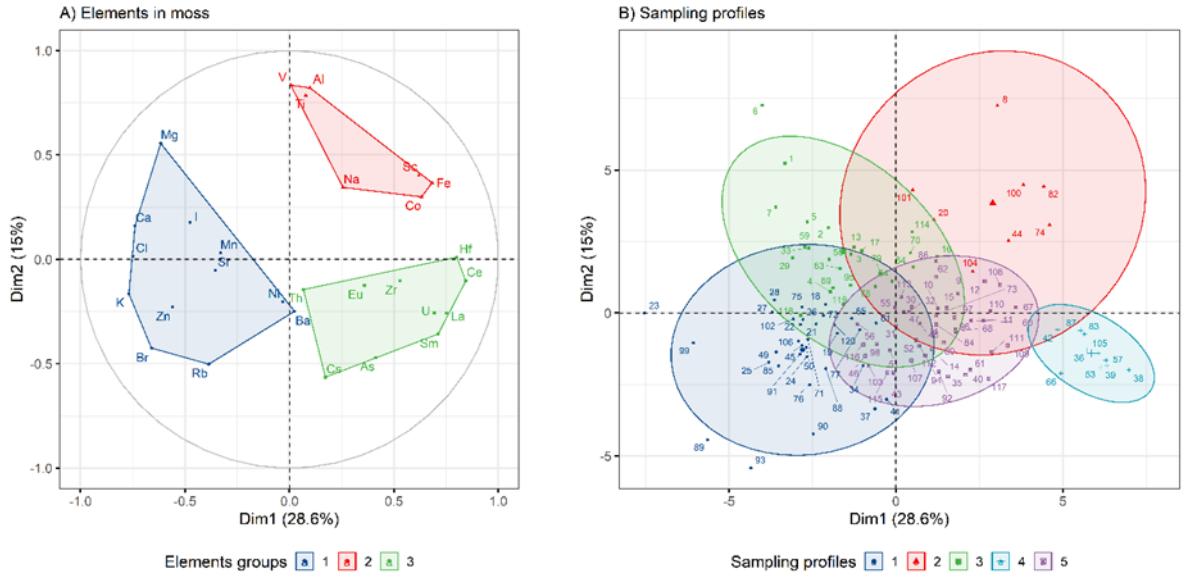

Figure 3.5. Biplot of the first two principal components analyzing 120 moss samples and 29 elements. Panel A highlights the clustering of elements (Clusters 3 and 5), and Panel B shows the corresponding distribution of moss samples from different sites based on the elemental composition.

The categorization of sampling sites was performed using R-mode PCA, with results visualized in the biplot of Figure 3.5B (95% confidence level). Five clusters are identified and grouped based on shared site characteristics. Cluster 1 consists of 44 locations. It is characterized by locations within Mn mining areas, with notable contributions from sites No. 112 and No. 113. Cluster 2, containing 10 locations, is distinguished by elevated arsenic, particularly at site No. 87 in As mining areas and site No. 38 near arsenic waste deposits. Cluster 3 consists of 25 locations and is defined by the inclusion of site No. 114, where the maximal Mn concentration was observed. The remaining locations are grouped into Clusters 4 (33 sites) and 5, both of which are characterized by a lack of identifiable proximate pollution sources.

PCA results revealed distinct clusters of neighboring sampling. A brief description of climatic regions is provided to clarify the rationale behind the clustering of sampling sites. The

climate of Georgia has been classified into three main regions: maritime subtropical humid, moderately humid subtropical, and a transitional subzone from moderately humid to Middle East highland dry subtropical climate [179, 297]. Additionally, it is demonstrated by the climatic zonation map of Tielidze et al. [297] that five distinct latitudinal and climatic zones are present. The transitional borders between these zones are reflected in the cluster formation in Figure 3.5B, with some overlap observed. In summary, the weathering and transport of elements from marine and mountainous sources are significantly influenced by predominant wind directions, the orographic effects of the Greater and Lesser Caucasus Mountains, and the distinct climatic zones of Eastern and Western Georgia. Consequently, the atmospheric accumulation of trace elements by moss species is affected by these factors, while the association with crustal rocks and soil reveals a significant and unavoidable geogenic contribution.

3.2. The Second Moss Survey in Georgia: Validation and Expansion (2019–2023)

The second comprehensive moss survey in Georgia took place from 2019 to 2023. The samples were collected from 95 distinct sites across the country. The dominant species sampled was *Hypnum cupressiforme*, supplemented by *Abietinella abietina*, *Pleurozium schreberi*, and *Hylocomium splendens* where the primary species was absent. Concentrations of Al, Ba, Cd, Co, Cr, Cu, Fe, Mn, Ni, Pb, S, Sr, V, and Zn were determined by ICP-OES, while Hg was analyzed using a DMA-80. All values are reported in mg/kg dry weight. Descriptive statistics for the 15 elements are presented in Table 3.3. The dataset for all elements is non-normally distributed and positively skewed. The highest variability was observed for Pb (CV% = 94%) and Mn (CV% = 74%), indicating potential outliers, which are discussed later. The extremely wide range for Pb (1.61 to 42.32 mg/kg) and Mn (26.2 to 835.7 mg/kg) confirms its high variability indicated by the CV. For the remaining elements, CV% values ranged from 26% to 53%. Elements like S (26%), Zn (30%), and Sr (31%) have the lowest CVs, indicating their concentrations are relatively consistent across the entire region, pointing towards more diffuse or uniform sources, such as widespread geological parent material or regional atmospheric background levels.

Table 3.3. Descriptive Statistics of Element Content (mg/kg) in 95 Moss Samples from the Second Georgian Moss Survey.

Element	Range	Mean ± SD	Median ± MAD	CV%	Q1	Q3	Percentile 90	Background
Al	674–6708	2361 ± 1106	2131 ± 616	47%	1601	2775	3862	1400
Ba	10.9–105.7	33 ± 17.5	28.6 ± 10.2	53%	20.9	43.6	54.9	17.8
Cd	0.06–0.49	0.15 ± 0.07	0.13 ± 0.03	49%	0.1	0.17	0.22	0.13
Co	0.33–3.17	0.99 ± 0.5	0.88 ± 0.22	51%	0.67	1.12	1.44	0.59
Cr	1.57–13.68	4.09 ± 1.9	3.71 ± 0.86	47%	2.88	4.58	6.02	2.69
Cu	3.81–22.08	7.56 ± 2.48	7.06 ± 1.26	33%	5.95	8.47	10.5	5.49
Fe	561–6548	1961 ± 890	1826 ± 457	45%	1370	2268	3113	1079
Hg	0.018–0.113	0.041 ± 0.016	0.037 ± 0.007	38%	0.031	0.046	0.054	0.033
Mn	26.2–835.7	141.2 ± 104.7	105.9 ± 36.7	74%	86.8	159	267	95.5
Ni	1.57–17.82	4.95 ± 2.36	4.41 ± 1.02	48%	3.48	5.55	7.77	3.77
Pb	1.61–42.32	5.38 ± 5.05	4.16 ± 1.05	94%	3.47	5.36	8.08	3.21
S	746–2281	1294 ± 331	1252 ± 199	26%	1054	1449	1703	1071
Sr	21.4–96.7	37.7 ± 11.6	36.2 ± 6.0	31%	31.3	42.6	50.2	34.8
V	1.91–19.62	5.86 ± 2.93	5.32 ± 1.41	50%	4.12	6.9	9.21	3.53
Zn	14.17–62.81	29.45 ± 8.92	28.25 ± 4.87	30%	23.3	32.7	41	23.8

The Interquartile Range (Q1–Q3) shows where the middle 50% of samples lie. For instance, for Cr, 50% of samples fall between 2.88 and 4.58 mg/kg, a relatively tight cluster. The 90th Percentile values are particularly useful for identifying upper-end concentrations that might trigger environmental concern. For example, while the median for Cu is 7.06 mg/kg, 10% of samples exceed 10.5 mg/kg, indicating localized areas of higher copper deposition.

A comparative analysis of the current biomonitoring data with prior regional and international studies [174, 179, 298, 299] is provided in Table 3.4, summarized by median values and concentration ranges.

The most appropriate local comparison is with Bulgaria [174], due to shared characteristics including sampled moss species, comparable latitudes, and influence from the Black Sea. Georgian samples exhibit significantly elevated median concentrations of lithogenic elements (Co, Cr, Fe, Ni, Sr, V), implying a stronger influence from local geochemistry. This is likely due to the geomorphology of Georgia, particularly its sloped terrain, enhances the role of soil composition through accelerated erosional processes. In contrast, median concentrations of Al, Cd, Cu, and Zn were comparable between the two countries, suggesting common anthropogenic sources such as vehicular emissions and road dust deposition. Bulgaria shows higher median concentrations for several elements, particularly Pb at 10.7 mg/kg compared to Georgia's 4.16 mg/kg, and Mn at 180 mg/kg versus Georgia's 106 mg/kg. Bulgaria's Pb levels are particularly noteworthy, as according to Hristozova et al. [174] atmospheric Pb deposition in Bulgaria has significantly declined due to the shutdown of major industrial polluters, though localized hotspots persist from remaining industrial activities and accidents. Historically, Bulgaria had the highest reported lead content in mosses among all participants in the European moss survey, primarily due to the Kardzhali lead-zinc smelter. Following its closure in 2011, both the median values and range of lead concentrations decreased markedly by the 2015/2016 survey. However, contemporary hotspots were still identified. The highest Pb levels in the 2015/2016 campaign were found near Bachkovo, attributed to tailings leaks and wastewater from fertilizer production, and near Iganovo, following a 2015 explosion at an ordnance plant. Persistent contamination was also recorded near the operating non-ferrous smelter in Plovdiv, copper-gold mines and tailings in Zlatitsa and Chelopech, and lignite coal mines in Gotse Delchev. The study concludes that while the situation improved after the Kardzhali closure, lead pollution now stems from a combination of ongoing industrial operations, legacy mining waste, and accidental industrial releases.

Table 3.4. Median and Range of Element Content (mg/kg) in Moss: Results from the Current 2020 Moss Survey, Previous 2015 Moss Survey [179], and Published Values from Hristozova et al. [174], Tepanosyan et al. [298], and Nurkassimova et al. [299].

Element	Georgia, 2019–2023 (n = 95)		Georgia, 2014–2017 (n = 120)		Bulgaria, 2015–2016 (n=115)		Armenia, 2016–2017 (n=65)		South Kazakhstan, 2019 (n=32)	
	Median	Range	Median	Range	Median	Range	Median	Range	Median	Range
Al	2131	674–6708	4295	759–24500	2310	569–10900	ND	ND	10550	33.8–40300
Ba	28.6	10.9–106	51.3	4.98–365	46	14.2–309	99.8	21.9–313	146.5	36.6–439
Cd	0.13	0.06–0.49	0.15	0.01–0.58	0.1	0.02–1.56	ND	ND	0.12	0.07–0.73
Co	0.88	0.33–3.17	1.43	0.23–8.12	0.59	0.197–3.29	3.7	0.9–15.4	3.06	0.66–10.1
Cr	3.71	1.57–13.68	7.75	2.04–39.00	2.73	0.219–25	22.3	5.7–243	16.75	2.6–60.7
Cu	7.06	3.81–22.08	5.54	0.13–143.07	7.36	3.2–46.88	14.2	5.3–212	3.95	1.59–15.3
Fe	1826	561–6548	2725	404–14100	1190	376–7240	7380	1840–29100	7940	1580–25900
Hg	0.037	0.018–0.113	ND	ND	ND	ND	ND	ND	ND	ND
Mn	106	26.2–835.7	141	21.7–2530.0	180	39–551	225	61.8–686	210.5	70.5–1260
Ni	4.41	1.57–17.82	5.56	1.92–24.20	2.1	0.45–13.5	ND	ND	7.38	0.2–36.6
Pb	4.16	1.61–42.32	5.57	0.18–19.1	10.7	3.72–102.8	6.1	2.5–34.3	3.31	1.26–43.46
S	1252	746–2281	ND	ND	ND	ND	ND	ND	ND	ND
Sr	36.3	21.4–96.7	43.9	17.2–157.0	25	11.3–122	82.5	37–286	86.25	29.3–521
V	5.32	1.91–19.62	9.4	1.71–54.00	3.89	1.3–22.7	24.4	6.5–84.0	16.65	0.47–64
Zn	28.25	14.17–62.81	28.9	7.15–75.20	28	9–101	42	22–149	65.35	22–177

Notable disparities are evident when comparing Georgia to Armenia, a neighboring country in the Caucasus with similar dominant emission sources from mining and metallurgy [298]. Median elemental concentrations in mosses were generally lower in Georgia. Armenia exhibits notably elevated levels of Ba (99.8 mg/kg), Co (3.7 mg/kg), Cr (22.3 mg/kg), Cu (14.2 mg/kg), Fe (7380 mg/kg), V (24.4 mg/kg), and Zn (42 mg/kg), with Cr and Fe concentrations being nearly six and four times higher than Georgia's recent medians. Two primary factors may explain this discrepancy. First, differences in land cover are significant: forest coverage is approximately 40.6% in Georgia compared to 11.1% in Armenia [300–302], potentially enhancing wind erosion and atmospheric dust loading in the latter. Second, a methodological bias exists, as the Armenian study predominantly utilized acrocarpous moss species (e.g., *Syntrichia ruralis*), whereas standardized protocols recommend pleurocarpous species for biomonitoring [256]. This difference in species may influence elemental accumulation patterns.

Comparison with a Kazakhstan study employing *Hylocomium splendens* near southern industrial centers [299] reveals substantially higher median concentrations for most elements in Kazakhstan, except for Cd, Cu, and Pb. Aluminum in Kazakhstan (10550 mg/kg) is approximately five times higher than in Georgia (2131 mg/kg), while Ba (146.5 vs. 28.6 mg/kg), Co (3.06 vs. 0.88 mg/kg), Cr (16.75 vs. 3.71 mg/kg), Fe (7940 vs. 1826 mg/kg), Mn (210.5 vs. 106 mg/kg), Ni (7.38 vs. 4.41 mg/kg), Sr (86.25 vs. 36.3 mg/kg), V (16.65 vs. 5.32 mg/kg), and Zn (65.35 vs. 28.25 mg/kg) all show significantly higher values in the Kazakhstan samples. These elevated concentrations likely reflect the influence of industrial activities in southern Kazakhstan, combined with regional geological characteristics and potential contributions from soil dust.

Cadmium median values were nearly identical (0.13 mg/kg in Georgia vs. 0.12 mg/kg in Kazakhstan), though maximum values were higher in Kazakhstan (0.73 vs. 0.49 mg/kg). Lead exhibited a higher median in Georgia (4.16 vs. 3.31 mg/kg), despite similar concentration ranges (Georgia: 1.61–42.32 mg/kg; Kazakhstan: 1.26–43.46 mg/kg). Copper concentrations were notably lower in Kazakhstan (3.95 mg/kg) compared to Georgia (7.06 mg/kg). This pronounced difference in Cu levels requires further study.

Comparative analysis with prior moss biomonitoring data from Georgia's moss survey 2015 indicates a general decline in median concentrations for most elements examined. Aluminum decreased substantially from 4295 mg/kg to 2131 mg/kg, Ba from 51.3 to 28.6 mg/kg, Co from 1.43 to 0.88 mg/kg, Cr nearly halved from 7.75 to 3.71 mg/kg, while Fe decreased from 2725 to 1826 mg/kg. Exceptions to this trend include Cd and Zn, whose median levels remained stable across both periods. In contrast, Cu exhibited an increase in its median value from 5.54 to 7.06 mg/kg. Mercury and Sulfur were only measured in the most recent Georgian study, with median

values of 0.037 mg/kg and 1252 mg/kg respectively, establishing important baseline data for future comparisons. Statistical evaluation via the Mann-Whitney U test revealed statistically significant differences ($p < 0.05$) between survey periods for all elements except Cd, Pb, and Zn [179, 223].

Only 33 of the original sampling sites remained identical or within a 10 km radius, permitting collection of the same moss species [179]. Analysis restricted to these locations also identified significant concentration differences for all elements between the 2014/2017 and 2019/2023 moss surveys. However, when CF (measured concentration divided by year-specific background levels) were evaluated, only minor, statistically insignificant variations for Pb and Cu were evident. Discrepancies between the two survey periods may be linked to changes in elemental bioavailability, potentially driven by variations in wet and dry deposition rates [303].

A noteworthy change between survey periods lies in the analytical method employed. The former primarily utilized INAA for elemental determination, employing AAS specifically for Cd, Cu, and Pb. The present research, however, uses only ICP-OES. NAA is a non-destructive technique capable of quantifying the total elemental content within a sample. In contrast, ICP-OES analysis follows an acid digestion step, which may be incomplete for certain refractory compounds. Consequently, these resistant phases might not be fully dissolved into the analytical solution, potentially leading to an underestimation of their total elemental contribution and affecting the accuracy of the analysis [304].

The correlation matrix (Figure 3.6) reveals strong positive correlations ($r = 0.74–0.91$) among Cr, Co, V, Al, and Fe. These high correlations are consistent with a common geogenic origin, likely indicating a shared source such as soil or mineral dust particles (e.g., from crustal weathering or natural geological deposits) [305].

The strong adsorption of vanadium onto iron oxide minerals is a widely recognized phenomenon that significantly influences its environmental distribution and concentration [306]. Several heavy metals, including Cu, Pb, Ni, and Zn, exhibit strong correlations with soil particles [307, 308]. Multiple sources may explain the strong correlation among Cu, Zn, Pb, and Cd though vehicle emissions likely represent a significant contributing source [309–313].

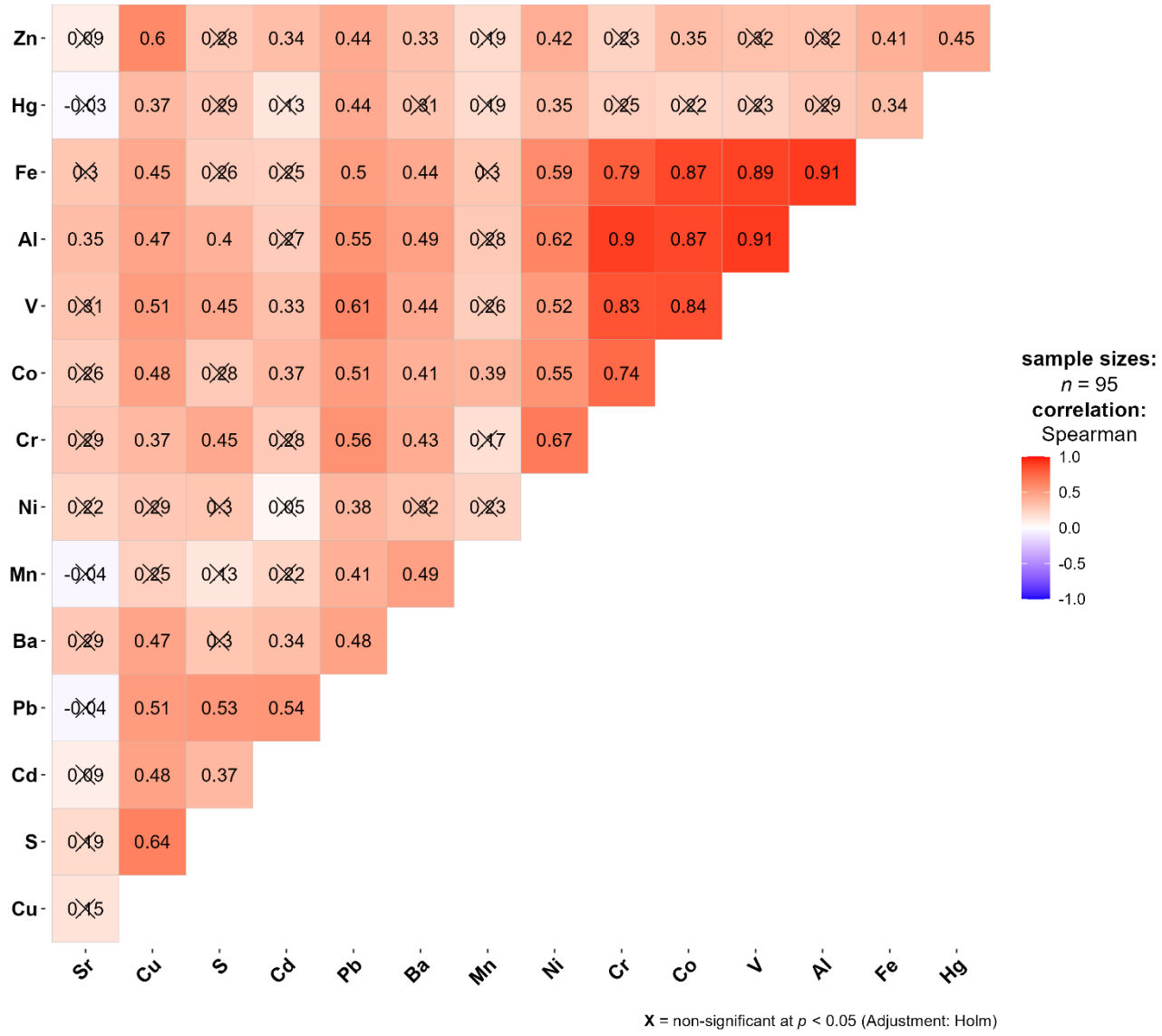

Figure 3.6. Spearman correlation matrix of measured variables from the second moss survey in Georgia.

Principal Component Analysis revealed that the first component (PC1), accounting for 43.4% of the variance, represents a geogenic signature characterized by elements such as Al, Co, Cr, Fe, and V (Figure 3.7). The highest loadings on PC1 were associated with samples from locations adjacent to agricultural fields (samples No. 87, 89, 92, 94, and 90). This pattern indicates that local farming practices, especially under dry conditions, contribute to the atmospheric release of soil particles. The open terrain in these areas likely facilitates the widespread dispersion of soil dust [314, 315].

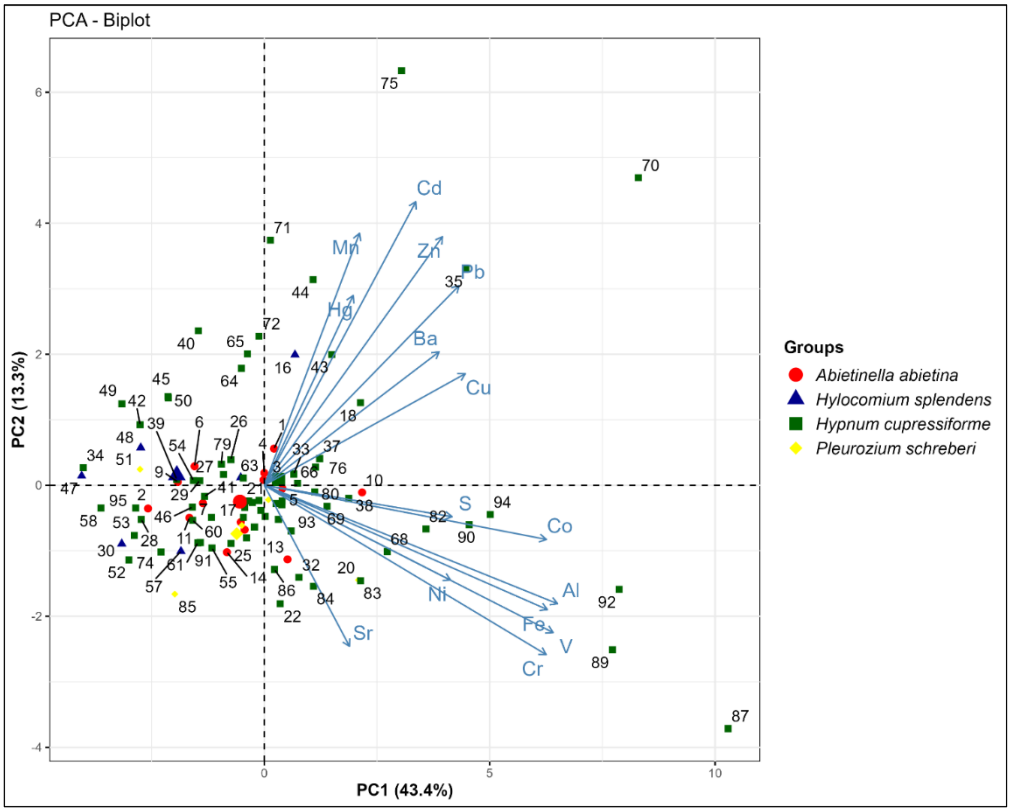

(a)

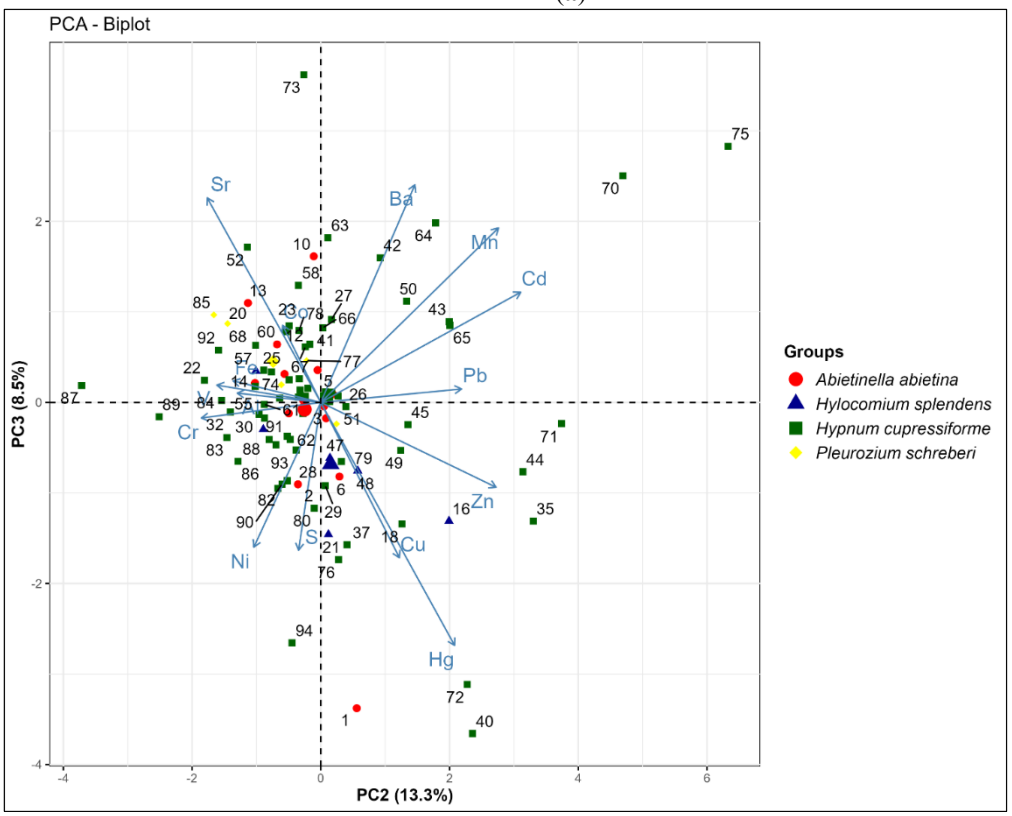

(b)

Figure 3.7. (a) Biplot of PC1 and PC2 denote the first two principal components explaining 56.7% of the variance in the data. (b) Biplot of PC2 and PC3 represent the second and third principal components explaining 21.8% of the variance in the data. Each point, distinguished by a unique combination of color and symbol, represents a sample of one of the four species. Arrows emanate from the origin, representing the variables.

The second principal component (PC2) accounts for 13.3% of the total data variance. It is characterized primarily by elevated loadings of Cd, Hg, Mn, Pb, and Zn, which are associated with anthropogenic pollution sources. These include emissions from highways, urban areas, and industrial activity, notably the Zestafoni ferro-alloy plant. Key samples representing this influence are No. 70 and No. 71 (both near Kutaisi), No. 75 (Zestafoni), and No. 35 (Rikoti Pass).

The third principal component (PC3) accounts for 8.5% of the total variance (Figure 3.7 b). Its composition is driven mainly by Ba, Cu, Hg, Mn, Ni, S, and Sr, suggesting association with local anomalies. Notable sample contributions to PC3 are observed in two distinct groups. Samples 1, 40, 72, 76, and 94 are strongly associated with the negatively loading elements (Cu, Hg, Ni, S). In contrast, samples 63, 64, 70, 73, and 75 align with the positively loading elements (Ba, Cd, Mn, Sr).

Sample 72, collected near the port city of Poti, showed elevated Cu levels likely linked to port operations. The widespread use of copper-based antifouling paints on vessels, while effective at preventing biofouling, is a chronic source of Cu pollution. The problem is acutely worsened during in-water cleaning events, which rapidly release high concentrations of copper into the local environment [316, 317]. Mercury emerged as a contaminant of particular concern at this sampling site. Its elevated concentration near the port city, at the Rioni River delta, is attributed to a combination of industrial sources and unique environmental conditions. One of such factors could be Mn mining in Chiatura [318, 319]. The Kvirila River carries manganese-rich sediments and runoff from the Chiatura mine into the Rioni River system [320]. These manganese oxides play a critical role in Hg dynamics, as they can adsorb, mobilize, and potentially enhance the bioavailability of Hg species in aquatic environments [321]. Furthermore, the unique conditions of the Black Sea, notably its extensive anoxic waters, create an environment conducive to the formation of highly toxic methylmercury [322]. Although the precise mechanisms require further study, current data indicate that the presence of manganese-rich sediments is a key factor likely enhancing both the transport and methylation of Hg within the Rioni River-Black Sea system. Consequently, developing effective monitoring and management strategies for these industrial impacts is essential. The patterns observed in remaining samples, detailed below, for items not covered, further investigation is recommended.

According to the PMF model's optimal three-factor solution, the primary source is soil dust (Figure 3.8). Its signature is defined by high loadings of lithophilic elements (e.g., Al at 64.8%, V at 63.0%, Cr at 61.2%) and siderophilic elements (e.g., Fe at 64.3%, Co at 60.5%, Ni at 49%), collectively pointing to a crustal origin.

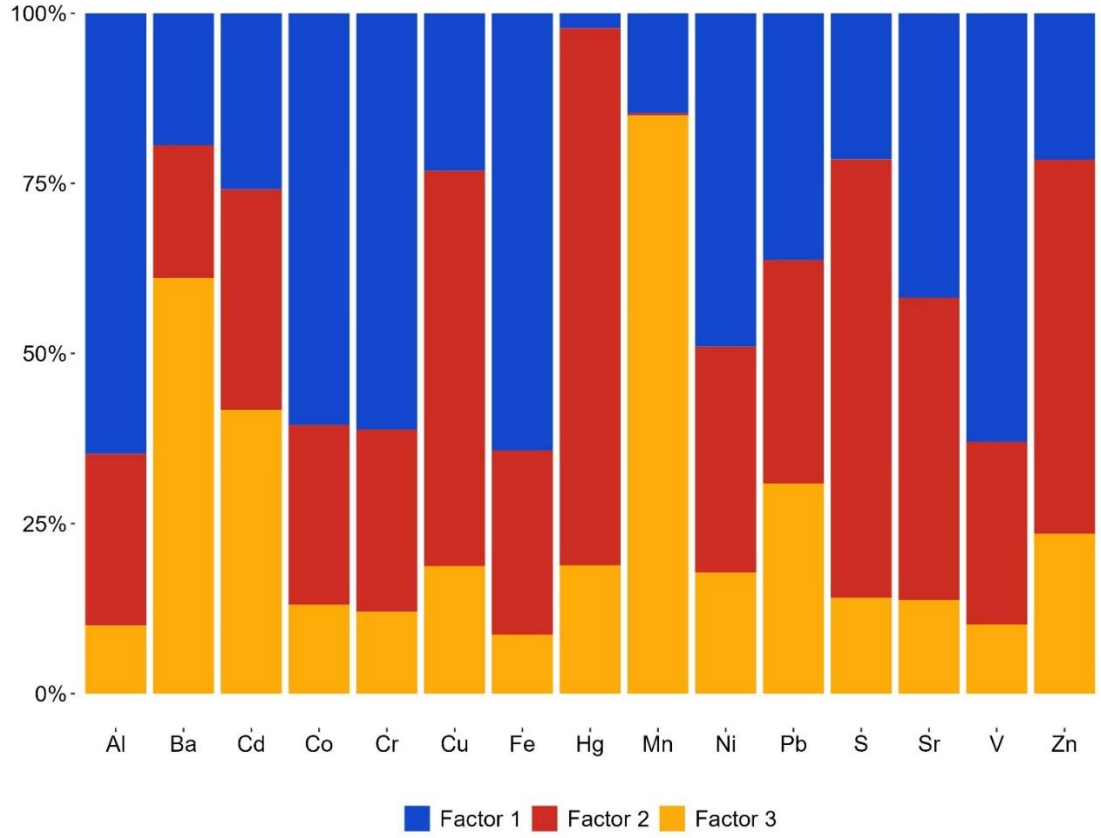

Figure 3.8. PMF analysis factor fingerprint showing the percentage contribution of three identified factors (Factor 1, Factor 2, Factor 3) across various elements measured in moss samples.

Characterized by chalcophilic elements (Hg, S, Cu, Zn), the second factor points strongly to an anthropogenic origin. These elements, which have a strong affinity for sulfur and commonly occur in sulfide minerals, show high loadings (Hg 78.9%, S 64.4%, Cu 58.1%, Zn 55%) and are commonly released through human activities like mining, industry, and improper waste disposal [323, 324].

A mixed anthropogenic-geogenic signature defines the third factor, which is strongly loaded with Mn (85%), Ba (61.1%), and Cd (41.7%). Cadmium and lead showed relatively even distributions across the three identified factors (Cd: 25.9%, 32.4%, 41.7%; Pb: 36.3%, 32.8%, 30.9%). Strontium, however, was primarily associated with the first two factors, with near-equal proportions of 41.8% and 44.4%.

The median CFs for most elements are lower in the current survey compared to previous survey, indicating a general reduction in contamination (Figure 3.9). Copper is a notable exception, with a significantly higher CF. While its mean CF decreased slightly from 1.44 to 1.38, the median actually increased from 1.04 to 1.29. The 2015 median of 1.04 was effectively at the threshold of "No Contamination" (CF < 1), whereas the 2020 median of 1.29 places it firmly within the

"Suspected" contamination category. This increase, coupled with a notable decrease in variability (SD dropping from 2.78 to 0.45), suggests that while the extreme outliers have been mitigated, a more widespread and consistent, albeit low-level, copper enrichment has become detectable across the survey area. Statistically significant differences between the two periods were observed for all elements tested, with the only exceptions being Fe and Pb, which showed no significant change (Mann-Whitney U Test, $p > 0.05$).

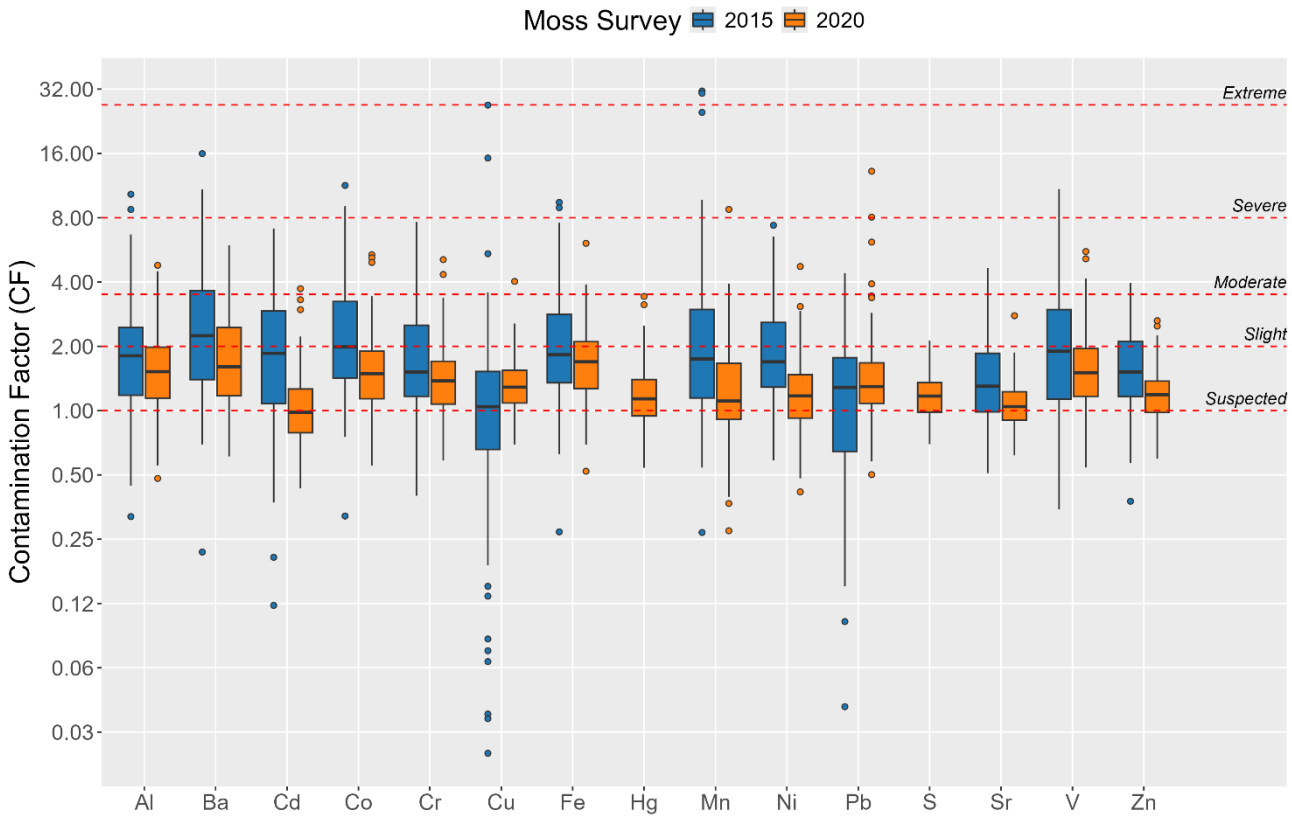

Figure 3.9. Comparison of Contamination Factors (CF) between current (95 Samples) and previous (120 Samples) moss surveys in Georgia.

Table 3.5 provides a detailed, element-by-element comparison of the CF and the overall PLI derived from the Georgian moss surveys conducted in 2015 and 2020. The data is presented using both the mean and median, accompanied by their respective measures of dispersion (Standard Deviation SD and Median Absolute Deviation MAD), offering a robust view of central tendency and variability for each element's contamination level across the sampling sites.

For the elements measured in both periods, a clear trend of decreasing CF values is most pronounced for Cd and Ni. In 2015, the median CF for Cd was 1.86 ("Suspected" contamination), but by 2020, this fell to 0.98, which falls below the threshold for "No Contamination". Similarly, Ni median dropped from 1.69 ("Suspected") to 1.17, a value now bordering on the "No Contamination" category. Other elements like Ba, Co, Mn, and V also show substantial median

reductions, generally moving from the lower end of the “Slight” category towards the upper boundary of “Suspected” or “No Contamination”.

The mean PLI fell from 1.74 to 1.41, and the median PLI decreased from 1.50 to 1.34, thus both surveys fall into the "Minimal to moderate pollution" category. The downward trend of the median, however, suggests a movement towards the lower end of this category, indicating a general improvement in overall atmospheric deposition quality. The reduction in variability (SD from 0.81 to 0.48; MAD from 0.47 to 0.22) also implies that the pollution levels across different sites have become more uniform, with fewer extreme hotspots.

Elevated CFs for Pb and Mn necessitate attention, with Mn pollution being particularly acute near Zestafoni’s industrial hub. The Zestafoni Ferroalloy Plant, processing ore from Chiatura, appears to be a key point source. This aligns with findings by Avkopashvili et al. [320], who recorded substantially higher Mn levels in soils around processing plants compared to mining regions. They attributed this disparity to airborne emissions from suboptimal ore processing, which release contaminants into the atmosphere that subsequently deposited into soils via precipitation. This study supports this pattern: Mn concentrations in mosses near the Chiatura mines (Samples 42, 43) were approximately 2.4 times lower than those near the Zestafoni plant (Sample 75).

Table 3.5. Values of Contamination Factor (CF) and Pollution Load Index (PLI) from the 2015 and 2020 Georgian Moss Surveys.

Element		Moss Survey 2015		Moss Survey 2020	
		Mean ± SD	Median ± MAD	Mean ± SD	Median ± MAD
CF	As	4.64 ± 17.41	2.41 ± 1.28	ND	ND
	Al	2.16 ± 1.56	1.81 ± 0.63	1.69 ± 0.79	1.52 ± 0.44
	Ba	3.06 ± 2.52	2.24 ± 1.04	1.86 ± 0.99	1.6 ± 0.57
	Cd	2.15 ± 1.47	1.86 ± 0.83	1.11 ± 0.54	0.98 ± 0.24
	Co	2.69 ± 2.02	1.99 ± 0.85	1.68 ± 0.85	1.49 ± 0.38
	Cr	1.99 ± 1.29	1.52 ± 0.52	1.52 ± 0.71	1.38 ± 0.32
	Cu	1.44 ± 2.78	1.04 ± 0.43	1.38 ± 0.45	1.29 ± 0.23
	Fe	2.43 ± 1.74	1.83 ± 0.7	1.82 ± 0.82	1.69 ± 0.42
	Hg	ND	ND	1.23 ± 0.47	1.14 ± 0.21
	Mn	2.95 ± 4.54	1.75 ± 0.68	1.48 ± 1.1	1.11 ± 0.38
	Ni	2.08 ± 1.24	1.69 ± 0.55	1.31 ± 0.63	1.17 ± 0.27
	Pb	1.56 ± 0.92	1.59 ± 0.66	1.68 ± 1.58	1.3 ± 0.33
	S	ND	ND	1.21 ± 0.31	1.17 ± 0.19
	Sr	1.49 ± 0.75	1.3 ± 0.38	1.09 ± 0.33	1.04 ± 0.17
	V	2.4 ± 1.8	1.9 ± 0.83	1.66 ± 0.83	1.51 ± 0.4
	Zn	1.66 ± 0.68	1.52 ± 0.47	1.24 ± 0.37	1.19 ± 0.2
PLI		1.74 ± 0.81	1.5 ± 0.47	1.41 ± 0.48	1.34 ± 0.22

Moss sampling in the vicinity of Zestafoni was not conducted in the previous moss survey. However, it should be noted that the mean Mn levels near the Chiatura mining sites were 6.5 times lower than earlier moss survey indicated [179, 223]. Several key factors may account for this notable disparity: differences in sampling sites, variations in analytical methodologies, and the recognized limitations of moss biomonitoring as a reliable measure of atmospheric manganese deposition. The use of mosses as biomonitors for atmospheric Mn deposition is complicated by several factors. Measurements are influenced by local environmental conditions, emission sources, and types. Consequently, moss Mn levels may not consistently reflect atmospheric deposition and can, in some cases, show decreases despite ongoing emissions [207].

Elevated Pb contamination factors are associated with samples collected in the vicinity of Kutaisi (Sample 70) and Lopota village (Sample 94). Lead near Kutaisi likely originates from multiple anthropogenic sources, including transport and industry, whereas the contamination at Lopota is probably linked to the recent construction of the 6-megawatt Lopota Hydro Power Station [223].

The elevated Pb concentrations observed in sample 94 could potentially be explained by contamination from sediment particles, as the sample was collected upstream, a location where, according to Tomczyk et al. [325], sediment Pb concentrations are greater than those downstream of hydro-power facilities. This potential source of contamination must be carefully considered in future studies to ensure accurate interpretation of results [223].

Variations in pollution levels across Georgia were visualized using a spatial map created in QGIS, with the Pollution Load Index (PLI) employed to quantify and highlight samples experiencing significant multi-element stress (Figure 3.10).

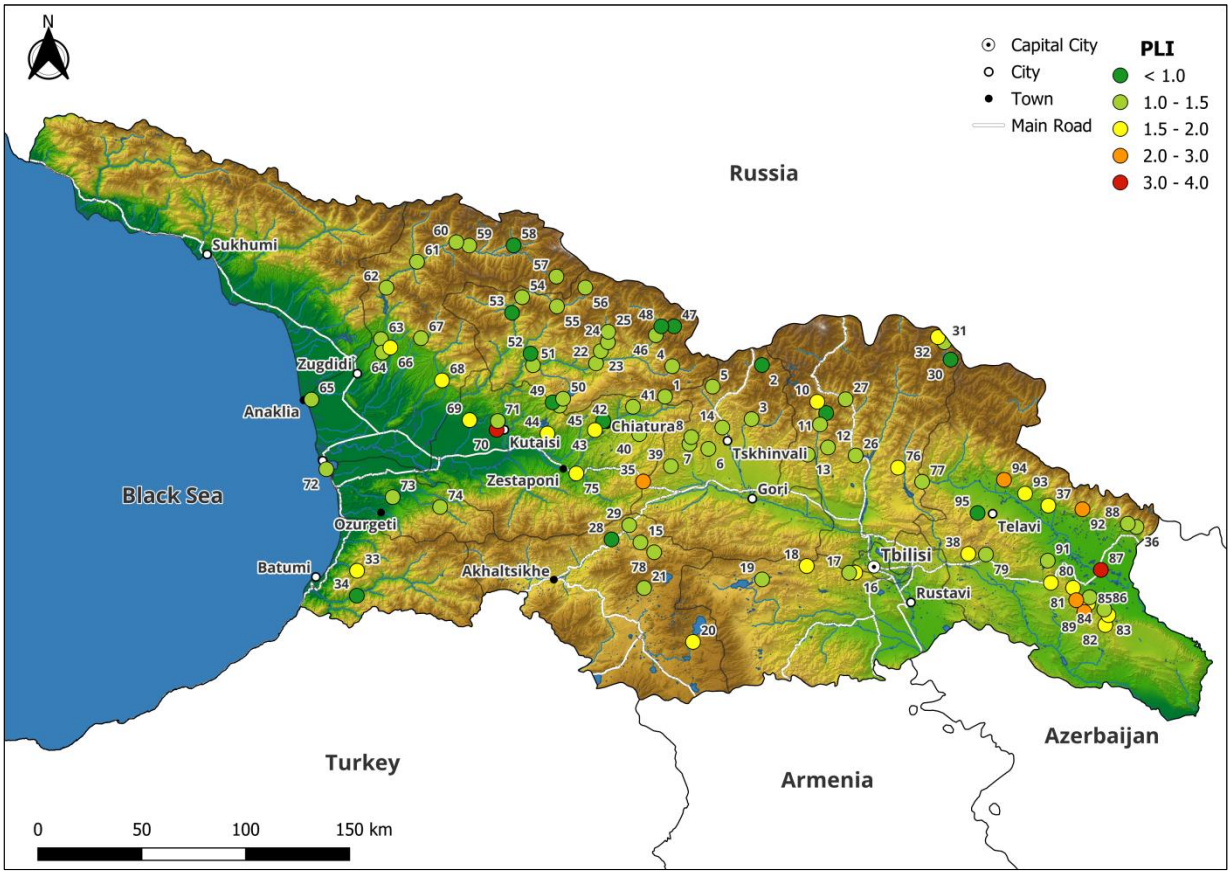

Figure 3.10. Spatial distribution of the Pollution Load Index (PLI) across the second moss survey in Georgia.

A moderate to severe pollution level was indicated by the highest PLI values, which were observed at sites No. 87 (Heretiskari) and No. 70 (Kutaisi), with recorded values of 3.21 and 3.06, respectively. The sampling location in Kutaisi, Georgia's third-largest city, is positioned about 3 km from an industrial zone that once was a crucial industrial center for the country. After the Soviet era, operations at many plants, such as the Auto Mechanical Plant (established in 1945), were ceased or substantially reduced. Present industries, including home appliance manufacturing, wood and stone processing, and metal construction, are concentrated in this zone. Furthermore, the highest $PM_{2.5}$ and PM_{10} concentrations in Kutaisi were reported by Surmava et al. [326] in close proximity to this sampling site.

Sample No. 87, collected near the village of Heretiskari and the Alazani River, exhibited the highest PLI of the study despite its location in an agricultural area, necessitating further investigation. Satellite imagery analysis revealed that the sample site was located within an old riverbed, a feature not evident on-site. It is plausible that the unusually high elemental content was caused by soil dust and river sediment transported via wind erosion onto the moss samples during drought periods [327].

The descending order of moderate PLI values (2.97 to 2.22) was observed in samples 92, 89, 94, 35, and 90. With the exception of sample 35, which is influenced by the internationally significant highway through the Rikoti Pass, the remaining samples are connected to agricultural soil particle erosion.

According to the Potential Environmental Risk Index (PER), significant risks were posed by Cd and Hg in several cases. In contrast, medium risks were identified by Pb in only two samples, with all remaining elements being characterized as low-risk (Figure 3.11).

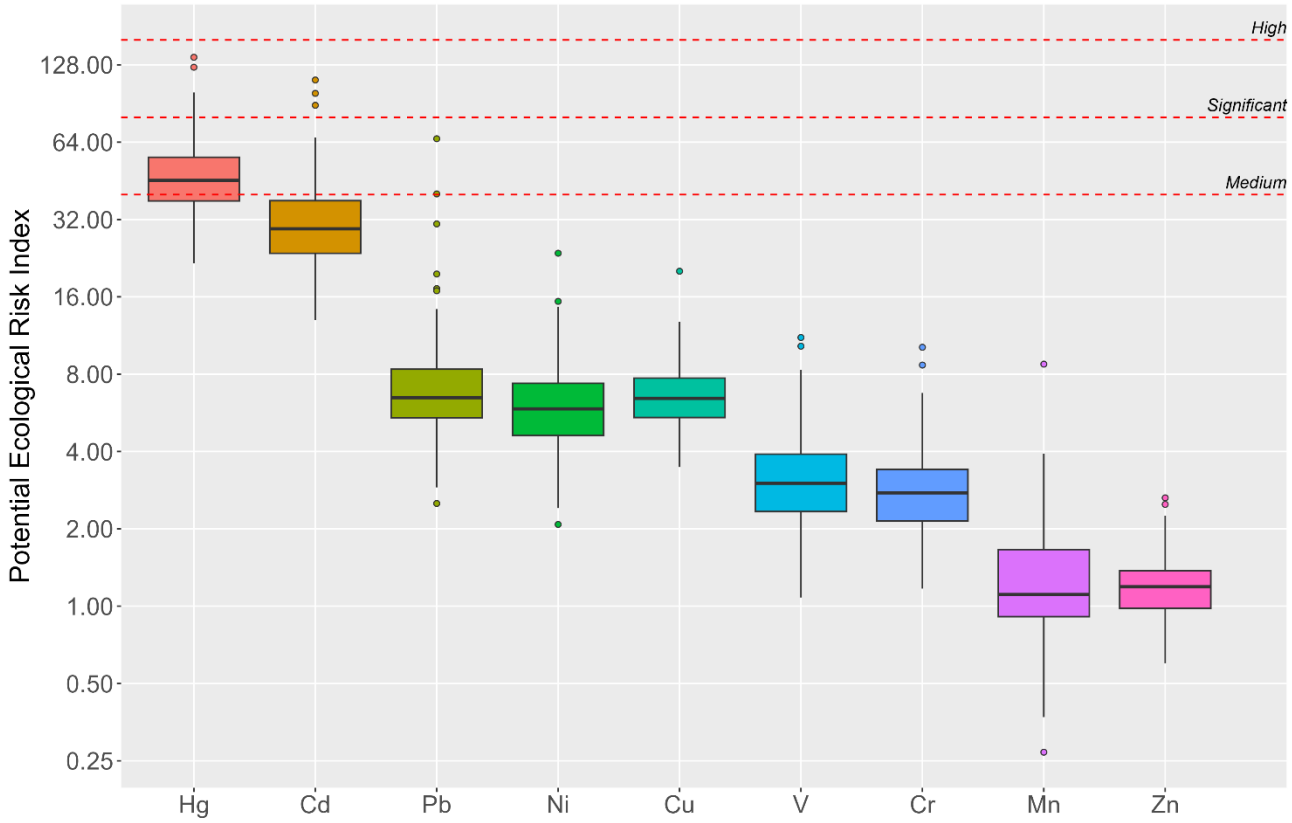

Figure 3.11. Boxplots of Potential Ecological Risk Index (PER) for selected elements accumulated by mosses.

The analysis revealed a significant PER (112) for Cd at coastal site No. 65 in Anaklia. This area was being developed for a deep-water port through the deepening of the water body and elevation of the shoreline. This elevation was achieved using excavated materials, but after construction was suspended, hazards from dust emissions from the abandoned materials emerged. A significant contribution to Cd contamination is plausibly attributed to this dust, therefore, further investigation is recommended [223, 328].

Kutaisi and Zestafoni were found to have significant Cd PER scores of 99 and 89, respectively. The substantial ecological concern indicated by these results is primarily linked to local industrial activities [320, 326, 329, 330].

Sample No. 40, found to contain the highest mercury content (0.113 mg/kg), was taken from a site roughly 5 km south of the Savane quartz sand quarry. In mineral extraction and processing, Hg is released through activities such as crushing, which liberates it from the host rock, and through atmospheric emissions and waste disposal [331]. Mercury contamination around the quarry requires assessment, and comprehensive strategies for environmental and public health monitoring and mitigation should be established.

An elevated PER of 125 was associated with sample No. 35 from Rikoti Pass. This site was impacted by the completion, in 2023, of a major 27-kilometer road section that included 65 bridges and 38 tunnels. In such contexts, anthropogenic mercury emissions are known to be generated by vehicle exhaust, motor fluids, and the abrasion of brakes and tires, and from the disturbance of geological materials through activities like drilling, blasting, and crushing during excavation. These emissions are also substantially increased by activities related to road construction and maintenance. Moreover, the release of mercury is further driven by the abrasion of paved surfaces caused by ongoing traffic [332].

The Ecological Risk Index (RI) indicated that a low level of ecological risk was present across most sampling locations. Moderate risk was confined to only 16 samples, with values ranging from 150.5 to 254.7. The highest RI values were recorded in samples No. 70 (Kutaisi) and No. 35 (Rikoti Pass), which are linked to an industrial zone and the construction of a major new east-west highway, respectively [223].

3.3. Conclusions for Chapter 3

The present study established, for the first time, a comprehensive baseline for trace element accumulation in mosses across Georgia, based on two large-scale surveys conducted during 2014–2017 and 2019–2023. Elevated concentrations of elements such as Al, Sc, Ti, V, Cr, Fe, Co, As, Se, Zr, Pb, Cd, Hf, Th, U, and rare earth elements (La, Ce, Sm, Eu, Tb, Yb) were identified, reflecting both geogenic background and anthropogenic influences. The results demonstrated that mean elemental concentrations were largely independent of moss species and sampling year, confirming the reliability of moss biomonitoring under varying environmental conditions. Multivariate statistical analysis (correlation analysis, PCA, and PMF) revealed a dominant geogenic signature associated with crustal materials derived from soil weathering, alongside significant anthropogenic contributions linked to mining, industrial activities, and transport emissions. Three principal geochemical clusters were consistently identified, including lithogenic elements (Na, Al, Sc, Ti, V, Fe, Co), mixed geogenic–anthropogenic associations involving rare earth elements and arsenic (notably influenced by historical mining activities such as those in

Uravi), and elements reflecting both marine input (Br, I) and anthropogenic enrichment (e.g., Mn from Chiatura mining and ferroalloy production). Spatial analysis confirmed a heterogeneous distribution of pollution across Georgia, with elevated contamination levels observed near industrial, mining, and urban areas, including the Zestafoni Ferroalloy Plant, Tkibuli coal mining region, and arsenic-contaminated sites such as Tsana and Koruldashi. The Pollution Load Index identified distinct hotspots, while ecological risk assessment highlighted significant contributions from As and Cd, indicating localized environmental risks associated with historical and ongoing industrial activities. Importantly, the spatial clustering of sampling sites showed clear correspondence with Georgia's latitudinal and climatic zonation, as well as with its complex mountainous relief. The observed patterns indicate that atmospheric transport, deposition, and accumulation of elements in mosses are not controlled solely by emission sources but are also significantly influenced by climatic variability (including precipitation regimes and wind patterns) and geomorphological features such as altitude and orographic barriers of the Greater and Lesser Caucasus. These factors modulate both long-range transport and local accumulation processes, contributing to the observed heterogeneity of element distribution.

The second moss survey (2019–2023) confirmed and expanded the initial findings, revealing a general decreasing trend in median concentrations for most elements, while Cd and Zn remained relatively stable and Cu exhibited a slight increasing tendency. The reduction in contamination factors and Pollution Load Index values suggests an overall improvement in atmospheric deposition quality, although localized hotspots persist, particularly in industrial and construction-affected areas such as Kutaisi, Rikoti Pass, and Anaklia. Despite these improvements, the study highlights that geogenic contributions from crustal materials represent a significant and unavoidable component of the biogeochemical system, particularly under conditions of complex terrain and active erosion. This aspect is especially relevant in regions with pronounced relief and dynamic climatic conditions, where soil resuspension and atmospheric transport processes are intensified.

Overall, the results confirm that moss biomonitoring is an effective and reliable tool for assessing atmospheric deposition in regions characterized by diverse climatic zones and complex relief. At the same time, the findings demonstrate that accurate interpretation of biomonitoring data requires the integrated consideration of emission sources, geogenic background, and physico-geographical factors. These results provide a robust foundation for the analysis of the role of climate and relief in shaping pollutant accumulation patterns.

The results presented in this chapter have been published in scientific journals indexed in the Web of Science and Scopus databases [179, 223, 285] and in the conference proceedings [284].

4. MOSS BIOMONITORING OF ATMOSPHERIC HEAVY METAL DEPOSITION IN THE REPUBLIC OF MOLDOVA

A second national moss biomonitoring survey was conducted across the Republic of Moldova to assess atmospheric deposition of potentially toxic elements. In May 2020, samples of the moss *Hypnum cupressiforme* Hedw. were collected from 41 sites distributed throughout the country. All samples were analyzed for 35 elements (Na, Mg, Al, Cl, K, Ca, Sc, Ti, V, Cr, Mn, Fe, Co, Ni, Cu, Zn, As, Br, Se, Rb, Sr, Sb, Cs, Ba, Cd, La, Ce, Sm, Eu, Tb, Hf, Ta, Th, Pb, and U) using NAA and AAS. Descriptive statistics for all elements are presented in Table 4.1. The table includes the range of observed concentrations, median ± median absolute deviation, the first quartile, third quartile, the 90th percentile, and finally the median ± MAD from the 2015 survey for direct temporal comparison.

A closer look at the major and crustal elements highlights specific trends between the 2020 and 2015 surveys. Potassium levels remained remarkably consistent, with the 2020 median (7250 ± 1000 mg/kg) aligning closely with the 2015 value (7100 ± 1500 mg/kg). Minor increases were observed for Al (3400 ± 1200 mg/kg, up from 3120 ± 1100 mg/kg) and Fe (2200 ± 600 mg/kg, up from 2100 ± 900 mg/kg). Conversely, Ca, the most abundant of these elements, experienced a slight decline, with its median falling to 9300 ± 1500 mg/kg from 9900 ± 1100 mg/kg in the previous survey.

An analysis of the trace metals and metalloids reveals a mixture of stability and change, with a notable trend toward decreasing concentrations for several elements. The most striking reductions were observed for Pb and Cd. The 2020 median for Cd (0.12 ± 0.04 mg/kg) is markedly lower than the 2015 value (0.39 ± 0.08 mg/kg), while Pb experienced a substantial drop, with its median falling to 3.1 ± 0.4 mg/kg from 12 ± 2.5 mg/kg. Copper also showed a strong downward trend, falling to 8.7 ± 1.0 mg/kg from 15 ± 3.0 mg/kg. Other elements, such as Cr and As, showed more moderate declines over the five-year period, with their medians shifting from 7.2 ± 3.1 mg/kg to 5.5 ± 1.06 mg/kg and from 0.85 ± 0.27 mg/kg to 0.77 ± 0.23 mg/kg, respectively. In contrast to these declining trends, Zn remained relatively stable, with its 2020 median of 39 ± 7 mg/kg aligning closely with the 37.2 ± 8.5 mg/kg reported in 2015.

The data for rare earth elements and other trace elements, such as La, Ce, and Sm, exhibit consistent medians between the two survey periods, suggesting stable geological background inputs. For instance, Ce shows a median of 4.6 ± 1.8 mg/kg in 2020 versus 4.4 ± 1.7 mg/kg in 2015, while La is recorded at 2.3 ± 0.6 mg/kg compared to 2.1 ± 0.8 mg/kg. Elements like Br and Sb show slight decreases, while Na and Ti display moderate increases in their median values.

Moderate variation in the mass fraction of all determined elements was indicated by CV in the 25%–75% range. It is suggested that for each element, such consistency reflects similar regional contamination levels and denotes stability in moss tissue content [288]. As demonstrated by Zhao et al. [333], particle grain size is an important indicator for variability, with CV values shown to increase significantly with larger particle size. Therefore, low CV values may be associated with very fine particles, whereas high CV values may be indicative of bigger particles.

Spatial analysis based on distribution mapping revealed pronounced spatial variability in Al content, with the highest levels detected near Balti (11,700 mg/kg), followed by Comrat (10,600 mg/kg), Briceni (9,520 mg/kg), and Chisinau (9,180 mg/kg) (Figure 4.1) [254]. A comparable pattern was observed for Fe content, which was notably elevated in moss samples collected from urban areas, particularly near Edinet (7,810 mg/kg), Balti (6,930 mg/kg), and Chisinau (6,150 mg/kg) [254]. These findings suggest that resuspended road dust and lithogenic inputs from rock weathering represent baseline sources of Al and Fe across Moldova. However, the marked increase in Al content in proximity to urban centers points to additional anthropogenic contributions, including coal combustion, motor vehicle emissions, waste incineration, and metallurgical industry exhaust gases [334]. For Fe, enhanced content levels are further attributable to fuel combustion for domestic heating, with coal and wood being the predominant fuels used in both urban and rural areas [97].

Table 4.1. Descriptive Statistics of Element Concentrations (mg/kg) in Moss Samples from the Moldova Moss Survey 2020 and a Comparative Analysis with the 2015 Campaign.

Element	2020/2022					2015/2016
	Range	Median ± MAD	Q1	Q3	Percentile 90	Median ± MAD
Al	1280 - 11700	3430 ± 1200	2515	4780	8784	3120 ± 1100
As*	0.31 - 2.03	0.77 ± 0.23	0.56	1.06	1.35	0.85 ± 0.27
Ba	24 - 117	50 ± 15	40.8	71.5	84	60 ± 24
Br*	1.07 - 7.6	3.2 ± 1.6	1.78	4	5.72	4.7 ± 1.0
Ca	5740 - 17200	9300 ± 1500	8165	11050	16200	9900 ± 1100
Cd*	0.06 - 0.56	0.12 ± 0.04	0.078	0.16	0.25	0.39 ± 0.08
Ce	1.83 - 16	4.6 ± 1.8	3.47	7.7	9.42	4.4 ± 1.7
Cl	23 - 453	110 ± 30	67.5	139	174	100 ± 40
Co	0.4 - 3.24	0.98 ± 0.29	0.7	1.32	1.96	0.79 ± 0.29
Cr*	3.2 - 21.3	5.5 ± 1.06	4.4	8.95	11.7	7.2 ± 3.1
Cs	0.18 - 1.5	0.42 ± 0.13	0.29	0.6	0.79	0.33 ± 0.14
Cu*	5.7 - 22.2	8.7 ± 1.0	7.12	9.42	11.7	15± 3.0
Eu	0.02 - 0.27	0.08 ± 0.04	0.058	0.12	0.15	0.08 ± 0.04
Fe	951 - 7810	2200 ± 600	1740	3125	4524	2100 ± 900
Hf	0.14 - 1.83	0.56 ± 0.19	0.41	0.86	1.15	0.45 ± 0.22
K	4170 - 12100	7250 ± 1000	5535	7830	9896	7100 ± 1500
La	0.78 - 8.1	2.3 ± 0.6	1.71	3.05	4.58	2.1 ± 0.8
Mn	41 - 335	90 ± 30	73.5	148	199	120 ± 50

Na	119 - 965	400 ± 120	248	506	670	308 ± 122
Ni	2.2 - 14.3	4.1 ± 1.0	3.27	5.4	7.74	4.7± 2.0
Pb*	1.56 - 8.82	3.1 ± 0.4	2.76	3.74	5.12	12 ± 2.5
Rb	3.2 - 26.6	9.9 ± 2.1	7.5	12.1	17.8	9.8 ± 3.9
Sb*	0.09 - 0.85	0.19 ± 0.04	0.15	0.26	0.41	0.25 ± 0.06
Sc	0.28 - 2.84	0.76 ± 0.24	0.59	1.07	1.61	0.69 ± 0.31
Se*	0.11 - 0.43	0.23 ± 0.04	0.18	0.26	0.29	0.32 ± 0.05
Sm	0.15 - 1.3	0.39 ± 0.14	0.28	0.57	0.77	0.31 ± 0.13
Sr	26.5 - 107	50 ± 15	38.3	68.5	92	40 ± 10
Ta	0.02 - 0.21	0.06 ± 0.02	0.046	0.095	0.12	0.06 ± 0.03
Tb	0.02 - 0.15	0.04 ± 0.01	0.032	0.068	0.087	0.05 ± 0.02
Th	0.23 - 2.5	0.73 ± 0.22	0.53	1	1.49	0.65 ± 0.27
Ti	80 - 1020	290 ± 80	207.5	379	668	230 ± 110
U	0.08 - 0.62	0.21 ± 0.07	0.16	0.29	0.35	0.22 ± 0.09
V	2.4 - 18.8	5.4 ± 1.6	3.9	8.2	13.7	5.5 ± 2.3
Zn	25 - 86	39 ± 7	32.3	47	70.4	37.2 ± 8.5

* Significantly different

The highest Zn content was recorded near Cahul (86 mg/kg), followed by Rezina (78 mg/kg), Vadul lui Voda (77 mg/kg), and Chisinau (73 mg/kg) [254]. Zinc emissions are commonly associated with vehicular activities, particularly tire wear [335]. Accordingly, transport has been identified as the primary source of Zn emissions in Moldova [336].

Elevated Cu content was observed in moss samples collected near Chisinau (22 mg/kg) and Balti (12.9 mg/kg), markedly exceeding values from other sampling sites [254]. Given Moldova's predominantly agricultural profile, the high Cu content, especially in the northern and central regions, can be attributed to the extensive use of copper-containing pesticides [254]. Such compounds are widely applied for the control of fungal and bacterial plant diseases, including downy mildew, potato late blight, fire blight, and apple scab [337].

Vanadium content was highest in Comrat (18.8 mg/kg) and Balti (18.5 mg/kg), while rural sites exhibited comparatively low values (2.4–9.3 mg/kg) [254]. This pattern supports the attribution of V accumulation to vehicular emissions, as V compounds are employed as catalysts in exhaust gas after-treatment technologies [338].

Similarly, elevated contents of Cr, Ni, As, Sb, and Pb were predominantly observed near Chisinau and Balti, underscoring the impact of urbanization and traffic density. Transport-related emissions and fuel combustion represent significant sources of Cu, V, Ni, Pb, and Sb [335, 338]. Industrial activities, including metal processing, non-ferrous metallurgy, paint and plastic manufacturing, together with waste incineration, further contribute to Cr, Ni, Cd, and Fe inputs.

The spatial distribution of Pb content indicated greater pollution levels in the central region of the country, particularly in the vicinity of Chisinau, as well as in Rezina, Balti, and Drochia [254]. The highest Cd content was detected around Cahul (0.56 mg/kg) and Rezina (0.42 mg/kg) [254]. In general, the data demonstrate that urban areas, especially Chisinau and Balti, exhibit the highest contents of the analyzed elements, confirming the spatial pattern reported by national monitoring authorities [339]. Notably, the moss bioindicator data specifically highlight the Balti region, where concentrations of nearly all analyzed elements reached peak national levels. This pronounced anthropogenic footprint is attributable to a high density of industrial point sources (registered 40 industrial manufacturers), including the Combined Heat and Power Plant "North," machinery manufacturers (e.g., "Moldagrotehnica," "Draexlmaier Automotivei"), and significant operations in construction materials ("Raut"), textiles, leather processing, and petroleum storage [254]. While the food and beverage sector dominate the industrial profile numerically, the emissions from heavy industry and energy production are likely the primary contributors to the elevated elemental deposition observed.

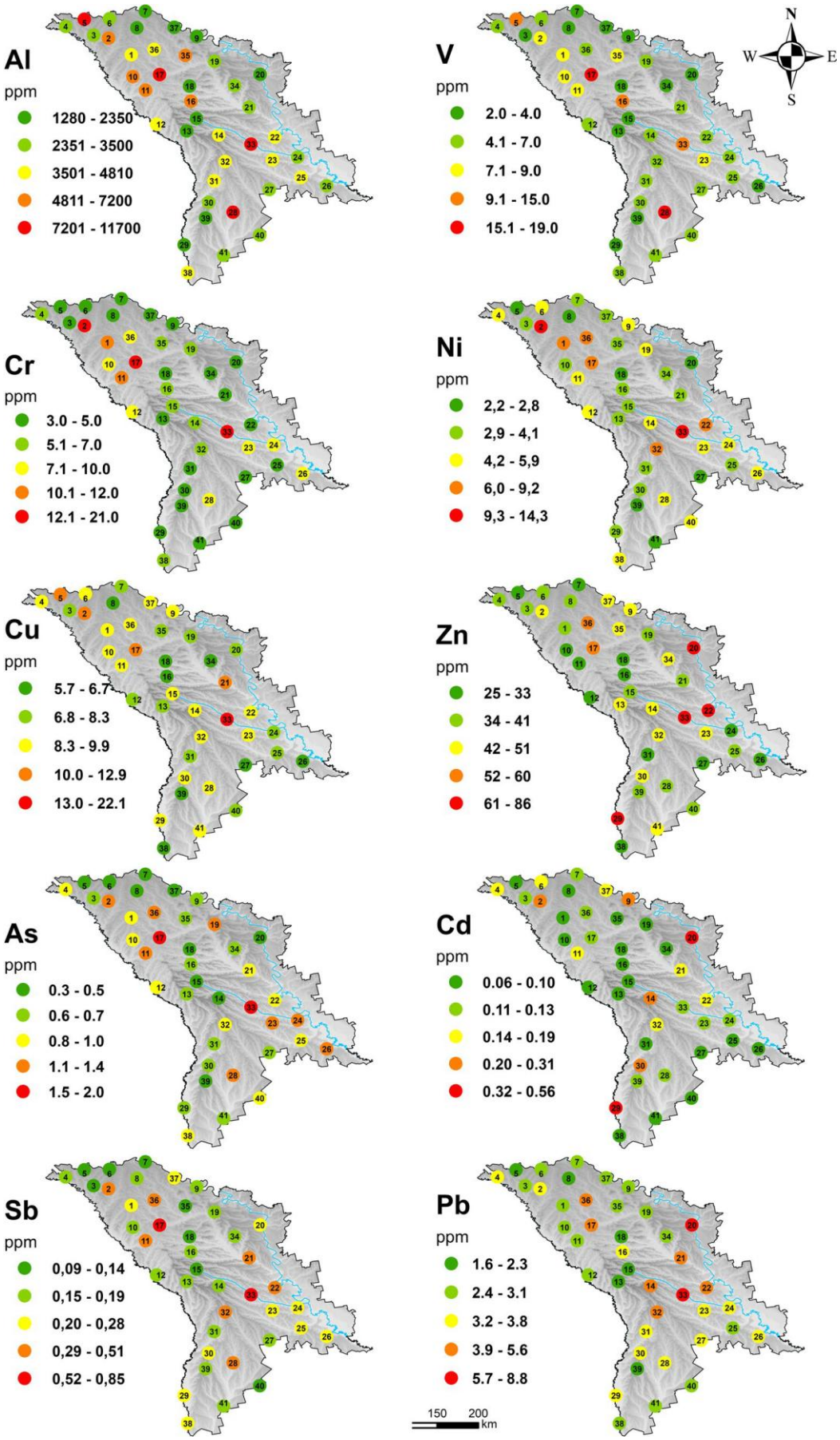

Figure 4.1. Spatial patterns of elemental distribution across the Republic of Moldova.

Comparisons between the two surveys were performed with the Mann–Whitney U test. It was determined that for most elements, measurements from 2015 and 2020 showed no significant differences ($p > 0.05$). In contrast, significant differences ($p < 0.05$) were observed for the mean mass fractions of Cr, As, Se, Br, Sb, Cd, Pb, and Cu, all of which exhibited lower median values in 2020. These disparities are potentially attributable to altered bioavailability of the elements, which may have been caused by differing wet and dry deposition rates in 2020 compared to 2015 [340].

A comparative analysis of 11 elemental concentrations at identical sampling sites between May 2015 and 2020 was conducted (Figure 4.2). Application of the Wilcoxon test revealed significant ($p < 0.05$) shifts in the median values for over half of the analyzed elements: Cr, As, Sb, Cd, Pb, and Cu. A general downward trend was evident, with mean concentrations lower in 2020 for all elements except Zn, which showed a slight increase of 8.9%. Reductions in median concentrations were most substantial for Pb (75% decrease) and Cd (66% decrease). Moderate declines were recorded for Cu (43%), and for V and Cr (31% each). The remaining elements (Al, Fe, Ni, As, Sb) demonstrated more modest decreases, all below 30%.

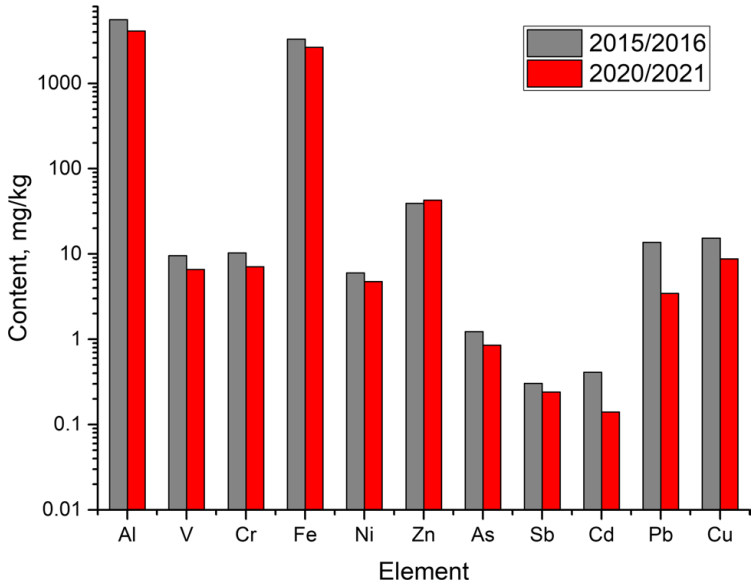

Figure 4.2. Comparison of the results from the two moss surveys in Moldova.

Interpretation of the PCA biplots (Figures 4.3) identifies key gradients and clusters in the previous and current Moldavian moss surveys. The extreme positions of Balti, Rezina, and Chisinau from the origin classify them as high-concentration outliers, a finding confirmed by their elevated elemental contents in both 2015 and 2020.

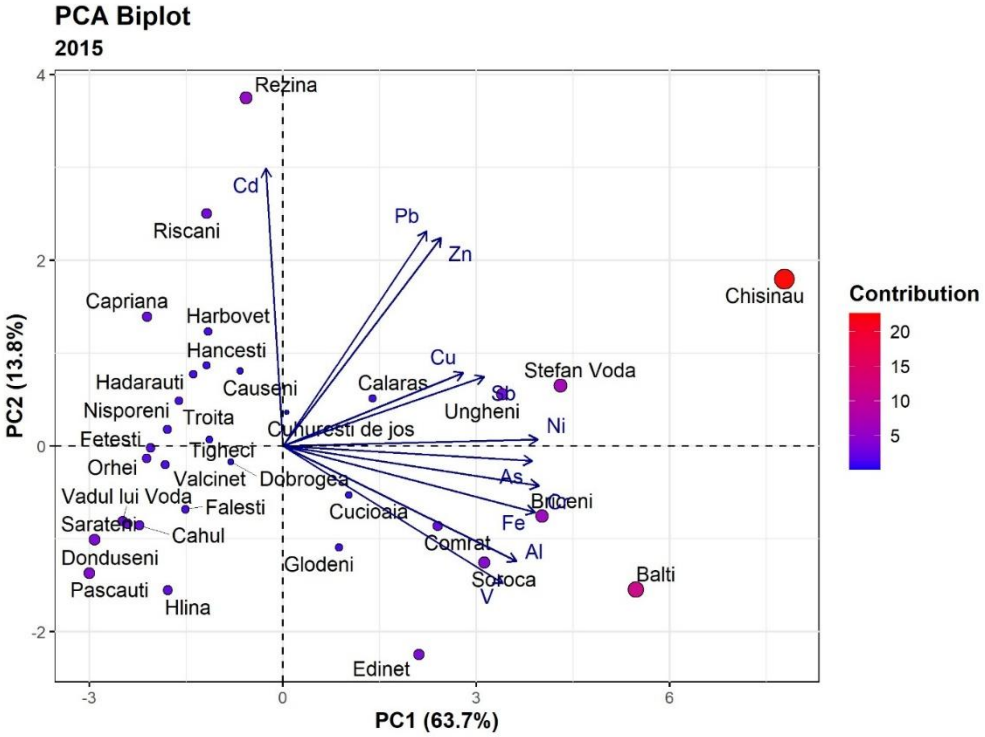

(a)

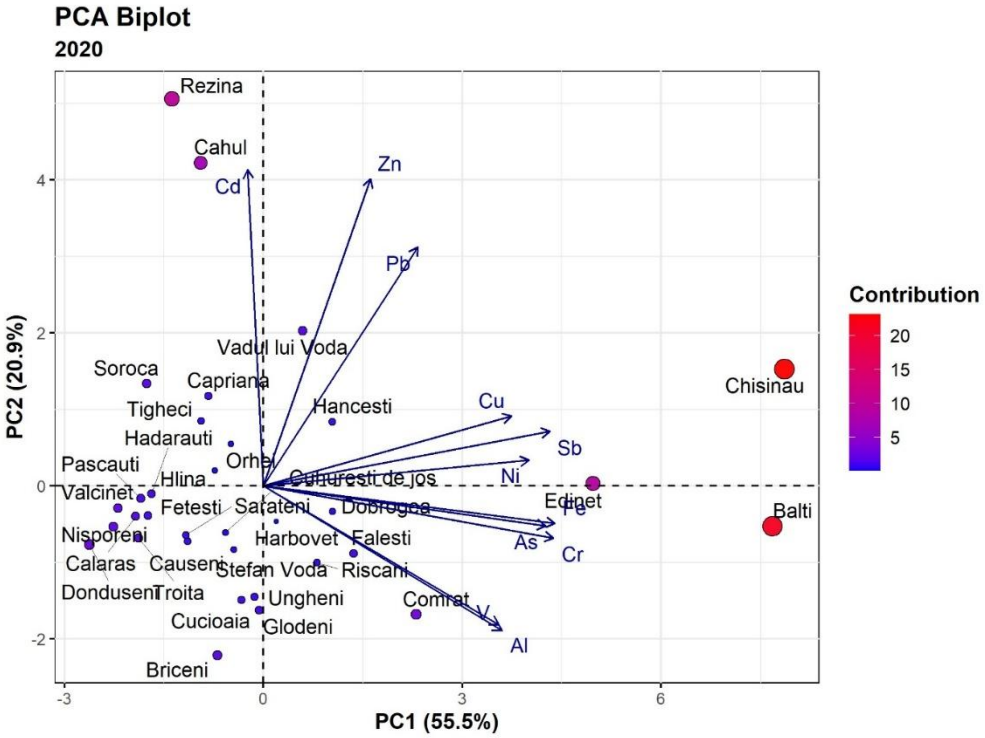

(b)

Figure 4.3. PCA biplots for the 2015 (a) and 2020 (b) surveys in Republic of Moldova. Points show individual sampling sites (colored by representation quality); vectors show component weights for each element.

Compositional similarity is inferred from spatial clustering on the diagram; the dominant cluster of rural sites (including Pascauti, Sarateni, Fetesti) suggests a common pollution profile driven by soil dust, vehicle emissions, and solid fuel combustion. Conversely, variable vectors near the origin show minimal influence, while short distances between vectors denote strong inter-element correlations [267].

The consistent strong correlations observed for specific element groups in the 2015 and 2020 surveys (Figure 4.3) indicate persistent common emission sources. The strong pairwise correlations observed for Cd, Zn, and Pb in both the 2015 and 2020 surveys point to traffic-related emissions as their dominant common source. In 2015, distinct correlation clusters were identified: one for Cu and Sb, geolocated to emissions from the Ungheni, Stefan Voda, and Chisinau areas, and another for Ni, Cr, Fe, Al, V, and As, primarily linked to sources in the Briceni, Comrat, Soroca, and Balți regions. The 2020 survey identified Chisinau as a probable source for Cu, Ni, and Sb. Additional correlations were observed for V-Al near Comrat and for As-Fe-Cr near Edineț and Balți. Overall, the consistent inter-element correlations across both sampling campaigns indicate predominant common sources for each element group. These sources are attributed to resuspended soil particles, thermal power generation, vehicular transport, and industrial activity [254].

A further comparison was made between median values from the Moldavian 2020 moss survey and corresponding data for neighboring countries (Ukraine, Romania, Bulgaria, Poland, Belarus, and Russia) from the 2015/2016 European Moss Atlas [47] (Table 4.2). Upon comparison, it was shown that, the median content of Al in Moldavian mosses stands at 3400 mg/kg, which is substantially higher than in any neighboring country. This pattern is also observed in the case of Fe, where the median value in Moldova (2200 mg/kg) significantly exceeds the values observed in Romania (1535 mg/kg), Bulgaria (1125 mg/kg), and especially Belarus (392 mg/kg). Furthermore, elements such as As, Ni, V, and Cr are also found in their highest concentrations within Moldova, with recorded medians of 0.7, 4.1, 5.4, and 5.4 mg/kg respectively. The only exception to this trend of Moldova's dominance in these elements is Romania, which surpasses Moldova in arsenic content with an average value of 1.08 mg/kg.

Conversely, Moldova records the lowest median concentration of Cd among all the countries surveyed, at just 0.1 mg/kg. This is considerably lower than the levels found in Ukraine (0.31 mg/kg) and Poland (0.21 mg/kg). Similarly, the median Pb concentration in Moldova (3.1 mg/kg) is among the lowest in the region, with only Russia (0.81 mg/kg) and Belarus (2.18 mg/kg)

showing lower values. For Zn, the values in Moldova (40 mg/kg) are observed to be lower than those recorded in Romania (40.1 mg/kg), Russia (43.1 mg/kg), and Poland (50.6 mg/kg).

Table 4.2. Comparison of the Median Element Concentrations (mg/kg) in Moldova and Adjacent Countries: 2015-2016 Moss Biomonitoring Survey [47].

	Al	As	Cd	Cr	Cu	Fe	Ni	Pb	Sb	V	Zn
Moldova	3400	0.7	0.1	5.4	8.7	2200	4.1	3.1	0.2	5.4	40
Belarus	595	0.23	0.39	ND	5.52	392	1.3	2.18	0.096	0.95	35
Bulgaria	2290	0.44	0.12	2.76	7.28	1125	2.21	10.7	0.11	3.81	28.1
Poland	967	0.38	0.21	2.22	7.6	535	2.94	4.98	0.2	1.59	50.6
Romania	2895	1.08	0.27	4.72	5.77	1535	3.11	4.2	0.2	4.32	40.1
Russia	1450	0.49	0.28	4.13	6.03	925	2.55	0.81	0.2	2.65	43.1
Ukraine	938	0.7	0.31	3.65	10.4	700	2.89	3.81	0.19	2.52	33.7

Elevated mass fractions of Al, Fe, Ni, V, and As in Moldovan moss samples are derived not only from anthropogenic sources but also from soil particles, which are typically responsible for increased elemental concentrations in moss within dry climates. In Moldova, mineral particle distribution and subsequent moss accumulation are substantially facilitated by the relatively dry weather, low precipitation, and widespread cropland [180]. The transfer of metals from soil to epigeal mosses is governed by two primary mechanisms, as outlined by Kłos et al. [341]. These include the physical resuspension and deposition of soil dust, and the chemical diffusion of metal cations via aqueous solutions that wet the moss surfaces [255]. Meanwhile, metal uptake efficiency by mosses is greatly diminished in rainy regions, where heavier rainfall is correlated with lower uptake [342].

The multivariate distribution of the elements was investigated, and the origins of their pollution sources were identified using factor and correlation analyses. The corresponding matrix of rotated factor loadings is provided in Table 4.3.

Table 4.3. Factor Loadings After Varimax Rotation and Explained Variance.

Element	Factor 1	Factor 2	Factor 3	Factor 4	Communality, %
Na	0.93	0.18	0.14	-0.02	98
Mg	0.53	0.68	0.26	0.17	95
Al	0.6	0.54	0.41	0.27	100
Cl	-0.18	0.18	0.82	-0.07	82
K	0.08	0.03	0.86	-0.15	85
Ca	0.02	-0.81	-0.06	0.38	76
Sc	0.97	0.14	0.12	-0.07	100
Ti	0.62	0.55	0.36	0.25	98

V	0.58	0.56	0.42	0.2	100
Cr	-0.91	-0.21	-0.09	0.11	94
Fe	-0.97	-0.14	-0.08	0.06	99
Co	-0.95	-0.12	-0.01	0.1	98
Ni	-0.86	0.02	-0.14	0.28	89
Zn	0.05	-0.13	-0.25	0.84	87
As	-0.87	-0.27	0	0.22	95
Br	0.46	-0.09	0.67	-0.22	91
Rb	0.89	-0.17	0.23	-0.02	94
Sr	0.24	0.81	-0.13	-0.19	87
Sb	-0.62	-0.14	0	0.61	92
Cs	-0.94	-0.24	-0.01	0.13	99
Th	0.96	0.11	0.15	-0.05	99
U	0.91	0.22	0.1	-0.25	98
Cd	-0.14	0.55	-0.19	0.61	85
Pb	0.38	0.12	0.15	-0.72	85
Cu	-0.45	0.1	-0.66	0.32	82
Expl.Var, %	**47**	**14**	**12**	**11**	

Four factors were extracted, encompassing 84% of the variability in total. Factor 1, explaining 47% of the total variance, is interpreted as representing a terrigenous source. This interpretation is supported by the high loadings of crustal tracer elements such as Al, Sc, Ti, and Th within the factor, which additionally includes Na, Cr, Fe, Co, Ni, As, Rb, Sb, Cs, and U. The dry climate and limited precipitation in Moldova promote soil erosion, which deposits windblown dust and mineral particles onto mosses. In contrast, Cr, Ni, and As are considered to be of anthropogenic origin. Support for this is provided by the highest factor scores, which were identified in the Balti and Chisinau areas (Figure 4.4). The areas with the highest mass fractions of Factor 1 elements shifted between 2015 and 2020. Initially detected at sites near Chisinau, Balti, Rezina, and Stefan Voda, the highest concentrations were later measured only in the Balti and Chisinau regions [180].

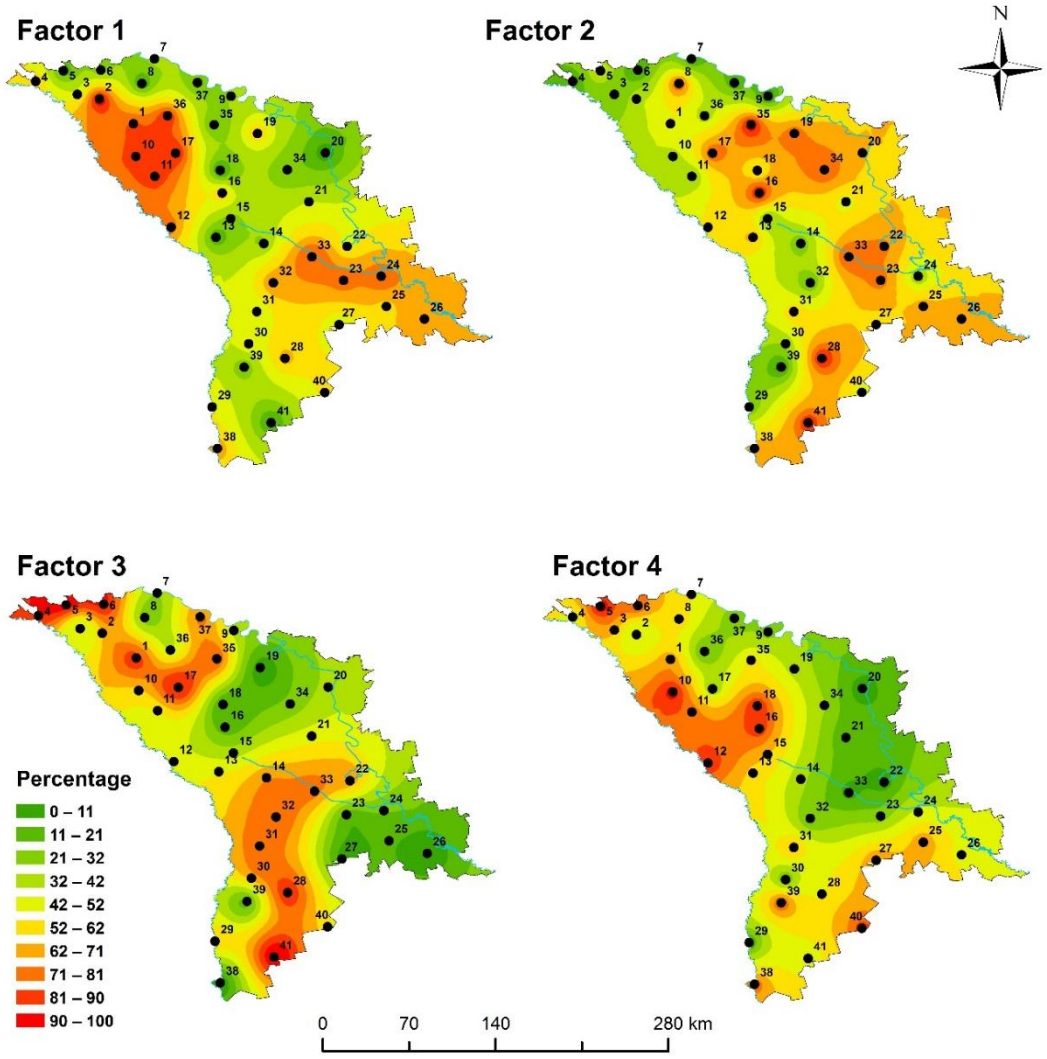

Figure 4.4. Map showing spatial distributions of Factors 1-4.

Magnesium, Ca, and Sr are linked to Factor 2, which explains 14% of the total contribution. A probable source for this elemental group is mineral extraction. In the Republic of Moldova, mineral resources are exploited from approximately 900 quarries across 411 prospected deposits, with limestone, gypsum, clay, sand, and granite [343]. Supporting this hypothesis, the most elevated mass fractions of Mg, Ca, and Sr were identified in moss specimens from regions hosting active limestone and gypsum quarries.

The third strongest factor (12% of total variability) is associated with elements indicative of agricultural activities (Cl, K, Br, Cu). Bromine and Cl are common components of fungicides and potassium fertilizers, while copper originates from micronutrient fertilizers and vineyard fungicides [306, 344, 345]. Elevated levels of Br have been documented in Moldavian soil [344].

In contrast, Factor 4 (11% of variability) presents an anthropogenic fingerprint of fossil fuel combustion, marked by Zn, Sb, Cd, and Pb. The distribution of this factor shows a clear spatial

trend, with the highest concentrations located in the north and north-east of the country (Figure 4.4).

The elemental distributions relative to Rb are presented in Figure 4.5. Correlation coefficients ranging from 0.75 to 0.90 for Cr, Fe, Ni, and As indicate that these elements are primarily of geogenic origin. Their accumulation in moss is strongly controlled by the atmospheric deposition of mineral particles generated by rock and soil weathering processes [173]. In Moldova, dry climatic conditions and limited plant cover favor soil erosion and enhance the entrainment of soil material, which readily deposits onto mosses. Nonetheless, elevated concentrations in urban areas suggest an additional contribution from resuspended road dust. Such dust is mainly produced by mechanical wear of vehicle components, road surfaces, and other traffic-related materials [288, 346].

The relatively low correlations observed for Sb/Rb and Cu/Rb ratios ($r < 0.7$) imply a combination of geogenic and anthropogenic sources. Agricultural activities represent a significant anthropogenic input, as Cu, Sb, and As are widely used in pesticide formulations applied in Moldova [347].

Clear anthropogenic signatures were identified for Zn, Cd, and Pb, as reflected by their respective ratios to Rb. The highest concentrations of these elements were found in the central part of the country, notably in Chisinau, Hincesti, Rezina, and Vadul lui Voda.

As already mentioned above, elevated concentrations of Al and V characterized samples from Chisinau, Balti, Comrat, and Briceni. In Chisinau and Comrat, elevated V concentrations are likely linked to emissions from the “Vitoil Trading” oil refinery, as well as from local thermal power plants. Although Al is typically governed by natural sources [348, 349], the weak Al/Rb–V/Rb correlation points to an anthropogenic contribution. The widespread use of coal for domestic and industrial heating, together with waste incineration, is considered the dominant anthropogenic source of Al in Moldova. The absence of identifiable local sources in Briceni suggests that long-range atmospheric transport is responsible for the observed enrichment [168].

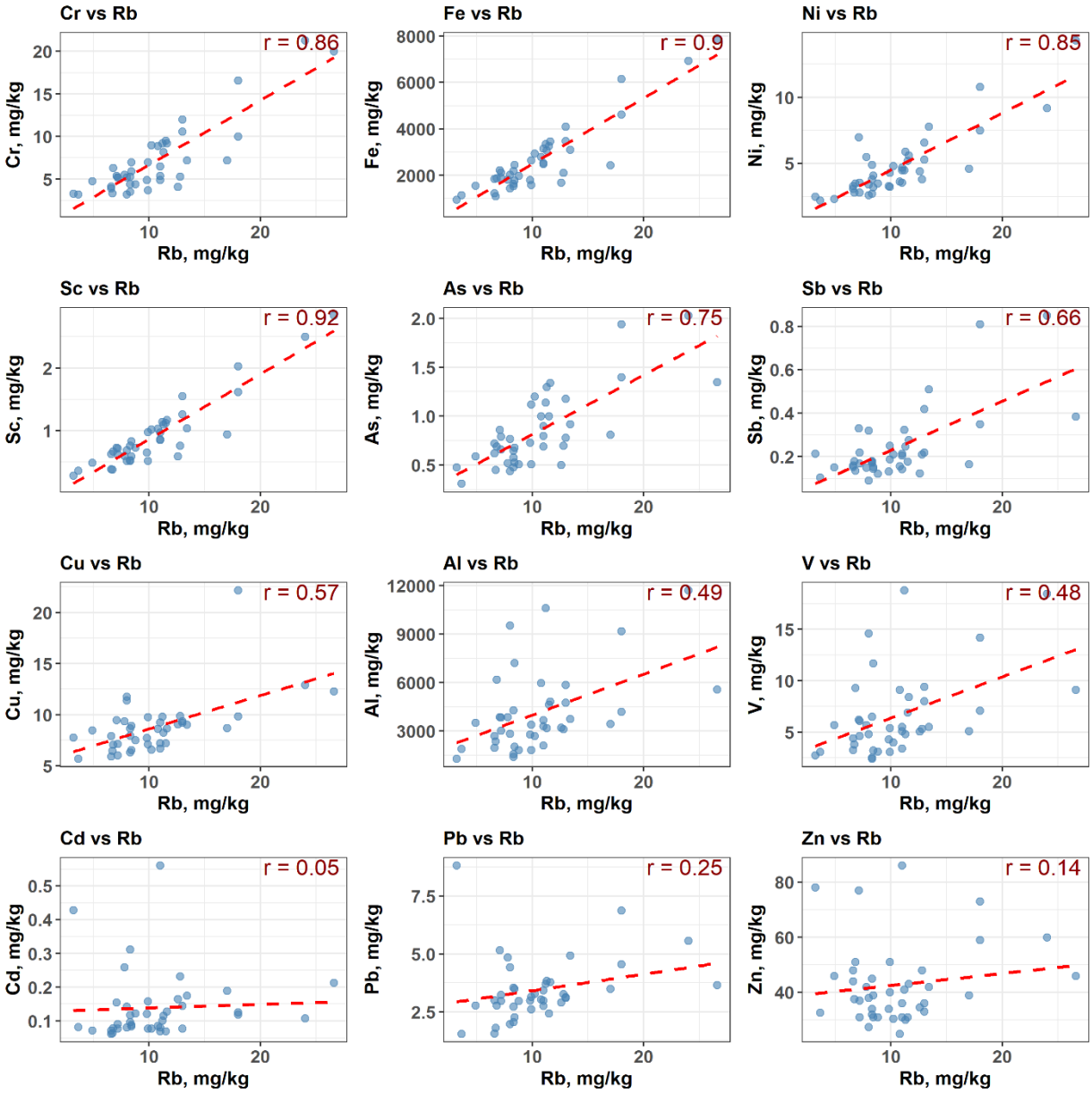

Figure 4.5. The ratio of the content of elements versus Rb content in moss samples.

The relationship between elements was assessed using correlation analysis (Figure 4.6). For clarity, the correlation matrix is presented in two parts: one for 19 naturally distributed elements, and another for 16 elements with potential mixed natural and anthropogenic origins. The correlation results are highly consistent with the factor analysis. Notably, elements characteristic of soil showed a strong positive correlation. Within the mixed-origin group, distinct associations emerged: K correlated with Cl; a Cd-Zn-Pb-Sb-Cu cluster was evident; and Co, Fe, and Cr formed a core group that correlated positively with Ni, As, V, and Cu. Furthermore, As, Sb, Ni, and Cu were intercorrelated and also showed positive correlations with V and Br, the latter of which also correlated with Se [255].

In the group of 19 elements the strong positive correlations among Al, Si, Ti, and rare earth elements, suggest a common control by aluminosilicate minerals, indicating minimal post-depositional fractionation of ambient particulate matter within the moss matrix. Turning to the 16 elements with mixed origins, K–Cl association points to agricultural influences such as fertilizer application. The Cd–Zn–Pb–Sb–Cu assemblage is particularly indicative of anthropogenic pressure, with Cd, Zn, and Pb commonly linked to non-ferrous metal smelting, road traffic (notably brake wear and tire abrasion), and long-range atmospheric transport, while Sb serves as a tracer for brake pad wear and Cu for vehicle-related emissions [350, 351].

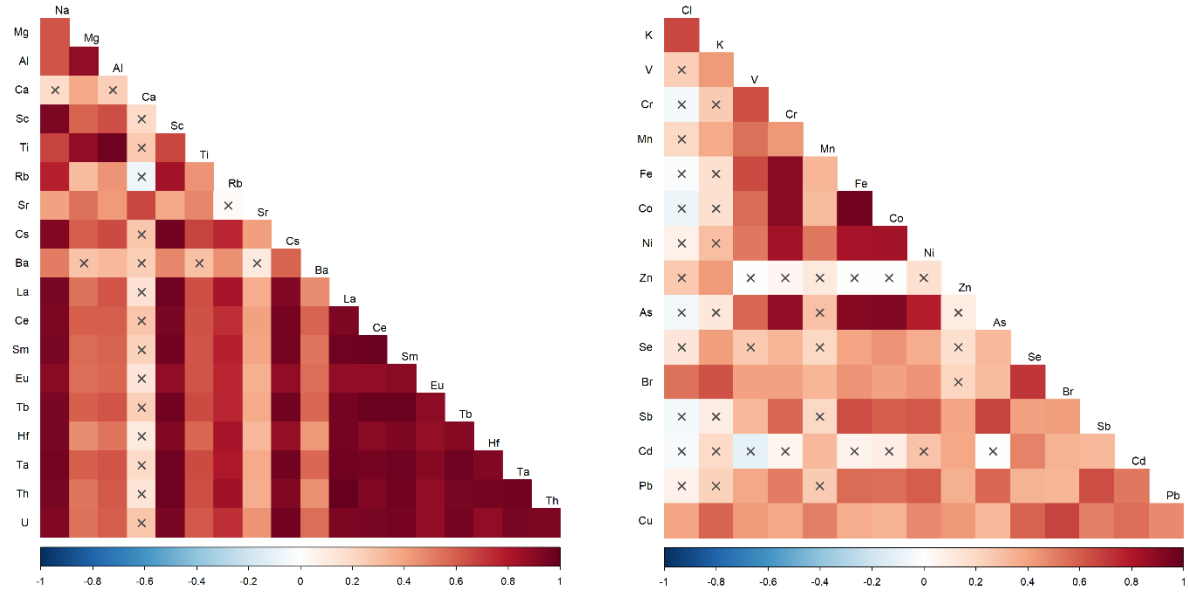

(a) (b)

Figure 4.6. Spearman correlation matrix of element content in mosses in Moldova: (a) 19 elements of natural origin, (b) 16 elements with mixed natural and anthropogenic sources.

While Fe and Cr are typically associated with crustal sources, their correlation with Ni, As, V, and Cu, elements often enriched in industrial emissions, fuel combustion, and metallurgical activities, implies that this cluster captures a gradient from natural background to anthropogenic enhancement. Notably, the intercorrelation among As, Sb, Ni, and Cu, along with their positive links to V and Br, reinforces the interpretation of a mixed industrial-traffic-combustion signature. The additional correlation of Br with Se further hints at coal combustion influences, as both elements are volatile and are released during high-temperature processes [351, 352].

To evaluate the extent of air pollution in Moldova, the Contamination Factor (CF) [353] and Pollution Load Index (PLI) [354] were applied to elements designated as priority pollutants by the European Economic Area [355]. These indices were calculated on a national scale and for the two major urban areas: Chisinau and Balti. The results are summarized in Table 4.4 and Figure 4.7.

Table 4.4. Mean Values of the Contamination Factor, and Pollution Load Index for the Entire Republic of Moldova, Chisinau and Balti.

Element	Background values, mg/kg	CF		
		Moldova	Chisinau	Balti
Cu	9.4	0.9±0.3	2.4	1.4
V	5.7	1.2±0.7	2.5	3.2
Cr	5.5	1.3±0.8	3	3.9
Fe	1820	1.5±0.8	3.4	3.8
As	0.52	1.6±0.7	3.7	3.9
Cd	0.26	0.5±0.4	0.4	0.5
Zn	42	1.0±0.3	1.1	1.4
Sb	0.15	1.6±1.1	5.4	5.6
Pb	4.8	0.7±0.3	1.1	1.4
U	0.13	1.8±0.9	4	4.1
PLI		1.1±0.4	2.4	2.3
PER		44.1		

Across Moldova, mean CF values below 1.0 for Cd indicate minimal anthropogenic impact and uncontaminated levels. While Pb and Cu CFs were also below 1.0 nationally, they exceeded this threshold in the cities of Chisinau and Balti, signaling suspected pollution level. Several elements, namely V (1.2±0.7), Cr (1.3±0.8), Fe (1.5±0.8), As (1.6±0.7), Zn (1.0±0.3), Sb (1.6±1.1), and U (1.8±0.9) display CF values above 1.0, pointing to suspected pollution.

Urban environments exhibit markedly higher contamination levels. In Chisinau, most elements show CF values in the slight to moderate range, with As (3.7), Sb (5.4), and U (4.0) reaching moderate contamination levels. Balti demonstrates comparable patterns, with Cr (3.9), Fe (3.8), As (3.9), Sb (5.6), and U (4.1) all falling within moderate contamination categories.

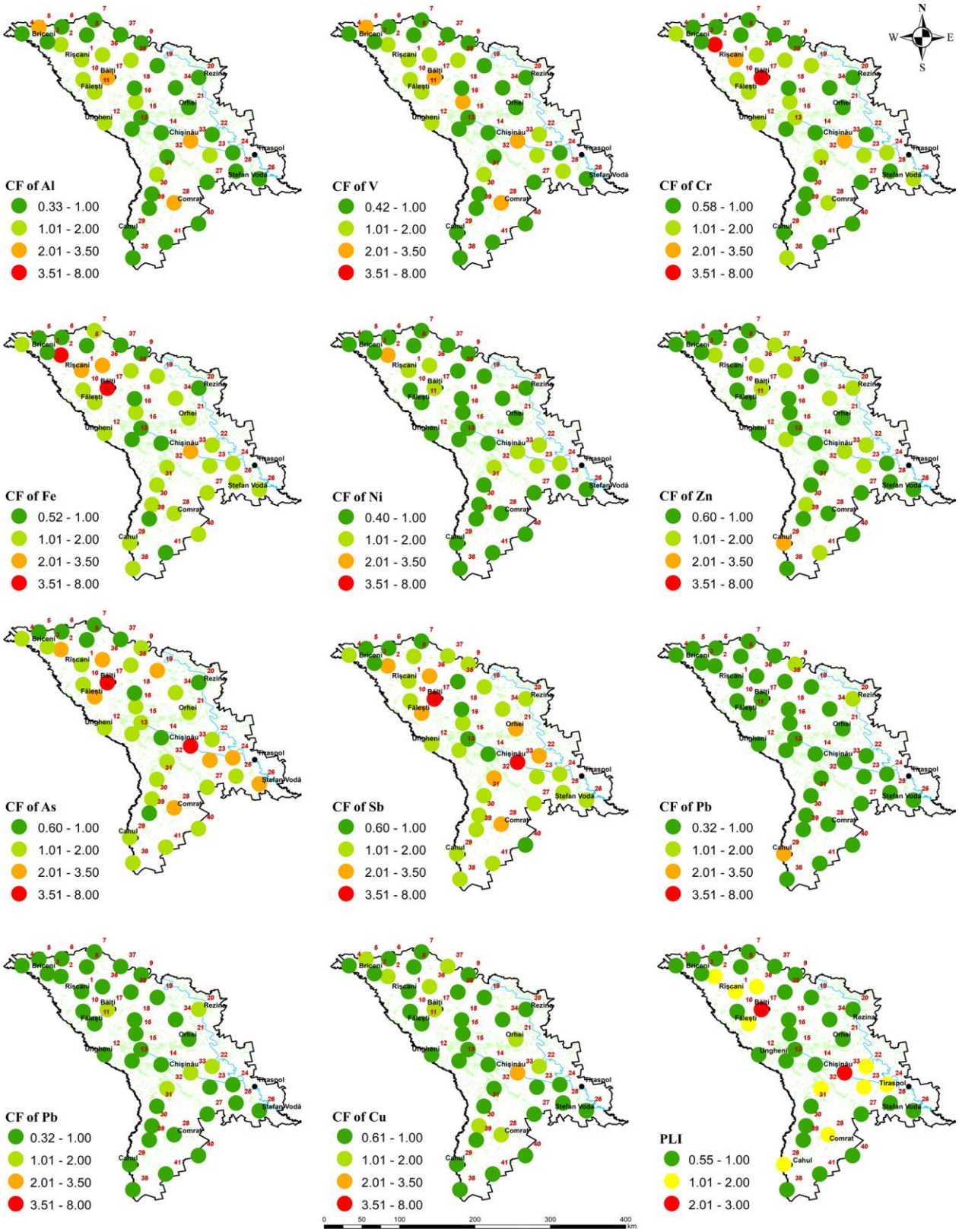

Figure 4.7. Distribution of the Contamination Factor (CF) and Pollution Load Index (PLI) values in Moldova 2020 moss survey.

Accordingly, the national mean PLI values of 1.1 indicates minimal to moderate pollution, while the cities of Chisinau and Balti, with PLI values of 2.4 and 2.3 respectively, are classified as moderately polluted.

The PER index serves as indicator of both the sensitivity of biological communities to toxicants and the risks posed by hazardous elements [288]. The single-metal ecological risk decreased in the order As > Cd > Cu > Pb > Cr > Zn, corresponding to mean PERs of 16.3, 16, 4.7, 3.6, 2.6, and 1.0. The mean RI was 44.1, indicating a low overall potential ecological risk.

4.1. Conclusions for Chapter 4

The results obtained for the Republic of Moldova demonstrate a heterogeneous spatial distribution of elements accumulated in moss samples, reflecting the combined influence of anthropogenic emissions and geogenic background. Elevated concentrations of elements such as Cu, Zn, V, Cr, Ni, Pb, and Sb were predominantly associated with urbanized and industrialized areas, particularly Chisinau and Balti, indicating the significant contribution of traffic, industrial activities, fossil fuel combustion, and agricultural practices.

Temporal analysis revealed a general decrease in the median concentrations of several potentially toxic elements, including Cr, As, Sb, Cd, Pb, and Cu, compared to the 2015/2016 survey, suggesting an overall improvement in atmospheric deposition quality. However, certain elements, such as Zn, remained relatively stable, while localized contamination hotspots persisted, particularly in urban and industrial regions.

Multivariate statistical analysis (PCA and factor analysis) enabled the identification of four principal source categories, including a dominant terrigenous factor associated with crustal elements (Al, Sc, Ti, Fe, Th), a factor related to mineral extraction activities (Mg, Ca, Sr), an agricultural factor characterized by elements such as Cl, K, Br, and Cu, and an anthropogenic factor linked to fossil fuel combustion and traffic emissions (Zn, Sb, Cd, Pb). The consistent correlations among specific element groups further confirm the presence of both geogenic and anthropogenic sources, with varying degrees of overlap.

The results indicate that environmental conditions specific to the Republic of Moldova, including relatively dry climate, low precipitation, and predominantly flat agricultural landscapes, play a crucial role in controlling the atmospheric transport and deposition of elements. Enhanced soil erosion and resuspension of fine mineral particles under these conditions significantly contribute to the accumulation of lithogenic elements in mosses, while reduced precipitation may increase the retention efficiency of deposited particles.

Spatial distribution patterns, including elevated concentrations of Al, Fe, and other crustal elements, as well as increased contamination factors in urban areas, further demonstrate that pollutant accumulation is strongly influenced by the interaction between emission sources and physico-geographical conditions. In particular, the combination of open terrain, intensive agricultural activity, and limited vegetation cover facilitates the dispersion and redeposition of particulate matter, reinforcing the role of environmental factors in shaping biomonitoring results.

The calculated Contamination Factor and Pollution Load Index indicate minimal to moderate pollution at the national scale, with moderate contamination levels observed in major urban centers. Ecological risk assessment (PER and RI) suggests generally low risk, although localized increases associated with elements such as As and Cd highlight the importance of targeted monitoring in specific areas.

The results confirm that moss biomonitoring is an effective tool for assessing atmospheric deposition in regions characterized by specific climatic and geomorphological conditions. At the same time, the results demonstrate that accurate interpretation of biomonitoring data requires the integrated consideration of emission sources, geogenic background, and environmental factors such as climate and relief. These findings provide a necessary foundation for the subsequent analysis of the influence of climatic and topographic conditions on pollutant accumulation patterns

The results presented in this chapter have been published in the in scientific journals indexed in the Web of Science and Scopus databases [254, 255].

5. CONTRASTING ENVIRONMENTAL DRIVERS OF POTENTIALLY TOXIC ELEMENT ACCUMULATION

To investigate the factors controlling elemental content in mosses, a comparative study was performed by combining two moss surveys from the Republic of Moldova and Georgia [223, 254]. The selection of a single moss species was driven by the need to control for interspecies variability in elemental uptake, a well-documented source of confounding influence in biomonitoring. This was underscored by Schröder et al. [356], who reported significant species-specific differences in the accumulation of Cd, Cu, Ni, Pb, Zn, N, and Hg. Therefore, *Hypnum cupressiforme*, geographically widespread and ecologically robust moss commonly employed in biomonitoring studies [357–360], was utilized. Moreover, it was the only species collected across both countries under study, thereby enabling a standardized comparison free from taxonomic bias. Finally, to ensure that the analysis reflected broader environmental factors rather than localized anthropogenic distortion, Grubbs' outlier test was applied at a significance level of 0.05 to identify and exclude statistical outliers from the dataset. This approach effectively removed sampling sites with anomalously high elemental concentrations attributable to point sources such as industrial facilities, mining operations, or construction activities. Following outlier removal, the dataset was reduced from 70 to 55 samples in Georgia and from 41 to 30 samples in Moldova. This filtering procedure enabled a more robust assessment of background environmental conditions, minimizing the confounding influence of local pollution hotspots and allowing clearer identification of the relationships between elemental accumulation and natural factors including climate, topography, and lithology.

Summary statistics of 13 elements and associated sampling-site characteristics are summarized in Table 5.1 for the original dataset and for a refined dataset generated by applying Grubbs' test to remove outliers and reduce the impact of local anomalies [260].

Table 5.1. Summary Statistics and Sample Site Characteristics from the 2020 Moss Survey of *Hypnum cupressiforme* in Georgia and Republic of Moldova, Including Both Initial and Adjusted (post-Grubbs' Test) Datasets.

Characteristic	Original/Initial Data		Adjusted Data	
	Georgia N = 70	**Moldova** N = 41	**Georgia** N = 55	**Moldova** N = 30
Land Cover *				
Coniferous forest	4 (5.7%)	0	4 (7.3%)	0
Deciduous forest	38 (54%)	0	28 (51%)	0
Mixed forest	28 (40%)	41 (100%)	23 (42%)	30 (100%)
Terrain *				
Plain	6 (8.6%)	19 (46%)	2 (3.6%)	9 (30%)
Slope	64 (91%)	22 (54%)	53 (96%)	21 (70%)
Köppen-Geiger climate classification *				
BSk (Arid, steppe, cold)	0	4 (9.8%)	0	3 (10%)
Cfa (Temperate, no dry season, hot summer)	36 (51%)	0	23 (42%)	0
Cfb (Temperate, no dry season, warm summer)	2 (2.9%)	0	2 (3.6%)	0
Dfa (Cold, no dry season, hot summer)	4 (5.7%)	20 (49%)	4 (7.3%)	16 (53%)
Dfb (Cold, no dry season, warm summer)	28 (40%)	17 (41%)	26 (47%)	11 (37%)
Population density *				
Very low density	49 (70%)	17 (41%)	38 (69%)	13 (43%)
Low density	10 (14%)	8 (20%)	8 (15%)	8 (27%)
Rural	6 (8.6%)	9 (22%)	6 (11%)	5 (17%)
Suburban	5 (7.1%)	6 (15%)	3 (5.5%)	4 (13%)
Urban	0	1 (2.4%)	0	0
Precipitation **				
Average Annual Precipitation in mm	848 (629, 1135)	362 (347, 383)	744 (629, 1033)	362 (347, 383)

Elevation zones *				
Lowland (0-500m)	20 (29%)	41 (100%)	12 (22%)	30 (100%)
Foothill (500-1000m)	32 (46%)	0	27 (49%)	0
Low-mountain (1000-1500m)	14 (20%)	0	12 (22%)	0
Upper-mountain (1500-2500m)	4 (5.7%)	0	4 (7.3%)	0
Altitude **				
Metres above mean sea level	749 (442, 1020)	148 (94, 200)	820 (557, 1133)	144(96, 199)
Topographic slope **				
Topographic slope in degree	11 (6, 18)	4 (2, 6)	12 (8, 19)	5 (2, 6)
Element content in mg/kg **				
Al	2288 (1660, 2840)	3430 (2680, 4750)	2184 (1636, 2771)	3,245 (2680, 4270)
Ba	29 (21, 43)	53 (41, 71)	26 (19, 35)	50 (41, 60)
Cd	0.13 (0.11, 0.17)	0.11 (0.08, 0.15)	0.13 (0.11, 0.15)	0.09 (0.08, 0.12)
Co	0.96 (0.69, 1.19)	0.94 (0.71, 1.28)	0.92 (0.67, 1.12)	0.94 (0.71, 1.28)
Cr	3.88 (2.91, 4.99)	5.40 (4.40, 8.90)	3.80 (2.89, 4.50)	5.35 (4.40, 8.20)
Cu	7.29 (6.16, 8.86)	8.62 (7.14, 9.38)	6.76 (5.64, 7.63)	7.83 (6.70, 9.05)
Fe	1898 (1367, 2436)	2190 (1790, 3100)	1798 (1335, 2208)	2130 (1790, 3070)
Mn	132 (88, 179)	93 (74, 144)	111 (86, 160)	87 (71, 106)
Ni	4.40 (3.52, 5.46)	4.10 (3.30, 5.30)	4.31 (3.42, 5.22)	3.72 (3.24, 4.80)
Pb	4.78 (3.88, 5.92)	3.14 (2.77, 3.70)	4.47 (3.60, 5.19)	3.00 (2.75, 3.29)
Sr	36 (31, 42)	51 (39, 68)	36 (32, 41)	50 (42, 67)
V	5.5 (4.2, 7.4)	5.4 (4.0, 8.0)	5.34 (4.11, 6.86)	5.20 (4.00, 6.90)
Zn	27 (23, 32)	39 (33, 46)	26 (22, 30)	36 (31, 43)

* n (%); ** Median (Q1, Q3).

The correlation matrix for the adjusted dataset revealed strong positive intercorrelations (r = 0.54–0.86) for the elements Al, Co, Cr, Fe, Ni, and V (Figure 5.1), suggesting a common natural origin, most likely related to crustal materials or soil dust contributions [254]. The homogeneity of these correlation coefficients, spanning a relatively narrow range, indicates a high degree of geochemical coherence among these elements, implying that their environmental distribution is governed by similar sources and transport mechanisms. The lower bound of this range (r = 0.54) still represents a substantial linear relationship, reinforcing the robustness of the lithogenic association across the entire dataset, despite potential variations in sampling conditions or local anthropogenic influences that could otherwise introduce heterogeneity. In contrast, topographic and climatic variables, namely average precipitation, slope, and altitude were negatively correlated (r = −0.42 to −0.61) with Zn, Ba, Cr, Al, and with Cu, Fe, and Sr depending on the specific variable considered. The strong intercorrelations among these environmental variables highlight their interconnected influence on elemental transport and accumulation processes.

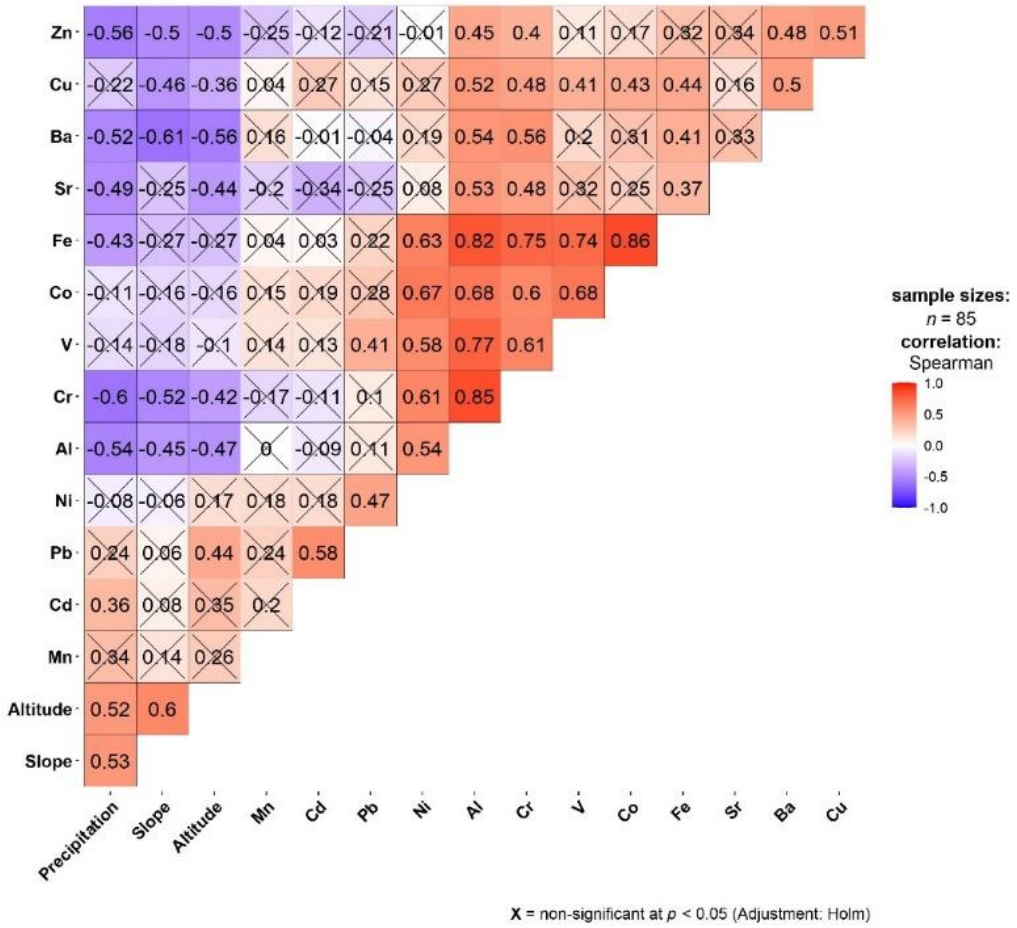

Figure 5.1. Spearman Correlation matrix between the elements of the entire adjusted data set.

Analysis of the correlation matrices for the Georgian and Moldovan moss surveys (Figure 5.2) revealed consistently strong positive correlations among the elements Al, Co, Cr, Fe, Ni, and V, suggesting a common lithogenic origin. The Georgian dataset exhibited stronger correlations between Al and other lithogenic elements relative to the Moldovan dataset, whereas Fe showed comparatively stronger associations in Moldova. A notable deviation from this pattern was the exceptionally strong V–Al correlation observed in the Republic of Moldova (r = 0.99). Additionally, several element pairs in Moldova displayed high correlation coefficients, including Cr–Co (r = 0.90), Fe–Co (r = 0.94), Fe–Cr (r = 0.91), Fe–Ni (r = 0.91), Co–Ni (r = 0.87), and Ni–Cr (r = 0.81). Among environmental variables, statistically significant negative correlations were detected exclusively in the Georgian survey, namely between slope degree and Ba (r = −0.46) and between slope degree and Pb (r = −0.50).

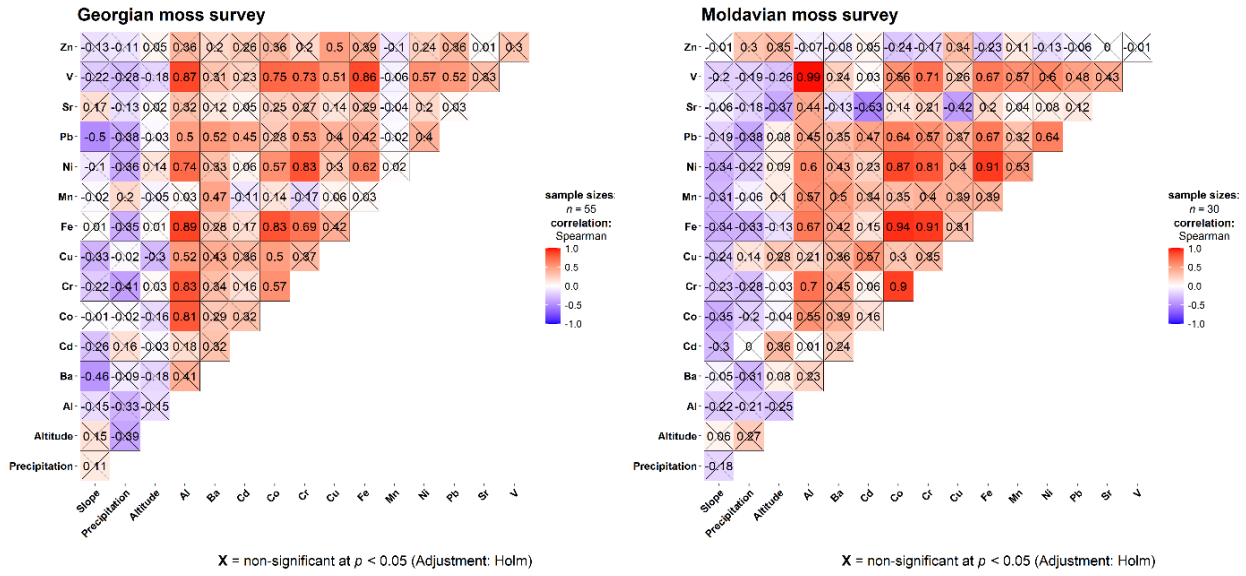

(**a**) (**b**)

Figure 5.2. Correlation matrices of Georgian (a) and Moldovan (b) moss surveys adjusted dataset.

The Kruskal–Wallis test indicated significant differences in elemental concentrations among lowland, foothill, and mountain zones. Al, Ba, Cr, Cu, Pb, and Zn differed significantly between lowland and both foothill and mountain areas, whereas Cd and Sr showed significant differences only between lowland and mountain zones. Median concentrations were typically greater in lowland zones, with the exception of Pb and Cd, which displayed higher values at higher elevations. A graphical overview of these findings is provided in Figure 5.3.

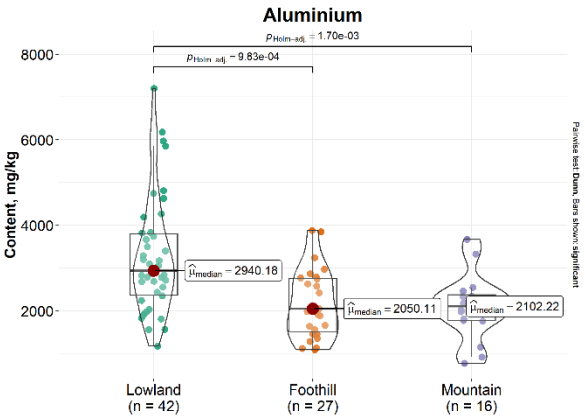
Aluminium
$p_{Holm-adj.}$ = 1.70e-03
$p_{Holm-adj.}$ = 9.83e-04
8000
6000
4000
2000
Content, mg/kg
$\hat{\mu}_{median}$ = 2940.18
$\hat{\mu}_{median}$ = 2050.11
$\hat{\mu}_{median}$ = 2102.22
Lowland (n = 42)
Foothill (n = 27)
Mountain (n = 16)
Pairwise test: Dunn, Bars shown: significant

(a)

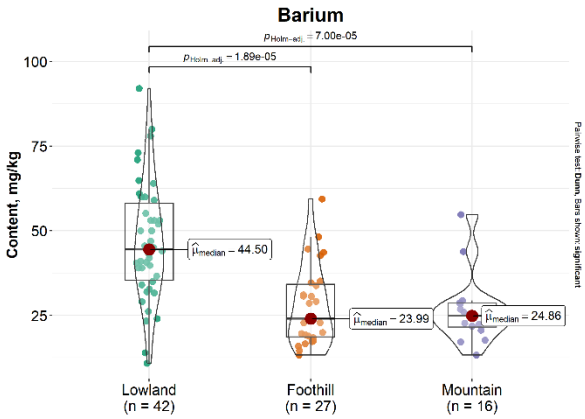
Barium
$p_{Holm-adj.}$ = 7.00e-05
$p_{Holm-adj.}$ = 1.89e-05
100
75
50
25
Content, mg/kg
$\hat{\mu}_{median}$ = 44.50
$\hat{\mu}_{median}$ = 23.99
$\hat{\mu}_{median}$ = 24.86
Lowland (n = 42)
Foothill (n = 27)
Mountain (n = 16)
Pairwise test: Dunn, Bars shown: significant

(b)

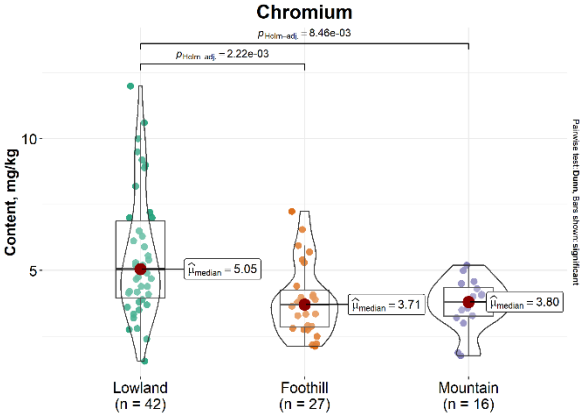
Chromium
$p_{Holm-adj.}$ = 8.46e-03
$p_{Holm-adj.}$ = 2.22e-03
10
5
Content, mg/kg
$\hat{\mu}_{median}$ = 5.05
$\hat{\mu}_{median}$ = 3.71
$\hat{\mu}_{median}$ = 3.80
Lowland (n = 42)
Foothill (n = 27)
Mountain (n = 16)
Pairwise test: Dunn, Bars shown: significant

(c)

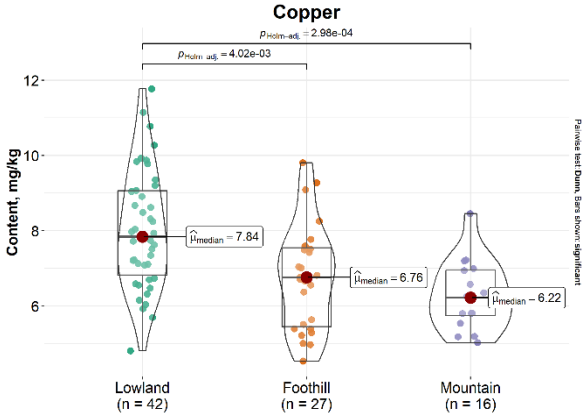
Copper
$p_{Holm-adj.}$ = 2.98e-04
$p_{Holm-adj.}$ = 4.02e-03
12
10
8
6
Content, mg/kg
$\hat{\mu}_{median}$ = 7.84
$\hat{\mu}_{median}$ = 6.76
$\hat{\mu}_{median}$ = 6.22
Lowland (n = 42)
Foothill (n = 27)
Mountain (n = 16)
Pairwise test: Dunn, Bars shown: significant

(d)

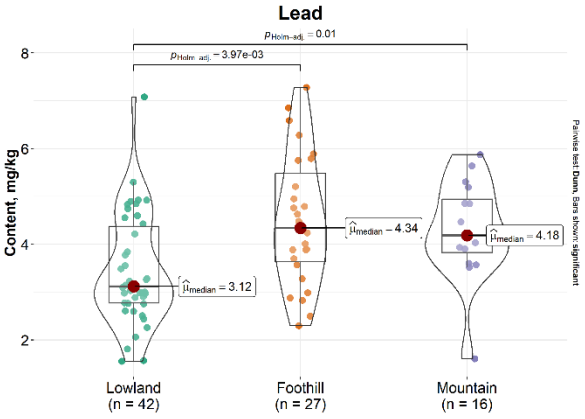
Lead
$p_{Holm-adj.}$ = 0.01
$p_{Holm-adj.}$ = 3.97e-03
8
6
4
2
Content, mg/kg
$\hat{\mu}_{median}$ = 3.12
$\hat{\mu}_{median}$ = 4.34
$\hat{\mu}_{median}$ = 4.18
Lowland (n = 42)
Foothill (n = 27)
Mountain (n = 16)
Pairwise test: Dunn, Bars shown: significant

(e)

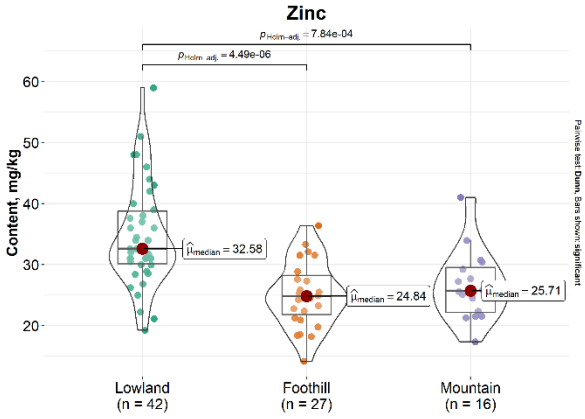
Zinc
$p_{Holm-adj.}$ = 7.84e-04
$p_{Holm-adj.}$ = 4.49e-06
60
50
40
30
20
Content, mg/kg
$\hat{\mu}_{median}$ = 32.58
$\hat{\mu}_{median}$ = 24.84
$\hat{\mu}_{median}$ = 25.71
Lowland (n = 42)
Foothill (n = 27)
Mountain (n = 16)
Pairwise test: Dunn, Bars shown: significant

(f)

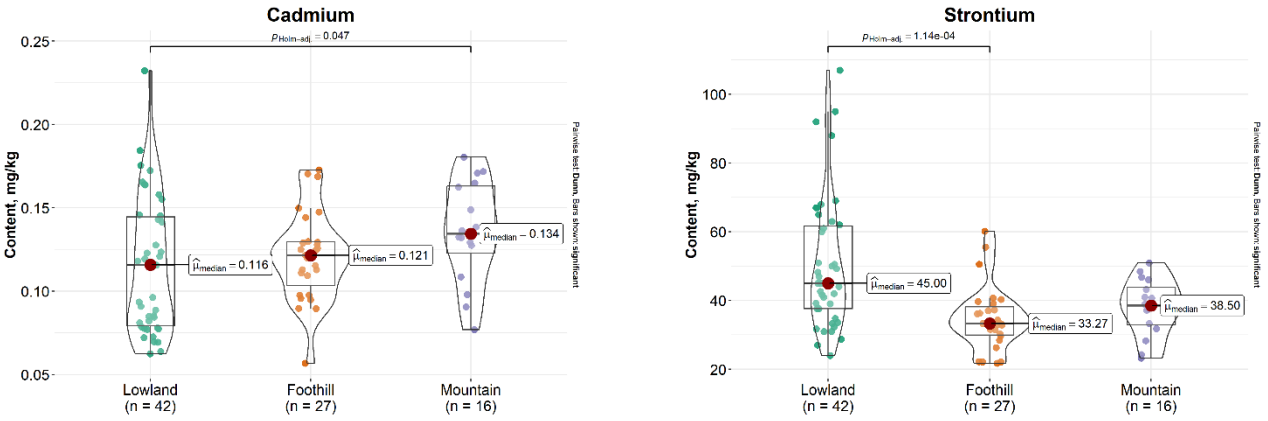

(g) (h)

Figure 5.3. Boxplots of elemental content across elevation zones. Significant pairwise differences (Kruskal–Wallis with Dunn's post-hoc, p < 0.05) are indicated with connecting lines.

Comparison across climate zones demonstrated significant differences in elemental concentrations, specifically Ba between Dfa and Dfb, Cd between BSk and Cfa, and Pb, Sr, and Zn between Cfa and Dfa (Figure 5.4) [260]. The Dfa and BSk climate zones are primarily represented by Moldovan sampling locations, while Dfb and Cfa are largely associated with Georgian sites. These climatic regimes also differ markedly in hydrological conditions, as Dfa and BSk generally receive considerably lower annual precipitation than Dfb and Cfa, potentially contributing to the observed geochemical variability.

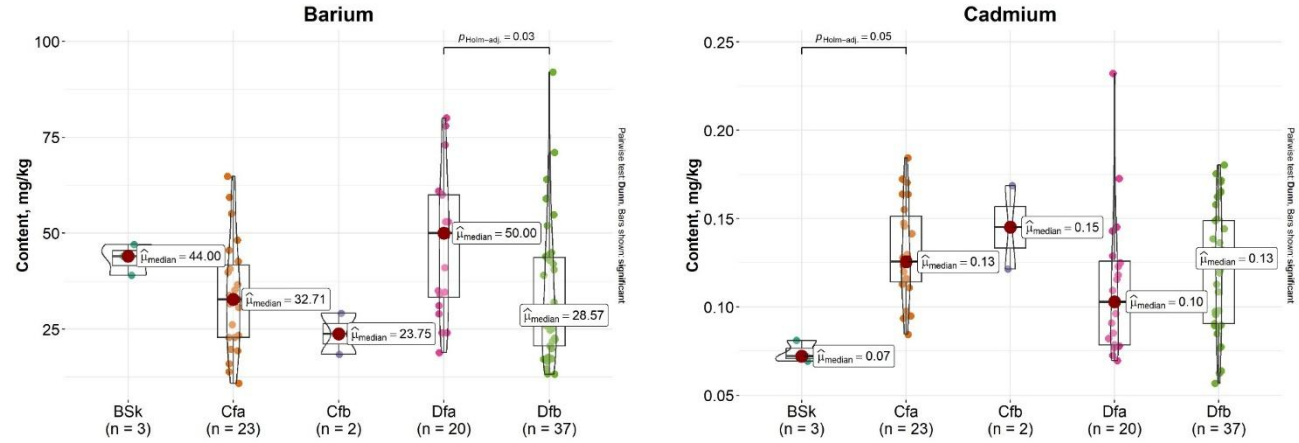

(a) (b)

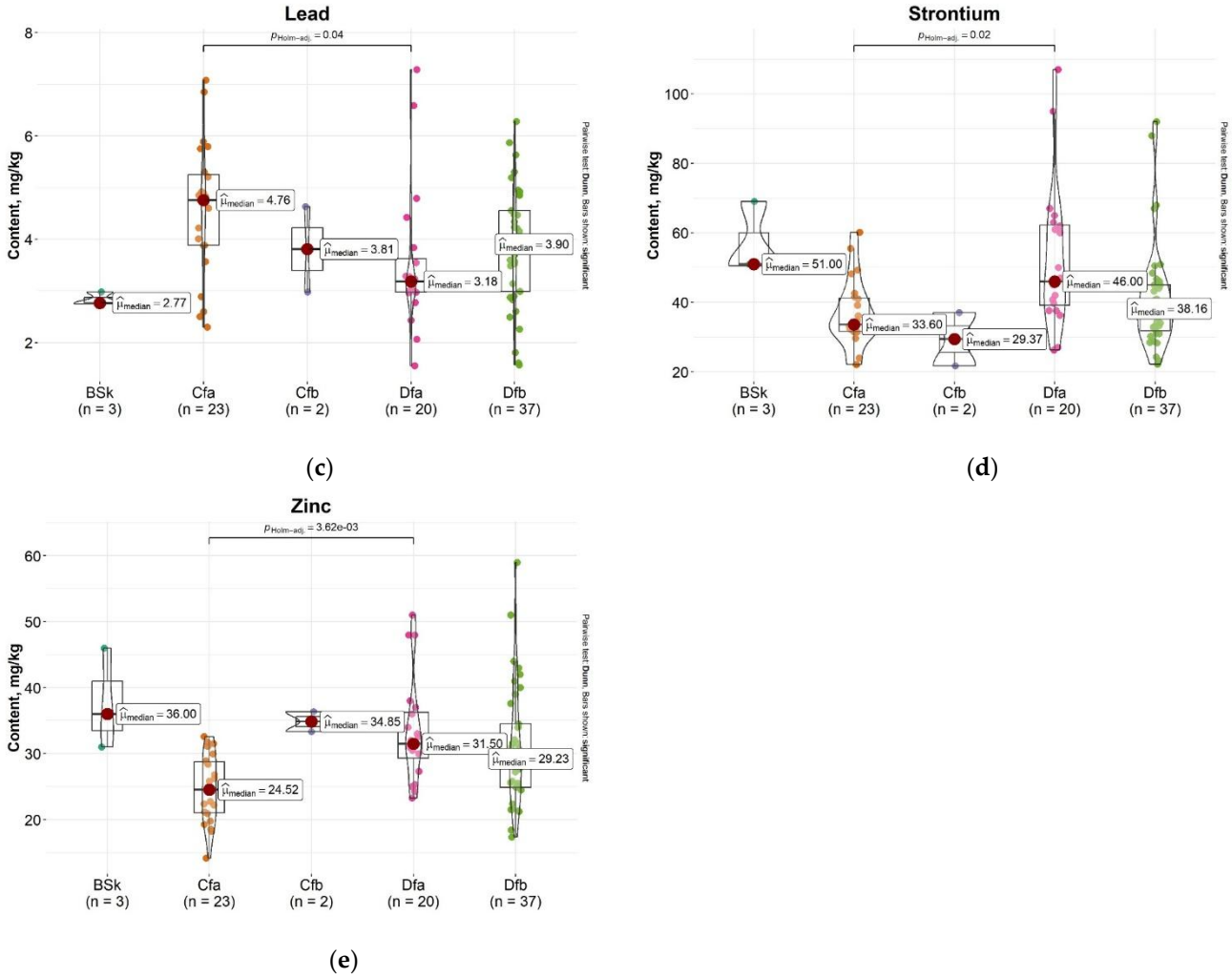

Figure 5.4. Boxplots of elemental content across climate zones. Significant pairwise differences (Kruskal–Wallis with Dunn's post-hoc, $p < 0.05$) are indicated with connecting lines.

The BSk-associated samples were characterized by elevated median concentrations of Al, Co, Cr, Fe, Sr, and Zn, alongside comparatively low concentrations of Cd and Pb. Such distributions may be attributable to wind erosion processes and the influence of local lithological characteristics, while low precipitation may further limit the accumulation of Cd and Pb [361]. Nonetheless, these interpretations are preliminary, as the number of samples representing the BSk climate zone is limited, and additional data are necessary to validate the observed patterns and identify the underlying environmental or geochemical controls.

Despite the absence of significant differences in analogous environmental and geographic parameters between the countries, including Dfb climate, mixed forest cover, population density, terrain slope, and lowland zones, distinct patterns in elemental composition were observed [260]. Specifically, Moldovan samples were enriched in Al, Ba, Cr, Sr, and Zn, whereas Georgian samples showed higher concentrations of Cd, Mn, and Pb.

To elucidate the multivariate relationships among elemental concentrations, topographic parameters, and categorical environmental variables, a Principal Component Analysis was performed on the dataset. The PCA results depicted in Figures 5.5 and 5.6 demonstrate that the first two components capture 58.7% of the total dataset variance, with PC1 contributing 40.3% and PC2 contributing 18.4%. This percentage of explained variance indicates a robust underlying structure within the dataset, suggesting that the two-component model effectively summarizes the dominant gradients influencing elemental composition across the sampling sites. The remaining 41.3% of variance, distributed across higher-order components, likely reflects more localized variability. The biplot indicates that PC1 is mainly associated with Fe, Cr, Al, Co, V, Ni, Cu, and Ba, while PC2 is largely governed by Pb, Cd, Sr, and Zn.

The pronounced contribution of Fe, Cr, Al, Co, V, Ni, and Ba to PC1 implies a dominant influence of geogenic sources, largely attributable to natural weathering processes affecting the Moldovan samples. The consistent alignment of these lithophilic elements, all major constituents of the Earth's upper continental crust, strongly suggests that the deposition of airborne mineral dust particles is the primary mechanism delivering these metals to the moss tissues. Such processes are likely enhanced by pronounced soil erosion and atmospheric suspension of mineral particles, driven by limited vegetation cover and arid climatic conditions [254, 362]. Under these conditions, the absence of a continuous vegetative buffer zone allows the wind to directly impact the soil surface, detaching and lofting fine-grained particulate matter into the air, which are subsequently deposited on moss biomonitors. Agricultural practices may also play a secondary role by enhancing the release and transport of these elements. Tillage breaks down soil aggregates and reduces surface roughness, which in turn increases the erosive capacity of the landscape and the atmospheric loading of crustal materials. Comparable findings have been reported for Georgia, where agricultural activities, especially under dry seasonal conditions, have been shown to increase soil particle emissions, and open terrain facilitate their widespread dispersion [223]. Nevertheless, in the current investigation, the representation of agricultural areas was limited, as most moss samples collected near such sites were excluded during outlier analysis [260]. This exclusion was methodologically necessary to isolate regional-scale atmospheric signals from the confounding influence of point-source agricultural inputs.

The comparatively low loading of copper on PC1 indicates that it has a reduced linkage to geogenic sources compared with the other elements. This divergence from the dominant lithogenic cluster suggests that Cu follows a distinct environmental pathway, likely decoupled from the soil erosion processes governing the other PC1 elements. This pattern may indicate an anthropogenic contribution, as Cu is extensively applied in agricultural practices in Moldova, particularly as a

fertilizer and fungicide [255]. The widespread use of copper-based agrochemicals in viticulture and horticulture results in the release of this metal into the environment through spraying, which can cause the formation of fine aerosol droplets capable of regional atmospheric transport.

The PCA biplot shows that altitude, slope degree, and precipitation, when projected as supplementary variables, align closely with the positive direction of PC2, where Pb and Cd also display positive correlations. This geometric convergence in the ordination space is statistically meaningful, indicating that the variance captured by PC2 is simultaneously explained by both the pollutant concentrations and the topoclimatic parameters. This pattern indicates that higher elevations, steeper terrain, and increased precipitation are associated with enhanced accumulation of these metals in moss tissues. The mechanistic basis for this relationship lies in orographic lifting: as air masses encounter topographic barriers, they ascend and cool adiabatically, leading to enhanced cloud formation and precipitation that efficiently remove both particulate and soluble atmospheric pollutants from the air column. This interpretation is consistent with the findings of Wang et al. [363], who demonstrated that mosses in alpine, high-precipitation environments efficiently capture soluble elements such as Cd and Pb via wet deposition. Furthermore, the strong relationships between Cd and Pb concentrations in mosses and bulk deposition observed by Aboal et al. [361] confirm the role of mosses as effective indicators of atmospheric metal inputs. Overall, the observed clustering suggests that topographic and climatic factors, particularly altitude-related precipitation gradients, may intensify atmospheric deposition and subsequent metal uptake by mosses.

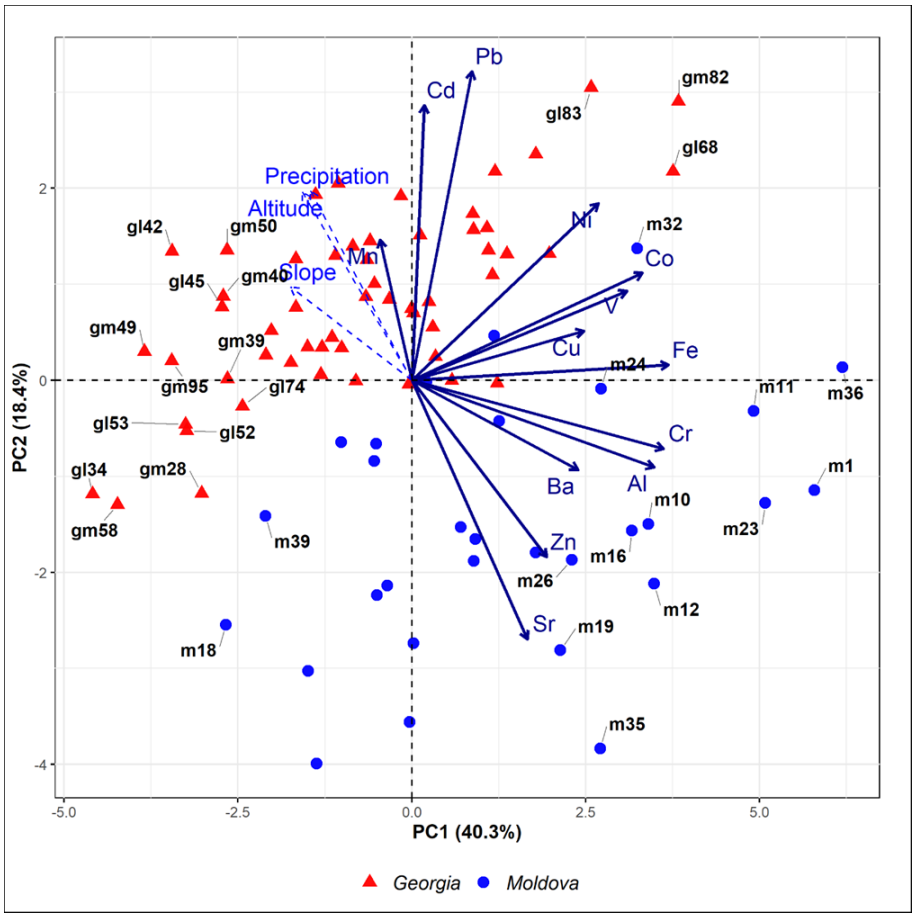

Figure 5.5. Biplot of the first two principal components express 58.7% of the variance in the data. Samples are marked with unique combination of color and symbol, dependent on the country. Variables appear as arrows from the origin, with qualitative variables shown as dashed arrows.

According to the Wilks' test p-values, country is the qualitative variable that contributes most to explaining the distances between individuals in the PC1–PC2 biplot, followed by elevation zones, land cover, climate, and terrain, in decreasing order of importance (Figure 5.6). This hierarchical ordering of categorical variables provides insight into the multiscale controls on elemental composition: national-level factors (such as geological parent material) have the strongest influence, followed by progressively finer-scale environmental gradients. The significance of elevation zones and climate as secondary factors reinforces the interpretation of PC2 as a topoclimatic deposition gradient, while the lesser but still significant contributions of land cover and terrain suggest that local landscape features modulate, but do not overwhelm, these regional patterns.

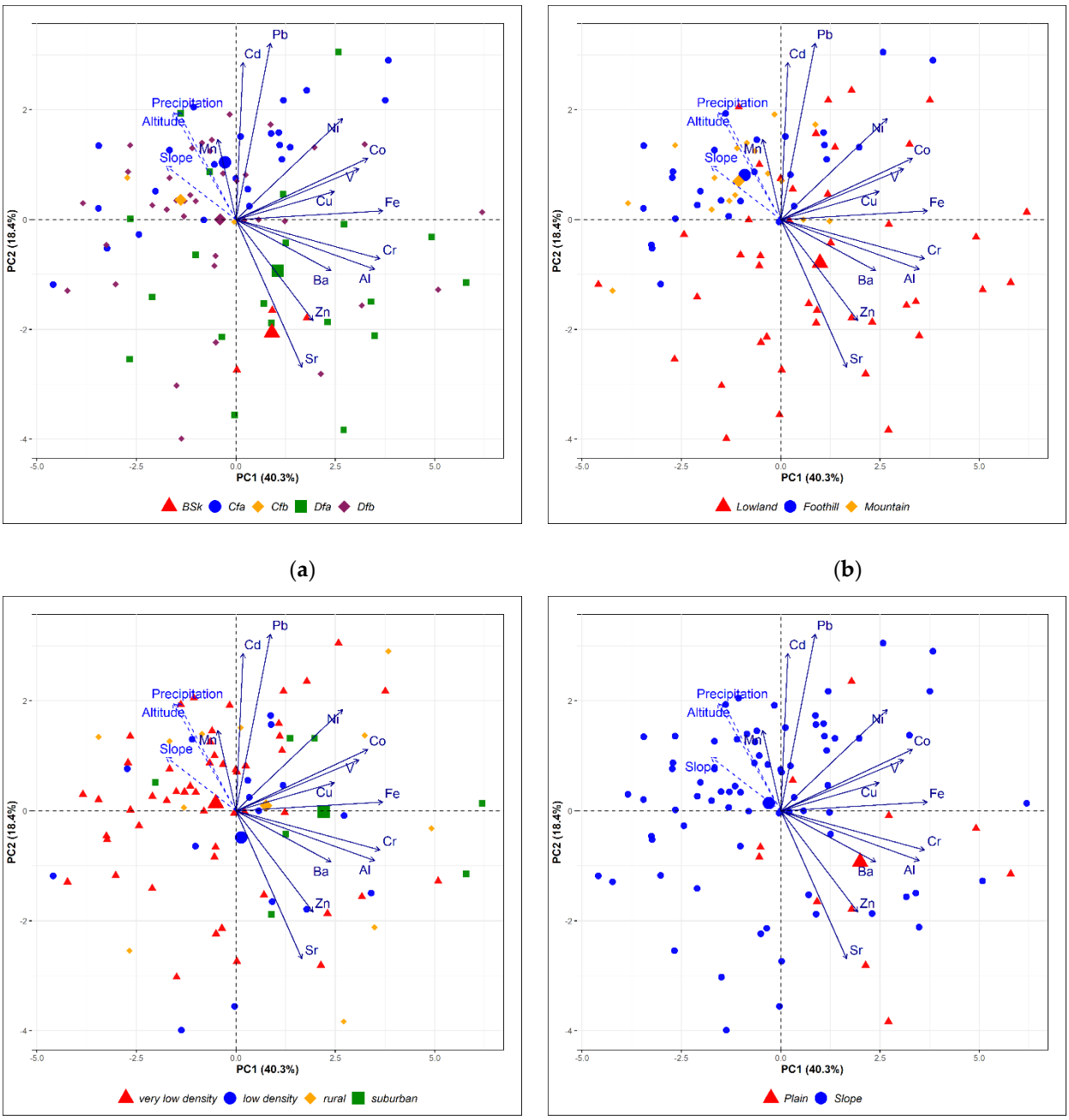

Figure 5.6. Biplots of the first two PCs. Samples are marked with unique combination of color and symbol, dependent on the climate (a), elevation zone (b), population density (c), terrain (d).

As shown in Figure 5.6, the distinct separation of sample groups by these categorical variables qualitatively supports the Wilks' test results. In panel (a), the distinction between samples from different climatic zones (e.g., Cfa vs. BSk) is evident, with the more humid Cfa samples tending toward the positive PC2 region associated with higher precipitation and pollutant accumulation. Panel (b) reveals a similar gradient with elevation, where samples from higher elevation zones project more strongly onto the positive PC2 axis. These visual patterns collectively

confirm that the multivariate structure captured by the PCA is systematically organized by the environmental gradients identified through statistical testing.

According to the PCA results, individuals m8, m19, m13, m34, m41, and m35 cluster on the negative side of the axis and are distinguished by high Sr and Zn loadings, coupled with low contributions from Cd, Pb, altitude, precipitation, and slope. This distinctive positioning in the ordination space indicates that these samples represent an anomalous geochemical environment that deviates from the dominant patterns governing the majority of the dataset.

According to Kabata-Pendias et al. [306], the highest concentrations of Sr are typically observed in heavy loamy soils, particularly those formed under hot and arid climatic conditions. This pedological context is essential for interpreting the Sr enrichment in these samples, as it establishes that elevated Sr is not necessarily indicative of anthropogenic pollution but may instead reflect the natural geochemical character of the underlying soil parent material. In the Republic of Moldova, soil erosion represents a major environmental issue, especially on sloped landscapes and in areas with complex and fragmented relief, as reported by Bejan et al. [362]. The convergence of these factors, namely, steep topography, erodible loamy soils, and intense erosional pressure, creates conditions favorable for the mobilization of Sr-rich soil particles into the atmosphere, where they become available for interception by moss through subsequent deposition. Carbonate chernozems, characterized by a loamy texture, are especially vulnerable to erosion and are mainly distributed in the southern and southeastern parts of the country, where BSk climatic conditions prevail (Figure 2.1).

The evidence indicates that soil erosion is the key driver of high Sr levels in Moldovan moss. The proposed mechanism involves three sequential steps: first, the physical detachment of Sr-bearing soil particles from carbonate chernozems through water and wind erosion; second, the atmospheric suspension and transport of these fine-grained materials; and third, the interception and retention of these particles by the moss, which effectively traps both the mineral grains and any surface-bound metals. This pathway represents an indirect geogenic signal, where mosses reflect not primary atmospheric deposition from distant sources, but rather the resuspension and redeposition of local soil materials. Furthermore, elevated Zn concentrations in Moldova are likely attributable to its naturally zinc-rich soils, which differ significantly from those in Georgia [364, 365].

5.1. Conclusions for Chapter 5

The comparative analysis of moss biomonitoring data from the Republic of Moldova and Georgia demonstrates that elemental accumulation in *Hypnum cupressiforme* is controlled by a

complex interaction between geogenic background, anthropogenic inputs, and environmental factors, particularly climatic conditions and relief characteristics. The applied approach, including outlier removal and the use of a single moss species, ensured that the observed patterns reflect regional-scale processes rather than localized contamination.

The results revealed strong and consistent associations among lithogenic elements (Al, Co, Cr, Fe, Ni, V), indicating a dominant influence of crustal materials and soil-derived particles. At the same time, significant negative correlations between these elements and environmental variables such as precipitation, altitude, and slope highlight the role of topoclimatic conditions in modulating their accumulation. In particular, dry climatic conditions and low precipitation, characteristic of the Republic of Moldova, favor soil erosion, resuspension, and atmospheric transport of mineral particles, leading to increased accumulation of lithogenic elements in moss tissues.

In contrast, elevated concentrations of Pb and Cd in Georgian samples were positively associated with altitude, slope, and precipitation, indicating the importance of orographic effects and wet deposition processes. The results demonstrate that in mountainous regions, atmospheric pollutants are efficiently scavenged through precipitation, leading to enhanced accumulation in mosses at higher elevations. This finding confirms that moss biomonitoring is highly sensitive to altitude-dependent deposition processes and reflects regional climatic gradients.

Principal Component Analysis further confirmed the existence of two dominant controlling gradients: a lithogenic gradient (PC1), associated with soil-derived elements and influenced primarily by erosion and resuspension processes, and a topoclimatic gradient (PC2), associated with pollutant deposition controlled by altitude, precipitation, and terrain slope. The alignment of Pb and Cd with topoclimatic variables provides strong evidence that these elements are predominantly deposited through wet atmospheric processes rather than direct local emission alone.

The comparative analysis between the two countries highlights the critical role of environmental context in shaping biomonitoring results. Moldovan samples were characterized by higher concentrations of elements such as Al, Ba, Cr, Sr, and Zn, reflecting the influence of arid conditions, agricultural land use, and open terrain, which enhance soil particle mobilization. In contrast, Georgian samples exhibited higher concentrations of Cd, Mn, and Pb, consistent with increased precipitation, complex mountainous relief, and enhanced wet deposition processes.

These findings demonstrate that the interpretation of moss biomonitoring data cannot be based solely on emission sources but must account for the modifying effects of climatic and geomorphological conditions. In regions with dry climates and low relief, pollutant accumulation

is largely controlled by resuspension and dry deposition of local materials, whereas in mountainous and humid regions, wet deposition and orographic effects play a significant role.

The results confirm that mosses are effective bioindicators of atmospheric deposition not only of pollution intensity but also of the environmental processes governing pollutant transport and accumulation. The study highlights that climatic variability and relief complexity represent key controlling factors in biomonitoring systems, and their integration into analytical frameworks is essential for accurate environmental assessment. These conclusions directly support the central objective of the thesis and demonstrate the applicability of moss biomonitoring in regions characterized by difficult climatic and relief conditions.

The results presented in this chapter have been published in scientific journal indexed in the Web of Science and Scopus databases [260].

CONCLUSIONS AND RECOMMENDATIONS

The present study confirms that moss biomonitoring represents an effective and reliable approach for assessing atmospheric deposition in regions characterized by contrasting physico-geographical conditions. Based on large-scale surveys conducted in Georgia (2014–2023) and the Republic of Moldova (2020), the research established baseline elemental concentrations, identified major pollution sources, and, importantly, demonstrated the significant role of climatic and geomorphological factors in controlling trace element accumulation in mosses.

1. Elemental accumulation patterns reflect both environmental conditions and emission sources. The results revealed distinct spatial patterns of elemental accumulation associated with differences in relief, climate, and land use. Georgian moss samples showed higher concentrations of lithogenic elements (Al, Sc, Ti, V, Cr, Fe, Co) and rare earth elements, reflecting the influence of mountainous terrain, complex geology, and enhanced weathering and erosion processes. In contrast, Moldovan samples exhibited elevated levels of Al, Fe, Ni, V, Cr, Sr, Zn, and As, which are consistent with lowland topography, dry climatic conditions, and intensive agricultural activity promoting soil resuspension and dry deposition processes.
2. Temporal trends indicate a general improvement in atmospheric deposition quality, with localized persistence of pollution sources. Comparative analysis between survey periods demonstrated a general decrease in median concentrations for most elements in both countries. In Moldova, substantial reductions were observed for Cr, As, Sb, Cd, Pb, and Cu between 2015 and 2020, while in Georgia, decreasing trends were recorded between 2014–2017 and 2019–2023, with Cd and Zn remaining relatively stable and Cu showing a slight increase. These trends reflect changes in emission intensity and environmental management, although persistent hotspots indicate ongoing local sources.
3. Multivariate analysis confirms the coexistence of geogenic and anthropogenic sources. Principal Component Analysis, Factor Analysis, and Positive Matrix Factorization identified three main source categories: (i) geogenic sources related to soil dust and crustal materials (Al, Fe, Cr, Co, V, rare earth elements); (ii) anthropogenic sources associated with traffic, industrial activity, and fossil fuel combustion (Pb, Zn, Cd, Cu, Hg); and (iii) mixed sources, including agricultural inputs (Cu, Br, Cl, K in Moldova) and mining-related contamination (Mn, As in Georgia). These findings highlight the complexity of atmospheric deposition systems and the need for integrated source interpretation.
4. Climatic and relief factors represent key controlling variables of atmospheric deposition. The study demonstrates that elemental accumulation in mosses is strongly influenced by

environmental conditions, particularly precipitation, altitude, and terrain characteristics. Lithogenic elements (Al, Cr, Ba, Zn) were negatively correlated with precipitation and altitude, indicating their dominance in regions characterized by dry conditions and active soil resuspension. Conversely, elements such as Cd and Pb were positively associated with altitude and precipitation, reflecting enhanced wet deposition and orographic effects in mountainous areas. Significant differences in elemental concentrations across elevation zones and Köppen–Geiger climate classes further confirm that climatic and geomorphological factors play a decisive role in shaping biomonitoring results.

5. Spatial analysis and pollution indices identify localized contamination hotspots within broader environmental gradients. The Pollution Load Index and Contamination Factor analyses revealed moderate to severe pollution in specific areas of Georgia, including the Chiatura manganese mining complex, the Zestafoni Ferroalloy Plant, and arsenic-contaminated regions such as Uravi and Tsana. In the Republic of Moldova, elevated concentrations were observed in urban and industrial areas such as Chisinau and Balti. Ecological risk assessment indicated predominantly low to moderate risk at the national scale, with localized increases associated with industrial and mining activities.
6. Methodological framework supports reliable comparative biomonitoring under different environmental conditions. The use of *Hypnum cupressiforme* as a common species, combined with the application of outlier filtering, enabled the identification of regional-scale patterns by minimizing the influence of local point sources. This approach allowed a clearer evaluation of environmental drivers, particularly climate and relief, while maintaining the comparability of datasets between countries.

Scientific contribution: integration of environmental drivers into biomonitoring interpretation. The study demonstrates that moss biomonitoring can be used not only to assess pollution levels but also to identify the environmental processes controlling atmospheric deposition. It provides evidence that climatic variability and relief complexity significantly modulate pollutant transport, deposition, and accumulation, which must be considered for accurate environmental assessment.

Practical recommendations:

1. Integration of environmental context into biomonitoring interpretation. The interpretation of moss biomonitoring data should explicitly account for climatic and geomorphological conditions. In dry, low-relief regions, elevated concentrations of lithogenic elements may reflect soil resuspension rather than direct pollution, whereas in mountainous and humid regions, increased accumulation of certain elements may be associated with wet deposition and

orographic processes. Ignoring these factors may lead to misinterpretation of pollution levels and sources.

2. Development and application of region-specific background values. Background concentrations established using the 10th percentile approach should be applied as reference values adapted to the specific physico-geographical conditions of each region. These values should be periodically updated to reflect environmental changes.
3. Implementation of standardized and comparable monitoring frameworks. Future biomonitoring programs should ensure methodological consistency, including the use of a single or comparable moss species, standardized sampling density, and harmonized analytical protocols, to allow reliable comparisons across regions with different environmental conditions.
4. Targeted environmental management of identified pollution sources. Mitigation strategies should focus on key pollution hotspots, including mining areas (Chiatura, Uravi), industrial facilities (Zestafoni, Kutaisi, Balti), and urban traffic emissions, as well as on reducing diffuse inputs from agricultural practices.

Expansion of monitoring to capture environmental variability. Future studies should extend spatial and temporal coverage to include a wider range of climatic zones, relief types, and land-use systems, enabling a more comprehensive understanding of atmospheric deposition dynamics in heterogeneous environments.

Suggestions for future research:

1. Expand spatial and temporal coverage: Future surveys should include remote and sensitive ecosystems (e.g., alpine zones in Georgia, protected areas in Moldova) to establish true background levels. Repeat surveys at 5-year intervals are essential to track the effectiveness of pollution control measures and assess the impact of climate change on deposition patterns.

2. Integrate complementary monitoring approaches: Combining moss biomonitoring with passive air samplers, deposition collectors, and soil analysis would provide a more comprehensive understanding of atmospheric pollution dynamics. Isotopic fingerprinting (e.g., Pb, Sr isotopes) could enhance source apportionment accuracy.

3. Investigate species-specific accumulation mechanisms: Controlled experiments should examine the physiological and morphological factors governing elemental uptake in different moss species. This would improve the comparability of studies using different biomonitors.

4. Assess health implications: Future research should link moss-derived deposition data with human biomonitoring and health studies in polluted areas (Kutaisi, Chisinau, mining

regions) to evaluate the public health impacts of air pollution and support evidence-based policy development.

5. Develop predictive models: Integrating moss biomonitoring data with GIS-based environmental variables (topography, climate, land use) and atmospheric transport models would enable spatial prediction of deposition patterns and identification of regions vulnerable to future contamination. This approach could be extended to other countries in the Black Sea basin with similar physico-geographical conditions.

REFERENCES

1. WORLD HEALTH ORGANIZATION. *World health statistics 2022: monitoring health for the SDGs, sustainable development goals*. Geneva, 2022. [Accessed 31 January 2024]. Available from: https://www.who.int/publications/i/item/9789240051157

2. VALAVANIDIS, A., FIOTAKIS, K., VLACHOGIANNI, T. Airborne particulate matter and human health: toxicological assessment and importance of size and composition of particles for oxidative damage and carcinogenic mechanisms. In: *Journal of Environmental Science and Health, Part C*. 2008. vol. 26, no. 4, pp. 339–362. ISSN 1059-0501. DOI: 10.1080/10590500802494538

3. KIM, K.H., KABIR, E., KABIR, S. A review on the human health impact of airborne particulate matter. In: *Environment International*. 2015. vol. 74, pp. 136-143. ISSN 0160-4120. DOI: 10.1016/j.envint.2014.10.005

4. WORLD HEALTH ORGANIZATION. *WHO global air quality guidelines: particulate matter ($PM_{2.5}$ and PM_{10}), ozone, nitrogen dioxide, sulfur dioxide and carbon monoxide*. . World Health Organization, 2021. ISBN 9240034226.

5. KELLY, F.J., FUSSELL, J.C. Size, source and chemical composition as determinants of toxicity attributable to ambient particulate matter. In: *Atmospheric environment*. 2012. vol. 60, pp. 504–526. ISSN 1352-2310. DOI: 10.1016/j.atmosenv.2012.06.039

6. MUKHTAR, A., LIMBECK, A. Recent developments in assessment of bio-accessible trace metal fractions in airborne particulate matter: A review. In: *Analytica chimica acta*. 2013. vol. 774, pp. 11–25. ISSN 0003-2670. DOI: 10.1016/j.aca.2013.02.008.

7. MARIRAJ MOHAN, S. An overview of particulate dry deposition: measuring methods, deposition velocity and controlling factors. In: *International Journal of Environmental Science and Technology*. 2016. vol. 13, no. 1, pp. 387–402. ISSN 1735-1472. DOI: 10.1007/s13762-015-0898-7.

8. AMODIO, M., CATINO, S., DAMBRUOSO, P.R., DE GENNARO, G., DI GILIO, A., GIUNGATO, P., LAIOLA, E., MARZOCCA, A., MAZZONE, A., SARDARO, A., TUTINO, M. Atmospheric deposition: Sampling procedures, analytical methods, and main recent findings from the scientific literature. *In: Advances in Meteorology.* 2014, vol. 2014, pp. 1–27. ISSN 1687-9309. DOI: 10.1155/2014/161730.

9. LORINȚ, C., TRAISTĂ, E., FLOREA, A., MARCHIȘ, D., RADU, S.M., NICOLA, A., REZMERIȚA, E. Spatiotemporal Distribution and Evolution of Air Pollutants Based on Comparative Analysis of Long-Term Monitoring Data and Snow Samples in Petroșani

Mountain Depression, Romania. In: *Sustainability*. 2025. vol. 17, no. 7, pp. 3141. ISSN 2071-1050. DOI: 10.3390/su17073141.

10. XU, B., LI, Y., ZHAO, S., ZHANG, B., LI, J., MA, J., HE, K., LU, L., WANG, X., CHEN, D., LI, J., ZHANG, G. Elevated wet deposition of micro- and nanoplastics in remote mountains driven by free tropospheric transport. In: *Journal of Hazardous Materials*. 2025. vol. 498, pp. 140010. ISSN 0304-3894. DOI: 10.1016/j.jhazmat.2025.140010.

11. ALI, H., KHAN, E., ILAHI, I. Environmental Chemistry and Ecotoxicology of Hazardous Heavy Metals: Environmental Persistence, Toxicity, and Bioaccumulation. In: *Journal of Chemistry*. 2019. vol. 2019, pp. 1–14. ISSN 2090-9063. DOI: 10.1155/2019/6730305.

12. KLAASSEN, C.D., AMDUR, M.O. *Casarett and Doull's toxicology: the basic science of poisons*. New York: McGraw-Hill Education, 2013. ISBN 978-0-07-176923-5.

13. TCHOUNWOU, P.B., YEDJOU, C.G., PATLOLLA, A.K., SUTTON, D.J. Heavy Metal Toxicity and the Environment. In: *Molecular, Clinical and Environmental Toxicology*. Basel: Springer Basel, 2012, pp. 133–164. ISBN 978-3-7643-8339-8. DOI: 10.1007/978-3-7643-8340-4_6.

14. PACYNA, J.M., PACYNA, E.G. *Environmental determinants of human health*. 1st ed. Cham: Springer International Publishing, 2016. Molecular and Integrative Toxicology. ISBN 978-3-319-43140-6. DOI: 10.1007/978-3-319-43142-0.

15. ALI, H., KHAN, E. Trophic transfer, bioaccumulation, and biomagnification of non-essential hazardous heavy metals and metalloids in food chains/webs—Concepts and implications for wildlife and human health. In: *Human and Ecological Risk Assessment: An International Journal*. 2019, vol. 25, no. 6, pp. 1353–1376. ISSN 1080-7039. DOI: 10.1080/10807039.2018.1469398.

16. NORDBERG, G.F., FOWLER, B.A., NORDBERG, M. *Handbook on the Toxicology of Metals*. 4th ed. Burlington, MA: Elsevier, 2015. ISBN 9780444594532. DOI: 10.1016/C2011-0-07884-5.

17. HASSANIEN, M.A. Atmospheric heavy metals pollution: exposure and prevention policies in mediterranean basin. In: *Environmental heavy metal pollution and effects on child mental development: risk assessment and prevention strategies*. Springer, 2011. p. 287–307. ISBN 9400702523.

18. UNITED NATIONS ECONOMIC COMMISSION FOR EUROPE. *Convention on Long-range Transboundary Air Pollution*. 1979. United Nations, Treaty Series, vol. 1302, p. 217. Registration no. 21623. [Accessed 1 May 2023]. Available from:

https://treaties.un.org/Pages/ViewDetails.aspx?src=TREATY&mtdsg_no=XXVII-1&chapter=27&clang=_en

19. XU, Z., FU, Y., YING, Q., HOPKE, P.K., SHU, X., YANG, X., QIAO, X., TANG, Y. Atmospheric deposition of pollutants at three altitudes on Mount Emei, Sichuan Basin, southwestern China. In: *Science of The Total Environment*. 2024. vol. 957, pp. 177806. ISSN 0048-9697. DOI: 10.1016/j.scitotenv.2024.177806.

20. COWAN, N., NEMITZ, E., WALKER, J.T., FOWLER, D., FINNIGAN, J.J., WEBSTER, H.N., LEVY, P., TWIGG, M., TANG, S.Y., BACHILLER-JARENO, N., TREMBATH, P., KINNERSLEY, R.P., BRABAN, C.F. Review of methods for assessing deposition of reactive nitrogen pollutants across complex terrain with focus on the UK. In: *Environmental Science: Atmospheres*. 2022. vol. 2, no. 5, pp. 829–851. DOI: 10.1039/D2EA00012A.

21. HEMOND, H.F., FECHNER, E.J. *Chemical fate and transport in the environment*. 3. 3rd ed. San Diego: Academic Press, 2015. ISBN 9780123982568. DOI: 10.1016/C2011-0-09677-1.

22. SEINFELD, J.H., PANDIS, S.N. *Atmospheric chemistry and physics: from air pollution to climate change*. 3rd ed. Hoboken, New Jersey: John Wiley & Sons, Inc., 2016. ISBN 978-1-118-94740-1

23. TODOROVIC, Z.N., RADULOVIC, J.M., SREDOVIC-IGNJATOVIC, I.D., IGNJATOVIC, L.M., ONJIA, A. Ambient air particles: The use of ion chromatography and multivariate techniques in the analysis of water-soluble substances. In: *Journal of the Serbian Chemical Society*. 2021. vol. 86, no. 7–8, pp. 753–766. ISSN 0352-5139. DOI: 10.2298/JSC200826077T.

24. DOS SANTOS, M., GÓMEZ, D., DAWIDOWSKI, L., GAUTIER, E., SMICHOWSKI, P. Determination of water-soluble and insoluble compounds in size classified airborne particulate matter. In: *Microchemical Journal*. 2009. vol. 91, no. 1, pp. 133–139. ISSN 0026-265X. DOI: 10.1016/j.microc.2008.09.001.

25. OCHSENKÜHN, K.-M., LYBEROPOULOU, T., KOUMARIANOU, G., OCHSENKÜHN-PETROPOULOU, M. Ion chromatographic and spectrometric determination of water-soluble compounds in airborne particulates, and their correlations in an industrial area in Attica, Greece. In: *Microchimica Acta*. 2008. vol. 160, no. 4, pp. 485–492. ISSN 0026-3672.

26. LIANG, S.X., WU, H., SUN, H.W. Determination of trace elements in airborne PM_{10} by inductively coupled plasma mass spectrometry. In: *International Journal of*

Environmental Science and Technology. 2015. vol. 12, no. 4, pp. 1373–1378. ISSN 1735-1472. DOI: 10.1007/s13762-014-0513-3.

27. CHANG, Y., HUANG, K., XIE, M., DENG, C., ZOU, Z., LIU, S., ZHANG, Y. First long-term and near real-time measurement of trace elements in China's urban atmosphere: temporal variability, source apportionment and precipitation effect. In: *Atmospheric Chemistry and Physics*. 2018. vol. 18, no. 16, pp. 11793–11812. ISSN 1680-7316. DOI: 10.5194/acp-18-11793-2018.

28. RADULESCU, C., IORDACHE, S., DUNEA, D., STIHI, C., DULAMA, I.D. Risks assessment of heavy metals on public health associated with atmospheric exposure to $PM_{2.5}$ in urban area. In: *Romanian Journal of Physics*. 2015, vol. 60, no. 7-8, pp. 1171–1182. ISSN 1221-146X.

29. HU, M., JING-HONG, Z., CHUN-FENG, D., LIANG, H.A.O., YA-FENG, G. Thermal desorption-gas chromatography or gas chromatography-mass spectrometry for analysis of semi-volatile compounds on atmospheric particulate matters. In: *Chinese Journal of Analytical Chemistry*. 2014. vol. 42, no. 7, pp. 931–936. ISSN 0253-3820.

30. FLORES, R.M., MERTOGLU, E. Optimization of a thermal desorption-gas chromatography/mass spectrometry method for characterization of semi-volatile organic compounds in high time resolved $PM_{2.5}$. In: *Atmospheric Pollution Research*. 2020. vol. 11, no. 3, pp. 619–629. ISSN 1309-1042.

31. ARETAKI, M.A., DESMET, J., VIANA, M., VAN DROOGE, B.L. Comprehensive methodology for semi-volatile organic compound determination in ambient air with emphasis on polycyclic aromatic hydrocarbons analysis by GC–MS/MS. In: *Journal of Chromatography A*. 2024. vol. 1730, pp. 465086. ISSN 0021-9673. DOI: 10.1016/j.chroma.2024.465086.

32. YAO, X., LEE, C.J., EVANS, G.J., CHU, A., GODRI, K.J., MCGUIRE, M.L., NG, A.C., WHITELAW, C. Evaluation of ambient SO2 measurement methods at roadside sites. In: *Atmospheric Environment*. 2011. vol. 45, no. 16, pp. 2781–2788. ISSN 1352-2310. DOI: 10.1016/j.atmosenv.2011.01.070.

33. WENG, W., ALDÉN, M., LI, Z. Quantitative SO2 detection in combustion environments using broad band ultraviolet absorption and laser-induced fluorescence. In: *Analytical chemistry*. 2019. vol. 91, no. 16, pp. 10849–10855. ISSN 0003-2700. DOI: 10.1021/acs.analchem.9b02505.

34. PELLIKKA, T., KAJOLINNA, T., PERÄLÄ, M. SO2 emission measurement with the European standard reference method, EN 14791, and alternative methods–observations from

laboratory and field studies. In: *Journal of the Air & Waste Management Association*. 2019. vol. 69, no. 9, pp. 1122–1131. ISSN 1096-2247. DOI: 10.1080/10962247.2019.1640809.

35. VILLENA, G., BEJAN, I., KURTENBACH, R., WIESEN, P., KLEFFMANN, J. Interferences of commercial NO 2 instruments in the urban atmosphere and in a smog chamber. In: *Atmospheric Measurement Techniques*. 2012. vol. 5, no. 1, pp. 149–159. ISSN 1867-1381. DOI: 10.5194/amt-5-149-2012.

36. MARTIN, C.R., ZENG, N., KARION, A., DICKERSON, R.R., REN, X., TURPIE, B.N., WEBER, K.J. Evaluation and environmental correction of ambient CO 2 measurements from a low-cost NDIR sensor. In: *Atmospheric measurement techniques*. 2017. vol. 10, no. 7, pp. 2383–2395. ISSN 1867-1381. DOI: 10.5194/amt-10-2383-2017.

37. KIM, J.-C., DINH, T.-V., CHOI, I.-Y., SONG, K.-Y. Physical and chemical factors influencing the continuous monitoring of carbon monoxide using NDIR sensor. In: *2015 9th International Conference on Sensing Technology (ICST)*. IEEE, 2015. p. 316–319. ISBN 1479963143.

38. GAO, R.S., BALLARD, J., WATTS, L.A., THORNBERRY, T.D., CICIORA, S.J., MCLAUGHLIN, R.J., FAHEY, D.W. A compact, fast UV photometer for measurement of ozone from research aircraft. In: *Atmospheric Measurement Techniques*. 2012. vol. 5, no. 9, pp. 2201–2210. ISSN 1867-1381. DOI: 10.5194/amt-5-2201-2012.

39. SPICER, C.W., JOSEPH, D.W., OLLISON, W.M. A re-examination of ambient air ozone monitor interferences. In: *Journal of the Air & Waste Management Association*. 2010. vol. 60, no. 11, pp. 1353–1364. ISSN 1096-2247. DOI: 10.3155/1047-3289.60.11.1353.

40. WORLD HEALTH ORGANIZATION. *WHO global air quality guidelines: particulate matter ($PM_{2.5}$ and PM_{10}), ozone, nitrogen dioxide, sulfur dioxide and carbon monoxide*. World Health Organization, 2021. ISBN 9240034226.

41. ZHAO, X., FIOLETOV, V., GRIFFIN, D., MCLINDEN, C., STAEBLER, R., MIHELE, C., STRAWBRIDGE, K., DAVIES, J., ABBOUD, I., LEE, S.C., CEDE, A., TIEFENGRABER, M., SWAP, R. The differences between remote sensing and in situ air pollutant measurements over the Canadian oil sands. In: *Atmospheric Measurement Techniques*. 2024. vol. 17, no. 23, pp. 6889–6912. DOI: 10.5194/amt-17-6889-2024.

42. ZHAO, S., YANG, Y., MA, L., BAI, Z., FENG, Y., LIU, Q., WANG, Q., CHEN, Y., WANG, F., TENG, J., ZHAO, L., XIE, Y., DAI, Y., YU, L., ZHOU, Y., XIONG, Y. A review of satellite remote sensing for pollution control and carbon reduction in China. In: *International Journal of Applied Earth Observation and Geoinformation*. 2026. vol. 146, pp. 105109. DOI: 10.1016/j.jag.2026.105109.

43. OECD. *Promoting Clean Urban Public Transportation and Green Investment in Moldova*. Paris: OECD Publishing, 2019. Green Finance and Investment. ISBN 978-92-64-41962-9. DOI: 10.1787/31925aae-en.

44. NATIONAL ENVIRONMENTAL AGENCY OF GEORGIA. Air Quality Portal. [Accessed 28 April 2023]. Available from: https://air.gov.ge/en/

45. UNECE. *Environmental Performance Reviews: Republic of Moldova: 3rd review*. UN: The United Nations, 2014. [Accessed 20 May 2025]. Available from: https://unece.org/environment-policy/publications/3rd-environmental-performance-review-republic-moldova

46. UNECE. *Environmental Performance Reviews: Georgia: 3rd review*. UN: The United Nations, 2016. [Accessed 2 February 2023]. Available from: https://unece.org/environment-policy/publications/3rd-environmental-performance-review-georgia

47. FRONTASYEVA, M., HARMENS, H., UZHINSKIY, A., CHALIGAVA, O. et al. Mosses as biomonitors of air pollution: 2015/2016 survey on heavy metals, nitrogen and POPs in Europe and beyond. Dubna: Joint Institute for Nuclear Research, 2020. ISBN 978-5-9530-0508-1.

48. MÜNZEL, T., GORI, T., AL-KINDI, S., DEANFIELD, J., LELIEVELD, J., DAIBER, A., RAJAGOPALAN, S. Effects of gaseous and solid constituents of air pollution on endothelial function. In: *European heart journal*. 2018, vol. 39, no. 38, pp. 3543–3550. ISSN 0195-668X. DOI: 10.1093/eurheartj/ehy481.

49. GLENCROSS, D.A., HO, T.-R., CAMINA, N., HAWRYLOWICZ, C.M., PFEFFER, P.E. Air pollution and its effects on the immune system. In: *Free Radical Biology and Medicine*. 2020, vol. 151, pp. 56–68. ISSN 0891-5849. DOI: 10.1016/j.freeradbiomed.2020.01.179.

50. FORTOUL, T.I., RODRIGUEZ-LARA, V., GONZALEZ-VILLALVA, A., ROJAS-LEMUS, M., COLIN-BARENQUE, L., BIZARRO-NEVARES, P., GARCÍA-PELÁEZ, I., USTARROZ-CANO, M., LÓPEZ-ZEPEDA, S., CERVANTES-YÉPEZ, S., LÓPEZ-VALDEZ, N., MELÉNDEZ-GARCÍA, N., ESPINOSA-ZURUTUZA, M., CANO-GUTIERREZ, G., CANO-RODRÍGUEZ, M.C. Health Effects of Metals in Particulate Matter. In: *Current Air Quality Issues*. InTech, 2015. ISBN 978-953-51-2180-0.

51. HEAL, M.R., KUMAR, P., HARRISON, R.M. Particles, air quality, policy and health. In: *Chemical Society Reviews*. 2012. vol. 41, no. 19, pp. 6606–6630. ISSN 0306-0012. DOI: 10.1039/c2cs35076a.

52. GLENCROSS, D.A., HO, T.-R., CAMINA, N., HAWRYLOWICZ, C.M., PFEFFER, P.E. Air pollution and its effects on the immune system. In: *Free Radical Biology and Medicine*. 2020. vol. 151, pp. 56–68. ISSN 0891-5849. DOI: 10.1016/j.freeradbiomed.2020.01.179.

53. GHIO, A.J., CARRAWAY, M.S., MADDEN, M.C. Composition of air pollution particles and oxidative stress in cells, tissues, and living systems. In: *Journal of Toxicology and Environmental Health, Part B*. 2012. vol. 15, no. 1, pp. 1–21. ISSN 1093-7404. DOI: 10.1080/10937404.2012.632359.

54. PISCITELLO, A., BIANCO, C., CASASSO, A., SETHI, R. Non-exhaust traffic emissions: Sources, characterization, and mitigation measures. In: *Science of the Total Environment*. 2021. vol. 766, pp. 144440. ISSN 0048-9697. DOI: 10.1016/j.scitotenv.2020.144440.

55. HASSANIEN, M.A. Atmospheric Heavy Metals Pollution: Exposure and Prevention Policies in Mediterranean Basin. In: *Environmental heavy metal pollution and effects on child mental development: risk assessment and prevention strategies*. Dordrecht: Springer, 2011, pp. 287–307. NATO Science for Peace and Security Series C: Environmental Security, vol. 1. ISBN 978-94-007-0252-3. DOI: 10.1007/978-94-007-0253-0_17.

56. WU, X., CHEN, B., WEN, T., HABIB, A., SHI, G. Concentrations and chemical compositions of PM_{10} during hazy and non-hazy days in Beijing. In: *Journal of Environmental Sciences*. 2020. vol. 87, pp. 1–9. ISSN 1001-0742. DOI: 10.1016/j.jes.2019.03.021.

57. ACOSTA, J.A., GABARRÓN, M., FAZ, A., MARTÍNEZ-MARTÍNEZ, S., ZORNOZA, R., AROCENA, J.M. Influence of population density on the concentration and speciation of metals in the soil and street dust from urban areas. In: *Chemosphere*. 2015. vol. 134, pp. 328–337. ISSN 0045-6535. DOI: 10.1016/j.chemosphere.2015.04.038.

58. ABUDUWAILIL, J., ZHAOYONG, Z., FENGQING, J. Evaluation of the pollution and human health risks posed by heavy metals in the atmospheric dust in Ebinur Basin in Northwest China. In: *Environmental Science and Pollution Research*. 2015. vol. 22, pp. 14018–14031. ISSN 0944-1344. DOI: 10.1007/s11356-015-4625-1.

59. NIEDER, R., BENBI, D.K. Potentially toxic elements in the environment – a review of sources, sinks, pathways and mitigation measures. In: *Reviews on Environmental Health*. 2024. vol. 39, no. 3, pp. 561–575. ISSN 0048-7554. DOI: 10.1515/reveh-2022-0161.

60. CHEN, R., ZHAO, Y., TIAN, Y., FENG, X., FENG, Y. Sources and uncertainties of health risks for $PM_{2.5}$-bound heavy metals based on synchronous online and offline filter-based

measurements in a Chinese megacity. In: *Environment International*. 2022. vol. 164, pp. 107236. ISSN 0160-4120. DOI: 10.1016/j.envint.2022.107236.

61. CHEN, L., FANG, L., YANG, X., LUO, X., QIU, T., ZENG, Y., HUANG, F., DONG, F., WHITE, J.C., BOLAN, N., RINKLEBE, J. Sources and human health risks associated with potentially toxic elements (PTEs) in urban dust: A global perspective. In: *Environment International*. 2024. vol. 187, pp. 108708. ISSN 0160-4120. DOI: 10.1016/j.envint.2024.108708.

62. KIM, S.C., HONG, Y.K., OH, S.J., OH, S.M., LEE, S.P., KIM, D.H., YANG, J.E. Effect of chemical amendments on remediation of potentially toxic trace elements (PTEs) and soil quality improvement in paddy fields. In: *Environmental Geochemistry and Health*. 2017. vol. 39, no. 2, pp. 345–352. ISSN 0269-4042. DOI: 10.1007/s10653-017-9921-x.

63. GHOSH, P., GHOSHAL, A. Potentially Toxic Elements (PTEs) in Plants and Animals: Environmental Pathways, Toxicity Mechanisms, and Biomonitoring Insights. In: *Environmental Quality Management*. 2026. vol. 35, no. 3. ISSN 1088-1913. DOI: 10.1002/tqem.70299.

64. KUNDU, S. Essential and Toxic: The Dual Nature of Heavy Metals in Human Physiology. In: *Functional Biochemistry of Metallic Elements*. Cham: Springer, 2026. pp. 259–274. ISBN 978-3-032-14444-7. DOI: 10.1007/978-3-032-14445-4_15.

65. BÁNFALVI, G. Heavy Metals, Trace Elements and Their Cellular Effects. In: *Cellular Effects of Heavy Metals*. Dordrecht: Springer Netherlands, 2011. p. 3–28. ISBN 978-94-007-0427-5. DOI: 10.1007/978-94-007-0428-2_1.

66. THOMSON, E.M., BREZNAN, D., KARTHIKEYAN, S., MACKINNON-ROY, C., VUONG, N.Q., DABEK-ZLOTORZYNSKA, E., CELO, V., CHARLAND, J.-P., KUMARATHASAN, P., BROOK, J.R., VINCENT, R. Contrasting biological potency of particulate matter collected at sites impacted by distinct industrial sources. In: *Particle and Fibre Toxicology*. 2016. vol. 13, no. 1, pp. 65. ISSN 1743-8977. DOI: 10.1186/s12989-016-0176-y.

67. SCHRAUFNAGEL, D.E. The health effects of ultrafine particles. In: *Experimental & Molecular Medicine*. 2020. vol. 52, no. 3, pp. 311–317. ISSN 1226-3613. DOI: 10.1038/s12276-020-0403-3.

68. SINGH, V., SINGH, N., VERMA, M., KAMAL, R., TIWARI, R., SANJAY CHIVATE, M., RAI, S.N., KUMAR, A., SINGH, A., SINGH, M.P., VAMANU, E., MISHRA, V. Hexavalent-Chromium-Induced Oxidative Stress and the Protective Role of Antioxidants against Cellular Toxicity. In: *Antioxidants*. 2022. vol. 11, no. 12, pp. 2375. ISSN 2076-3921. DOI: 10.3390/antiox11122375.

69. HUANG, L., YU, C.H., HOPKE, P.K., SHIN, J.Y., FAN, Z. (TINA). Trivalent chromium solubility and its influence on quantification of hexavalent chromium in ambient particulate matter using EPA method 6800. In: *Journal of the Air & Waste Management Association*. 2014. vol. 64, no. 12, pp. 1439–1445. ISSN 1096-2247. DOI: 10.1080/10962247.2014.951745.

70. LIU, Q. Sources and Control Strategies of Arsenic in the Atmosphere. In: *Journal of Environmental & Earth Sciences*. 2025. vol. 7, no. 7, pp. 209–226. ISSN 2661-3190. DOI: 10.30564/jees.v7i7.9955.

71. JIANG, X., CHEN, C., ZHAO, W., ZHANG, Z. Sodium arsenite and arsenic trioxide differently affect the oxidative stress, genotoxicity and apoptosis in A549 cells: An implication for the paradoxical mechanism. In: *Environmental Toxicology and Pharmacology*. 2013. vol. 36, no. 3, pp. 891–902. ISSN 1382-6689. DOI: 10.1016/j.etap.2013.08.002.

72. BREUNINGER, E.S., TOLU, J., AEMISEGGER, F., THURNHERR, I., BOUCHET, S., MESTROT, A., OSSOLA, R., MCNEILL, K., TUKHMETOVA, D., VOGL, J., MEERMANN, B., SONKE, J.E., WINKEL, L.H.E. Marine and terrestrial contributions to atmospheric deposition fluxes of methylated arsenic species. In: *Nature Communications*. 2024. vol. 15, no. 1, pp. 9623. ISSN 2041-1723. DOI: 10.1038/s41467-024-53974-z.

73. JAKOB, R., ROTH, A., HAAS, K., KRUPP, E.M., RAAB, A., SMICHOWSKI, P., GÓMEZ, D., FELDMANN, J. Atmospheric stability of arsines and the determination of their oxidative products in atmospheric aerosols (PM_{10}): evidence of the widespread phenomena of biovolatilization of arsenic. In: *J. Environ. Monit.* 2010. vol. 12, no. 2, pp. 409–416. ISSN 1464-0325. DOI: 10.1039/B915867G.

74. MESTROT, A., MERLE, J.K., BROGLIA, A., FELDMANN, J., KRUPP, E.M. Atmospheric Stability of Arsine and Methylarsines. In: *Environmental Science & Technology*. 2011. vol. 45, no. 9, pp. 4010–4015. ISSN 0013-936X. DOI: 10.1021/es2004649.

75. MARTIN, R., DOWLING, K., PEARCE, D., SILLITOE, J., FLORENTINE, S. Health Effects Associated with Inhalation of Airborne Arsenic Arising from Mining Operations. In: *Geosciences*. 2014. vol. 4, no. 3, pp. 128–175. ISSN 2076-3263. DOI: 10.3390/geosciences4030128.

76. LIU, Q. Toxicology of Airborne Inorganic Arsenic: Oxidative Stress, Molecular Mechanisms, and Organ-Specific Pathologies. In: *Toxics*. 2025. vol. 13, no. 9, pp. 753. ISSN 2305-6304. DOI: 10.3390/toxics13090753.

77. SHEN, S., LI, X.-F., CULLEN, W.R., WEINFELD, M., LE, X.C. Arsenic Binding to Proteins. In: *Chemical Reviews*. 2013. vol. 113, no. 10, pp. 7769–7792. ISSN 0009-2665. DOI: 10.1021/cr300015c.

78. GENCHI, G., SINICROPI, M.S., LAURIA, G., CAROCCI, A., CATALANO, A. The Effects of Cadmium Toxicity. In: *International Journal of Environmental Research and Public Health*. 2020. vol. 17, no. 11, pp. 3782. ISSN 1661-7827. DOI: 10.3390/ijerph17113782.

79. HAYAT, M.T., NAUMAN, M., NAZIR, N., ALI, S., BANGASH, N. Environmental Hazards of Cadmium: Past, Present, and Future. In: *Cadmium Toxicity and Tolerance in Plants*. London: Academic Press, 2019, pp. 163–183. ISBN 978-0-12-814864-8. DOI: 10.1016/B978-0-12-814864-8.00007-3.

80. RANI, A., KUMAR, A., LAL, A., PANT, M. Cellular mechanisms of cadmium-induced toxicity: a review. In: *International Journal of Environmental Health Research*. 2014. vol. 24, no. 4, pp. 378–399. ISSN 0960-3123. DOI: 10.1080/09603123.2013.835032.

81. SATARUG, S., GARRETT, S.H., SENS, M.A., SENS, D.A. Cadmium, Environmental Exposure, and Health Outcomes. In: *Environmental Health Perspectives*. 2010. vol. 118, no. 2, pp. 182–190. ISSN 0091-6765. DOI: 10.1289/ehp.0901234.

82. YANG, H., SHU, Y. Cadmium Transporters in the Kidney and Cadmium-Induced Nephrotoxicity. In: *International Journal of Molecular Sciences*. 2015. vol. 16, no. 1, pp. 1484–1494. ISSN 1422-0067. DOI: 10.3390/ijms16011484.

83. SAHA, R., NANDI, R., SAHA, B. Sources and toxicity of hexavalent chromium. In: *Journal of Coordination Chemistry*. 2011. vol. 64, no. 10, pp. 1782–1806. ISSN 0095-8972. DOI: 10.1080/00958972.2011.583646.

84. MURTHY, M.K., KHANDAYATARAY, P., PADHIARY, S., SAMAL, D. A review on chromium health hazards and molecular mechanism of chromium bioremediation. In: *Reviews on Environmental Health*. 2023. vol. 38, no. 3, pp. 461–478. ISSN 0048-7554. DOI: 10.1515/reveh-2021-0139.

85. SHIN, D.Y., LEE, S.M., JANG, Y., LEE, J., LEE, C.M., CHO, E.-M., SEO, Y.R. Adverse Human Health Effects of Chromium by Exposure Route: A Comprehensive Review Based on Toxicogenomic Approach. In: *International Journal of Molecular Sciences*. 2023. vol. 24, no. 4, pp. 3410. ISSN 1422-0067. DOI: 10.3390/ijms24043410.

86. YAN, G., GAO, Y., XUE, K., QI, Y., FAN, Y., TIAN, X., WANG, J., ZHAO, R., ZHANG, P., LIU, Y., LIU, J. Toxicity mechanisms and remediation strategies for chromium exposure in the environment. In: *Frontiers in Environmental Science*. 2023. vol. 11. ISSN 2296-665X. DOI: 10.3389/fenvs.2023.1131204.

87. PAVESI, T., MOREIRA, J.C. Mechanisms and individuality in chromium toxicity in humans. In: *Journal of Applied Toxicology*. 2020. vol. 40, no. 9, pp. 1183–1197. ISSN 0260-437X. DOI: 10.1002/jat.3965.

88. SIMONSEN, L.O., HARBAK, H., BENNEKOU, P. Cobalt metabolism and toxicology—A brief update. In: *Science of The Total Environment*. 2012. vol. 432, pp. 210–215. ISSN 0048-9697. DOI: 10.1016/j.scitotenv.2012.06.009.

89. BIBI, M. Essential and non-essential heavy metals sources and impacts on human health and plants. In: *Pure and Applied Biology*. 2023. vol. 12, no. 2. ISSN 2304-2478. DOI: 10.19045/bspab.2023.120083.

90. ORTEGA, R., BRESSON, C., DAROLLES, C., GAUTIER, C., ROUDEAU, S., PERRIN, L., JANIN, M., FLORIANI, M., ALOIN, V., CARMONA, A., MALARD, V. Low-solubility particles and a Trojan-horse type mechanism of toxicity: the case of cobalt oxide on human lung cells. In: *Particle and Fibre Toxicology*. 2014. vol. 11, no. 1, pp. 14. ISSN 1743-8977. DOI: 10.1186/1743-8977-11-14.

91. GAETKE, L.M., CHOW-JOHNSON, H.S., CHOW, C.K. Copper: toxicological relevance and mechanisms. In: *Archives of Toxicology*. 2014. vol. 88, no. 11, pp. 1929–1938. ISSN 0340-5761. DOI: 10.1007/s00204-014-1355-y.

92. CHEN, J., JIANG, Y., SHI, H., PENG, Y., FAN, X., LI, C. The molecular mechanisms of copper metabolism and its roles in human diseases. In: *Pflügers Archiv - European Journal of Physiology*. 2020. vol. 472, no. 10, pp. 1415–1429. ISSN 0031-6768. DOI: 10.1007/s00424-020-02412-2.

93. HUSAK, V. Copper and Copper-Containing Pesticides: Metabolism, Toxicity and Oxidative Stress. In: *Journal of Vasyl Stefanyk Precarpathian National University*. 2015. vol. 2, no. 1, pp. 38–50. ISSN 2311-0155. DOI: 10.15330/jpnu.2.1.38-50.

94. PEASE, C., RÜCKER, T., BIRK, T. Review of the Evidence from Epidemiology, Toxicology, and Lung Bioavailability on the Carcinogenicity of Inhaled Iron Oxide Particulates. In: *Chemical Research in Toxicology*. 2016. vol. 29, no. 3, pp. 237–254. ISSN 0893-228X. DOI: 10.1021/acs.chemrestox.5b00448.

95. ANDERSON, G.J. Mechanisms of iron loading and toxicity. In: *American journal of hematology*. 2007. vol. 82, no. S12, pp. 1128–1131. ISSN 0361-8609. DOI: 10.1002/ajh.21075.

96. TAYAL, A., KAUR, J., SADEGHI, P., MAITTA, R.W. Molecular Mechanisms of Iron Metabolism and Overload. In: *Biomedicines*. 2025. vol. 13, no. 9, pp. 2067. ISSN 2227-9059. DOI: 10.3390/biomedicines13092067.

97. WANG, R., BALKANSKI, Y., BOUCHER, O., BOPP, L., CHAPPELL, A., CIAIS, P., HAUGLUSTAINE, D., PEÑUELAS, J., TAO, S. Sources, transport and deposition of iron in the global atmosphere. In: *Atmospheric Chemistry and Physics*. 2015. vol. 15, no. 11, pp. 6247–6270. ISSN 1680-7316. DOI: 10.5194/acp-15-6247-2015.

98. GENERALOVA, A., DAVIDOVA, S., SATCHANSKA, G. The Mechanisms of Lead Toxicity in Living Organisms. In: *Journal of Xenobiotics*. 2025. vol. 15, no. 5, pp. 146. ISSN 2039-4705. DOI: 10.3390/jox15050146.

99. BOLDYREV, M. Lead: properties, history, and applications. In: *WikiJournal of Science*. 2018. vol. 1, no. 2, pp. 7. ISSN 2470-6345. DOI: 10.15347/wjs/2018.007.

100. YANG, J., LI, X., XIONG, Z., WANG, M., LIU, Q. Environmental Pollution Effect Analysis of Lead Compounds in China Based on Life Cycle. In: *International Journal of Environmental Research and Public Health*. 2020. vol. 17, no. 7, pp. 2184. ISSN 1661-7827. DOI: 10.3390/ijerph17072184.

101. COLLIN, M.S., VENKATRAMAN, S.K., VIJAYAKUMAR, N., KANIMOZHI, V., ARBAAZ, S.M., STACEY, R.G.S., ANUSHA, J., CHOUDHARY, R., LVOV, V., TOVAR, G.I., SENATOV, F., KOPPALA, S., SWAMIAPPAN, S. Bioaccumulation of lead (Pb) and its effects on human: A review. In: *Journal of Hazardous Materials Advances*. 2022. vol. 7, pp. 100094. ISSN 2772-4166. DOI: 10.1016/j.hazadv.2022.100094.

102. OBENG-GYASI, E. Sources of lead exposure in various countries. In: *Reviews on Environmental Health*. 2019. vol. 34, no. 1, pp. 25–34. ISSN 0048-7554. DOI: 10.1515/reveh-2018-0037.

103. SANGEETHA, K.S., UMAMAHESWARI, S. Human Exposure to Lead, Mechanism of Toxicity and Treatment Strategy - A Review. In: *Journal of Clinical and Diagnostic Research*. 2020. vol. 14, no. 12. ISSN 2249-782X. DOI: 10.7860/JCDR/2020/45615.14345.

104. KOYAMA, H., KAMOGASHIRA, T., YAMASOBA, T. Heavy Metal Exposure: Molecular Pathways, Clinical Implications, and Protective Strategies. In: *Antioxidants*. 2024. vol. 13, no. 1, pp. 76. ISSN 2076-3921. DOI: 10.3390/antiox13010076.

105. CHEN, P., CULBRETH, M., ASCHNER, M. Exposure, epidemiology, and mechanism of the environmental toxicant manganese. In: *Environmental Science and Pollution Research*. 2016. vol. 23, no. 14, pp. 13802–13810. ISSN 1614-7499. DOI: 10.1007/s11356-016-6687-0.

106. MICHALKE, B., FERNSEBNER, K. New insights into manganese toxicity and speciation. In: *Journal of Trace Elements in Medicine and Biology*. 2014. vol. 28, no. 2, pp. 106–116. ISSN 0946-672X. DOI: 10.1016/j.jtemb.2013.08.005.

107. PERES, T. V., SCHETTINGER, M.R.C., CHEN, P., CARVALHO, F., AVILA, D.S., BOWMAN, A.B., ASCHNER, M. Manganese-induced neurotoxicity: a review of its behavioral consequences and neuroprotective strategies. In: *BMC Pharmacology and Toxicology*. 2016. vol. 17, no. 1, pp. 57. ISSN 2050-6511. DOI: 10.1186/s40360-016-0099-0.

108. TINKOV, A.A., PAOLIELLO, M.M.B., MAZILINA, A.N., SKALNY, A. V., MARTINS, A.C., VOSKRESENSKAYA, O.N., AASETH, J., SANTAMARIA, A., NOTOVA, S. V., TSATSAKIS, A., LEE, E., BOWMAN, A.B., ASCHNER, M. Molecular Targets of Manganese-Induced Neurotoxicity: A Five-Year Update. In: *International Journal of Molecular Sciences*. 2021. vol. 22, no. 9, pp. 4646. ISSN 1422-0067. DOI: 10.3390/ijms22094646.

109. WU, Y.-S., OSMAN, A.I., HOSNY, M., ELGARAHY, A.M., ELTAWEIL, A.S., ROONEY, D.W., CHEN, Z., RAHIM, N.S., SEKAR, M., GOPINATH, S.C.B., MAT RANI, N.N.I., BATUMALAIE, K., YAP, P.-S. The Toxicity of Mercury and Its Chemical Compounds: Molecular Mechanisms and Environmental and Human Health Implications: A Comprehensive Review. In: *ACS Omega*. 2024. vol. 9, no. 5, pp. 5100–5126. ISSN 2470-1343. DOI: 10.1021/acsomega.3c07047.

110. BEGUM, W., RAI, S., BANERJEE, S., BHATTACHARJEE, S., MONDAL, M.H., BHATTARAI, A., SAHA, B. A comprehensive review on the sources, essentiality and toxicological profile of nickel. In: *RSC Advances*. 2022. vol. 12, no. 15, pp. 9139–9153. ISSN 2046-2069. DOI: 10.1039/D2RA00378C.

111. DAS, K.K., REDDY, R.C., BAGOJI, I.B., DAS, S., BAGALI, S., MULLUR, L., KHODNAPUR, J.P., BIRADAR, M.S. Primary concept of nickel toxicity – an overview. In: *Journal of Basic and Clinical Physiology and Pharmacology*. 2019. vol. 30, no. 2, pp. 141–152. ISSN 0792-6855. DOI: 10.1515/jbcpp-2017-0171.

112. GENCHI, G., CAROCCI, A., LAURIA, G., SINICROPI, M.S., CATALANO, A. Nickel: Human Health and Environmental Toxicology. In: *International Journal of Environmental Research and Public Health*. 2020. vol. 17, no. 3, pp. 679. ISSN 1661-7827. DOI: 10.3390/ijerph17030679.

113. SCHOOFS, H., SCHMIT, J., RINK, L. Zinc Toxicity: Understanding the Limits. In: *Molecules*. 2024. vol. 29, no. 13, pp. 3130. ISSN 1420-3049. DOI: 10.3390/molecules29133130.

114. PLUM, L.M., RINK, L., HAASE, H. The Essential Toxin: Impact of Zinc on Human Health. In: *International Journal of Environmental Research and Public Health*. 2010. vol. 7, no. 4, pp. 1342–1365. ISSN 1661-7827. DOI: 10.3390/ijerph7041342.

115. STULL, R. *An algebra-based survey of atmospheric science*. 3rd Edition. University of British Columbia, 2015. ISBN 978-0-88865-178-5.

116. LIN, J., QIAN, T., BECHTOLD, P., GRELL, G., ZHANG, G.J., ZHU, P., FREITAS, S.R., BARNES, H., HAN, J. Atmospheric Convection. In: *Atmosphere-Ocean*. 2022. vol. 60, no. 3–4, pp. 422–476. ISSN 0705-5900. DOI: 10.1080/07055900.2022.2082915.

117. JACOBSON, M.Z. *Air pollution and global warming: history, science, and solutions*. 2nd ed. Cambridge: Cambridge University Press, 2012.ISBN 110769115X.

118. GKIKAS, A., BASART, S., HATZIANASTASSIOU, N., MARINOU, E., AMIRIDIS, V., KAZADZIS, S., PEY, J., QUEROL, X., JORBA, O., GASSÓ, S. Mediterranean intense desert dust outbreaks and their vertical structure based on remote sensing data. In: *Atmospheric Chemistry and Physics*. 2016. vol. 16, no. 13, pp. 8609–8642. ISSN 1680-7316. DOI: 10.5194/acp-16-8609-2016.

119. ALIZADEH-CHOOBARI, O., STURMAN, A., ZAWAR-REZA, P. A global satellite view of the seasonal distribution of mineral dust and its correlation with atmospheric circulation. In: *Dynamics of atmospheres and oceans*. 2014. vol. 68, pp. 20–34. ISSN 0377-0265.

120. DENJEAN, C., FORMENTI, P., DESBOEUFS, K., CHEVAILLIER, S., TRIQUET, S., MAILLÉ, M., CAZAUNAU, M., LAURENT, B., MAYOL-BRACERO, O.L., VALLEJO, P. Size distribution and optical properties of African mineral dust after intercontinental transport. In: *Journal of Geophysical Research: Atmospheres*. 2016. vol. 121, no. 12, pp. 7117–7138. ISSN 2169-897X. DOI: 10.1002/2016JD024783.

121. GRIFFIN, D.W. Atmospheric movement of microorganisms in clouds of desert dust and implications for human health. In: *Clinical microbiology reviews*. 2007. vol. 20, no. 3, pp. 459–477. ISSN 0893-8512. DOI: 10.1128/CMR.00039-06.

122. BI, J., LI, Z., ZUO, D., YANG, F., LI, B., MA, J., HUANG, Z., HE, Q. Dust aerosol vertical profiles in the hinterland of Taklimakan Desert during summer 2019. In: *Frontiers in Environmental Science*. 2022. vol. 10, pp. 851915. ISSN 2296-665X. DOI: 10.3389/fenvs.2022.851915.

123. FENG, X., WEI, S., WANG, S. Temperature inversions in the atmospheric boundary layer and lower troposphere over the Sichuan Basin, China: Climatology and impacts on air pollution. In: *Science of The Total Environment*. 2020. vol. 726, pp. 138579. ISSN 0048-9697. DOI: 10.1016/j.scitotenv.2020.138579.

124. LEHNER, M., ROTACH, M.W. Current Challenges in Understanding and Predicting Transport and Exchange in the Atmosphere over Mountainous Terrain. In: *Atmosphere*. 2018. vol. 9, no. 7, pp. 276. ISSN 2073-4433. DOI: 10.3390/atmos9070276.

125. CLAEYS, M.J., RAJAGOPALAN, S., NAWROT, T.S., BROOK, R.D. Climate and environmental triggers of acute myocardial infarction. In: *European heart journal*. 2017. vol. 38, no. 13, pp. 955–960. ISSN 0195-668X. DOI: 10.1093/eurheartj/ehw151.

126. PÖSCHL, U., SHIRAIWA, M. Multiphase chemistry at the atmosphere–biosphere interface influencing climate and public health in the anthropocene. In: *Chemical reviews*. 2015. vol. 115, no. 10, pp. 4440–4475. ISSN 0009-2665.

127. TANG, M., HUANG, X., LU, K., GE, M., LI, Y., CHENG, P., ZHU, T., DING, A., ZHANG, Y., GLIGOROVSKI, S. Heterogeneous reactions of mineral dust aerosol: implications for tropospheric oxidation capacity. In: *Atmospheric Chemistry and Physics*. 2017. vol. 17, no. 19, pp. 11727–11777. ISSN 1680-7316. DOI: 10.5194/acp-17-11727-2017.

128. WANG, Z., UNO, I., YUMIMOTO, K., PAN, X., CHEN, X., LI, J., WANG, Z., SHIMIZU, A., SUGIMOTO, N. Dust heterogeneous reactions during long-range transport of a severe dust storm in May 2017 over East Asia. In: *Atmosphere*. 2019. vol. 10, no. 11, pp. 680. ISSN 2073-4433. DOI: 10.3390/atmos10110680.

129. CREAMEAN, J.M., SUSKI, K.J., ROSENFELD, D., CAZORLA, A., DEMOTT, P.J., SULLIVAN, R.C., WHITE, A.B., RALPH, F.M., MINNIS, P., COMSTOCK, J.M. Dust and biological aerosols from the Sahara and Asia influence precipitation in the western US. In: *Science*. 2013. vol. 339, no. 6127, pp. 1572–1578. ISSN 0036-8075. DOI: 10.1126/science.1227279.

130. WANG, Z., ZHANG, H., JING, X., WEI, X. Effect of non-spherical dust aerosol on its direct radiative forcing. In: *Atmospheric Research*. 2013. vol. 120, pp. 112–126. ISSN 0169-8095.

131. PARK, J., KIM, H., KIM, Y., HEO, J., KIM, S.-W., JEON, K., YI, S.-M., HOPKE, P.K. Source apportionment of $PM_{2.5}$ in Seoul, South Korea and Beijing, China using dispersion normalized PMF. In: *Science of The Total Environment*. 2022. vol. 833, pp. 155056. ISSN 0048-9697.

132. TSEDENDAMBA, P., DULAM, J., BABA, K., HAGIWARA, K., NODA, J., KAWAI, K., SUMIYA, G., MCCARTHY, C., KAI, K., HOSHINO, B. Northeast Asian dust transport: A case study of a dust storm event from 28 March to 2 April 2012. In: *Atmosphere*. 2019. vol. 10, no. 2, pp. 69. ISSN 2073-4433. DOI: 10.3390/atmos10020069.

133. UNO, I., UEMATSU, M., HARA, Y., HE, Y.J., OHARA, T., MORI, A., KAMAYA, T., MURANO, K., SADANAGA, Y., BANDOW, H. Numerical study of the atmospheric input of anthropogenic total nitrate to the marginal seas in the western North Pacific region. In: *Geophysical Research Letters*. 2007. vol. 34, no. 17. ISSN 0094-8276. DOI: 10.1029/2007GL030338.

134. ABOUCHAMI, W., NÄTHE, K., KUMAR, A., GALER, S.J.G., JOCHUM, K.P., WILLIAMS, E., HORBE, A.M.C., ROSA, J.W.C., BALSAM, W., ADAMS, D. Geochemical and isotopic characterization of the Bodélé Depression dust source and implications for transatlantic dust transport to the Amazon Basin. In: *Earth and Planetary Science Letters*. 2013. vol. 380, pp. 112–123. ISSN 0012-821X. DOI: 10.1016/j.epsl.2013.08.028.

135. JIN, L., HE, Q., LI, Z., DENG, M., ABBAS, A. Interannual and seasonal variations of sand-dust events in Tarim Basin, China. Preprint. 2021. DOI: 10.21203/rs.3.rs-327333/v1.

136. SHAO, Y., KLOSE, M., WYRWOLL, K. Recent global dust trend and connections to climate forcing. In: *Journal of Geophysical Research: Atmospheres*. 2013. vol. 118, no. 19, pp. 11,107–11,118. ISSN 2169-897X. DOI: 10.1002/jgrd.50836.

137. HUO, W., YANG, F., WU, Y., ZHI, X., SONG, M., ZHOU, C., YANG, X., MAMTIMIN, A., HE, Q., WEN, C. Influence of Topographic Relief on Sand Transport in the Near-Surface Layer During Dust Storms in the Taklimakan Desert. In: *Frontiers in Environmental Science*. 2022. vol. 10, pp. 931529. ISSN 2296-665X.

138. KATRA, I. Soil erosion by wind and dust emission in semi-arid soils due to agricultural activities. In: *Agronomy*. 2020. vol. 10, no. 1, pp. 89. ISSN 2073-4395. DOI: 10.3390/agronomy10010089.

139. AZIMI, S., LUDWIG, A., THÉVENOT, D.R., COLIN, J.-L. Trace metal determination in total atmospheric deposition in rural and urban areas. In: *Science of The Total Environment*. 2003. vol. 308, no. 1–3, pp. 247–256. ISSN 0048-9697. DOI: 10.1016/S0048-9697(02)00678-2.

140. SAITANIS, C.J., FRONTASYEVA, M. V., STEINNES, E., PALMER, M.W., OSTROVNAYA, T.M., GUNDORINA, S.F. Spatiotemporal distribution of airborne elements monitored with the moss bags technique in the Greater Thriasion Plain, Attica, Greece. In: *Environmental Monitoring and Assessment*. 2013. vol. 185, no. 1, pp. 955–968. ISSN 0167-6369. DOI: 10.1007/s10661-012-2606-0.

141. MARKERT, B.A., BREURE, A.M., ZECHMEISTER, H.G. *Bioindicators & Biomonitors: Principles and concepts*. Amsterdam; Boston: Elsevier, 2003. vol. 6. ISBN 9780080527970.

142. CHAKRABORTTY, S., PARATKAR, G.T. Biomonitoring of Trace Element Air Pollution Using Mosses. In: *Aerosol and Air Quality Research*. 2006. vol. 6, no. 3, pp. 247–258. ISSN 2071-1409 DOI: 10.4209/aaqr.2006.09.0002.

143. ZHANG, Z.H., CHAI, Z.F., MAO, X.Y., CHEN, J.B. Biomonitoring trace element atmospheric deposition using lichens in China. In: *Environmental Pollution*. 2002. vol. 120, no. 1, pp. 157–161. ISSN 0269-7491.

144. GUÉGUEN, F., STILLE, P., MILLET, M. Air quality assessment by tree bark biomonitoring in urban, industrial and rural environments of the Rhine Valley: PCDD/Fs, PCBs and trace metal evidence. In: *Chemosphere*. 2011. vol. 85, no. 2, pp. 195–202. ISSN 0045-6535.

145. ZHOU, X., LI, J., YAN, P., LU, N., LU, L., NI, Q., ZHANG, J., FANG, Y. Mosses as Biomonitors of Atmospheric Trace Metal and Nitrogen Deposition: Spatial Distribution and Temporal Trend in Yancheng, China. In: *Plants*. 2025. vol. 14, no. 9, pp. 1315. ISSN 2223-7747.

146. KHODADADI, M., WIDOM, E., KOUSEHLAR, M., KREKELER, M.P.S. Long-Term Changes in Particulate Matter Abundance and Sources in an Industrial City: Insights from Microscopy and Elemental and Pb Isotopic Compositions of Bio-monitors. In: *Environmental Pollution*. 2025. P. 126590. ISSN 0269-7491. DOI: 10.1016/j.envpol.2025.126590.

147. RUHLING, A., TYLER, G. Ecology of heavy metals – a regional and historical study. In: *Botaniska Notiser (Sweden)*. 1969. vol. 122. ISSN 0006-8195.

148. RUHLING, A., TYLER, G. Regional Differences in the Deposition of Heavy Metals Over Scandinavia. In: *The Journal of Applied Ecology*. 1971. vol. 8, no. 2, pp. 497. ISSN 0021-8901. DOI: 10.2307/2402886.

149. STEINNES, E. Biomonitors of Air Pollution by Heavy Metals. In: *Control and Fate of Atmospheric Trace Metals*. Dordrecht: Springer, 1989, pp. 321–338. NATO ASI Series. ISBN 978-94-010-7527-5. DOI: 10.1007/978-94-009-2315-7_15.

150. GJENGEDAL, E., STEINNES, E. Uptake of metal ions in moss from artificial precipitation. In: *Environmental Monitoring and Assessment*. 1990. vol. 14, no. 1, pp. 77–87. ISSN 0167-6369. DOI: 10.1007/BF00394359.

151. VERGEL, K., ZINICOVSCAIA, I., YUSHIN, N., CHALIGAVA, O., NEKHOROSHKOV, P., GROZDOV, D. Moss Biomonitoring of Atmospheric Pollution with Trace Elements in the Moscow Region, Russia. In: *Toxics*. 2022. vol. 10, no. 2. ISSN 2305-6304. DOI: 10.3390/toxics10020066.

152. GATZIOLIS, D., JOVAN, S., DONOVAN, G., AMACHER, M., MONLEON, V. Elemental atmospheric pollution assessment via moss-based measurements in Portland, Oregon. In: *General Technical Report PNW-GTR-938.* United States Department of Agriculture. *55 p.* 2016. DOI:10.2737/PNW-GTR-938

153. YURUKOVA, L., TSAKIRI, E., CAYIR, A. Cross-border response of moss, *Hypnum cupressiforme* Hedw., to atmospheric deposition in southern Bulgaria and northeastern

Greece. In: *Bulletin of environmental contamination and toxicology*. 2009. vol. 83, pp. 174–179. ISSN 0007-4861.

154. HARMENS, H., NORRIS, D., MILLS, G. *Heavy metals and nitrogen in mosses: spatial patterns in 2010/2011 and long-term temporal trends in Europe*. NERC/Centre for Ecology & Hydrology, 2013. ISBN 1906698384.

155. HARMENS, H., NORRIS, D.A., STEINNES, E., KUBIN, E., PIISPANEN, J., ALBER, R., ALEKSIAYENAK, Y., BLUM, O., COŞKUN, M., DAM, M., DE TEMMERMAN, L., FERNÁNDEZ, J.A., FROLOVA, M., FRONTASYEVA, M., GONZÁLEZ-MIQUEO, L., GRODZIŃSKA, K., JERAN, Z., KORZEKWA, S., KRMAR, M., KVIETKUS, K., LEBLOND, S., LIIV, S., MAGNÚSSON, S.H., MAŇKOVSKÁ, B., PESCH, R., RÜHLING, Å., SANTAMARIA, J.M., SCHRÖDER, W., SPIRIC, Z., SUCHARA, I., THÖNI, L., URUMOV, V., YURUKOVA, L., ZECHMEISTER, H.G. Mosses as biomonitors of atmospheric heavy metal deposition: Spatial patterns and temporal trends in Europe. In: *Environmental Pollution*. 2010. vol. 158, no. 10, pp. 3144–3156. ISSN 0269-7491. DOI: 10.1016/j.envpol.2010.06.039.

156. COŞKUN, M., YURUKOVA, L., ÇAYIR, A., COŞKUN, M., GECHEVA, G. Cross-border response of mosses to heavy metal atmospheric deposition in Southeastern Bulgaria and European Turkey. In: *Environmental monitoring and assessment*. 2009. vol. 157, pp. 529–537. ISSN 0167-6369.

157. NICKEL, S., SCHRÖDER, W. Correlating elements content in mosses collected in 2015 across Germany with spatially associated characteristics of sampling sites and their surroundings. In: *Environmental Sciences Europe*. 2019. vol. 31, pp. 1–21. ISSN 2190-4707.

158. ZINICOVSCAIA, I., CHERNYAGINA, O., CHALIGAVA, O., YUSHIN, N., DEVYATOVA, E., GROZOV, D. Moss biomonitoring in areas affected by ashfalls of Shiveluch volcano (Kamchatka). In: *Environmental Science and Pollution Research*. 2024. vol. 31, no. 52, pp. 61730–61739. ISSN 1614-7499. DOI: 10.1007/s11356-024-35383-3.

159. STIHI, C., POPESCU, I. V, FRONTASYEVA, M., RADULESCU, C., ENE, A., CULICOV, O., ZINICOVSCAIA, I., DULAMA, I.D., CUCU-MAN, S., TODORAN, R. Characterization of heavy metal air pollution in Romania using moss biomonitoring, neutron activation analysis, and atomic absorption spectrometry. In: *Analytical Letters*. 2017. vol. 50, no. 17, pp. 2851–2858. ISSN 0003-2719.

160. STEINNES, E. Atmospheric deposition of trace elements in Norway studied by means of moss analysis. No. KR-154. Institutt for Atomenergi, Kjeller, Norway, 1977.

161. RUHLING, A., BRUMELIS, G., GOLTSOVA, N., KVIETKUS, K., KUBIN, E., LIIV, S., MAGNUSSON, S., MAEKINEN, A., PILEGAARD, K., RASMUSSEN, L., SANDER,

E., STEINNES, E. Atmospheric heavy metal deposition in Northern Europe 1990. Copenhagen: Nordic Council of Ministers, 1992. ISBN 9291200158.

162. HARMENS, H., BUSE, A., BÜKER, P., NORRIS, D., MILLS, G., WILLIAMS, B., REYNOLDS, B., ASHENDEN, T.W., RÜHLING, Å., STEINNES, E. Heavy Metal Concentrations in European Mosses: 2000/2001 Survey. In: *Journal of Atmospheric Chemistry*. 2004. vol. 49, no. 1–3, pp. 425–436. ISSN 0167-7764. DOI: 10.1007/s10874-004-1257-0.

163. HARMENS, H., NORRIS, D., MILLS, G. Heavy metals and nitrogen in mosses: spatial patterns in 2010/11 and long-term temporal trends (1990-2010) in Europe. ECE/EB.AIR/WG.1/2013/13. Bangor: ICP Coordination Centre, 2013.

164. RÜHLING, Å. *Atmospheric Heavy Metal Deposition in Europe – estimation based on moss analysis*. Copenhagen: Nordic Council of Ministers, 1994. ISBN 9291204277.

165. KOSONEN, Z., THIMONIER, A., SCHNYDER, E., THÖNI, L. Nitrogen concentration in moss compared with N load in precipitation and with total N deposition in Switzerland. In: *Environmental Pollution*. 2018. vol. 239, pp. 169–178. ISSN 0269-7491. DOI: https://doi.org/10.1016/j.envpol.2018.03.063.

166. OISHI, Y. Seasonal differences in nitrogen deposition affect nitrogen content in mosses: Implications for biomonitoring. In: *Environmental Nanotechnology, Monitoring & Management*. 2023. vol. 20, pp. 100783. ISSN 2215-1532. DOI: 10.1016/j.enmm.2023.100783.

167. SCHLABACH, M., STEINNES, E., UGGERUD, H.T. Atmospheric deposition of organic contaminants in Norway. National survey 2015. In: *NILU rapport, 28/2016*. Kjeller: Norwegian Institute for Air Research, 2016. ISBN 978-82-425-2837-7.

168. MOTYKA, O., PAVLÍKOVÁ, I., BITTA, J., FRONTASYEVA, M., JANČÍK, P. Moss biomonitoring and air pollution modelling on a regional scale: delayed reflection of industrial pollution in moss in a heavily polluted region? In: *Environmental Science and Pollution Research*. 2020. vol. 27, no. 26, pp. 32569–32578. ISSN 1614-7499. DOI: 10.1007/s11356-020-09466-w.

169. MESSAGER, M.L., DAVIES, I.P., LEVIN, P.S. Low-cost biomonitoring and high-resolution, scalable models of urban metal pollution. In: *Science of The Total Environment*. 2021. vol. 767, pp. 144280. ISSN 0048-9697. DOI: 10.1016/j.scitotenv.2020.144280.

170. ROBLIN, B., AHERNE, J. Moss as a biomonitor for the atmospheric deposition of anthropogenic microfibres. In: *Science of The Total Environment*. 2020. vol. 715, pp. 136973. ISSN 0048-9697. DOI: 10.1016/j.scitotenv.2020.136973.

171. BERTRIM, C., AHERNE, J. Moss Bags as Biomonitors of Atmospheric Microplastic Deposition in Urban Environments. In: *Biology*. 2023. vol. 12, no. 2. ISSN 2079-7737. DOI: 10.3390/biology12020149.

172. BARANDOVSKI, L., CEKOVA, M., FRONTASYEVA, M. V, PAVLOV, S.S., STAFILOV, T., STEINNES, E., URUMOV, V. Atmospheric deposition of trace element pollutants in Macedonia studied by the moss biomonitoring technique. In: *Environmental Monitoring and Assessment*. 2008. vol. 138, no. 1, pp. 107–118. ISSN 0167-6369. DOI: 10.1007/s10661-007-9747-6.

173. BARANDOVSKI, L., FRONTASYEVA, M. V, STAFILOV, T., ŠAJN, R., OSTROVNAYA, T.M. Multi-element atmospheric deposition in Macedonia studied by the moss biomonitoring technique. In: *Environmental Science and Pollution Research*. 2015. vol. 22, no. 20, pp. 16077–16097. ISSN 1614-7499. DOI: 10.1007/s11356-015-4787-x.

174. HRISTOZOVA, G., MARINOVA, S., SVOZILÍK, V., NEKHOROSHKOV, P., FRONTASYEVA, M. V. Biomonitoring of elemental atmospheric deposition: spatial distributions in the 2015/2016 moss survey in Bulgaria. In: *Journal of Radioanalytical and Nuclear Chemistry*. 2020. vol. 323, no. 2, pp. 839–849. ISSN 0236-5731. DOI: 10.1007/s10967-019-06978-9.

175. HRISTOZOVA, G., MARINOVA, S., MOTYKA, O., SVOZILÍK, V., ZINICOVSCAIA, I. Multivariate assessment of atmospheric deposition studies in Bulgaria based on moss biomonitors: trends between the 2005/2006 and 2015/2016 surveys. In: *Environmental Science and Pollution Research*. 2020. vol. 27, no. 31, pp. 39330–39342. ISSN 1614-7499. DOI: 10.1007/s11356-020-10005-w.

176. BARANDOVSKI, L., STAFILOV, T., ŠAJN, R., FRONTASYEVA, M., BAČEVA ANDONOVSKA, K. Atmospheric Heavy Metal Deposition in North Macedonia from 2002 to 2010 Studied by Moss Biomonitoring Technique. In: *Atmosphere*. 2020. vol. 11, no. 9. ISSN 2073-4433. DOI: 10.3390/atmos11090929.

177. SHETEKAURI, S., SHETEKAURI, T., KVLIVIDZE, A., CHALIGAVA, O., KALABEGISHVILI, T., KIRKESALI, E.I., FRONTASYEVA, M. V, CHEPURCHENKO, O.E. Preliminary results of atmospheric deposition of major and trace elements in the greater and lesser Caucasus Mountains studied by the moss technique and neutron activation analysis. In: *Annali di Botanica*. 2015. vol. 5, pp. 89–95. ISSN 0365-0812.

178. SHETEKAURI, S., CHALIGAVA, O., SHETEKAURI, T., KVLIVIDZE, A., KALABEGISHVILI, T., KIRKESALI, E., FRONTASYEVA, M.V., CHEPURCHENKO, O.E., TSELMOVICH, V.A. Biomonitoring air pollution using moss in Georgia. In: *Polish Journal of*

Environmental Studies. 2018. vol. 27, no. 5, pp. 2259–2266. ISSN 1230-1485. DOI: 10.15244/pjoes/73798.

179. CHALIGAVA, O., SHETEKAURI, S., BADAWY, W.M., FRONTASYEVA, M. V., ZINICOVSCAIA, I., SHETEKAURI, T., KVLIVIDZE, A., VERGEL, K., YUSHIN, N. Characterization of Trace Elements in Atmospheric Deposition Studied by Moss Biomonitoring in Georgia. In: *Archives of Environmental Contamination and Toxicology*. 2021. vol. 80, no. 2. ISSN 0090-4341. DOI: 10.1007/s00244-020-00788-x.

180. ZINICOVSCAIA, I., HRAMCO, C., DULIU, O.G., VERGEL, K., CULICOV, O.A., FRONTASYEVA, M. V, DUCA, G. Air pollution study in the Republic of Moldova using moss biomonitoring technique. In: *Bulletin of environmental contamination and toxicology*. 2017. vol. 98, no. 2, pp. 262–269. ISSN 0007-4861. DOI: 10.1007/s00128-016-1989-y.

181. PROCTOR, M.C.F., GOFFINET, B. Physiological ecology. In: SHAW, A. Jonathan (ed.), In: *Bryophyte Biology*. 2nd ed. Cambridge: Cambridge University Press, 2008. pp. 237–268. ISBN 978-0-521-87225-6.

182. CRANDALL-STOTLER, B., BARTHOLOMEW-BEGAN, S. Morphology of Mosses (Phylum Bryophyta). In: *Flora of North America North of Mexico*. 2007. vol. 27, pp. 3–17. ISBN 978-0-19-531823-4.

183. BÜDEL, B., FRIEDL, T., BEYSCHLAG, W. *Biology of Algae, Lichens and Bryophytes*. Berlin, Heidelberg: Springer Berlin Heidelberg, 2024. ISBN 978-3-662-65711-9.

184. SHARMA, O.P. *Bryophyta*. McGraw Hill Education, 2014. ISBN 1259062872.

185. PRESSEL, S., LIGRONE, R., DUCKETT, J.G. Effects of de-and rehydration on food-conducting cells in the moss Polytrichum formosum: a cytological study. In: *Annals of Botany*. 2006. vol. 98, no. 1, pp. 67–76. ISSN 0305-7364. DOI: 10.1093/aob/mcl092.

186. HE, X., HE, K.S., HYVÖNEN, J. Will bryophytes survive in a warming world? In: *Perspectives in Plant Ecology, Evolution and Systematics*. 2016. vol. 19, pp. 49–60. ISSN 1433-8319. DOI: 10.1016/j.ppees.2016.02.005.

187. O'NEILL, K.P. Role of bryophyte-dominated ecosystems in the global carbon budget. In: *Bryophyte Biology*. 2000. P. 344–368. ISBN 0-521-66097-1. DOI: 10.1017/CBO9781139171304.012.

188. VITT, D.H., WIEDER, R.K. The structure and function of bryophyte-dominated peatlands. In: *Bryophyte Biology, Second Edition*. 2008. P. 357–392. ISBN 978-0-521-87225-6. DOI: 10.1017/CBO9780511754807.010.

189. VAN TOOREN, B.F., HERTOG, J. DEN, VERHAAR, J. Cover, biomass and nutrient content of bryophytes in Dutch chalk grasslands. In: *Lindbergia: a journal of bryology*. 1988. ISSN 0105-0761.

190. TAMM, C. Growth, yield and nutrition in carpets of a forest moss (*Hylocomium splendens).*1953. [Accessed 31 January 2023]. Available from: https://pub.epsilon.slu.se/9960/1/medd_statens_skogsforskningsinst_043_01.pdf

191. OECHEL, W.C., VAN CLEVE, K. The role of bryophytes in nutrient cycling in the taiga. In: *Forest ecosystems in the Alaskan taiga: a synthesis of structure and function*. New York, NY: Springer-Verlag, 1986. vol. 57, pp. 121–137. ISBN 978-1-4612-9353-8.

192. VAN TOOREN, B.F., VAN DAM, D., DURING, H.J. The relative importance of precipitation and soil as sources of nutrients for *Calliergonella cuspidata* (Hedw.) Loeske in chalk grassland. In: *Functional Ecology*. 1990, vol. 4, no. 1, pp. 101–107. ISSN 0269-8463.

193. TUBA, Z., SLACK, N.G., STARK, L.R. *Bryophyte Ecology and Climate Change*. Cambridge University Press, 2011. ISBN 9780521767637.

194. BACZEWSKA-DĄBROWSKA, A.H., GWOREK, B., DMUCHOWSKI, W. The Use of Mosses in Biomonitoring of Air Pollution in the Terrestrial Environment: A Review. In: *Environmental Protection and Natural Resources*. 2023. vol. 34, no. 2, pp. 19–30. ISSN 2353-8589. DOI: 10.2478/oszn-2023-0005.

195. GERDOL, R., MARCHESINI, R., IACUMIN, P., BRANCALEONI, L. Monitoring temporal trends of air pollution in an urban area using mosses and lichens as biomonitors. In: *Chemosphere*. 2014. vol. 108, pp. 388–395. ISSN 0045-6535. DOI: 10.1016/j.chemosphere.2014.02.035.

196. GONZÁLEZ, A.G., POKROVSKY, O.S. Metal adsorption on mosses: Toward a universal adsorption model. In: *Journal of Colloid and Interface Science*. 2014. vol. 415, pp. 169–178. ISSN 0021-9797. DOI: 10.1016/j.jcis.2013.10.028.

197. TYLER, G. Bryophytes and heavy metals: a literature review. In: *Botanical Journal of the Linnean Society*. 1990. vol. 104, no. 1–3, pp. 231–253. ISSN 0024-4074. DOI: 10.1111/j.1095-8339.1990.tb02220.x.

198. STEINNES, E., RAMBÆK, J.P., HANSSEN, J.E. Large scale multi-element survey of atmospheric deposition using naturally growing moss as biomonitor. In: *Chemosphere*. 1992. vol. 25, no. 5, pp. 735–752. ISSN 0045-6535. DOI: 10.1016/0045-6535(92)90435-T.

199. STEINNES, E. Monitoring of trace element deposition by means of mosses. In: *Fresenius' Zeitschrift für analytische Chemie*. 1984. vol. 317, no. 3–4, pp. 350–350. ISSN 0016-1152. DOI: 10.1007/BF00494490.

200. ROSS, H.B. On the use of mosses (*Hylocomium splendens* and *Pleurozium schreberi*) for estimating atmospheric trace metal deposition. In: *Water, Air, and Soil Pollution*. 1990. vol. 50, no. 1–2. ISSN 0049-6979. DOI: 10.1007/BF00284784.

201. BERG, T., STEINNES, E. Use of mosses (*Hylocomium splendens and Pleurozium schreberi*) as biomonitors of heavy metal deposition: From relative to absolute deposition values. In: *Environmental Pollution*. 1997. vol. 98, no. 1, pp. 61–71. ISSN 0269-7491. DOI: 10.1016/S0269-7491(97)00103-6.

202. BROWN, D.H., BATES, J.W. Bryophytes and nutrient cycling. In: *Botanical Journal of the Linnean Society*. 1990. vol. 104, no. 1–3, pp. 129–147. ISSN 0024-4074. DOI: 10.1111/j.1095-8339.1990.tb02215.x.

203. RAO, D.N. Responses of Bryophytes to Air Pollution. In: *Bryophyte Ecology*. Dordrecht: Springer Netherlands, 1982. pp. 445–471. ISBN 978-94-009-5893-7. DOI: 10.1007/978-94-009-5891-3_12.

204. GANDOIS, L., AGNAN, Y., LEBLOND, S., SÉJALON-DELMAS, N., LE ROUX, G., PROBST, A. Use of geochemical signatures, including rare earth elements, in mosses and lichens to assess spatial integration and the influence of forest environment. In: *Atmospheric Environment*. 2014. vol. 95, pp. 96–104. ISSN 1352-2310. DOI: 10.1016/j.atmosenv.2014.06.029.

205. MEYER, M., SCHRÖDER, W., HOFFMANN, A. Effect of canopy drip on accumulation of nitrogen and heavy metals in moss. In: *Pollution atmosphérique*. 2015. vol. 226, pp. 1–29. ISSN 2268-3798. DOI: 10.4267/pollution-atmospherique.5159.

206. SCHRÖDER, W., NICKEL, S. Site-specific investigation and spatial modeling of canopy drip effect on element concentrations in moss. In: *Environmental Science and Pollution Research*. 2018. vol. 25, no. 27, pp. 27173–27186. ISSN 1614-7499. DOI: 10.1007/s11356-018-2763-y.

207. BOQUETE, M.T., FERNÁNDEZ, J.A., ABOAL, J.R., CARBALLEIRA, A. Are terrestrial mosses good biomonitors of atmospheric deposition of Mn? In: *Atmospheric Environment*. 2011. vol. 45, no. 16, pp. 2704–2710. ISSN 1352-2310. DOI: 10.1016/j.atmosenv.2011.02.057.

208. ZECHMEISTER, H.G., HOHENWALLNER, D., RISS, A., HANUS-ILLNAR, A. Variations in heavy metal concentrations in the moss species *Abietinella abietina* (Hedw.) Fleisch. according to sampling time, within site variability and increase in biomass. In: *The Science of the total environment*. 2003. vol. 301, no. 1–3, pp. 55–65. ISSN 0048-9697. DOI: 10.1016/S0048-9697(02)00296-6.

209. BERG, T., RØYSET, O., STEINNES, E. Moss (*Hylocomium splendens*) used as biomonitor of atmospheric trace element deposition: Estimation of uptake efficiencies. In: *Atmospheric Environment*. 1995. vol. 29, no. 3, pp. 353–360. ISSN 1352-2310. DOI: 10.1016/1352-2310(94)00259-N.

210. MÄKINEN A. *Biomonitoring of Atmospheric Deposition in the Kola Peninsula (Russia) and Finnish Lapland, Based on the Chemical Analysis of Mosses*. 1994.

211. ZECHMEISTER, H.G. Correlation between altitude and heavy metal deposition in the Alps. In: *Environmental Pollution*. 1995. vol. 89, no. 1, pp. 73–80. ISSN 0269-7491. DOI: 10.1016/0269-7491(94)00042-C.

212. GERDOL, R., BRAGAZZA, L., MARCHESINI, R. Element concentrations in the forest moss *Hylocomium splendens*: variation associated with altitude, net primary production and soil chemistry. In: *Environmental Pollution*. 2002. vol. 116, no. 1, pp. 129–135. ISSN 0269-7491. DOI: 10.1016/S0269-7491(01)00198-1.

213. XIAO, J., HAN, X., SUN, S., WANG, L., RINKLEBE, J. Heavy metals in different moss species in alpine ecosystems of Mountain Gongga, China: Geochemical characteristics and controlling factors. In: *Environmental Pollution*. 2021. vol. 272, pp. 115991. ISSN 0269-7491. DOI: 10.1016/j.envpol.2020.115991.

214. WILSCHEFSKI, S.C., BAXTER, M.R. Inductively coupled plasma mass spectrometry: introduction to analytical aspects. In: *The Clinical Biochemist Reviews*. 2019. vol. 40, no. 3, pp. 115. ISSN 1838-0212.

215. CHAJDUK, E., KALBARCZYK, P. Comparison of the Analytical Performance of Inductively Coupled Plasma Mass Spectrometry and Instrumental Neutron Activation Analysis Techniques in the Elemental Analysis of Coal Fly Ash. In: *Minerals*. 2023. vol. 13, no. 12, pp. 1484. ISSN 2075-163X.

216. FRONTASYEVA, M. V. Neutron activation analysis in the life sciences. In: *Physics of Particles and Nuclei*. 2011. vol. 42, no. 2, pp. 332–378. ISSN 1063-7796. DOI: 10.1134/S1063779611020043.

217. OYEDOTUN, T.D.T. X-ray fluorescence (XRF) in the investigation of the composition of earth materials: a review and an overview. In: *Geology, Ecology, and Landscapes*. 2018. vol. 2, no. 2, pp. 148–154. ISSN 2474-9508. DOI: 10.1080/24749508.2018.1452459.

218. KATAKAM, L.N.R., ABOUL-ENEIN, H.Y. Elemental Impurities Determination by ICP-AES / ICP-MS: A review of Theory, Interpretation of Concentration Limits, Analytical Method Development Challenges and Validation Criterion for Pharmaceutical Dosage Forms. In:

Current Pharmaceutical Analysis. 2020. vol. 16, no. 4, pp. 392–403. ISSN 1573-4129. DOI: 10.2174/1573412915666190225160512.

219. KHAN, S.R., SHARMA, B., CHAWLA, P.A., BHATIA, R. Inductively Coupled Plasma Optical Emission Spectrometry (ICP-OES): a Powerful Analytical Technique for Elemental Analysis. In: *Food Analytical Methods*. 2022. vol. 15, no. 3, pp. 666–688. ISSN 1936-9751. DOI: 10.1007/s12161-021-02148-4.

220. HE, S., NIU, Y., XING, L., LIANG, Z., SONG, X., DING, M., HUANG, W. Research progress of the detection and analysis methods of heavy metals in plants. In: *Frontiers in Plant Science*. 2024. vol. 15. ISSN 1664-462X. DOI: 10.3389/fpls.2024.1310328.

221. OLIVARES, I.R.B., SOUZA, G.B., NOGUEIRA, A.R.A., TOLEDO, G.T.K., MARCKI, D.C. Trends in developments of certified reference materials for chemical analysis - Focus on food, water, soil, and sediment matrices. In: *TrAC Trends in Analytical Chemistry*. 2018. vol. 100, pp. 53–64. ISSN 0165-9936. DOI: 10.1016/j.trac.2017.12.013.

222. BECK, H.E., MCVICAR, T.R., VERGOPOLAN, N., BERG, A., LUTSKO, N.J., DUFOUR, A., ZENG, Z., JIANG, X., VAN DIJK, A.I.J.M., MIRALLES, D.G. High-resolution (1 km) Köppen-Geiger maps for 1901–2099 based on constrained CMIP6 projections. In: *Scientific Data*. 2023. vol. 10, no. 1, pp. 724. ISSN 2052-4463. DOI: 10.1038/s41597-023-02549-6.

223. CHALIGAVA, O., ZINICOVSCAIA, I., PESHKOVA, A., YUSHIN, N., FRONTASYEVA, M., VERGEL, K., NURKASSIMOVA, M., CEPOI, L. Major and Trace Airborne Elements and Ecological Risk Assessment: Georgia Moss Survey 2019–2023. In: *Plants*. 2024. vol. 13, no. 23. ISSN 2223-7747. DOI: 10.3390/plants13233298.

224. BOLASHVILI, N., NEIDZE, V. *The Physical Geography of Georgia*. Springer Nature, 2022. ISBN 3030907538.

225. ABUSELIDZE, G. Competitiveness Analysis of the Georgian Transport and Logistics System in the Black Sea Region: Challenges and Perspectives. In: Computational Science and Its Applications – ICCSA 2021. Cham: Springer, 2021. p. 133–148. ISBN 978-3-030-86973-1. DOI: 10.1007/978-3-030-86973-1_10.

226. GUGUSHVILI, T., SALUKVADZE, G., ROEP, D., CHKHAIDZE, V. Land fragmentation: Is it a curse or a blessing for small family farms? In: *Dela*. 2025. No. 64, p. 109–140. ISSN 0354-0596. DOI: 10.4312/dela.64.109-140.

227. KHELASHVILI, I., SHARIA, M. Economic Impact of Tourism Industry Development in Georgia: Current Trends. In: *Economics & Business (1987-5789)*. 2025. No. 3. ISSN 1987-5789.

228. NATALIA ROBITASHVILI. Tourism Statistics in Georgia. In: *International Journal of Innovative Technologies in Economy*. 2018. vol. 2, no. 6(18), pp. 51–53. ISSN 2415-3877. DOI: 10.31435/rsglobal_ijite/01072018/5945.

229. KATSITADZE, N., NATSVLISHVILI, I. The Role of State Regulation and Policy in Tourism Development: The Case of Georgia. In: Eurasian Economic Perspectives. Cham: Springer International Publishing, 2020. p. 419–434. ISBN 978-3-030-40374-4. DOI: 10.1007/978-3-030-40375-1_28.

230. KATAMADZE, D., KATAMADZE, G. Prospects for the formation of the transport and logistics hub of Georgia. In: *Access Journal - Access to Science, Business, Innovation in the digital economy*. 2022. vol. 4, no. 1, pp. 71–84. ISSN 2683-1007. DOI: 10.46656/access.2023.4.1(6).

231. TVALCHRELIDZE, A., SILAGADZE, A., KESHELASHVILI, G., GEGIA, D. *Georgia's Social Economic Development Program*. Tbilisi: Nekeri, 2011.

232. BOCHORISHVILI, N., KHOMERIKI, D., MATARADZE, E., CHIKHRADZE, N., KVAVADZE, S., ROBAKIDZE, D., KHOMERIKI, S. Mining Waste Complex Research and Development of Technologies for their Use in Georgia. In: *IOP Conference Series: Earth and Environmental Science*. 2021. vol. 906, no. 1, pp. 012133. ISSN 1755-1307. DOI: 10.1088/1755-1315/906/1/012133.

233. JAPOSHVILI, B., COUTO, T.B.A., MUMLADZE, L., EPITASHVILI, G., MCCLAIN, M.E., JENKINS, C.N., ANDERSON, E.P. Hydropower development in the Republic of Georgia and implications for freshwater biodiversity conservation. In: *Biological Conservation*. 2021. vol. 263, pp. 109359. ISSN 0006-3207. DOI: 10.1016/j.biocon.2021.109359.

234. KINKLADZE, R. Modern Trends and Prospects to Develop the Agrarian Sector of Georgia. In: *Procedia - Social and Behavioral Sciences*. 2015. vol. 213, pp. 562–568. ISSN 1877-0428. DOI: 10.1016/j.sbspro.2015.11.450.

235. WORLD BANK. *Georgia: From Reformer to Performer*. Washington, DC, 2018. [Accessed 24 April 2025]. Available from: http://hdl.handle.net/10986/29790

236. WORLD HEALTH ORGANIZATION. *World health statistics 2020*. Geneva, 2022. [Accessed 25 January 2023]. Available from: https://www.who.int/publications/i/item/9789240005105

237. OECD. *Developing a Water Policy Outlook for Georgia, the Republic of Moldova and Ukraine*. Paris: OECD Publishing, 2021. ISBN 9789264905184.

238. WORLD BANK. *Georgia Country Environmental Analysis: Institutional, Economic, and Poverty Aspects of Georgia's Road to Environmental Sustainability*. Washington,

DC: World Bank, 2015. [Accessed 25 January 2023] Available from: https://openknowledge.worldbank.org/handle/10986/22287

239. EEA. *Country Briefing on State of the Environment in Georgia*. Copenhagen, 2018.

240. POTOP, V. Evolution of drought severity and its impact on corn in the Republic of Moldova. In: *Theoretical and Applied Climatology*. 2011. vol. 105, no. 3, pp. 469–483. ISSN 0177-798X. DOI: 10.1007/s00704-011-0403-2.

241. DUCA, G., XIAO, H., NEDEALCOV, M. Regional climatic changes and small river's water quality in Republic of Moldova's south (Danube River basin). In: *Present Environment and Sustainable Development*. 2017. vol. 11, no. 1, pp. 21–33. ISSN 1843-5971. DOI: 10.1515/pesd-2017-0002.

242. DUCA, G., NEDEALCOV, M., GLADCHI, V., TRAVIN, S. Climatic changes and surface water quality on Republic of Moldovas territory. In: *Advances in Intelligent Systems and Computing*. Springer Verlag, 2020. p. 325–334. ISBN 9783030212544. DOI: 10.1007/978-3-030-21255-1_25.

243. PETREA, ȘTEFAN-M., CRISTEA, D.S., TUREK RAHOVEANU, M.M., ZAMFIR, C.G., TUREK RAHOVEANU, A., ZUGRAVU, G.A., NANCU, D. Perspectives of the Moldavian Agricultural Sector by Using a Custom-Developed Analytical Framework. In: *Sustainability*. 2020. vol. 12, no. 11, pp. 4671. ISSN 2071-1050. DOI: 10.3390/su12114671.

244. COJOCARU, A., CIMPOIES, L. Unlocking Potential: Assessing Opportunities and Challenges for Moldovan Agri-Food Exports. In: *SSRN Electronic Journal*. 2025. ISSN 1556-5068. DOI: 10.2139/ssrn.5937417.

245. SAFIROVA, E. *The Mineral Industry of Moldova*. 2023. [Accessed 25 March 2025]. Available from: https://pubs.usgs.gov/myb/vol3/2019/myb3-2019-moldova.pdf

246. WORLD BANK. *Blueing the Black Sea: Turning the Tide of Pollution: Regional Marine Pollution Diagnostics*. Washington, DC: World Bank, 2025. [Accessed 01 March 2026]. Available from: https://documents.worldbank.org/en/publication/documents-reports/documentdetail/099063025112017220

247. IVANOVA, A., WIBERG, K., AHRENS, L., ZUBCOV, E., DAHLBERG, A.-K. Spatial distribution of legacy pesticides in river sediment from the Republic of Moldova. In: *Chemosphere*. 2021. vol. 279, pp. 130923. ISSN 0045-6535. DOI: 10.1016/j.chemosphere.2021.130923.

248. RABOSAPCA, I., BARTA, A.-I. Management of Environmental Risks Induced by Building Materials Industry in the Republic of Moldova. In: *Economy and Sociology*. 2012. No. 4, p. 131–135. ISSN 1857-4130.

249. TALMACI, I., GALUPA, D., ȘPITOC, L., VEDUTENCO, D. Promoting Agroforestry Within the Agricultural Competitiveness Project in Moldova. In: *Regenerative Agriculture*. Cham: Springer International Publishing, 2021. p. 329–340. ISBN 978-3-030-72223-4. DOI: 10.1007/978-3-030-72224-1_30.

250. BOIKO, M.O. Ecological consequences of burning crop residues. In: *Taurian Scientific Herald*. 2024. vol. 1, no. 135, pp. 206–211. ISSN 2226-0099. DOI: 10.32782/2226-0099.2024.135.1.27.

251. BRAGA, D., GUTU-CHETRUSCA, C., HLUSOV, V., TVERDOHLEB, A. The Biomass Use for Heat Supply. A Study Case for the Republic of Moldova. In: *2024 IEEE International Conference and Exposition on Electric and Power Engineering (EPEi)*. IEEE, 2024. p. 605–610. ISBN 979-8-3503-5619-9. DOI: 10.1109/EPEi63510.2024.10758174.

252. CHAUDHURI, S., ROY, M. Global ambient air quality monitoring: Can mosses help? A systematic meta-analysis of literature about passive moss biomonitoring. In: *Environment, Development and Sustainability*. 2024. vol. 26, no. 3, pp. 5735–5773.

253. ŠAJN, R., BAČEVA ANDONOVSKA, K., STAFILOV, T., BARANDOVSKI, L. Moss as a Biomonitor to Identify Atmospheric Deposition of Minor and Trace Elements in Macedonia. In: *Atmosphere*. 2024. vol. 15, no. 3, pp. 297.

254. ZINICOVSCAIA, I., CHALIGAVA, O., YUSHIN, N., GROZDOV, D., VERGEL, K., HRAMCO, C. Moss Biomonitoring of Atmospheric Trace Element Pollution in the Republic of Moldova. In: *Archives of Environmental Contamination and Toxicology*. 2022. DOI: 10.1007/s00244-022-00918-7.

255. ZINICOVSCAIA, I., HRAMCO, C., CHALIGAVA, O., YUSHIN, N., GROZDOV, D., VERGEL, K., DUCA, G. Accumulation of Potentially Toxic Elements in Mosses Collected in the Republic of Moldova. In: *Plants*. 2021. vol. 10, no. 3, pp. 471. DOI: 10.3390/plants10030471.

256. HARMENS HARRY, FRONTASYEVA MARINA. *Monitoring of Atmospheric Deposition of Heavy Metals, Nitrogen and Pops in Europe Using Bryophytes*. 2020. [Accessed 3 April 2024]. Available from: https://icpvegetation.ceh.ac.uk/get-involved/manuals/moss-survey

257. PAVLOV, S.S., DMITRIEV, A.Y., FRONTASYEVA, M. V. Automation system for neutron activation analysis at the reactor ibr-2, frank laboratory of neutron physics, joint

institute for nuclear research, Dubna, Russia. In: *Journal of Radioanalytical and Nuclear Chemistry*. 2016. vol. 309, no. 1, pp. 27–38.

258. MELENDEZ-PEREZ, J.J., FOSTIER, A.H. Assessment of Direct Mercury Analyzer® to quantify mercury in soils and leaf samples. In: *Journal of the Brazilian Chemical Society*. 2013. vol. 24, pp. 1880–1886.

259. ZINTWANA, M.P., CAWTHORN, R.G., ASHWAL, L.D., ROELOFSE, F., CRONWRIGHT, H. Mercury in the Bushveld complex, South Africa, and the Skaergaard intrusion, Greenland. In: *Chemical Geology*. 2012. vol. 320, pp. 147–155.

260. CHALIGAVA, O., ZINICOVSCAIA, I., CEPOI, L. Environmental Drivers of Trace Element Variability in *Hypnum cupressiforme* Hedw.: A Cross-Regional Moss Biomonitoring Study in Georgia and the Republic of Moldova. In: *Plants*. 2025. vol. 14, no. 13, pp. 2040.

261. CHAUDHURI, S., ROY, M. Global ambient air quality monitoring: Can mosses help? A systematic meta-analysis of literature about passive moss biomonitoring. In: *Environment, Development and Sustainability*. 2024. vol. 26, no. 3, pp. 5735–5773. ISSN 1387-585X.

262. PATIL, I. Visualizations with statistical details: The'ggstatsplot'approach. In: *Journal of Open Source Software*. 2021. vol. 6, no. 61, pp. 3167. ISSN 2475-9066. DOI: 10.21105/joss.03167.

263. LÊ, S., JOSSE, J., HUSSON, F. FactoMineR: an R package for multivariate analysis. In: *Journal of statistical software*. 2008. vol. 25, pp. 1–18. ISSN 1548-7660. DOI: 10.18637/jss.v025.i01.

264. KASSAMBARA, A., MUNDT, F. *factoextra: Extract and Visualize the Results of Multivariate Data Analyses*. Version 2.0.0. 2017 DOI: 10.32614/CRAN.package.factoextra.

265. BETSOU, C., DIAPOULI, E., TSAKIRI, E., PAPADOPOULOU, L., FRONTASYEVA, M., ELEFTHERIADIS, K., IOANNIDOU, A. First-time source apportionment analysis of deposited particulate matter from a moss biomonitoring study in northern Greece. In: *Atmosphere*. 2021. vol. 12, no. 2, pp. 208. ISSN 2073-4433.

266. NORRIS, G., DUVALL, R., BROWN, S., BAI, S. EPA positive matrix factorization (PMF) 5.0 Fundamentals and User Guide. Washington, DC: *U.S. Environmental Protection Agency, Office of Research and Development,* 2014. [Accessed 24 March 2024]. Available from: https://www.epa.gov/air-research/epa-positive-matrix-factorization-50-fundamentals-and-user-guide

267. KRAKOVSKÁ, A.S., SVOZILÍK, V., ZINICOVSCAIA, I., VERGEL, K., JANČÍK, P. Analysis of spatial data from moss biomonitoring in Czech–Polish border. In: *Atmosphere*. 2020. vol. 11, no. 11, pp. 1237. ISSN 2073-4433. DOI: 10.3390/atmos11111237.

268. FERNÁNDEZ, J.A., CARBALLEIRA, A. Evaluation of contamination, by different elements, in terrestrial mosses. In: *Archives of environmental contamination and toxicology*. 2001. vol. 40, pp. 461–468. ISSN 0090-4341. DOI: 10.1007/s002440010198.

269. RAI, P.K., LEE, S.S., ZHANG, M., TSANG, Y.F., KIM, K.-H. Heavy metals in food crops: Health risks, fate, mechanisms, and management. In: *Environment international*. 2019. vol. 125, pp. 365–385. ISSN 0160-4120. DOI: 10.1016/j.envint.2019.01.067.

270. WEISSMANNOVÁ, H.D., MIHOČOVÁ, S., CHOVANEC, P., PAVLOVSKÝ, J. Potential ecological risk and human health risk assessment of heavy metal pollution in industrial affected soils by coal mining and metallurgy in Ostrava, Czech Republic. In: *International journal of environmental research and public health*. 2019. vol. 16, no. 22, pp. 4495. ISSN 1661-7827. DOI: 10.3390/ijerph16224495.

271. QGIS DEVELOPMENT TEAM. *QGIS Geographic Information System (Version 3.40)*. 2025. [Accessed 16 February 2025]. Available from: https://qgis.org

272. WORLD METEOROLOGICAL ORGANIZATION. *WMO guidelines on the calculation of climate normals.* WMO-No. 1203. Geneva: World Meteorological Organization, 2017

273. PESARESI, M., SCHIAVINA, M., POLITIS, P., FREIRE, S., KRASNODĘBSKA, K., UHL, J.H., CARIOLI, A., CORBANE, C., DIJKSTRA, L., FLORIO, P. Advances on the Global Human Settlement Layer by joint assessment of Earth Observation and population survey data. In: *International Journal of Digital Earth*. 2024. vol. 17, no. 1, pp. 2390454. ISSN 1753-8947.

274. YAN, G., TANG, G., LU, D., MA, J., YANG, X., LI, F. Distinguishing the Intervalley Plain from the Intermountain Flat for Landform Mapping Using the Sightline Algorithm. In: *ISPRS International Journal of Geo-Information*. 2024. vol. 13, no. 3, pp. 86. ISSN 2220-9964. DOI: 10.3390/ijgi13030086

275. WOODS, T., MCKEEN, T., CUNNINGHAM, A., PRIYATIKANTO, R., SORICHETTA, A., TATEM, A., BONDARENKO, M. WorldPop high resolution, harmonised annual global geospatial covariates. Version 1.0. Dataset. University of Southampton, 2025. DOI: 10.5258/SOTON/WP00772

276. YAMAZAKI, D., IKESHIMA, D., NEAL, J.C., O'LOUGHLIN, F., SAMPSON, C.C., KANAE, S., BATES, P.D. MERIT DEM: A new high-accuracy global digital elevation

model and its merit to global hydrodynamic modeling. In: *AGU fall meeting abstracts*. 2017. abstract H12C-04.

277. ABATZOGLOU, J.T., DOBROWSKI, S.Z., PARKS, S.A., HEGEWISCH, K.C. TerraClimate, a high-resolution global dataset of monthly climate and climatic water balance from 1958–2015. In: *Scientific data*. 2018. vol. 5, no. 1, pp. 1–12. ISSN 2052-4463. DOI: 10.1038/sdata.2017.191.

278. NAGARAJAN, R., ARMSTRONG-ALTRIN, J.S., KESSLER, F.L., JONG, J. Petrological and geochemical constraints on provenance, paleoweathering, and tectonic setting of clastic sediments from the Neogene Lambir and Sibuti Formations, northwest Borneo. In: *Sediment Provenance: Influences on Compositional Change from Source to Sink*. Amsterdam: Elsevier, 2017, pp. 123–153. ISBN 9780128033869.

279. BABA, A.A., IBRAHIM, L., ADEKOLA, F.A., BALE, R.B., GHOSH, M.K., SHEIK, A.R., PRADHAN, S.R., AYANDA, O.S., FOLORUNSHO, I.O. Hydrometallurgical Processing of Manganese Ores: A Review. In: *Journal of Minerals and Materials Characterization and Engineering*. 2014. vol. 02, no. 03, pp. 230–247. ISSN 2327-4077. DOI: 10.4236/jmmce.2014.23028.

280. SALUKVADZE, E., CHALADZE, T., KHARDZIANI, T., GOGIDZE, K. Present Landscapes and Their Ecological States in the Ore Mining Region of Chiatura. In: *Earth Sciences*. 2017. vol. 6, no. 5–1, pp. 8–16. ISSN 2328-5974.

281. CHIRAKADZE, A., BUACHIDZE, Z., KHOMERIKI, I.O., GVAKHARIA, V., STAMATELI, M., CHAKVETADZE, N., CHOKHELI, M., TOSCANO, W.A., CHIGOGIDZE, K., GVERTSITELI, L. Arsenic pollution of soils and morbidity prevalence in Racha-Lower Svaneti district of Georgia. In: *International Journal of Global Warming*. 2016. vol. 10, no. 1–3, pp. 92–114. ISSN 1758-2083. DOI: 10.1504/IJGW.2016.077908.

282. TEBIDZE, V., ZURABISHVILI, E., TATANASHVILI, G., VARAZI, T., BUNIN, E., BAKRADZE, E. *Arsenic Pollution and Human Health Risk Assessment in the Region of Racha-Lechkhumi and Kvemo Svaneti of Georgia*. Preprint. 2022. DOI: 10.21203/rs.3.rs-1744446/v1

283. GURGULIANI, I. Arsenic contamination in Georgia. Environment related security risks from old soviet legacy. In: *Proceedings of the 22nd OSCE Economic and Environmental Forum "Responding to Environmental Challenges with a View to Promoting Cooperation and Security in the OSCE Area", Vienna, Austria*, 27-28 January 2014.Vienna: OSCE, 2014. p. 27–28.

284. CHALIGAVA, O. Moss biomonitoring of air pollution in the vicinity of mines: Georgia case study. In: *Conferința tehnico-științifică a studenților, masteranzilor și doctoranzilor*. Chișinău, Republica Moldova, 5-7 aprilie 2023. Chișinău: Tehnica-UTM, 2023, vol. 4, pp. 39–42. ISBN 978-9975-45-960-0. [Accessed 25 May 2024] Available from: https://ibn.idsi.md/vizualizare_articol/198428/

285. CHALIGAVA, O., NIKOLAEV, I., KHETAGUROV, K., LAVRINENKO, Y., BAZAEV, A., FRONTASYEVA, M., VERGEL, K., GROZDOV, D. First results on moss biomonitoring of trace elements in the central part of Georgia, Caucasus. In: *Atmosphere*. 2021. vol. 12, no. 3. ISSN 2073-4433. DOI: 10.3390/atmos12030317.

286. HAIR, J.F., SARSTEDT, M., PIEPER, T.M., RINGLE, C.M. The use of partial least squares structural equation modeling in strategic management research: a review of past practices and recommendations for future applications. In: *Long range planning*. 2012. vol. 45, no. 5–6, pp. 320–340. ISSN 0024-6301. DOI: 10.1016/j.lrp.2012.09.008.

287. ALLAJBEU, S., YUSHIN, N.S., QARRI, F., DULIU, O.G., LAZO, P., FRONTASYEVA, M. V. Atmospheric deposition of rare earth elements in Albania studied by the moss biomonitoring technique, neutron activation analysis and GIS technology. In: *Environmental Science and Pollution Research*. 2016. vol. 23, no. 14, pp. 14087–14101. ISSN 1614-7499.

288. ZHOU, X., CHEN, Q., LIU, C., FANG, Y. Using moss to assess airborne heavy metal pollution in Taizhou, China. In: *International journal of environmental research and public health*. 2017. vol. 14, no. 4, pp. 430. ISSN 1661-7827. DOI: 10.3390/ijerph14040430.

289. MARKERT, B. Establishing of 'Reference Plant'for inorganic characterization of different plant species by chemical fingerprinting. In: *Water, Air, and Soil Pollution*. 1992. vol. 64, no. 3, pp. 533–538. ISSN 0049-6979.

290. STAFILOV, T., ŠAJN, R., BARANDOVSKI, L., ANDONOVSKA, K.B., MALINOVSKA, S. Moss biomonitoring of atmospheric deposition study of minor and trace elements in Macedonia. In: *Air Quality, Atmosphere & Health*. 2018. vol. 11, no. 2, pp. 137–152. ISSN 1873-9318.

291. STEINNES, E., UGGERUD, H.T., PFAFFHUBER, K.A., BERG, T. Atmospheric deposition of heavy metals in Norway. National moss survey 2015. Kjeller: NILU, 2017. NILU rapport, 28/2016. [Accessed 5 February 2023]. Available from: https://www.environmentagency.no/globalassets/publikasjoner/M594/M594.pdf

292. BUNIN, E., KHATISASHVILI, G., VARAZI, T., KARTVELISHVILI, T., ASATIANI, N., SAPOJNIKOVA, N. Study of arsenic-contaminated soil bacterial community

using biochip technology. In: *Water, Air, & Soil Pollution*. 2020. vol. 231, no. 5, pp. 198. ISSN 0049-6979. DOI: 10.1007/s11270-020-04575-1.

293. SHAVLIASHVILI, L., KUCHAVA, G., TABATADZE, M., SHUBLADZE, E., BAKRADZE, E. Influence of waste products of arsenic industries on soil pollution in Racha-Lechkhumi and Kvemo Svaneti regions of Georgia. In: *The Journal of Solid Waste Technology and Management*. 2025. vol. 51, no. 1, pp. 111–124. ISSN 1088-1697.

294. OKROSTSVARIDZE, A., POPKHADZE, N., BLUASHVILI, D., CHANG, SKHIRTLADZE, I. Pliocene-Quaternary Samtskhe-Javakheti Volcanic Highland, Lesser Caucasus-as a Result of Mantle Plumes Activity. In: *IGCP 610 Fourth Plenary Meeting and Field Trip: From the Caspian to Mediterranean: Environmental Change and Human Response during the Quaternary*. Tbilisi, 2016. p. 127–129. [Accessed 2 September 2023]. Available from: http://www.avalon-institute.org/IGCP610

295. PARFENOV, A. V, LEBEDEV, V.A., VASHAKIDZE, G.T., YAKUSHEV, A.I., EDIBERIDZE, B.D. The History of the Formation of Pliocene–Quaternary Valley Lava Rivers in the Northeast Part of the Javakheti Volcanic Highland, Lesser Caucasus. In: *Journal of Volcanology and Seismology*. 2023. vol. 17, no. 3, pp. 187–209. ISSN 0742-0463. DOI:10.1134/S0742046323700070.

296. RUDNICK, R.L., GAO, S. Composition of the Continental Crust. In: *Treatise on Geochemistry*. Volume 4, The Crust. 2nd ed. Amsterdam: Elsevier, 2014, pp. 1–51. ISBN 978-0-08-099945-6.

297. TIELIDZE, L., TRAPAIDZE, V., MATCHAVARIANI, L., WHEATE, R. Climate, Hydrography, and Soils of Georgia. In: *Geomorphology of Georgia*. 2019. p. 15–34. ISBN 978-3-319-77763-4. DOI: 10.1007/978-3-319-77764-1_2.

298. TEPANOSYAN, G., SAHAKYAN, L., GEVORGYAN, A., FRONTASYEVA, M. Factors conditioning the content of chemical elements in soil and mosses in Armenia. In: *Journal of Trace Elements and Minerals*. 2022. vol. 2, pp. 100029. ISSN 2773-0506.

299. NURKASSIMOVA, M., OMAROVA, N., YUSHIN, N., GROZDOV, D., VERGEL, K., ZINICOVSCAIA, I. Assessment of air pollution in South Kazakhstan using moss (*Hylocomium splendens*) biomonitoring technique and neutron activation analysis. In: *Journal of Radioanalytical and Nuclear Chemistry*. 2024. P. 1–10. ISSN 0236-5731.

300. UNECE. *Overview of the State of Forests and Forest Management in Armenia*. United Nations, 2020. ISBN 9789210048163. [Accessed 15 November 2024]. Available from: https://unece.org/DAM/timber/publications/2020/Armenia_DP78_1922453_E_WEB.pdf

301. UNECE. *Overview of the State of Forests and Forest Management in Georgia*. United Nations, 2020. ISBN 9789210048170. [Accessed 15 November 2024]. Available from: https://unece.org/DAM/timber/publications/2020/Georgia_DP80_1922467_E_WEB.pdf

302. UNECE. *State of Forests of the Caucasus and Central Asia*. Geneva, 2024. ISBN 9789213632918. [Accessed 15 November 2024]. Available from: https://unece.org/DAM/timber/publications/sp-47-soccaf-en.pdf

303. SCHLUTOW, A., SCHRÖDER, W., NICKEL, S. Atmospheric deposition and element accumulation in moss sampled across Germany 1990–2015: trends and relevance for ecological integrity and human health. In: *Atmosphere*. 2021. vol. 12, no. 2, pp. 193. ISSN 2073-4433. DOI: 10.3390/atmos12020193.

304. OJEDA, C.B., ROJAS, F.S. Separation and preconcentration by cloud point extraction procedures for determination of ions: recent trends and applications. In: *Microchimica Acta*. 2012. vol. 177, pp. 1–21. ISSN 0026-3672.

305. GIRÁLDEZ, P., VARELA, Z., ABOAL, J.R., FERNÁNDEZ, J.Á. Testing different methods of estimating edaphic inputs in moss biomonitoring. In: *Science of The Total Environment*. 2021. vol. 778, pp. 146332. ISSN 0048-9697. DOI: 10.1016/j.scitotenv.2021.146332.

306. KABATA-PENDIAS, A., SZTEKE, B. *Trace elements in abiotic and biotic environments*. 1st ed. Boca Raton, FL: CRC Press, 2015. ISBN 1482212811.

307. LEQUY, E., SABY, N.P.A., ILYIN, I., BOURIN, A., SAUVAGE, S., LEBLOND, S. Spatial analysis of trace elements in a moss bio-monitoring data over France by accounting for source, protocol and environmental parameters. In: *Science of the Total Environment*. 2017. vol. 590, pp. 602–610. ISSN 0048-9697. DOI: 10.1016/j.scitotenv.2017.02.240.

308. QARRI, F., LAZO, P., ALLAJBEU, S., BEKTESHI, L., KANE, S., STAFILOV, T. The evaluation of air quality in Albania by moss biomonitoring and metals atmospheric deposition. In: *Archives of environmental contamination and toxicology*. 2019. vol. 76, pp. 554–571. ISSN 0090-4341. DOI: 10.1007/s00244-019-00608-x.

309. KUKLOVÁ, M., KUKLA, J., HNILIČKOVÁ, H., HNILIČKA, F., PIVKOVÁ, I. Impact of Car Traffic on Metal Accumulation in Soils and Plants Growing Close to a Motorway (Eastern Slovakia). In: *Toxics*. 2022. vol. 10, no. 4, pp. 183. ISSN 2305-6304. DOI: 10.3390/toxics10040183.

310. JEONG, H. Toxic metal concentrations and Cu–Zn–Pb isotopic compositions in tires. In: *Journal of Analytical Science and Technology*. 2022. vol. 13, pp. 1–10. ISSN 2093-3134. DOI: 10.1186/s40543-021-00312-3.

311. WANG, J.M., JEONG, C.-H., HILKER, N., HEALY, R.M., SOFOWOTE, U., DEBOSZ, J., SU, Y., MUNOZ, A., EVANS, G.J. Quantifying metal emissions from vehicular traffic using real world emission factors. In: *Environmental Pollution*. 2021. vol. 268, pp. 115805. ISSN 0269-7491. DOI: 10.1016/j.envpol.2020.115805.

312. NAWROT, N., WOJCIECHOWSKA, E., REZANIA, S., WALKUSZ-MIOTK, J., PAZDRO, K. The effects of urban vehicle traffic on heavy metal contamination in road sweeping waste and bottom sediments of retention tanks. In: *Science of the Total Environment*. 2020. vol. 749, pp. 141511. ISSN 0048-9697. DOI: 10.1016/j.scitotenv.2020.141511.

313. RADZIEMSKA, M., MAZUR, Z., BES, A., MAJEWSKI, G., GUSIATIN, Z.M., BRTNICKY, M. Using mosses as bioindicators of potentially toxic element contamination in ecologically valuable areas located in the vicinity of a road: a case study. In: *International journal of environmental research and public health*. 2019. vol. 16, no. 20, pp. 3963. ISSN 1661-7827. DOI: 10.3390/ijerph16203963.

314. DROR, I., YARON, B., BERKOWITZ, B. The human impact on all soil-forming factors during the anthropocene. In: *ACS Environmental Au*. 2021. vol. 2, no. 1, pp. 11–19. ISSN 2694-2518. DOI: 10.1021/acsenvironau.1c00010.

315. GILTRAP, D., CAVANAGH, J., STEVENSON, B., AUSSEIL, A.-G. The role of soils in the regulation of air quality. In: *Philosophical Transactions of the Royal Society B*. 2021. vol. 376, no. 1834, pp. 20200172. ISSN 0962-8436. DOI: 10.1098/rstb.2020.0172.

316. LAGERSTRÖM, M., YTREBERG, E., WIKLUND, A.-K.E., GRANHAG, L. Antifouling paints leach copper in excess–study of metal release rates and efficacy along a salinity gradient. In: *Water Research*. 2020. vol. 186, pp. 116383. ISSN 0043-1354. DOI: 10.1016/j.watres.2020.116383.

317. MILLER, R.J., ADELEYE, A.S., PAGE, H.M., KUI, L., LENIHAN, H.S., KELLER, A.A. Nano and traditional copper and zinc antifouling coatings: Metal release and impact on marine sessile invertebrate communities. In: *Journal of Nanoparticle Research*. 2020. vol. 22, no. 5, pp. 1–15. ISSN 1388-0764. DOI: 10.1007/s11051-020-04875-z.

318. ZHANG, Y., SUN, T., MA, M., WANG, X., XIE, Q., ZHANG, C., WANG, Y., WANG, D. Distribution of mercury and methylmercury in river water and sediment of typical manganese mining area. In: *Journal of Environmental Sciences*. 2022. vol. 119, pp. 11–22. ISSN 1001-0742.

319. ZHANG, Y., ZHOU, X., MA, W., YIN, D., WANG, Y., ZHANG, C., WANG, D. Distribution of mercury and methylmercury in farmland soils affected by manganese mining and

smelting activities. In: *International Journal of Environmental Research and Public Health*. 2022. vol. 19, no. 16, pp. 10288. ISSN 1661-7827. DOI: 10.3390/ijerph191610288.

320. AVKOPASHVILI, M., GONGADZE, A., MATCHAVARIANI, L., AVKOPASHVILI, G., AVKOPASHVILI, I. Soil, Water and Air Pollution by Manganese Industry in The Imereti Region, Georgia. In: 19th International Multidisciplinary Scientific GeoConference SGEM 2019. Albena, Bulgaria, 30 June - 6 July 2019. Sofia: International Multidisciplinary Scientific Geoconference, 2019, vol. 19, no. 3.2, pp. 417–424. ISSN 1314-2704. DOI: 10.5593/sgem2019/3.2/S13.055.

321. ALEKU, D.L., LAZAREVA, O., PICHLER, T. Mercury in Groundwater–Source, Transport and Remediation. In: *Applied Geochemistry*. 2024. vol. 170, pp. 106060. ISSN 0883-2927. DOI: 10.1016/j.apgeochem.2024.106060.

322. ROSATI, G., HEIMBÜRGER, L.E., MELAKU CANU, D., LAGANE, C., LAFFONT, L., RIJKENBERG, M.J.A., GERRINGA, L.J.A., SOLIDORO, C., GENCARELLI, C.N., HEDGECOCK, I.M. Mercury in the Black Sea: New insights from measurements and numerical modeling. In: *Global biogeochemical cycles*. 2018. vol. 32, no. 4, pp. 529–550. ISSN 0886-6236. DOI: 10.1002/2017GB005700.

323. BARAGO, N., MASTROIANNI, C., PAVONI, E., FLOREANI, F., PARISI, F., LENAZ, D., COVELLI, S. Environmental impact of potentially toxic elements on soils, sediments, waters, and air nearby an abandoned Hg-rich fahlore mine (Mt. Avanza, Carnic Alps, NE Italy). In: *Environmental Science and Pollution Research*. 2023. vol. 30, no. 23, pp. 63754–63775. ISSN 1614-7499. DOI: 10.1007/s11356-023-26629-7.

324. OHTA, A., IMAI, N., TERASHIMA, S., TACHIBANA, Y. The spatial distribution of multiple elements in the Kanto region of Japan: Transport of chalcophile elements from land to sea. In: *Journal of Geochemical Exploration*. 2015. vol. 154, pp. 156–170. ISSN 0375-6742.

325. TOMCZYK, P., GAŁKA, B., WIATKOWSKI, M., BUTA, B., GRUSS, Ł. Analysis of spatial distribution of sediment pollutants accumulated in the vicinity of a small hydropower plant. In: *Energies*. 2021. vol. 14, no. 18, pp. 5935. ISSN 1996-1073. DOI: 10.3390/en14185935.

326. SURMAVA, A.A., KUKHALASHVILI, V.G., GIGAURI, N.G., INTSKIRVELI, L.N. $PM_{2.5}$ and PM_{10} in the Atmosphere of Kutaisi City. In: *Journals of Georgian Geophysical Society*. 2023. vol. 26, no. N2. ISSN 1512-1127.

327. POUILLÉ, S., TALBOT, J., TAMALAVAGE, A.E., KESSLER-NADEAU, M.É., KING, J. Impacts of mineral dust on trace element concentrations (As, Cd, Cu, Ni and Pb) in

lichens and soils at Lhù'ààn Mân' (Yukon Territory, Canada). In: *Journal of Geophysical Research: Biogeosciences*. 2024. vol. 129, no. 6. ISSN 2169-8953. DOI: 10.1029/2023JG007927.

328. GELOVANI, I., LOMINADZE, G., KAVLASHVILI, G., RUSSO, G. Examples of Coastal Hazard Along the Georgian Black Sea Coast. In: *Building Knowledge for Geohazard Assessment and Management in the Caucasus and other Orogenic Regions*. Springer, 2021. p. 317–326. ISBN 9402420452.

329. SURMAVA, A.A., KUKHALASHVILI, V.G., GIGAURI, N.G., INTSKIRVELI, L.N. Study of Kutaisi City Atmospheric Air Pollution with PM_{10} Particles using Numerical Modeling. A Case of Fresh Western Background Breeze. In: *Journals of Georgian Geophysical Society*. 2024. vol. 27, no. N1. ISSN 1512-1127.

330. SURMAVA, A.A. Numerical Modeling of Zestafoni City Dust Dispersion in case of Western Wind. In: *Journals of Georgian Geophysical Society*. 2018. vol. 21, no. 2. ISSN 1512-1127.

331. KOSAI, S., NAKAJIMA, K., YAMASUE, E. Mercury mitigation and unintended consequences in artisanal and small-scale gold mining. In: *Resources, Conservation and Recycling*. 2023. vol. 188, pp. 106708. ISSN 0921-3449. DOI: 10.1016/j.resconrec.2022.106708.

332. RODRIGUES, Y.O.S., DÓREA, J.G., LANDIM, P.M.B., BERNARDI, J.V.E., MONTEIRO, L.C., DE SOUZA, J.P.R., PINTO, L. DE C.M., FERNANDES, I.O., DE SOUZA, J.V.V., SOUSA, A.R. Mercury spatiality and mobilization in roadside soils adjacent to a savannah ecological reserve. In: *Environmental Research*. 2022. vol. 205, pp. 112513. ISSN 0013-9351. DOI: 10.1016/j.envres.2021.112513.

333. ZHAO, H., WANG, X., LI, X. Quantifying grain-size variability of metal pollutants in road-deposited sediments using the coefficient of variation. In: *International Journal of Environmental Research and Public Health*. 2017. vol. 14, no. 8, pp. 850. ISSN 1661-7827. DOI: 10.3390/ijerph14080850.

334. BARABASZ, W., ALBINSKA, D., JASKOWSKA, M., LIPIEC, J. Ecotoxicology of Aluminium. In: *Polish journal of environmental studies*. 2002. vol. 11, no. 3, pp. 199–204. ISSN 1230-1485.

335. AKSU, A. Sources of metal pollution in the urban atmosphere (A case study: Tuzla, Istanbul). In: *Journal of Environmental Health Science and Engineering*. 2015. vol. 13, no. 1, pp. 79. ISSN 2052-336X. DOI: 10.1186/s40201-015-0224-9.

336. ZINICOVSCAIA, I., HRAMCO, C., DULIU, O.G., VERGEL, K., CULICOV, O.A., FRONTASYEVA, M. V, DUCA, G. Air pollution study in the Republic of Moldova using

moss biomonitoring technique. In: *Bulletin of environmental contamination and toxicology*. 2017. vol. 98, pp. 262–269. ISSN 0007-4861. DOI: 10.1007/s00128-016-1989-y.

337. KÜHNE, S., ROSSBERG, D., RÖHRIG, P., MEHRING, F. VON, WEIHRAUCH, F., KANTHAK, S., KIENZLE, J., PATZWAHL, W., REINERS, E., GITZEL, J. The use of copper pesticides in Germany and the search for minimization and replacement strategies. In: *Organic Farming*. 2017, vol. 3, no. 1, pp. 66-70. ISSN 2297-6485. DOI: 10.12924/of2017.03010066.

338. VISSCHEDIJK, A.H.J., VAN DER GON, H.A.C.D., HULSKOTTE, J.H.J., QUASS, U. Anthropogenic Vanadium emissions to air and ambient air concentrations in North-West Europe. In: *E3S web of conferences*. EDP Sciences, 2013. p. 03004. ISBN 2267-1242.

339. Inspectorate for Environmental Protection (Moldova). IPM Yearbook – 2018 "Environmental Protection in the Republic of Moldova". Chișinău: Pontos, 2019. ISBN 978-9975-72-346-6. [Accessed 09 February 2023]. Available from: https://ipm.gov.md/upfiles/menu_files/ANUAR%20-%202018.pdf

340. QARRI, F., LAZO, P., ALLAJBEU, S., BEKTESHI, L., KANE, S., STAFILOV, T. The evaluation of air quality in Albania by moss biomonitoring and metals atmospheric deposition. In: *Archives of environmental contamination and toxicology*. 2019. vol. 76, no. 4, pp. 554–571. ISSN 0090-4341. DOI: 10.1007/s00244-019-00608-x.

341. KŁOS, A., CZORA, M., RAJFUR, M., WACŁAWEK, M. Mechanisms for translocation of heavy metals from soil to epigeal mosses. In: *Water, Air, & Soil Pollution*. 2012. vol. 223, no. 4, pp. 1829–1836. ISSN 0049-6979.

342. ČEBURNIS, D., VALIULIS, D. Investigation of absolute metal uptake efficiency from precipitation in moss. In: *Science of the Total Environment*. 1999. vol. 226, no. 2–3, pp. 247–253. ISSN 0048-9697. DOI: 10.1016/S0048-9697(98)00399-4.

343. Ministry of Ecology and Natural Resources National Institute of Ecology. *REPUBLIC OF MOLDOVA STATE OF THE ENVIRONMENT REPORT 2004*. Chişinău, 2005. [Accessed 10 February 2023]. Available from: https://www.unep.org/resources/report/state-environment-report-moldova

344. ZINICOVSCAIA, I., STURZA, R., DULIU, O., GROZDOV, D., GUNDORINA, S., GHENDOV-MOSANU, A., DUCA, G. Major and trace elements in moldavian orchard soil and fruits: Assessment of anthropogenic contamination. In: *International Journal of Environmental Research and Public Health*. 2020. vol. 17, no. 19, pp. 7112. ISSN 1661-7827. DOI: 10.3390/ijerph17197112.

345. MARTINS, G., MIOT-SERTIER, C., LONVAUD-FUNEL, A., MASNEUF-POMARÈDE, I. Grape berry bacterial inhibition by different copper fungicides. In: *BIO web of conferences*. EDP Sciences, 2016. p. 01043. ISBN 2117-4458.

346. ADAMIEC, E., JAROSZ-KRZEMIŃSKA, E., WIESZAŁA, R. Heavy metals from non-exhaust vehicle emissions in urban and motorway road dusts. In: *Environmental monitoring and assessment*. 2016. vol. 188, no. 6, pp. 369. ISSN 0167-6369. DOI: 10.1007/s10661-016-5377-1.

347. WAGNER, S.E., PERYEA, F.J., FILBY, R.A. Antimony impurity in lead arsenate insecticide enhances the antimony content of old orchard soils. In: *Journal of environmental quality*. 2003. vol. 32, no. 2, pp. 736–738. ISSN 0047-2425. DOI: 10.2134/jeq2003.7360.

348. NIU, Q. Overview of the relationship between aluminum exposure and human health. In: *Neurotoxicity of Aluminum*. 2nd ed. Singapore: Springer, 2023, pp. 1–32. ISBN 978-981-99-1591-0. DOI: 10.1007/978-981-99-1592-7_1.

349. INGERMAN, L., JONES, D.G., KEITH, S., ROSEMOND, Z.A. Toxicological profile for aluminum. Atlanta, Georgia: U.S. Department of Health and Human Services, Public Health Service, Agency for Toxic Substances and Disease Registry, September 2008 [Accessed 8 February 2026]. Available from: https://www.ncbi.nlm.nih.gov/books/NBK597308/

350. QI, M., WU, Y., ZHANG, S., LI, G., AN, T. Pollution Profiles, Source Identification and Health Risk Assessment of Heavy Metals in Soil near a Non-Ferrous Metal Smelting Plant. In: *International Journal of Environmental Research and Public Health*. 2023. vol. 20, no. 2, pp. 1004. ISSN 1661-7827. DOI: 10.3390/ijerph20021004.

351. SAGER, M. Urban Soils and Road Dust—Civilization Effects and Metal Pollution—A Review. In: *Environments*. 2020. vol. 7, no. 11, pp. 98. ISSN 2076-3298. DOI: 10.3390/environments7110098.

352. SENIOR, C., GRANITE, E., LINAK, W., SEAMES, W. Chemistry of Trace Inorganic Elements in Coal Combustion Systems: A Century of Discovery. In: *Energy & Fuels*. 2020. vol. 34, no. 12, pp. 15141–15168. ISSN 0887-0624. DOI: 10.1021/acs.energyfuels.0c02375.

353. FERNÁNDEZ, J.A., CARBALLEIRA, A. Evaluation of contamination, by different elements, in terrestrial mosses. In: *Archives of environmental contamination and toxicology*. 2001. vol. 40, pp. 461–468. ISSN 0090-4341. DOI: 10.1007/s002440010198.

354. WU, W., WU, P., YANG, F., SUN, D., ZHANG, D.-X., ZHOU, Y.-K. Assessment of heavy metal pollution and human health risks in urban soils around an electronics manufacturing facility. In: *Science of the Total Environment*. 2018. vol. 630, pp. 53–61. ISSN 0048-9697.

355. EUROPEAN ENVIRONMENT AGENCY. *Air quality in Europe - 2017 report*. Luxembourg, 2017. ISBN 9789292139216. [Accessed 2 October 2025]. https://www.eea.europa.eu/en/analysis/publications/air-quality-in-europe-2017

356. SCHRÖDER, W., NICKEL, S. Moss species-specific accumulation of atmospheric deposition? In: *Environmental Sciences Europe*. 2019. vol. 31, pp. 1–18. ISSN 2190-4715. DOI: 10.1186/s12302-019-0262-5.

357. ANIČIĆ UROŠEVIĆ, M., ILIĆ, M., RADNOVIĆ, D., VERGEL, K., YUSHIN, N., CHALIGAVA, O., ZINICOVSCAIA, I. Comparative biomonitoring of airborne potentially toxic elements using mosses (*Hypnum cupressiforme*, *Brachythecium* spp.) and lichen (Evernia prunastri) over remote areas. In: *Environmental Science and Pollution Research*. 2024. vol. 31, no. 35, pp. 48296–48312. ISSN 1614-7499. DOI: 10.1007/s11356-024-34353-z.

358. CAPOZZI, F., DI PALMA, A., SORRENTINO, M.C., ADAMO, P., GIORDANO, S., SPAGNUOLO, V. Morphological traits influence the uptake ability of priority pollutant elements by *Hypnum cupressiforme* and *Robinia pseudoacacia* Leaves. In: *Atmosphere*. 2020. vol. 11, no. 2, pp. 148. ISSN 2073-4433.

359. BETSOU, C., TSAKIRI, E., KAZAKIS, N., VASILEV, A., FRONTASYEVA, M., IOANNIDOU, A. Atmospheric deposition of trace elements in Greece using moss *Hypnum cupressiforme* Hedw. as biomonitors. In: *Journal of Radioanalytical and Nuclear Chemistry*. 2019. vol. 320, pp. 597–608. ISSN 0236-5731. DOI: 10.1007/s10967-019-06535-4.

360. RENAUDIN, M., LEBLOND, S., MEYER, C., ROSE, C., LEQUY, E. The coastal environment affects lead and sodium uptake by the moss *Hypnum cupressiforme* used as an air pollution biomonitor. In: *Chemosphere*. 2018. vol. 193, pp. 506–513. ISSN 0045-6535. DOI: 10.1016/j.chemosphere.2017.11.045.

361. ABOAL, J.R., FERNÁNDEZ, J.A., BOQUETE, T., CARBALLEIRA, A. Is it possible to estimate atmospheric deposition of heavy metals by analysis of terrestrial mosses? In: *Science of the Total Environment*. 2010. vol. 408, no. 24, pp. 6291–6297. ISSN 0048-9697. DOI: 10.1016/j.scitotenv.2010.09.013.

362. BEJAN, I., SOCHIRCĂ, V., NAGACEVSCHI, T., ŢÎŢU, P. Spatial study of soil erosion in the Republic of Moldova. In: *Present Environment and Sustainable Development*. 2022, vol. 16, no. 2, pp. 259-271. ISSN 1843-5971. DOI: 10.47743/pesd2022162021.

363. WANG, X., YUAN, W., FENG, X., WANG, D., LUO, J. Moss facilitating mercury, lead and cadmium enhanced accumulation in organic soils over glacial erratic at Mt. Gongga, China. In: *Environmental Pollution*. 2019. vol. 254, pp. 112974. ISSN 0269-7491. DOI: 10.1016/j.envpol.2019.112974.

364. TARITA, A., BRAŞOVEANU, V., JIGĂU, G. The content of heavy metals in the soils of the state protected natural areas in the south-eastern area of the Republic of Moldova. In: *Lucrări Ştiinţifice. Seria Horticultură*. 2021. P. 147–154. ISSN 2286-1580.

365. GAMBASHIDZE, G.O., URUSHADZE, T.F., BLUM, W.E., MENTLER, A.F. Heavy metals in some soils of Western Georgia. In: *Eurasian Soil Science*. 2014. vol. 47, pp. 834–843. ISSN 1064-2293. DOI: 10.1134/S1064229314080031

DECLARATION ABOUT ASSUMING RESPONSIBILITY

The undersigned, Omari Chaligava, announce on my own responsibility that the materials presented in PhD thesis are the results of proper investigations and scientific advances. Comprehend that in opposite case, follow to be accountable for the consequences in compliance with current legislation.

Signature 

Data 27.07.2026

CURRICULUM VITAE

Full Name	Omari Chaligava
Address	0152 Georgia, Tbilisi, Isani-Samgori District, Vazisubani Settlement, III Micro-District, II Block, Building 9, Flat 182
Phone	+995 599 56 16 28
E-mail	o.chaligava@gmail.com
Nationality	Georgian
Date of birth	04.01.1994
Gender	Male

Languages:	Georgian – native; English – B2; Russian – C1
Education	
2012 – 2016	Bachelor's degree, Ivane Javakhishvili Tbilisi State University
2016 – 2018	Master's degree, Ivane Javakhishvili Tbilisi State University
2022 – 2026	PhD student, Moldova State University
Professional Experience	
2017 − 2025	Junior Researcher, SNAAPI Sector, Division of Nuclear Physics, Frank Laboratory of Neutron Physics, Joint Institute for Nuclear Research
2026 – present.	Acting Head of the Data Processing Group, SNAAPI Sector, Division of Nuclear Physics, Frank Laboratory of Neutron Physics, Joint Institute for Nuclear Research
Research Interests	Elemental analysis, Biomonitoring, Gamma-ray Spectrometry
Research Project Participation	
2015-2017	Georgia Shota Rustaveli National Science Foundation Grant No. AR/198/9-240/14, “Investigation of atmospheric deposition of heavy metals in Georgia using moss biomonitoring and physical analytical techniques”.
2016	Grant of the Plenipotentiary of Georgia at the Joint Institute for Nuclear Research, Order No.18.
2020	Grant of the Plenipotentiary of Georgia at the Joint Institute for Nuclear Research, Order No.37.

2022	Grant for young scientists and specialists of JINR No. 22-402-10.
2023	Grant for young scientists and specialists of JINR No. 23-402-12.
2024-2028	Neutron Nuclear Physics Project No. 03-4-1146-2024/2028
Awards And Honors	
2020	Second Prize of the FLNP for Cycle of works “Athmospheric Deposits of Heavy Metals– Assessment Based on Analysis of Moss-Biomonitors: results of the 2015/2016 moss survey”.
2021	Second Prize of the JINR for Cycle of works “Atmospheric deposits of heavy metals – estimation based on analysis of moss-biomonitors: results of a single-stage accumulation of moss-biomonitors for 2015-2016”.
2022	Encouraging Prize of the JINR for “Application of the neutron activation analysis for the estimation of the chemical quality in mussels from different parts of the World Ocean for the characterization of relation to the environment”.
2022	Third Prize of the FLNP for Paper “Distribution of natural and anthropogenic radionuclides in soil samples in recreational zones of Moscow”.
2024	First Prize of the FLNP for series of papers “Neutron activation analysis and complementary techniques in meeting environmental and food safety issues”.
Internships	
2021	International Youth Training Program "EcoLogica", Baku, Azerbaijan.
Publications	
Articles in international peer-reviewed journals	43
Reports at scientific meetings	25
Patents	1